REMARKS

The Finality of the Office Action

On August 30, 2006, Applicant petitioned the Director under C.F.R. § 1.181 to withdraw the finality of the instant Office Action.

The Claim Amendments

Claim 23 has been amended to recite a method of inhibiting ERK or AKT activity *in vitro* in selected biological samples. Support for this amendment is found in the specification on page 42, lines 4 to 8.

Claim 27, *inter alia*, and claim 28 have been amended to recite a method of treating a cancer selected from breast cancer, colon cancer, kidney carcinoma, lung cancer, melanoma, ovarian cancer, pancreatic cancer, or prostate cancer. Support for these amendments is found in the specification on page 45, line 10, to page 46, line 13 and in the claims as originally filed.

Claim 27, *inter alia*, and claim 33 have been amended to recite a method of treating Alzheimer's disease. Support for these amendments is found in the specification on page 45, line 10, to page 46, line 13 and in the claims as originally filed.

Claim 27, *inter alia*, and claim 35 have been amended to recite a method of treating cardiovascular disease selected from stroke, restenosis, cardiomegaly, atherosclerosis, myocardial infarction, or congestive heart failure. Support for these amendments is found in the specification on page 45, line 10, to page 46, line 13 and in the claims as originally filed.

Claim 27, *inter alia*, and claim 38 have been amended to recite a method of treating asthma. Support for these amendments is found in the specification on page 45, line 10, to page 46, line 13 and in the claims as originally filed.

Claims 29, 31-21, 34, 36, and 39-43 have been canceled.

None of the amendments contain new matter. Their entry is requested.

Applicants reserve the right to pursue canceled subject matter in the application or in an application claiming priority therefrom.

The Response

Rejection under 35 U.S.C. § 112

The Examiner has rejected claims 23 and 27-41 under 35 U.S.C. § 112, first paragraph, for allegedly lacking enablement. In particular, the Examiner asserts that the specification does not reasonably provide enablement for (*i*) a method of inhibiting ERK or AKT activity in a biological sample (claim 23); (*ii*) a method of treating neurological disorders generally or specific neurological disorders, such as, for example, Alzheimer's disease, Parkinson's disease, ALS, or Huntington's disease (claims 27 and 33-34); (*iii*) a method of treating inflammatory disorders, such as, for example, asthma (claims 27 and 38-39); (*iv*) a method of treating cardiovascular disease generally or individual cardiovascular disorders, such as, for example, stroke, restenosis, cardiomegaly, atherosclerosis, myocardial infarction, or congestive heart failure (claims 27 and 35-36); or (*v*) a method of treating cancer generally or a cancer selected from a list of specific cancers (claims 27-29).

Regarding item (*i*), claim 23 has been amended to incorporate the term "*in vitro*" to and to recite specific biological samples in which ERK activity is inhibited, thus clearly differentiating the inhibition of ERK in a biological sample from the *in vivo* inhibition of ERK for the treatment of disease. The specification provides ample support for the inhibition of ERK and AKT3 kinase (see, e.g., Tables 6 and & on pages 59-63) and this amendment obviates the Examiner's implied objection to claim 23 as reciting a method of treating disease in general by inhibiting AKT or ERK.

Regarding item (*ii*), amended claims 27 and 33 recite a method of treating Alzheimer's disease. At the time of the invention, it was known that the neuronal microtubule-associated protein tau becomes highly phosphorylated, loses its binding properties, and aggregates into paired helical filaments in patients with Alzheimer's disease. In one study, the physiological phosphorylation of endogenous tau protein in metabolically labeled human neuroblastoma cells and in Chinese hamster ovary cells stably transfected with tau was measured and 17 phosphorylation sites were identified, comprising 80-90% of the total phosphate incorporated. See the abstract of Illenberger et al., *Mol. Biol. Cell* 9(6): 1495-512, 1998 (Exhibit A; hereafter, "Illenberger"). ERK2 was known at the time of the invention to mediate the phosphorylation of tau. See page 1057, paragraph 2, of Raghunandan et al., *Biochem. Biophys. Res. Commun.* 215(3):1056-66, 1995 (Exhibit B; hereafter, "Raghunandan"). Further, Fukunaga et al., *Mol. Neurobiol.* 16(1): 79-95, 1998

(Exhibit C; hereafter, "Fukunaga") have postulated that ERKs are attractive candidates to mediate morphological differentiation and promote survival in neurons, and their inhibition may mediate physiological and pathological events such as Alzheimer's disease and cerebral ischemia. See the abstract of Fukunaga. Taken together with the specification, Illenberger, Raghunandan, and Fukunaga clearly show that there is a reasonable correlation between the inhibitors of the invention, their ERK2 inhibitory activity, and the use of these compounds to treat Alzheimer's disease.

Regarding item (*iii*), amended claims 27 and 38 recite a method of treating asthma in a patient in need thereof by compounds of the invention. The role of ERK in allergy and asthma was established at the time of the invention, as it was known that the survival and apoptosis of eosinophils is of pivotal importance for controlling allergic diseases, such as asthma. See page 36 of Chang et al., *Cell Immunol.* 203(1):29-38, 2000 (Exhibit D; hereafter "Chang") showed that a MAP/ERK kinase inhibitor was partly able to block augmentation of eosinophil viability in cell culture studies. Taken together with the specification, Chang clearly shows that there is a reasonable correlation between the inhibitors of the invention, their ERK2 inhibitory activity, and the use of these compounds to treat allergy/asthma.

Regarding item (*iv*), amended claims 27 and 35 recite a method of treating a cardiovascular disease selected from stroke, restenosis, cardiomegaly, artherosclerosis, myocardial infarction, or congestive heart failure in a patient in need thereof by compounds of the invention. The role of ERK in cardiovaacular disease has been demonstrated. For instance, the chronic activation of tyrosine phosphorylation, in particular the redistribution and phosphorylation of ERK1/ERK2 in the brain tissue of ischemic stroke victims, was known at the time of the invention. See page 2762, column 2, to page 2763, column 1, of Slevin et al. in *Neuroreport* 11(12): 2759-64, 2000 (Exhibit E; hereafter "Slevin"). Further, the intravenous administration of an ERK inhibitor afforded brain protection against forebrain ischemia and focal cerebral ischemia in an animal model. See the abstract and page 11572, column 2, in Namura et al., *Proc. Natl. Acad. Sci. U S A* 98(20): 11569-74, 2001 (Exhibit F; hereafter "Namura").

Osteopontin was known to play role in matrix reorganization after tissue injury, including vascular conditions such as atherosclerosis and restenosis. Using an inhibitor of the MEK/ERK pathway, it was known at the time of the invention that ERK is involved in the regulation of osteopontin expression. See the abstract and concluding paragraph on page 136

of Moses et al., *Arch. Biochem. Biophys.* 396(1): 133-7, 2001 (Exhibit G; hereafter, "Moses"). Further, a link between the ERK pathway and endothelial cell migration, an important event in the development of atherosclerotic plaque, had been established. See the concluding paragraph on page 600 of Pintucci et al., *FASEB J.* 16(6): 598-600, 2002 (Exhibit H; hereafter, "Pintucci").

In addition, the role of ERK in cardiac hypertrophy was established at the time the invention was made. Markers indicative of hypertrophy could be suppressed by a MEK/ERK inhibitor in stimulated neonatal rat cardiomyocytes. See the abstract and page H1641, right column, to page H1642, left column, of Kodama et al. in *Am. J. Physiol. Heart Circ. Physiol.* 279(4): H1635-44, 2000 (Exhibit I; hereafter, "Kodama"). Cardiac hypertrophy is also associated with congestive heart failure and myocardial infarction. It had been reported that the mean activity of ERK was significantly greater in failing hearts vs. non-failing human hearts. See the first paragraph of the discussion on page 133 of Takeishi et al., *Cardiovasc. Res.* 53(1): 131-7, 2002 (Exhibit J; hereafter, "Takeishi"). Taken together with the specification, Slevin, Namura, Moses, Pintucci, Kodama, and Takeishi clearly show that there is a reasonable correlation between the inhibitors of the invention, their ERK2 inhibitory activity, and the use of these compounds to treat the cardiovascular diseases recited in amended claims 27 and 35.

Regarding item (*v*), amended claims 27 and 28 recite a method of treating a cancer selected from breast cancer, colon cancer, kidney carcinoma, lung cancer, melanoma, ovarian cancer, pancreatic cancer, or prostate cancer. A link between ERK kinase activity and various cancers had been established at the time of the invention. For instance, it was known that MAP/ERK kinases play a pivotal role in mitogenic signal transduction and that the aberrant activation of signal transducing molecules, such as Ras and Raf-1, via MAP/ERK kinases was linked with the recited cancers. See, e.g., page 2, lines 11-19 of the specification. Constitutive activation of MAP/ERK kinases had been found in primary tumor cell lines derived from human pancreas, colon, lung, ovary and kidney. See the abstract of Hoshino et al., *Oncogene* 18: 813-22, 1999 (Exhibit K; hereafter, "Hoshino"). ERK had also been shown to be constitutively active in human melanoma tumor cell lines. See page 302, right column, of Kortylewski et al., *Biochem. J.* 357(Pt 1): 297-303, 2001 (Exhibit L; hereafter, "Kortylewski"). Additionally, it had been demonstrated that transforming growth factor beta-2 potently activates ERK2 in a human tumor cell line for breast cancer. See page

47, left column, in Frey et al., *Cancer Lett.* 117(1): 41-50, 1997 (Exhibit M; hereafter, "Frey"). Further, it was known that EGF and IGF-1 are potent mitogens that play a regulatory role in the proliferation of prostate cancer cells and that a monoclonal antibody against the EGF receptor abrogates p42/ERK2 activation in a human tumor cell line for prostate cancer. See page 231, right column, in Putz et al., *Cancer Res.* 59(1): 227-33, 1999 (Exhibit N; hereafter, "Putz"). Taken together with the specification, Kortylewski, Hoshino, Frey, and Putz clearly show that there is a reasonable correlation between the activation of ERK in various cancers, the use of an ERK inhibitor to inhibit cancer cell growth, and the use of the ERK inhibitors of the invention to treat the cancers recited in claims 27 and 28.

As discussed above, applicants have demonstrated that ERK and AKT3 inhibition is useful in the treatment of the diseases recited in amended claims 23, 27-28, 30, 33, 35, and 37-38. Further, for each of the therapeutic methods discussed above, a skilled artisan would be able to discern an appropriate dosage and method of use based upon the information provided in the specification (see page 48, line 4, to page 52, line 5) along with the general knowledge of one skilled in the art. Accordingly, one skilled in the art would find it reasonable to use the ERK/AKT3 inhibitors of the present invention for the treatment of the recited diseases without undue experimentation. Thus, the teachings of the specification, combined with the state of the art at the time of the invention, fully enable the claimed invention with respect to the aforementioned diseases. For all of the reasons set forth above, applicants respectfully request that the Examiner withdraw her rejection over 35 U.S.C. § 112, first paragraph.

Conclusion

Applicants request that the Examiner enter the above amendments, consider the matters taken up in the remarks, and allow the claims to pass to issue. Should the Examiner deem expedient a telephone discussion to further the prosecution of the above application, Applicants request that the Examiner contact the undersigned.

Respectfully submitted,

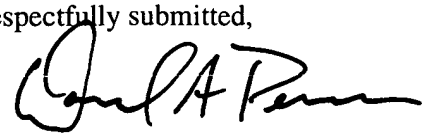

Daniel A. Pearson (Reg. No. 58,053)
Agent for Applicants
c/o Vertex Pharmaceuticals Incorporated
130 Waverly Street
Cambridge, MA 02139-4242
Tel.: (617) 444-6790
Fax.: (617) 444-6483

Exhibit A

Molecular Biology of the Cell
Vol. 9, 1495–1512, June 1998

The Endogenous and Cell Cycle-dependent Phosphorylation of tau Protein in Living Cells: Implications for Alzheimer's Disease

Susanne Illenberger, Qingyi Zheng-Fischhöfer, Ute Preuss,* Karsten Stamer, Karlheinz Baumann,† Bernhard Trinczek, Jacek Biernat, Robert Godemann, Eva-Maria Mandelkow, and Eckhard Mandelkow‡

Max-Planck-Unit for Structural Molecular Biology, D-22603 Hamburg, Germany

Submitted October 14, 1997; Accepted March 23, 1997
Monitoring Editor: J. Richard McIntosh

In Alzheimer's disease the neuronal microtubule-associated protein tau becomes highly phosphorylated, loses its binding properties, and aggregates into paired helical filaments. There is increasing evidence that the events leading to this hyperphosphorylation are related to mitotic mechanisms. Hence, we have analyzed the physiological phosphorylation of endogenous tau protein in metabolically labeled human neuroblastoma cells and in Chinese hamster ovary cells stably transfected with tau. In nonsynchronized cultures the phosphorylation pattern was remarkably similar in both cell lines, suggesting a similar balance of kinases and phosphatases with respect to tau. Using phosphopeptide mapping and sequencing we identified 17 phosphorylation sites comprising 80–90% of the total phosphate incorporated. Most of these are in SP or TP motifs, except S214 and S262. Since phosphorylation of microtubule-associated proteins increases during mitosis, concomitant with increased microtubule dynamics, we analyzed cells mitotically arrested with nocodazole. This revealed that S214 is a prominent phosphorylation site in metaphase, but not in interphase. Phosphorylation of this residue strongly decreases the tau–microtubule interaction in vitro, suppresses microtubule assembly, and may be a key factor in the observed detachment of tau from microtubules during mitosis. Since S214 is also phosphorylated in Alzheimer's disease tau, our results support the view that reactivation of the cell cycle machinery is involved in tau hyperphosphorylation.

INTRODUCTION

Microtubule-associated proteins (MAPs)[1] are key factors regulating microtubule dynamics in living cells. These proteins bind to microtubules in a nucleotide-insensitive way, leading to an overall stabilization of the microtubule network. Microtubules are involved in highly dynamic cellular events: they drive neurite outgrowth and are responsible for correct chromosome segregation at mitosis (reviewed by Kosik and McConlogue, 1994; Schoenfeld and Obar, 1994; Hyman and Karsenti, 1996). There is much evidence that the modulation of the MAP–microtubule interaction is regulated by the phosphorylation state of MAPs. Tau protein, a class of mammalian MAPs in brain, is predominantly found in the axons of neurons (Binder *et al.*, 1985), where it is thought to support axonal transport by stabilizing axonal microtubules. As in the related proteins MAP2 and MAP4, the microtubule-binding region of tau (Figure 1) is located in the C-terminal half of the protein. It includes three or four

* Present address: Institute of Genetics, University of Bonn, D-53117 Bonn, Germany.
† Present address: Nervous System Research, Novartis Pharma Inc., CH-4002 Basel, Switzerland.
‡ Corresponding author. E-mail address: mandelkow.mpasmb.desy.de.

[1] Abbreviations: AD, Alzheimer's disease; GFP, green fluorescent protein; GSK-3, glycogen synthase kinase-3; MAPs, microtubule-associated proteins; PHFs, paired helical filaments; TLE/TLC, thin layer electrophoresis/TLC.

pseudorepeats of ~31 residues each depending on the isoform (Lee *et al.*, 1988; Goedert *et al.*, 1989; Himmler *et al.*, 1989). The repeats are flanked by basic, proline-rich stretches that help to target the protein to the microtubule (Butner and Kirschner, 1991; Brandt *et al.*, 1994; Goode and Feinstein, 1994; Gustke *et al.*, 1994). The N-terminal part of the molecule is more acidic and does not interact with microtubules (projection domain). In Alzheimer's disease (AD), tau becomes detached from microtubules and aggregates into the paired helical filaments (PHFs), a hallmark in the AD neurofibrillary pathology (review by Kosik and Greenberg, 1994). Tau isolated from these aggregates is highly phosphorylated, about 4 times as much as tau from brain tissue of nondemented individuals (Ksiezak-Reding *et al.*, 1992; Köpke *et al.*, 1993). Mapping of phosphorylation sites of PHF-tau by mass spectrometry revealed that many of the residues phosphorylated are of the Ser-Pro/Thr-Pro type, predominantly located in the proline-rich region (Morishima-Kawashima *et al.*, 1995). Some of these can be detected with phosphorylation-dependent antibodies (reviewed by Kosik and Greenberg, 1994; Mandelkow *et al.*, 1995).

There is increasing evidence that mitotic mechanisms may be involved in the abnormal phosphorylation of tau in AD neurons: 1) Tau from fetal brain tissue, still undergoing cell division, has an elevated phosphate content and is recognized by diagnostic phosphorylation-dependent AD antibodies (Kanemaru *et al.*, 1992; Brion *et al.*, 1993; Kenessey and Yen, 1993, Matsuo *et al.*, 1994). 2) In several cell lines the phosphorylation of tau is increased specifically during mitosis (Pope *et al.*, 1994; Preuss *et al.*, 1995; Vincent *et al.*, 1996; Preuss and Mandelkow, 1998). 3) There is a tight link between apoptosis and the cell cycle machinery (for reviews see Pandey and Wang, 1995; King and Cidlowski, 1995) and induction of mitosis in postmitotic neuronal cells leads inevitably to cell death (Park *et al.*, 1996). 4) Furthermore, apoptosis is indeed elevated in hippocampal brain tissue in AD (Smale *et al.*, 1995; Li *et al.*, 1997). A current hypothesis for the AD-specific phosphorylation of tau therefore states that the affected neurons try to reenter the proliferative phase as a result of some hitherto unknown insult. Thus, turning on the "inappropriate" program ultimately drives the cells into apoptosis, explaining the massive loss of neurons from AD brains.

Many of the investigations of tau phosphorylation in living cells have concentrated on immunocytochemical detection of phosphorylation sites with diagnostic AD antibodies, thus limiting the analysis to those sites where antibodies were available (reviewed by Friedhoff and Mandelkow, 1998). To overcome these limitations we have analyzed tau from metabolically radiolabeled cells by two-dimensional (2D) phosphopeptide mapping. This approach allows the detection of all phosphorylation sites, including those not seen by antibody labeling, and allows relative quantification (Boyle *et al.*, 1991). We investigated two cell lines in parallel, the LAN-5 neuroblastoma cells (Seeger *et al.*, 1982) that express moderate levels of tau protein endogenously (Greenwood and Johnson, 1995), and a Chinese hamster ovary (CHO) cell line stably transfected with the longest human tau isoform (htau40; Preuss *et al.*, 1995). Using recombinant tau protein phosphorylated in vitro with different kinases to generate reference phosphopeptides, we identified the 17 major in vivo phosphorylation sites in the two cell lines corresponding to 80–90% of the total radiolabel incorporated. The overall pattern in the neuronal and nonneuronal cells was remarkably similar, showing that transfected CHO cells can function as a cell model to study tau phosphorylation. Most of the sites are of the Ser-Pro/Thr-Pro type except S214 and S262. Transfected CHO cells arrested in metaphase show enhanced phosphorylation in several peptides, including T153, T181, S202/T205, T212/T217, and S214. The first four peptides are phosphorylated by cdc2 in vitro, suggesting that this kinase could be involved in the phosphorylation of MAPs during mitosis. S214 can be rapidly and selectively phosphorylated in vitro by PKA, and this single site strongly affects tau's ability to bind and stabilize microtubules. Thus, phosphorylation at S214 by PKA or an equivalent kinase could contribute to the increase in microtubule dynamics during mitosis. In addition, S214 has recently been shown to be part of the epitope of the antibody AT 100 that specifically recognizes PHF-tau (Hoffmann *et al.*, 1997; Zheng-Fischhöfer *et al.*, 1998). The knowledge of the physiological phosphorylation sites will be also applicable to primary neurons to monitor the changes in tau phosphorylation due to various insults (e.g., amyloid toxicity, oxidative stress).

MATERIALS AND METHODS

Proteins

Human tau cDNA clones were kindly provided by M. Goedert (Goedert *et al.*, 1989), mitogen-activated protein kinase (MAPK) and its activating kinase (MEK) were kindly provided by F. Döring and B. Berling (Döring *et al.*, 1993). Proteins were expressed in *Escherichia coli* using variants of the pET vector (Studier *et al.*, 1990). Recombinant tau protein was purified by making use of its heat stability and by Mono S fast protein liquid chromatography (Hagestedt *et al.*, 1989). MAP/microtubule affinity-regulating kinase (MARK) and the neuronal cdc2-like kinase cdk5 were prepared from porcine brain as described previously (MARK, Drewes *et al.*, 1995; cdk5, Baumann *et al.*, 1993). GSK-3β was expressed in active form in *E. coli* following the procedure of Wang *et al.* (1994); the original clone was generously provided by J.R. Woodgett. cAMP-dependent protein kinase (PKA) was obtained from Promega (Madison, WI).

The kinase cdc2 was immunoprecipitated from HeLa-S3 cells after mitotic arrest with 0.4 μg/ml nocodazole. Cells were initially lysed in hypotonic 10 mM phosphate buffer (pH 7.0) containing 5 mM $MgCl_2$, 1 mM EDTA, 1 mM EGTA, 10 mM NaF, 10 mM β-glycerophosphate, 1 mM PMSF, 1 μg/ml leupeptin, 1 μg/ml

pepstatin, 1 μg/ml aprotinin. After the addition of 0.5 M NaCl (final concentration) and further homogenization, the homogenate was centrifuged at 4°C for (148,000 × *g*). The supernatant was dialyzed against SP-Sepharose buffer A (50 mM 2-(*N*-morpholino)ethanesulfonic acid, pH 6.5, 2 mM EGTA, 0.5 mM dithiothreitol, 0.2 mM PMSF, 3 mM $MgCl_2$, 0.5 mM benzamidine, 0.2 mM sodium vanadate, 0.02 mM sodium fluoride, 0.01% Brij 35), loaded onto a SP-Sepharose column, and eluted in 40 ml buffer B (buffer A with 0.5 M NaCl). Fractions (2 ml) were assayed for cdc2 activity on phosphocellulose paper discs (Life Technologies, Gaithersburg, MD) (Casnellie, 1991), using the modified histone H1 peptide PKTPKKAKKL as substrate (Beaudette *et al.*, 1993). Active fractions were pooled and immunoprecipitated with an anti-cyclinB-antibody (generous gift from G. Draetta, Mitotix, Cambridge, MA).

Construction of the GFP-tau Vector

The multicloning site in the pEGFP-N1 vector (Clontech, Palo Alto, CA) upstream of GFP was removed with the restriction endonucleases *Nhe*I and *Bam*HI. Oligonucleotides carrying *Xba*I and *Bgl*II restriction sites were ligated into the open frame to omit the *Nhe*I and *Bam*HI restriction sites. To create a new multicloning site downstream of GFP, the vector was cut open with Bsp1407 I and *Not*I. 36-oligomers containing *Nde*I, *Esp*I, *Nhe*I, and *Bam*HI restriction sites were inserted. Tau protein was excised from a bacterial expression vector (pNG2; Gustke *et al.*, 1994) and cloned into the *Nde*I *Bam*HI site to gain a fusion protein with GFP fused to the N terminus of tau.

Transfection

CHO cells were plated onto LabTek chambered cover glass (NUNC, Naperville IL) at 70% confluency the day before transfection. Transfection was carried out with Dotap (Boehringer, Mannheim, Germany) according to manufacturer's instructions.

Phosphorylation Reactions

Phosphorylation reactions were carried out in 40 mM HEPES (pH 7.2) containing 10 μM tau protein, 5 mM $MgCl_2$, 2 mM dithiothreitol, 5 mM EGTA, 0.2 mM PMSF, and 1 mM [γ^{32}P]-ATP (100–200 Ci/mol). Phosphorylation was assayed in SDS gels (Steiner *et al.*, 1990).

Cell Culture

CHO cells stably transfected with the longest human tau isoform htau40 (Preuss *et al.*, 1995) or with a GFP-htau40 construct were grown in HAM's F12 medium supplemented with 10% FCS (Biochrom, Berlin, Germany) in the presence of 600 μg/ml Geneticin (G-418). LAN-5 human neuroblastoma cells (Seeger *et al.*, 1982) and HeLa-S3 cells were grown in RPMI 1640 medium supplemented with 10% FCS. HeLa-S3 cells grown in spinner cultures were mitotically arrested by overnight treatment with 0.4 μg/ml nocodazole (Sigma, Deisenhofen, Germany).

Cell Extracts

For Western blot analysis of tau protein only, total cell extracts of CHO cells transfected with htau40 and LAN-5 neuroblastoma cells were prepared by lysing subconfluent cells on ice in a hypotonic buffer containing 50 mM Tris (pH 7.4), 2 mM EGTA, 2 mM EDTA, 20 mM NaF, 0.1 mM PMSF, 1 μg/ml leupeptin, 1 μg/ml aprotinin, 1 μg/ml pepstatin, 10 mM benzamidine, 1 μM microcystine, and 0.1 M ocadaic acid. Extracts were centrifuged immediately at 15,800 × *g* for 10 min at 4°C. Supernatants were treated with perchloric acid (2.5% final concentration) for 15 min at room temperature. After centrifugation (15,800 × *g* for 10 min at 4°C) tau protein remaining in the supernatant was precipitated with trichloroacetic acid (15% final concentration, 15 min on ice) and centrifuged (15,800 × *g* for 10 min at 4°C). Trichloroacetic acid pellets were either resuspended directly in sample buffer or, for dephosphorylation with alkaline phosphatase, they were washed with ice-cold ethanol, air-dried, and dephosphorylated according to manufacturer's instructions. Samples were run on 10% SDS gels. To analyze the tau and tubulin content of interphase and nocodazole-treated cells without and after extraction, cells were treated with 1% Triton-X 100 in an MT-stabilizing buffer (MTSB: 80 mM piperazine-*N*,*N*'-bis(2-ethanesulfonic acid), pH 6.9, 1 mM $MgCl_2$, 1 mM EGTA, 4% polyethyleneglycol) for 10 s. Triton and the extracted proteins were removed by a brief wash in MTSB and subsequent lysis in hypotonic buffer. After centrifugation (15,800 × *g* for 10 min at 4°C) SDS sample buffer was added to the supernatants.

SDS-PAGE and Western Blotting

Extract samples were electrophoresed on 10% SDS-polyacrylamide gels (perchloric acid-soluble fraction from 1 × 10^6 CHO cells and 1 × 10^7 LAN-5 cells, respectively, per lane) and transferred electrophoretically to polyvinylidene difluoride membranes (Millipore, Eschborn, Germany). Residual membrane-binding sites were blocked with 5% nonfat dry milk in Tris-buffered saline after incubation with the monoclonal antibody T46 (1:6000). Bound antibody was detected with a peroxidase-conjugated antibody and visualized using ECL according to manufacturer's instructions (Amersham-Buchler, Braunschweig, Germany). Densitometric analysis was carried out using the TINA 2.09f software from Raytest GmbH (Straubenhardt, Germany). For immunoblot analysis, recombinant htau23 and htau40 from *E. coli* were isolated by fast protein liquid Mono S (Pharmacia, Freiburg, Germany) chromatography on the basis of its heat stability (for details see Hagestedt *et al.*, 1989).

Immunofluorescence and Microscopy

Cells were washed in an MTSB (80 mM piperazine-*N*,*N*'-bis(2-ethanesulfonic acid), pH 6.9, 1 mM $MgCl_2$, 1 mM EGTA, 4% polyethyleneglycol) and subsequently fixed in methanol (5 min at −20°C). For extraction experiments, cells were extracted with 1% Triton-X 100 in MTSB for 10 s before methanol fixation. Time and fixative were crucial for differential extraction. Prolonged incubation with Triton-X 100 almost completely removed tau protein from all cells irrespective of cell cycle stage and also affected cellular microtubules (our unpublished observations). Paraformaldehyde fixation was not applicable, since the cellular localization of tau is altered: instead of colocalizing with microtubules, tau protein is distributed throughout the cytoplasm, a phenomenon that has been described previously (Schliwa *et al.*, 1981). Hence, only methanol fixation represented the in vivo distribution of tau as was determined by live observation of EGFP-Tau-expressing CHO cells. The rabbit polyclonal anti-tau antibody (Dako, Hamburg, Germany) and the monoclonal anti-α-tubulin antibody DM1A (Sigma, Deisenhofen, Germany) were used at 1:300 and 1:200 dilutions, respectively. Fluorescently labeled (FITC and TRITC) secondary antibodies were obtained from Dianova (Hamburg, Germany). Samples were examined using an Axioplan fluorescence microscope (Zeiss, Jena, Germany). Pictures were taken with a cooled CCD camera (Visicam, Visitron, Puchheim, Germany) using the MetaMorph software package (Visitron). In vivo observation of cells transfected with GFP-htau40 was conducted with an inverted Axiovert 10 microscope (Zeiss) using filters for FITC fluorescence.

Metabolic Labeling and Immunoprecipitation

Both stably transfected CHO cells and LAN-5 neuroblastoma cells grown in 75-cm^2 culture flasks were preincubated for 60 min in phosphate-free MEM (Life Technologies) containing 10% FCS dialyzed against 20 mM HEPES. Subsequently [^{32}P]-orthophosphate (0.7 mCi/ml) was added to the media and cells were then incubated for 4 h. Cells were lysed on ice in the hypotonic 10 mM phosphate buffer (pH 7.0) described above and immediately centrifuged at 15,800 × *g* for 10 min. The supernatant was boiled for 5 min and again centrifuged at 15,800 × *g* for 10 min. (15 μg) Polyclonal rabbit

anti-Tau antibody (Dako) was added and incubated under constant agitation at 4°C for 2 h. (50 μl) Protein-A/G-Sepharose beads (Dianova, Hamburg, Germany) were added and incubation was continued overnight. The immune complexes were recovered by centrifugation and rinsed four times in immunoprecipitation buffer. To arrest CHO cells in metaphase, 0.4 μg/ml nocodazole (Sigma) was added to the phosphate-free medium (DeBrabander *et al.*, 1986). Mitotic cells were detached by mechanical shake-off. Lysis of cells and immunoprecipitation were carried out as described above.

Sequencing and Mass Spectrometric Analysis of Peptides

Fractionated peptides were sequenced on a 476-A Liquid Phase Protein Sequencer (Applied Biosystems, Weiterstadt, Germany). Mass spectrometry was performed using a MALDI II instrument (Matrix Assisted Laser Desorption/Ionization, Shimadzu, Duisburg, Germany). Phosphorylated serine was determined by the formation of the dithiothreitol adduct of dehydroalanine (Meyer *et al.*, 1993). Phosphothreonine was determined by the loss of the threonine peak in the sequence and by the 80-Da mass increase (as seen by MALDI) due to the incorporated phosphate.

Phosphopeptide Mapping by Thin-Layer Electrophoresis/Chromatography and HPLC

After in vitro phosphorylation, kinase proteins were removed by boiling the samples in 0.5 M NaCl, 5 mM dithiothreitol and centrifugation. Tau remains in the supernatant and was precipitated by 15% trichloroacetic acid on ice. Tau protein immunoprecipitated from cells was resolubilized in SDS-sample buffer and boiled for 5 min. Electrophoresis was carried out on a 10% SDS polyacrylamide gel, and the unstained gel was subjected to autoradiography to identify labeled tau protein. Tau bands were cut out of the gel and eluted overnight in 50 mM NH_4HCO_3 buffer (pH 7.4) containing 0.1% SDS and 5% β-mercaptoethanol. Before precipitation by 15% trichloroacetic acid, 20 μg recombinant htau 40 were added. Cysteine residues were modified by performic acid (Hirs, 1967). The protein was digested overnight with trypsin (Promega, sequencing grade) in the presence of 0.1 mM $CaCl_2$, using two additions of the enzyme in a ratio of 1:10–1:20 (wt/wt).

2D phosphopeptide mapping on thin-layer cellulose plates (Macherey and Nagel, Düren, Germany) was performed according to Boyle *et al.* (1991). First-dimension electrophoresis was carried out at pH 1.9 in formic acid (88%)/glacial acetic acid/water (50:156:1794), second-dimension chromatography at pH 3.5 in n-butyl alcohol/pyridine/glacial acetic acid/water (150:100:30:120). For the mapping of phosphorylation sites by sequencing, 400 μg of recombinant htau40 were phosphorylated with cdc2, cdk5, MEK/MAPK, and GSK-3β in the presence of 1 mM [γ^{32}P]-ATP (150 Ci/mol) for 16 h. Samples were treated as described above and digested with trypsin. Separation of peptides was performed by HPLC on a Vydac 218TP52 column using a gradient of 0% acetonitrile, 0.075% trifluoroacetic acid to 50% acetonitrile, 0.05% trifluoroacetic acid in 150 min with a flow rate of 80 μl/min (Smart System, Pharmacia). Radioactive fractions were rechromatographed on a μRPC C2/C18 SC2.1/10 column (Pharmacia) using a gradient of 0% acetonitrile, 0.075% trifluoroacetic acid to 50% acetonitrile, 0.05% trifluoroacetic acid in 60 min with a flow rate of 0.1 ml/min. Sequence analysis of peptides was performed using 476-A pulsed liquid phase sequencer and a 120-A online phenylthiohydantoin-derivative analyzer (Applied Biosystems). Phosphoserines and -threonines were modified with ethanethiol before sequencing and subsequently identified as *S*-ethylcysteine and β-methyl-*S*-ethylcysteine, respectively (Meyer *et al.*, 1993). For the case of phosphorylation by GSK-3β, 100 μg of htau40 were phosphorylated with [γ^{32}P]-ATP, digested with trypsin, and separated on 10 TLC plates (10 μg peptide mix per plate). The peptide spots were then scratched out of the plates and recovered as described by Boyle *et al.* (1991) and further purified on a Vydac reverse phase column. The radioactive fractions were then analyzed by MALDI and sequencing.

Phosphoamino Acid Analysis

Aliquots of digestion samples were partially hydrolyzed in 6 N HCl (110°C, 60 min) and analyzed by 2D electrophoresis at pH 1.9 and pH 3.5 according to Boyle *et al.* (1991).

Tau-Microtubule Binding Assay

Binding curves between tau and microtubules were obtained as described (Gustke *et al.*, 1994). Microtubules were stabilized by taxol, which allows one to measure binding independently of microtubule dynamics. Microtubule-bound and free tau fractions were separated by centrifugation, run on SDS gels, and stained with Coomassie brilliant blue R250. The gels were scanned on an HP ScanJet 4c and evaluated with the Tina 2.0 software (Raytest, Straubenhardt, Germany). The data can be fitted by nonlinear regression using the standard binding equation for a macromolecule containing equivalent and noninteracting ligand-binding sites: $[Tau_{bound}] = n[Mt_o][Tau_{free}]/\{K_d + [Tau_{free}]\}$.

Video Microscopy of Microtubule Assembly

This was done as described previously (Trinczek *et al.*, 1995): 25 μM PC-tubulin and 10 μM tau isoforms or constructs were mixed. A portion of the samples (0.5 μl) was put on a slide, covered with 18 × 18 mm coverslips, sealed, and warmed up to 37°C with a controlled air flow within 5 s. Observation began ~15 s after temperature shift to 37°C; the number of microtubules per volume of the monitor field was recorded by focussing through the whole depth of the field and counted later from the video frames. Each assay was done for 10 fields and repeated three times. The monitor field contained an area of 73 × 54 μm² (~4000 μm²), the depth of the solution was ~3–4 μm, and focal depth was ~1–2 μm.

RESULTS

Expression and Phosphorylation of tau in Nonsynchronized LAN-5 and CHO Cells

The major function of the neuronal MAP tau is to bind to and hence stabilize axonal microtubules. This is important for maintaining axonal transport and defining the polarity of a neuron. Tau protein can roughly be subdivided into two domains, the N-terminal projection domain, followed by the C-terminal microtubule-binding domain (Figure 1). Phosphorylation is thought to be the key factor regulating tau–microtubule interaction. Earlier studies on tau phosphorylation have shown that tau protein can be phosphorylated by several kinases in vitro and that most phosphorylation sites lie in the microtubule-binding domain. Several of these sites are recognized by phosphorylation-dependent antibodies that have been used to characterize Alzheimer tau and to monitor phosphorylation in living cells (reviews by Johnson and Jenkins, 1996; Friedhoff and Mandelkow, 1998). However, the immunocytochemical detection of phosphorylation sites is limited to the antibodies available. We therefore used 2D phosphopeptide mapping of metabolically radiolabeled cells to visualize all phosphopeptides present. In addition, the amount of radio-

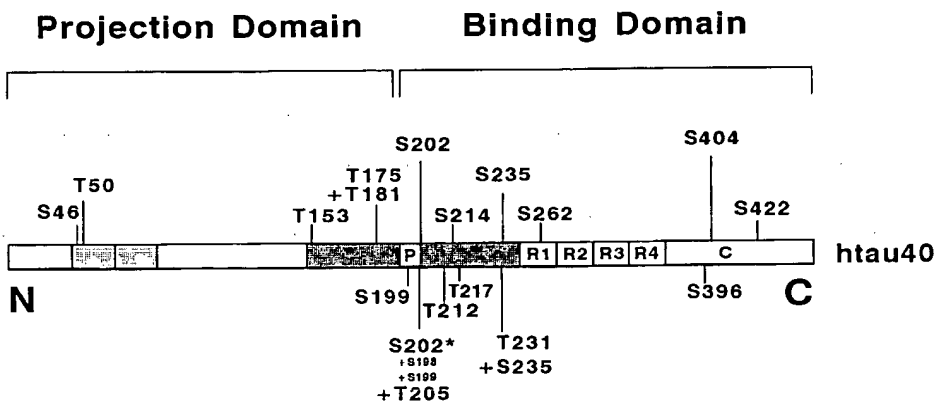

Figure 1. Bar diagram of the longest human tau isoform (htau40) in human CNS, used for transfection of CHO cells in this study. The identified phosphorylation sites are shown. Tau protein can be subdivided into an N-terminal projection domain and a C-terminal binding domain. Only the latter interacts with microtubules. It contains three or four repeats (R1-R4) that are flanked N-terminally by a proline-rich region (P) that extends into the projection domain and harbors most of the Ser/Thr-Pro motifs. The six tau isoforms in human CNS are generated by alternative splicing (0, 1, or 2 inserts near the N terminus shown as shaded boxes, and repeat R2 present or absent). The endogenous tau in LAN-5 cells consists of only two isoforms, htau23 and htau24 (no inserts, repeat R2 absent or present). The identified phosphorylation sites are located mainly in the proline-rich region upstream of the repeats. Except for S214, all of these sites are of the proline-directed type. The only KXGS motif found to be phosphorylated in vivo is S262 located in the first repeat.

label incorporated can be used for relative quantification.

LAN-5 cells (a human neuroblastoma cell line; Seeger *et al.*, 1982) express the two smallest tau isoforms, htau23 and htau24, endogenously (Figure 2, lanes 4,5). This is sufficient for analysis if a large number of cells are averaged without regard to stages of the cell cycle. However, to monitor tau phosphorylation in different stages of the cell cycle, we had to turn to CHO cells stably transfected with tau (htau40 isoform, Figure 2, lane 2) which express 5–10 times the amount of tau compared with LAN-5 cells (200–300 ng tau/10^7 cells in CHO cells, compared with 20–50 ng/10^7 LAN-5 cells). The justification for using transfected CHO cells overexpressing tau protein as a model for cells of neuronal origin comes from the similarity of their tau phosphorylation patterns (as shown below). Judging from Western blots, the phosphorylation of tau in both cell lines generates several subspecies of each isoform that migrate at higher apparent Mr values (Figure 2, lanes 2 and 4), but dephosphorylation with alkaline phosphatase increases the electrophoretic mobility to that of the corresponding recombinant proteins expressed in *E. coli* (shown for LAN-5 in Figure 2, lane 5). The Mr shift is a rough indicator of phosphorylation but cannot be used to quantify the extent since the various phosphorylation sites differ greatly in their effect on the electrophoretic mobility of tau in the gel (Lichtenberg-Kraag *et al.*, 1992).

When LAN-5 cells were metabolically labeled with [^{32}P]-orthophosphate (0.7 mCi/ml) for 4 h, their 2D maps of tau phosphopeptides revealed a complex pattern of 23 individual spots (Figure 3a). For CHO cells this procedure yielded a surprisingly similar map in spite of the different origins of these cell types and the different isoforms expressed (Figure 3b). Some minor spots occurring in CHO, but not in LAN-5, cells are due to the phosphorylation of S46 and T50 in the additional inserts present in htau40. The two maps are similar not only in terms of signals detected, but also in their relative intensities (Table 1). This is strong evidence that the balance of kinases and phosphatases is similar in the two cell lines. The major spots correspond to peptides S396/S404, T175/T181, S202, S202/T205* (peptide S195-R209 with two phosphate groups, one at S202, the other at either T205 or S199 or S198), S235, and S404. As additional phosphopeptides we found T153, T181, S199, T212, S214, T217, T231/S235, S262, and S422 (for identification see below and Figure 6). All identified signals together comprise 88% of the incorporated phosphate in CHO cells, and 78% in LAN-5 cells (Table 1 and Illenberger, unpublished results). The most intense signal in both peptide maps (Ser396/Ser404, Figure 3, a and b) contained 31% and 24%, respectively, leaving only a residual 12% (CHO) and 22% (LAN-5) phosphate incorporated into a few minor unidentified phosphopeptides. Note, however, that the total extent of phosphorylation cannot be obtained from the maps because nonphosphorylated peptides cannot be detected with this method. It is probably much smaller than suggested by the number of sites; from immunocytochemical analyses with phosphorylation-dependent antibodies we estimate that the average tau molecule contains about two to three phosphates in

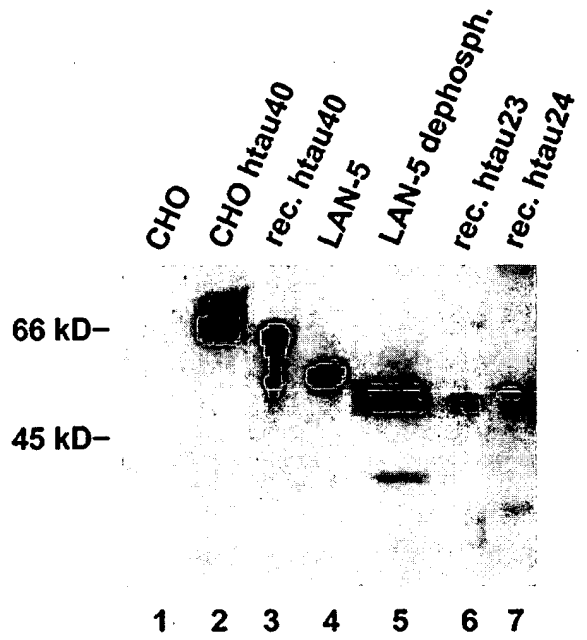

Figure 2. Western blot analysis of tau protein in stably transfected CHO cells and LAN-5 neuroblastoma cells. Lane 1, nontransfected CHO cells, showing that there is no endogenous tau; lane 2, CHO cells stably transfected with htau40. There are bands of higher Mr representing different phosphorylation states of the protein. Lane 3, recombinant htau40 (longest human tau isoform, 441 residues), showing a single band at Mr 65 kDa; lane 4, tau isolated from LAN-5 neuroblastoma cells. Lane 5, tau from LAN-5 cells after dephosphorylation with alkaline phosphatase, showing two bands that comigrate with htau23 (lower) and htau24 (upper) indicating that LAN-5 cells contain these two isoforms (3 or 4 repeats, no N-terminal inserts) and their phosphorylated derivatives. Lane 6, recombinant fetal tau (htau23, 352 residues); lane 7, recombinant htau24 (383 residues).

LAN-5 cells and probably even less in CHO cells (apart from mitosis, see below).

Tau Phosphorylation in Interphase and in Mitotically Arrested CHO Cells

In a previous immunocytochemical study we had shown that in stably transfected CHO cells tau protein becomes highly phosphorylated during mitosis (sevenfold increase), which appeared to correlate with the detachment of tau from the microtubules and the rearrangement of the microtubule network (Preuss *et al.*, 1995). To further analyze the tau–microtubule interaction, we observed living CHO cells expressing a GFP-tau fusion protein. The microtubule network is stained in interphase cells due to GFP-tau binding to cellular microtubules (Figure 4a, left panel) in agreement with Ludin *et al.* (1996). In mitotic cells (Figure 4a, right panel) the green fluorescence is mainly distributed throughout the whole cytosol with some more intense staining of the mitotic spindle, suggesting that a significant amount of tau protein becomes detached from microtubules. To be able to visualize tau and microtubules at the same time, we performed indirect immunofluorescence in stably transfected CHO cells expressing the longest human tau isoform, htau40 (Preuss *et al.*, 1995). Cells were fixed in methanol, either without prior extraction of cytosolic proteins or after treatment for 10 s with 1% Triton-X 100 (Figure 4b). In untreated interphase cells, tau protein colocalizes with microtubules. In mitotic cells, however, there is pronounced tau staining in the cytosol in addition to staining of the mitotic spindle (Figure 4b, upper right panel), similar to mitotic living cells expressing GFP-tau (compare Figure 4a, right panel). If cytosolic proteins were removed by brief extraction with Triton-X 100 (Figure 4b, lower two panels; according to the procedure of Melan and Sluder, 1992), the distribution of tau in interphase cells was not altered, whereas in mitotic cells the cytosolic tau staining had disappeared. Only tau bound to spindle microtubules remained in these cells (Figure 4b, lower right panel). This result further indicated that a significant fraction of tau protein did not bind to microtubules during mitosis. The fixation procedure was crucial for the demonstration of this effect. Prolonged extraction washed out all tau protein from the cell. Paraformaldehyde, for some reason, detaches tau from microtubules (also described by Schliwa *et al.*, 1981) abolishing the colocalization of tau and microtubules.

To get a more quantitative estimate of the changes in the binding of tau during mitosis, we performed a Western blot analysis of cell extracts from nonsynchronized (interphase) and nocodazole-treated (M-phase) cells and compared the tau and tubulin levels before and after Triton extraction (Figure 4c). Western blots were analyzed densitometrically to asses relative tau to tubulin ratios. The amount of tubulin between untreated and extracted cell pellets did not significantly change throughout the cell cycle (lanes 1–4), indicating that the nonextractable polymer mass of tubulin essentially remains the same. In interphase cells, Triton extraction had no effect on the amount of tau remaining in the pellet, indicating that most tau protein in interphase cells is bound to microtubules (lanes 6 and 7). In contrast, the tau level remaining in the pellet of mitotic cells was drastically reduced to about 22% due to detergent extraction (lanes 8 and 9). This result confirmed that tau becomes indeed detached from microtubules during mitosis. It is widely accepted that tau phosphorylation is a key factor regulating tau–microtubule interactions. Hence, we wanted to determine the phosphorylation sites responsible for the changes in tau–microtubule interaction during mitosis. We therefore performed a mitotic arrest in tau-transfected CHO cells since they allow separation of metaphase and remaining interphase

cells by mechanical shake-off, in contrast to LAN-5 cells where this procedure is not applicable.

In nonsynchronized CHO cell cultures, approximately 10–15% of the cells are mitotic. Synchronization with nocodazole arrests cells mainly in metaphase (DeBrabander *et al.*, 1986; Jordan *et al.*, 1992). Stably transfected CHO cells were treated with 0.4 μg/ml nocodazole while labeled with [^{32}P]-orthophosphate. Mitotic cells were separated from the remaining interphase cells by mechanical shake-off. Interphase and metaphase cells were analyzed separately with 2D thin-layer electrophoresis (TLE)/TLC (Figure 5). The sevenfold increase in phosphorylation in metaphase can be attributed to the occurrence of five additional phosphopeptides as well as a relative increase in the phosphorylation of T181, T212/T217, and S235 (compare Figure 5, a and b). Table 1 summarizes the relative intensities of the identified spots. Three of the additional five peptides could be identified as S202/T205*, S214, and T153 in similar comparative analyses as for nonsynchronized cells (Illenberger, unpublished results). The incorporation of an additional phosphate group into the peptide S202 (^{195}SGYSSPGSPGTPGSR^{209}), which is faintly seen in the interphase sample (Figure 5a), shifts this peptide to the more acidic position of S202/T205* (further left in the map). The asterisk indicates that this doubly phosphorylated peptide contains a phosphate at S202 plus another one at either T205, S199, or S198. Since the phosphorylation-dependent antibody AT-8 recognizes phosphorylated S202 and T205, this result confirms our earlier findings that AT-8 reactivity is only observed in mitotic cells (Preuss *et al.*, 1995; hence our nomenclature of this peak as S202/T205*). The strong signal labeled S396/S404 in nonsynchronized cells (Figure 3), corresponding to the doubly phosphorylated peptide T386-R406, has disappeared from interphase and metaphase cells. Instead, two new spots have appeared closer to the anode (Figure 5b, short arrows), probably corresponding to this peptide in triply phosphorylated forms. These peptides would be recognized by the antibody PHF-1 (Otvos *et al.*, 1994), which is known to immunostain mitotic cells (Pope *et al.*, 1994; Preuss *et al.*, 1995). The diffuse spot at the bottom of the interphase pattern labeled with an asterisk (*) has disappeared in metaphase (Figure 5, a and b). This spot contains peptides doubly phosphorylated at S46 and T50 (Figure 3b and Table 1). The pattern observed for tau protein from metaphase cells partly resembles the phosphorylation pattern of recombinant tau phosphorylated by the cyclin-dependent kinases cdc2 and cdk5 (see below, Figure 6, a and b). Since cdc2 activity is high in mitotic cells, it seems likely that this proline-directed kinase is involved in the in vivo phosphorylation of tau protein. It is notable that the fraction of phosphothreonine in mitotic cells, 33% of all sites, is much higher than in nonsynchronized cells (12%, unpublished results), indicating that the mitotic kinases preferentially phosphorylate TP motifs.

When comparing the signals in interphase and metaphase CHO cells (Figure 5, a and b) with the pattern from nonsynchronized CHO cells (Figure 3b), it becomes obvious that there are significant differences in signal intensities for certain spots (especially for S214 and T153, the latter being hardly visible in nonsynchronized cells; Figure 3b). In addition, not all signals found in the bulk analysis are represented by

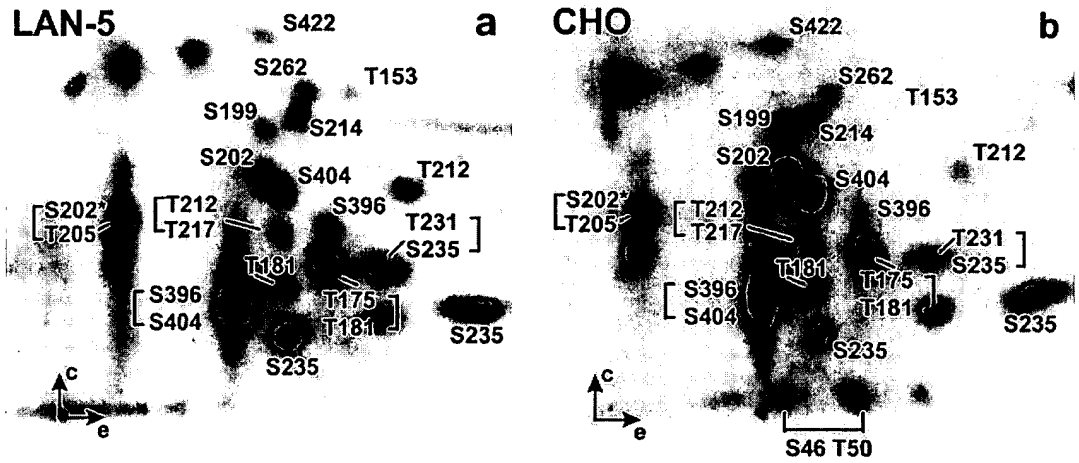

Figure 3. Analysis of tau phosphorylation in LAN-5 and CHO cell lines by 2D thin layer electrophoresis/chromatography. A portion of the tryptic digest (1000 cpm) was loaded per sample, and autoradiographs were exposed for 6 wk. (a) Tryptic phosphopeptide map of tau protein immunoprecipitated from transfected LAN-5 neuroblastoma cells. (b) Tryptic phosphopeptide map of endogenous tau protein immunoprecipitated from CHO cells.

Table 1. Identification of phosphorylated residues in vivo and in vitro

Spot		Sequence		LAN-5 relative intensity	CHO relative intensity	Interphase relative intensity	Metaphase relative intensity	cdc2	CDK5	MAPK	GSK3β	MARK
S46/T50[a]	25	KDQGGYT...	67	−	+	++	−			*	*	
S46/T50[b]	24	DQGGYT...	67	−	+	++	−			*	*	
T153	151	IATPR	155	+	(+)	−	+++	*	*	*		
T175	171	IPAKTPPAPK	180	−	−	−	−			*		
T181	175	TPPAPKTPPSSGEPPK	190	+	+	+	++			*		
T175/T181	171	IPAKTPPAPKTPPSSGEPPK	190	++	++	n.d.	n.d.			*		
S199[c]	195	SGYSSPGSPGTPGSR	209	+	++					*		
S202[d]	195	SGYSSPGSPGTPGSR	209	++	+++	+	−	*	*			
S202/T205*[e]	195	SGYSSPGSPGTPGSR	209	++	++	−	++	*	*	*		
T212	210	SRTPSLPTPPTR	221	+	+	n.d	n.d.	*	*	*		
T212/T217	210	SRTPSLPTPPTR	221	+	+	+	+++			*		
S214	212	TPSLPTPPTR	221	+	+	−	+++		*			
T231/S235	226	VAVVRTPPKSPSSAK	240	++	+	n.d.	n.d.	*				
S235[f]	231	TPPKSPSSAK	240	++	++	++	++	*	*	*		
S262	260	IGSTENLK	267	+	+	−	−					*
S293	291	CGSK	294	−	−	−	−					*
S324	322	CGSLGNIHHK	331	−	−	−	−					*
S356	354	IGSLDNITHVPGGGNK	369	−	−	−	−					*
S396	386	TDHGAEIVYKSPVVSGDTSPR	406	+	+	n.d.	n.d.			*		
S404	396	SPVVSGDTSPR	406	++	+++	++	+	*	*	*	*	
S396/S404[g]	386	TDHGAE...	−	++++	++++	−	−				*	
S422	407	HLSNVSSTGSIDMVDSPQ...	−	+	+	−	+			*		

*, Kinase phosphorylating this site; n.d., not determined; −, phosphorylation of this site not detected; + to ++++, phosphorylation detected with increasing intensity.

[a,b] Doubly phosphorylated peptides as determined by MALDI, equal amounts of P-Ser and P-Thr in phosphoamino acid analysis.

[c] S199 was determined for MAPK, but for the in vivo analysis it can only be concluded to be peptide 195-209 bearing a single phosphate.

[d] S202 was identified for cdc2 and cdk5; in the vivo analysis it corresponds to peptide 195-209 bearing a single phosphate.

[e] S202 with an additional phosphorylation at either S198, S199 or T205. Due to AT8 reactivity we conclude that this peptide is phosphorylated at S202 and T205.

[f] May occur at two different coordinates in the 2D maps.

[g] Doubly phosphorylated peptide as determined by MALDI, only P-Ser by phosphoamino acid analysis, containing a small fraction phosphorylated at S400.

simply adding interphase and metaphase signals. This is, for instance, the case for S262 (not visible in Figure 5), and for the pronounced spot S396/S404, which is only seen in nonsynchronized cells (not seen in Figure 5 but seen in Figure 3). This peptide could have partially acquired a further phosphate and therefore shifted to the left in Figure 5b (short arrows), or could, in part, be dephosphorylated (thus becoming invisible). These results suggest that the phosphorylation of tau protein is not only generally higher during mitosis, but furthermore, that tau is differentially phosphorylated during individual phases of mitosis, so that analyzing interphase and metaphase cells is not sufficient to generate all phosphopeptides that occur throughout the whole cell cycle. This would be consistent with the variations of microtubule dynamics during the phases of mitosis (e.g., Olmsted *et al.*, 1989; Belmont *et al.*, 1990), which could involve different states of tau phosphorylation.

Phosphorylation of tau In Vitro with Kinases cdc2, cdk5, MAPK, GSK-3β, and MARK, and Identification of Phosphorylation Sites

In principle, the phosphorylation sites in each spot of the in vivo maps could be identified by phosphopeptide sequencing using established procedures (Meyer *et al.*, 1993). This would require at least 10 pmol of material (0.46 μg htau40, assuming phosphorylation is 100%), more than 1000 times the amount present in a spot of medium intensity. To circumvent this problem, we expressed tau in *E. coli*, phosphorylated it in vitro with several kinases in the presence of [γ-^{32}P]-ATP, and after tryptic digestion we separated the radiolabeled peptides by TLE/TLC and by HPLC chromatography, respectively. The HPLC experiments yielded sufficient material to identify the individual peptides by mass spectroscopy and sequencing. The spots in the 2D map were determined by running an aliquot of the total digest together with the identified

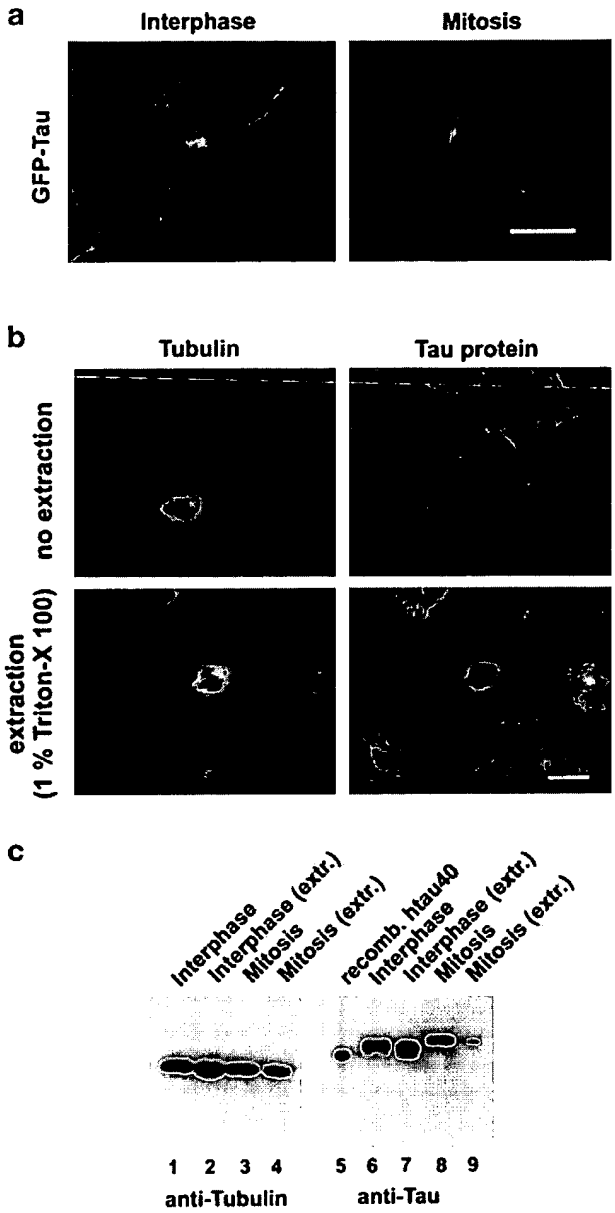

Figure 4. Tau–microtubule interaction in transfected CHO cells in interphase and during mitosis. (a) Observation of a living CHO cell expressing GFP-tau in interphase (left) and metaphase (right) CHO cell expressing GFP-tau. Bar, 20 μm. The increased cytosolic GFP-tau fluorescence in mitotic cells indicates that a large fraction of tau is not bound to microtubules during mitosis in contrast to interphase, where nearly all tau is associated with microtubules (exposure time of the metaphase cell was one-fifth of that for interphase cells, since when equal exposure times were used, mitotic cells would be overexposed and the mitotic spindle would not be discernible). (b) Indirect immunofluorescence analysis of CHO cells overexpressing the longest human tau isoform (htau40) without (upper panels) and after extraction (lower panels) with Triton X-100. No cytosolic stain, but only tau bound to the mitotic spindle, is observed after extraction (lower right). Tubulin staining with DM1A (left panels) and tau staining with polyclonal anti-tau antibody (right panels). Bar, 15 μm. (c) Western blot analysis of total cell extracts, lanes 1–4 DM1A against tubulin, lanes 5–9 T46 against tau protein. Tau levels in interphase cells are unaffected by extraction (lanes 6 and 7) whereas the tau signal is decreased to 22% in mitotic cells (lanes 8 and 9).

peptides (because of their higher concentration, the marker peptides could be identified in the mixture). Figure 6 shows experiments in which 400 μg of recombinant tau protein were phosphorylated with the kinases cdc2, cdk5, MAPK, GSK-3β (100 μg tau), and MARK. We chose cdc2 and cdk5 (Figure 6, a and b) because they have been shown to phosphorylate tau in vitro (Arioka *et al.*, 1993; Baumann *et al.*, 1993; Paudel *et al.*, 1993), and because tau's phosphorylation is upregulated in mitotic CHO cells (Preuss *et al.*, 1995). Since most of the phosphorylation sites detected by diagnostic phosphorylation-dependent PHF antibodies are of the SP or TP type, we also included mitogen-activated protein kinase (MAPK), which phosphorylates most of the SP or TP motifs in tau and is associated with microtubules (Drewes *et al.*, 1992; Morishima-Kawashima and Kosik, 1996; Figure 6c), as well as GSK-3β (Figure 6d), which is known to be active in nonsynchronized cells (Woodgett, 1991; Mandelkow *et al.*, 1992; Lovestone *et al.*, 1994; Song and Yang, 1995). Finally, we chose MARK (Figure 6e) because it phosphorylates the KXGS motifs in the repeats, particularly S262, a residue that has a strong influence on tau's binding to microtubules (Biernat *et al.*, 1993; Drewes *et al.*, 1995; 1997) and shows elevated phosphorylation in AD (Morishima-Kawashima *et al.*, 1995).

The kinases cdc2 and cdk5 show a rather similar phosphorylation pattern. Sites of major phosphate incorporation after phosphorylation with cdc2 (Figure 6a) comprise S202, S235, and S404 as well as the doubly phosphorylated peptides T231/S235 and S202/T205*. Minor signals were detected corresponding to peptides with phosphorylated T153 or T212. No phosphorylation at T231 could be observed for cdk5, since the peptide T231/S235 was missing (Figure 6b). Furthermore, T181, T175/T181, and S396 could be identified as additional phosphorylation sites. The non-proline-directed phosphorylation site S214 apparently generated by cdk5 is probably caused by a minor contamination with a different kinase since cdk5 was prepared from brain tissue. Phosphorylation with recombinant MAPK (activated by recombinant MEK) yielded 22 phosphopeptides. The following phosphorylation sites were identified: T153, T175, T181, T175/T181, S199, S202, S202/T205*, T212, T212/T217, S235, S396, S404, and S422. The prominent spots generated by GSK-3β (brief phosphorylation) include S404 and S396/S404 (containing a small fraction phosphorylated at S400), and in addition the doubly phosphor-

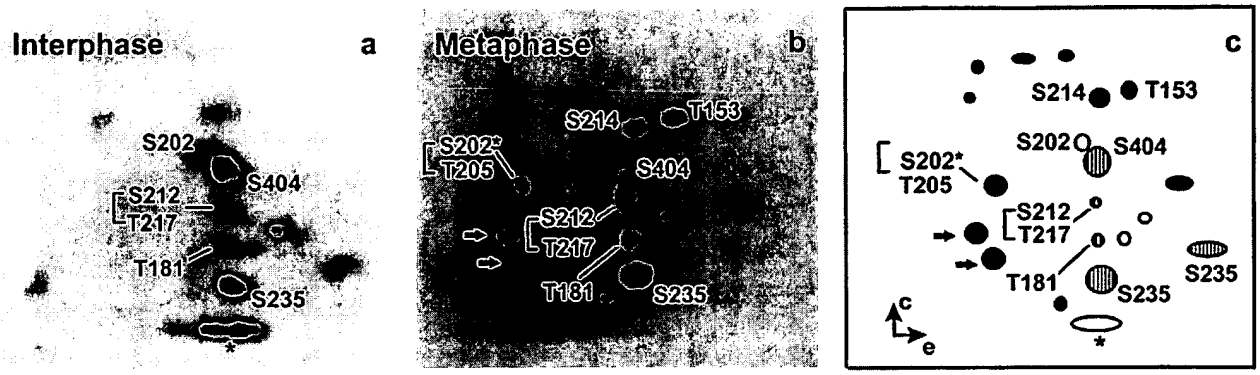

Figure 5. 2D maps of htau40 transfected CHO cells in interphase and metaphase. Cells were treated with 0.4 μg/ml nocodazole for 5 h. A portion (1000 cpm) of the tryptic digest was loaded per sample, and autoradiographs were exposed for 6 wk. (a) Interphase pattern revealing phosphorylation at T181, S202, S235, and S404. (b) Tau isolated from metaphase cells shows additional phosphorylation mainly at T153, S202/T205* (corresponding to the peptide 195–202 in htau40 bearing two phosphates), T212/217, S214, and two peptides (short arrows) corresponding to S386-R406 containing phosphorylated S396, S404, and another site. (c) Schematic diagram of phosphopeptides. Open circles represent signals present in interphase only, filled circles are phosphopeptides that only occur in metaphase, and gray circles are constitutively phosphorylated sites. The asterisks in Figure 5a represent the peptides containing phosphorylated S46 and T50 (see Figure 4b).

ylated peptides from the inserts (S46/T50), and S202/T205*. The spot S396/S404 is also the most prominent spot in nonsynchronized CHO and LAN-5 cells (Figure 3, a and b), consistent with the known activity of GSK-3β in interphase (Lovestone *et al.*, 1994). The MAP/microtubule affinity-regulating kinase (MARK) mainly phosphorylates the KXGS motifs, S262, S293, S324, and S356, as published in Drewes *et al.*, 1995. The identified phosphopeptides and corresponding kinases as well as relative intensities for signals identified in CHO and LAN-5 cells (compare Figures 3 and 5) are compiled in Table 1. These peptides served as a basis to interpret the phosphopeptide pattern of tau in cells and to identifiy 17 phosphorylation sites. Phosphopeptides in the in vivo samples were determined by running the samples shown in Figure 3 together with samples derived from in vitro phosphorylation with MAPK, MARK, and cdc2 (immunoprecipitated from mitotically arrested HeLa-S3 cells).

As an example for the analysis to identify in vivo phosphorylation sites, Figure 7 shows the comparison of the LAN-5 phosphorylation pattern with that of recombinant tau protein phosphorylated with a crude immunoprecipitate of cdc2 from mitotically arrested HeLa cells in vitro. Preliminary experiments (our unpublished data) had shown that if one immunoprecipitates cdc2 directly from supernatants of mitotically arrested HeLa cells, omitting the SP-Sepharose purification step, a S214- phosphorylating activity was also present in the immunoprecipitate. Therefore, we were able to use this "contaminated" fraction to investigate both the cdc2 pattern and the position of S214, irrespective of the kinase phosphorylating this residue. This explains why the pattern observed in Figure 7c differs from that in Figure 6a. However, this does not affect the identification of phosphopeptides since the identity of the peptides labeled in Figure 7c had been confirmed by additional in vitro analysis (our unpublished results). By comparing the in vivo pattern (Figure 7a) with the cdc2 pattern (Figure 7c) in the control run (Figure 7b, with aliquots of a and c run on the same plate), the following signals were identified: T153, T181, T175/T181, T212/T217, S214, T231/S235, S235, and S404. Similar analyses were conducted for both cell lines with MAP kinase, and MARK (our unpublished results). The prominent spot S396/S404 in both cell lines (Figure 3, a and b) was interpreted on the basis of the GSK-3β pattern (Figure 6d). Among the identified phosphopeptides, only four (T181, S202/T205*, T231/S235, and S396/S404) would be detected immunocytochemically with the monoclonal antibodies AT270, AT8, AT180, and PHF-1, respectively (Biernat *et al.*, 1992; Goedert *et al.*, 1995). Thus, the phosphopeptide maps confirm the increase of these antibody reactions during mitosis, and in addition they reveal the greater complexity of the phosphorylation of tau.

The Mitotic Phosphorylation Site Ser214 Strongly Affects the tau–Microtubule Interaction

In mitosis, microtubules are known to become highly dynamic (Belmont *et al.*, 1990). At the same time, tau becomes hyperphosphorylated in transfected CHO cells (Preuss *et al.*, 1995) concomitant with detachment of tau from microtubules (Figure 4). This led us to investigate whether the observed detachment of tau is due to its phosphorylation state. Among the phosphorylation sites elevated in nocodazole-treated cells, only S214 is not of the SP or TP type. In a previous

study (Trinczek *et al.*, 1995) we had concluded that phosphorylation at SP or TP sites has only a moderate effect on the dynamic instability of microtubules in vitro, compared with others, such as S262 (in the KXGS motif of the first repeat; Biernat *et al.*, 1993). We therefore wanted to determine directly the effect of the phosphorylation of S214 on the binding of tau to microtubules. S214 can selectively be phosphorylated by PKA in vitro, if appropriate conditions are chosen. By 15 min incubation time with PKA, almost 1 mol phosphate per mol tau is incorporated, and isolation and sequencing of the radioactive phosphopeptide show that phosphate incorporation occurs almost exclusively at S214 (Figure 8). Extended incubation times led to the incorporation of three to four phosphates by PKA, and these were distributed over more than 10 sites, including the KXGS motifs located in each of the repeats (S262, S324, S356).

The binding curves of Figure 9 show that the phosphorylation at S214 alone can account for the strong reduction in tau's affinity for microtubules (the dissociation constant K_d for phosphorylated tau protein is increased by approximately 10). Next, we asked whether this decrease in tau–microtubule interactions had any impact on microtubule stability. Figure 10 shows microtubule assembly monitored by video microscopy. The upper images show normal microtubule assembly in the absence of ATP (so that the added PKA remained inactive). However, when phosphorylation proceeds in the presence of ATP (Figure 10, bottom left), microtubule assembly is essentially suppressed. The effect is clearly due to the phosphorylation of S214 since the mutant Ser214Ala supports normal microtubule assembly, irrespective of phosphorylation by PKA (Figure 10, right). These data argue that the mitotic phosphorylation of S214 in tau could play a role in the detachment of tau from microtubules during mitosis and the concomitant increase in microtubule dynamics.

DISCUSSION

The interaction of tau and other MAPs with microtubules is regulated by phosphorylation, and this in turn affects the structure and dynamics of the microtubule cytoskeleton. In particular, tau becomes highly phosphorylated in the neurofibrillary pathology of Alzheimer's disease and hence loses its binding capability to

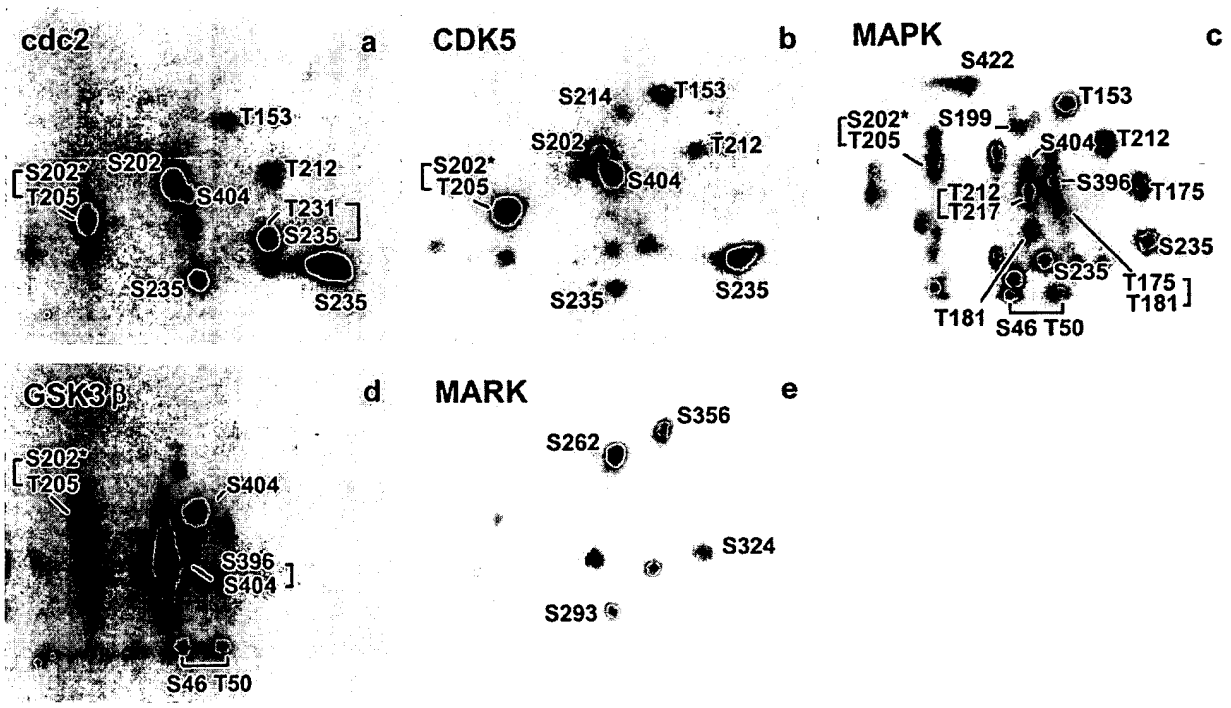

Figure 6. Tryptic 2D phosphopeptide maps of htau40 generated by different kinases in vitro. The peptides were obtained by tryptic digestion and separated by 2D TLE/TLC after phosphorylation. Aliquots of the tryptic digests (10.000 cpm per sample) were loaded and autoradiographs were exposed overnight. (a) htau40 phosphorylated with cdc2 immunoprecipitated from mitotically arrested HeLa-S3 cells for 16 h. (b) htau40 phosphorylated with cdk5, prepared from porcine brain (Baumann *et al.*, 1993) for 16 h. (c) htau40 phosphorylated with recombinant MAPK (activated by MEK, Döring *et al.*, 1993) for 16 h. (d) htau40 phosphorylated with recombinant GSK-3β for 1 h. (e) htau40 phosphorylated with MARK prepared from porcine brain (Drewes *et al.*, 1995) for 2 h. Phosphorylation sites were identified by 2D analysis of HPLC-purified and sequenced peptides derived from the same phosphorylation assay for each kinase.

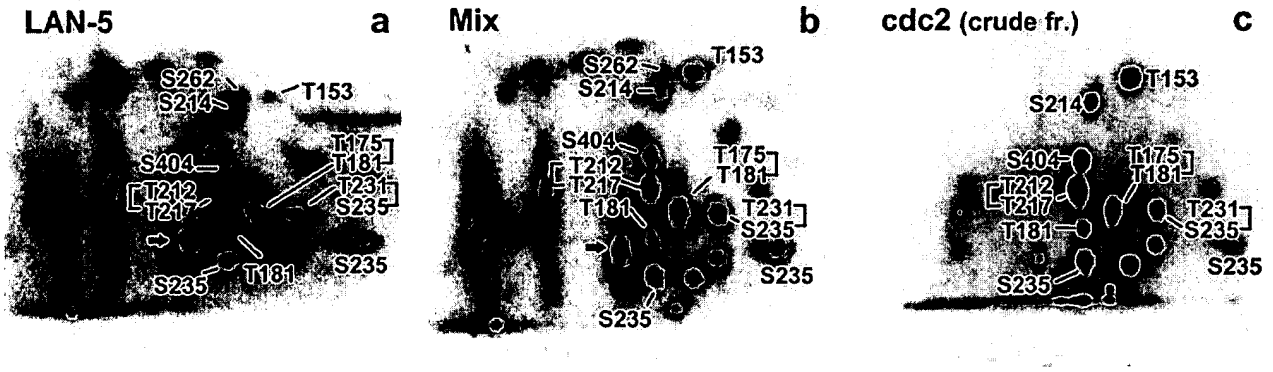

Figure 7. Identification of phosphopeptides generated in vivo, represented by the analysis of LAN-5 cells with tau phosphorylated with a crude fraction (see text for explanation) of cdc2. (a) 2D phosphopeptide map of tau from LAN-5 cells (same as in Figure 3a). (b) Control analysis with aliquots of the in vivo probe and of the cdc2 phosphorylated recombinant tau protein spotted onto the same plate. (c) In vitro sample of recombinant tau protein phosphorylated with cdc2 used in the control run in b. Phosphorylated residues are labeled; for identification of peptides see Table 1.

microtubules (Yoshida and Ihara, 1993). It has recently been discussed that the events leading to the abnormal phosphorylation of the MAP tau in AD involves mitotic mechanisms (Preuss *et al.*, 1995; Vincent *et al.*, 1996). Due to some insult yet to be identified, affected neurons may try to reenter the cell cycle. Since postmitotic neurons are unable to undergo cell division, this frustrated attempt finally leads to cell death and could explain the massive loss of neurons in AD. To investigate this hypothesis, we first had to check whether tau protein becomes detached from microtubules during mitosis in analogy with PHF-tau. Using three different methods, we could show that during mitosis a large fraction of tau becomes cytosolic (Figure 4) and that this is not due to a dramatic decrease in tubulin polymer (Figure 4c). This is in good agreement with studies showing that the level of tubulin polymer essentially remains constant throughout the cell cycle (Zhai and Borisy, 1994). In our previous investigation (Preuss *et al.*, 1995) we had already shown that the extent of tau phosphorylation is increased during mitosis and that tau presumably detaches from microtubules. However, to understand the role of phosphorylation, it is necessary to determine the specific phosphorylation sites of tau protein in living cells. In this study we therefore attempted to identify endogenous phosphorylation sites of the microtubule-associated protein tau in interphase and mitosis, as well as protein kinases that could be responsible for the phosphorylation. Many earlier studies aimed at phosphorylation sites in cells or tissues have relied on phosphorylation-dependent antibodies (reviews by Kosik and Greenberg, 1994; Trojanowski and Lee, 1995; Friedhoff and Mandelkow, 1998). However, these antibodies detect only a fraction of the potential phosphorylation sites, and in addition they are difficult to quantify, especially at low cellular concentrations. These limitations can be overcome by metabolic labeling of cells with ^{32}P and detection of phosphorylation sites by 2D phosphopeptide mapping.

Since many kinases are capable of phosphorylating tau in vitro (e.g., cdc2, cdk5, MAP kinase, GSK-3, PKA,

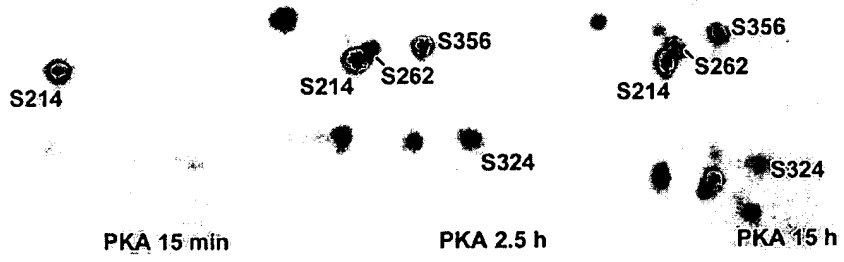

Figure 8. Phosphopeptide map of tau (htau23, 0.5 mg/ml) phosphorylated with PKA (1.5 U/μl) for (a) 15 min, (b) 2.5 h, (c) 15 h. Note that at 15 min nearly all phosphate is incorporated into Ser214. This condition was used for binding studies and the microtubule assembly assay (Figures 9 and 10).

MARK, for review see Mandelkow *et al.*, 1995; Johnson and Jenkins, 1996), these experiments provide little information about the kinases phosphorylating tau in vivo. In our approach, however, they were valuable tools to generate reference phosphopeptides to identify phosphorylation sites in proliferating cells. In our experiments we included two members of the cell cycle-related kinase family, cdc2 and cdk5. Since cdc2 activity is up-regulated during mitosis, it seemed to be the most promising candidate for mitotic phosphorylation of tau protein in living cells as observed in our earlier study (Preuss *et al.*, 1995). In postmitotic neurons, cdk5 is the most abundant kinase of the cdc2 family (Beaudette *et al.*, 1993). Since the patterns of both kinases resemble one another, it is likely that cdks in general have a similar effect on tau in cells. Other potent kinases for tau are MAP kinase and GSK-3β, both of which are capable of phosphorylating many of the SP/TP sites and are associated with the microtubule network (Drewes *et al.*, 1992; Hanger *et al.*, 1992; Mandelkow *et al.*, 1992; Morishima-Kawashima and Kosik, 1996; Roder *et al.*, 1997). MARK is a novel kinase that has recently been described to phosphorylate tau protein in vitro and in vivo at S262 (Drewes *et al.*, 1995, 1997), which has a pronounced effect on microtubule binding increasing microtubule dynamics (Biernat *et al.*, 1993) and was therefore chosen as a non-proline-directed kinase.

LAN-5 neuroblastoma cells expressing moderate levels of the two smallest isoforms htau23 and htau24 (3 or 4 repeats, no inserts, Figure 2), and a CHO cell line transfected with htau40, the largest human isoform in the CNS, were investigated (Figures 1 and 2). Comparison of the overall phosphorylation pattern of tau in both cell lines revealed a surprising similarity in terms of tau phosphorylation irrespective of the different isoforms expressed (Figure 3) indicating similar kinase and phosphatase activities in both cell lines. This enabled us to use transfected CHO cells expressing tenfold more tau protein as a cell model to monitor tau phosphorylation in interphase and metaphase after nocodazole treatment (Figure 5). Moreover, with the phosphopeptides generated in vitro and sequenced we were able to identify 17 phosphorylation sites (Figures 6–8). Most of these (except S214 and S262) are of the SP/TP type, attesting to the activity of proline-directed kinases. Among the nonproline-directed motifs, S214 can be phosphorylated in vitro by PKA and to some extent by PKC (Steiner *et al.*, 1990; Scott *et al.*, 1993; Brandt *et al.*, 1994) and S262 is phosphorylated mainly by MARK (Drewes *et al.*, 1995, 1997) and to a lesser extent by PKA (Figures 6 and 8).

The bulk analysis of the phosphorylation sites (Figure 3) represents an average over the cell cycle, with about 10–15% of the cells undergoing mitosis at any time (this applies to both LAN-5 and CHO cells). Thus even sites that appear minor in the average population could play a major role at a particular stage or compartment. This question can be addressed only if one can subfractionate and compare different stages, such as interphase versus metaphase (see below). In support of this view, one should note that the overall extent of phosphorylation is quite low (2–3 phosphate groups per tau molecule, estimated from immunocytochemical analysis with phosphorylation-dependent antibodies (cf. Ksiezak-Reding *et al.*, 1992; Köpke *et al.*, 1993). This means that a given tau molecule is unlikely

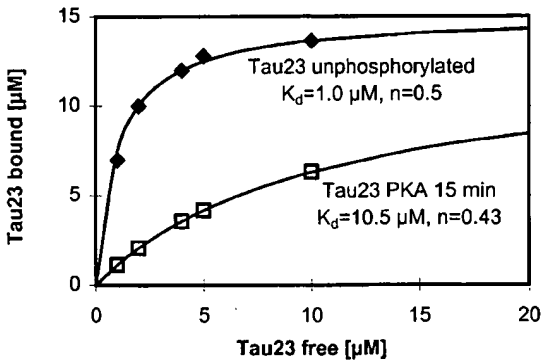

Figure 9. Binding of tau (isoform htau23) to microtubules (30 μM) before and after phosphorylation with PKA. Inserts, dissociation constant K_d and stoichiometry n. Conditions were chosen such that Ser214 is essentially the only phosphorylated residue (for details see Figure 8). Note that the phosphorylation strongly reduces the binding (K_d increases 10-fold).

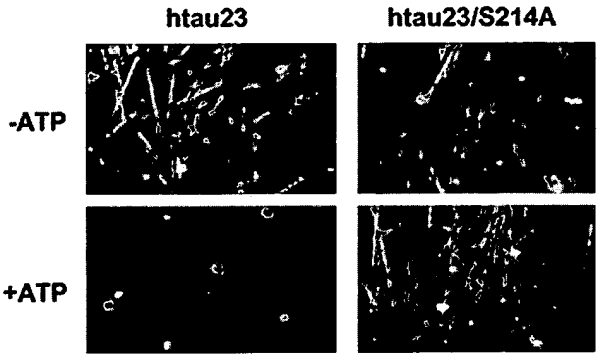

Figure 10. Dynamic instability of microtubules before and after phosphorylation of tau with PKA. The initial solution contained tubulin (25 μM), tau (10 μM), and PKA (1.5 U/μl, activity as in Figure 8). The images were taken 8 min after raising the temperature to 37°C. Left, isoform htau23; right, isoform htau23 with Ser214 mutated into Ala. Top, no ATP; bottom, prephosphorylated with 2 mM ATP. The top images show that microtubules grow well under the stabilizing influence of tau. The bottom left shows that microtubule formation is almost totally suppressed when PKA is allowed to phosphorylate tau (note that PKA has no direct effect on tubulin; our unpublished observations). The bottom right shows that the effect of PKA is mainly due to the phosphorylation of Ser214; when this residue is mutated to Ala, microtubules assemble normally.

to contain all of the phosphorylation sites detected in 2D phosphopeptide mapping. Direct evidence for this comes from the reactions with antibodies whose epitopes require a pair of phosphorylation sites, such as AT-8 (S202 and T205), AT-180 (T231 and S235), or PHF-1 (S396 and S404; Biernat *et al.*, 1992; Otvos *et al.*, 1994; Goedert *et al.*, 1995). These antibodies are nearly undetectable in interphase (except PHF-1) but enhanced in mitosis (Pope *et al.*, 1994; Preuss *et al.*, 1995), implying that, at most, one but not both of their required sites is phosphorylated during interphase.

The mitotic arrest with nocodazole was performed in the transfected CHO cells, due to their significantly higher expression of tau protein. Phosphorylation of tau increases sevenfold during mitosis in transfected CHO and N2a cells (Preuss *et al.*, 1995; Preuss and Mandelkow, 1998), particularly at T153, T181, S202/T205*, T212/T217, S235, and S214 (Figure 5). Except for S214 these sites are of the proline-directed type, particularly TP motifs. Considering the up-regulation of cdc2 during mitosis (for review see Stern and Nurse, 1996) and the fact that all the proline-directed sites are phosphorylated by this kinase in vitro, cdc2 is a strong candidate for causing the enhanced phosphorylation. However, strictly speaking, the up-regulation of other proline-directed kinases, or the down-regulation of tau phosphatases (particularly PP-2a and PP-2b, Drewes *et al.*, 1993; Trojanowski and Lee, 1995; Wang *et al.*, 1995; Merrick *et al.*, 1996), cannot be excluded.

Mitosis is accompanied with a rearrangement of microtubules, higher dynamics, and a loosening of the MAP–microtubule interactions (Belmont *et al.*, 1990; Verde *et al.*, 1992; Ookata *et al.*, 1995). If this is due to MAP phosphorylation, one would expect that some of the up-regulated sites have an influence on tau's binding to microtubules. Proline-directed phosphorylation does have an effect (Drechsel *et al.*, 1992; Trinczek *et al.*, 1995), but it is rather moderate, at least in vitro, when compared with the much larger effect of S262 phosphorylation (Illenberger *et al.*, 1996; Drewes *et al.*, 1997). It was therefore unexpected that the major increase at a non-proline-directed site in metaphase was at S214 and not at S262. Since PKA phosphorylates S214 in vitro (Scott *et al.*, 1993; Brandt *et al.*, 1994; Zheng-Fischhöfer *et al.*, 1998), we further investigated whether this could have an effect on the interaction of tau with microtubules and on the dynamic behavior of microtubules in vitro. There was indeed a strong decrease in tau's microtubule binding and nucleation activity in vitro (Figures 9 and 10). This influence was eliminated when Ser214 was mutated into Ala. Thus, PKA or an equivalent kinase could contribute to the rearrangement of the microtubule network during mitosis. These results are consistent with recent results by Brandt *et al.* (1994) and Leger *et al.* (1997) showing the influence of PKA on tau's ability to bundle microtubules and support neurite outgrowth. PKA activity can be stimulated in situ in brain slices (Fleming and Johnson, 1995), and one of its effects is to increase the rate of axonal transport in neurons, possibly by phosphorylating tau and other MAPs (Sato-Harada *et al.*, 1996). In addition to its direct effects, PKA could influence the tau–microtubule interaction indirectly by altering its susceptibility to other proline-directed kinases, e.g., MAP kinase or GSK-3 (Raghunandan and Ingram, 1995; Singh *et al.*, 1995). The close association of PKA with the microtubule cytoskeleton is demonstrated by the observation that some MAPs (e.g., MAP2) provide anchoring sites for PKA (Obar *et al.*, 1989; Faux and Scott, 1996). Interestingly, PKA can be detached and activated by phosphorylating their RII-regulatory subunit with cdc2 (Keryer *et al.*, 1993). Furthermore, it has been shown that PKA activity is crucial for cell cycle progression, since blocking PKA activity in metaphase prevented the transition from mitosis to interphase (Grieco *et al.*, 1996). We note, however, that S214 can also be phosphorylated by PKC, albeit with lower efficiency. Since some PKC isoforms are up-regulated in mitosis (Watanabe *et al.*, 1992; Lehrich and Forest, 1994, Thompson and Fields, 1996), this kinase or a related one could also contribute to the increase in microtubule dynamics.

In the nonsynchronized cells, S262 is the only one of the four KXGS motifs phosphorylated. Our result is in good agreement with earlier observations by Seubert *et al.* (1995). In their immunocytochemical study with the phosphorylation-dependent antibody 12E8, which recognizes the phosphorylated KXGS motifs S262 and S356, respectively, they could show that only S262 was phosphorylated in fetal human brain tissue. S262 is the major target site for MARK in vitro (Biernat *et al.*, 1993; Drewes *et al.*, 1995) and in vivo (Drewes *et al.*, 1997) and to a far lesser extent for PKA (Drewes *et al.*, 1995). In addition, MARK also phosphorylates the closely related MAP2 and MAP4 at the corresponding, highly conserved KXGS motifs (Illenberger *et al.*, 1996). All three MAPs fail to bind to microtubules upon phosphorylation by MARK, rendering microtubules highly dynamic. These data suggest that MARK is responsible for the phosphorylation at S262 in eukaryotic cells. Since phosphorylation at S262 is neither observed during interphase or metaphase in the cells (after mitotic arrest with nocodazole) and phosphorylation at this particular site is rather weak in the nonsynchronized cell population (Figure 2a), it is likely that this residue is only briefly phosphorylated during mitosis, possibly in prophase, where cellular microtubules are rearranged to form the mitotic spindle. By analogy, S214 has a similar low intensity in the bulk analysis, but gives a strong signal in metaphase (compare Figures 3 and 5). However, since the activation of MARK is not yet known, it remains to be shown that MARK is active in proliferating cells and that its activity is regulated during the cell cycle.

Finally, we note that the hyperphosphorylation and aggregation of tau protein (PHFs) is one of the hallmarks of AD pathology. Events that trigger the obvious imbalance of protein kinases and phosphatases in the affected neurons remain hitherto unknown. Several lines of evidence suggest that mitotic mechanisms might be involved, since earlier immunocytochemical studies have shown that tau protein from mitotic cells is recognized by phosphorylation-dependent antibodies diagnostic of Alzheimer neurofibrillary tangles (Pope *et al.*, 1994; Preuss *et al.*, 1995; Vincent *et al.*, 1996). The present investigation supports these studies in that the phosphorylation pattern of tau in metaphase cells closely resembles that generated by cdc2 and cdk5 in vitro except for the non-proline-directed site S214. These results help explain why tau protein from fetal brain tissue shows a higher degree of phosphorylation (Kanemaru *et al.*, 1992; Bramblett *et al.*, 1993; Yoshida and Ihara, 1993) and can also be detected with the same PHF antibodies (Goedert *et al.*, 1994; Matsuo *et al.*, 1994; Seubert *et al.*, 1995), because these cells also undergo mitosis during embryogenesis. Furthermore, the antibody MPM-2, a marker antibody for mitotic phospho-epitopes (Vandre *et al.*, 1991), strongly reacts with neurofibrillary tangles (Vincent *et al.*, 1996). These findings have led to the hypothesis that in AD the neurons may respond to some insult, such as ischemia, oxidative stress, or β-amyloid toxicity, by a final attempt to reinitiate mitosis. Since postmitotic neurons are incapable of reentering the cell cycle, activating mitotic protein kinases, with the cdks being the most prominent, may lead to cell death instead. This implies a tight relationship between the cell cycle and cell death machinery, which seem to converge at the level of cdks that show indeed increased activity in apoptosis (for reviews see King and Cidlowski, 1995; Pandey and Wang, 1995). Furthermore, it has been shown that increasing cdk activity in differentiated neuronal cell lines causes apoptosis (Meikrantz and Schlegel, 1996), whereas treating differentiated cells with mitotic inhibitors after nerve growth factor depletion prevents cell death (Farinelli and Greene, 1996; Park *et al.*, 1996). Consistent with this, cdc2 is up-regulated in Alzheimer brain tissue (Vincent *et al.*, 1997). In addition, our finding that S214 is highly phosphorylated in metaphase also strongly suggests mitotic mechanisms to be involved. S214 is a prominent site in PHF tau (Morishima-Kawashima *et al.*, 1995) and is part of the epitope of the antibody AT100, which is the only specific antibody for Alzheimer tau so far known (Hoffmann *et al.*, 1997; Zheng-Fischhöfer *et al.*, 1998). Thus, the 2D phosphopeptide maps will provide a valuable tool with which to monitor changes in tau phosphorylation in neuronal cells exposed to various conditions (e.g., stress, kinase and phosphatase inhibitors) and help elucidate mechanisms leading to the hyperphosphorylation of tau protein in AD.

ACKNOWLEDGMENTS

We are grateful to U. Böning, B. Krüger, and K. Alm for excellent technical assistance and to H.E. Meyer and H. Korte (Ruhr-University, Bochum) for peptide sequencing during the initial stage of this work. The clone of GSK-3 was generously provided by J.R. Woodgett (Toronto, Ontario, Canada). The pEGFP-N1 vector was a generous gift from Dr. Pongs (ZMNH, Hamburg, Germany). The monoclonal antibody T46 was obtained from Dr. V.M.Y. Lee (University of Pennsylvania, Philadelphia, PA). This work was supported by a grant from the Deutsche Forschungsgemeinschaft.

REFERENCES

Arioka, M., Tsukamoto, M., Ishiguro, K., Kato, R., Sato, K., Imahori, K., and Uchida, T. (1993). Tau protein kinase II is involved in the regulation of the normal phosphorylation state of tau protein. J. Neurochem. *60*, 461–468.

Baumann, K., Mandelkow, E.-M., Biernat, J., Piwnica-Worms, H., and Mandelkow, E. (1993). Abnormal Alzheimer-like phosphorylation of tau by cyclin-dependent kinases cdk2 and cdk5. FEBS Lett. *336*, 417–424.

Beaudette, K., Lew, J., and Wang, J.H. (1993). Substrate specificity characterization of a cdc2-like protein kinase purified from bovine brain. J. Biol. Chem. *268*, 20825–20830.

Belmont, L.D., Hyman, A.A., Sawin, K.E., and Mitchison, T.J. (1990). Real-time visualization of cell-cycle dependent changes in microtubule dynamics in cytoplasmic extracts. Cell *62*, 579–589.

Biernat, J., Gustke, N., Drewes, G., Mandelkow, E.-M., and Mandelkow, E. (1993). Phosphorylation of serine 262 strongly reduces the binding of tau protein to microtubules: Distinction between PHF-like immunoreactivity and microtubule binding. Neuron *11*, 153–163.

Biernat, J., Mandelkow, E.-M., Schröter, C., Lichtenberg-Kraag, B., Steiner, B., Berling, B., Meyer, H.E., Mercken, M., Vandermeeren, A., Goedert, M., and Mandelkow, E. (1992). The switch of tau protein to an Alzheimer-like state includes the phosphorylation of two serine-proline motifs upstream of the microtubule binding region. EMBO J. *11*, 1593–1597.

Binder, L.I., Frankfurter, A., and Rebhun, L. (1985). The distribution of tau in the mammalian central nervous system. J. Cell Biol. *101*, 1371–1378.

Boyle, W.J., van der Geer, P., and Hunter, T. (1991). Phosphopeptide mapping and phosphoamino acid analysis by two-dimensional separation on thin layer cellulose plates. Methods Enzymol. *201*, 110–149.

Bramblett, G.T., Goedert, M., Jakes, R., Merrick, S.E., Trojanowski, J.Q., and Lee, V.M.Y. (1993). Abnormal tau phosphorylation at Ser(396) in Alzheimer's disease recapitulates development and contributes to reduced microtubule binding. Neuron *10*, 1089–1099.

Brandt, R., Lee, G., Teplow, D.B., Shalloway, D., and Abdelghany, M. (1994). Differential effect of phosphorylation and substrate modulation on tau's ability to promote microtubule growth and nucleation. J. Biol. Chem. *269*, 11776–11782.

Brion, J.P., Smith, C., Couck, A.M., Gallo, J.M., and Anderton, B.H. (1993). Developmental changes in tau phosphorylation: Fetal tau is transiently phosphorylated in a manner similar to paired helical filament tau characteristic of Alzheimers disease. J. Neurochem. *61*, 2071–2080.

Butner, K.A., and Kirschner, M.W. (1991). Tau-protein binds to microtubules through a flexible array of distributed weak sites. J. Cell Biol. *115*, 717–730.

Casnellie, J.E. (1991). Assay of protein kinases using peptides with basic residues for phosphocellulose binding. Methods Enzymol. *200*, 115–120.

DeBrabander, M., Geuens, G., Nuydens, R., Willebrords, R., Aerts, F., and DeMey, J. (1986). Microtubule dynamics during the cell cycle: the effects of taxol and nocodazole on the microtubule system of PtK2 cells at different stages of the mitotic cycle. Int. Rev. Cytol. *101*, 215–274.

Döring, F., Drewes, G., Berling, B., and Mandelkow, E.-M. (1993). Cloning and sequencing of a cDNA encoding rat brain mitogen activated protein (MAP) kinase activator. Gene *131*, 303–304.

Drechsel, D.N., Hyman, A.A., Cobb, M.H., and Kirschner, M.W. (1992). Modulation of the dynamic instability of tubulin assembly by the microtubule-associated protein tau. Mol. Biol. Cell *3*, 1141–1154.

Drewes, G., Lichtenberg-Kraag, B., Döring, F., Mandelkow, E.-M., Biernat, J., Goris, J., Doree, M., and Mandelkow, E. (1992). Mitogen-activated protein (MAP) kinase transforms tau protein into an Alzheimer-like state. EMBO J. *11*, 2131–2138.

Drewes, G., Mandelkow, E.-M., Baumann, K., Goris, J., Merlevede, W., and Mandelkow, E. (1993). Dephosphorylation of tau protein and Alzheimer paired helical filaments by calcineurin and phosphatase-2A. FEBS Lett. *336*, 425–432.

Drewes, G., Ebneth, A., Preuss, U., Mandelkow, E.-M., and Mandelkow, E. (1997). MARK—a novel family of protein kinases that phosphorylate microtubule-associated proteins and trigger microtubule disruption. Cell *89*, 297–308.

Drewes, G., Trinczek, B., Illenberger, S., Biernat, J., Schmitt-Ulms, G., Meyer, H.E., Mandelkow, E.-M., and Mandelkow, E. (1995). MAP/microtubule affinity regulating kinase (p110/mark): a novel protein kinase that regulates tau-microtubule interactions and dynamic instability by phosphorylation at the Alzheimer-specific site Serine 262. J. Biol. Chem. *270*, 7679–7688.

Farinelli, S.E., and Greene, L.A. (1996). Cell cycle blockers mimosine, ciclopirox, and deferoxamine prevent the death of PC12 cells and postmitotic sympathetic neurons after removal of trophic support. J. Neurosci. *16*, 1150–1162.

Faux, M.C., and Scott, J.D. (1996). Molecular glue-kinase anchoring and scaffold proteins. Cell *85*, 9–12.

Fleming, L.M., and Johnson, G.V.W. (1995). Modulation of the phosphorylation state of tau in situ: the roles of calcium and cyclic AMP. Biochem. J. *309*, 41–47.

Friedhoff, P., and Mandelkow, E. (1998). Tau Protein. In: Guidebook to the Cytoskeletal and Motor Proteins, ed. Th. Kreis and R. Vale, Oxford, England: Oxford University Press (*in press*).

Goedert, M., Jakes, R., Crowther, R.A., Cohen, P., Vanmechelen, E., Vandermeeren, M., and Cras, P. (1994). Epitope mapping of monoclonal antibodies to the paired helical filaments of Alzheimers disease: identification of phosphorylation sites in tau protein. Biochem. J. *301*, 871–877.

Goedert, M., Jakes, R., and Vanmechelen, E. (1995). Monoclonal antibody AT8 recognizes tau protein phosphorylated at both serine 202 and threonine 205. Neurosci. Lett. *189*, 167–170.

Goedert, M., Spillantini, M., Jakes, R., Rutherford, D., and Crowther, R.A. (1989). Multiple isoforms of human microtubule-associated protein-tau: Sequences and localization in neurofibrillary tangles of Alzheimers-disease. Neuron *3*, 519–526.

Goode, B.L., and Feinstein, S.C. (1994). Identification of a novel microtubule binding and assembly domain in the developmentally regulated inter-repeat region of tau. J. Cell Biol. *124*, 769–782.

Greenwood, J.A., and Johnson, G.V.W. (1995). Localization and in situ phosphorylation state of nuclear tau. Exp. Cell Res. *220*, 332–337.

Grieco, D., Porcellini, A., Avvedimento, E.V., and Gottesmann, M.E. (1996). Requirement for cAMP-PKA pathway activation by Mphase-promoting factor in the transition from mitosis to interphase. Science *271*, 1718–1723.

Gustke, N., Trinczek, B., Biernat, J., Mandelkow, E.-M., and Mandelkow, E. (1994). Domains of tau protein and interactions with microtubules. Biochemistry *33*, 9511–9522.

Hagestedt, T., Lichtenberg, B., Wille, H., Mandelkow, E.-M., and Mandelkow, E. (1989). Tau protein becomes long and stiff upon phosphorylation: Correlation between paracrystalline structure and degree of phosphorylation. J. Cell Biol. *109*, 1643–1651.

Hanger, D., Hughes, K., Woodgett, J., Brion, J., and Anderton, B. (1992). Glycogen-synthase kinase-3 induces Alzheimer's disease-like phosphorylation of tau: Generation of paired helical filament epitopes and neuronal localization of the kinase. Neurosci. Lett. *147*, 58–62.

Himmler, A., Drechsel, D., Kirschner, M., and Martin, D. (1989). Tau consists of a set of proteins with repeated C-terminal microtubule-binding domains and variable N-terminal domains. Mol. Cell. Biol. *9*, 1381–1388.

Hirs, C.H. (1967). Modification of cysteine residues. Methods Enzymol. *11*, 325–329.

Hoffmann, R., Lee, V.M.Y., Leight, S., Varga, I., and Otvos, L. (1997). Unique Alzheimer's disease paired helical filament specific epitopes involve double phosphorylation at specific sites. Biochemistry *36*, 8114–8124.

Hyman, A.A., and Karsenti, E. (1996). Morphogenetic properties of microtubules and mitotic spindle assembly. Cell *84*, 401–410.

Illenberger, S., Drewes, G., Trinczek B., Biernat, J., Meyer, H.E., Olmsted, J.B., Mandelkow, E.-M., and Mandelkow, E. (1996). Phosphorylation of microtubule associated proteins MAP2 and MAP4 by the protein kinase p110/mark: phosphorylation sites and regulation of microtubule dynamics. J. Biol. Chem. *271*, 10834–10843.

Johnson, G., and Jenkins, S. (1996). Tau protein and Alzheimer's disease brain. Alzheimer's Dis. Rev. *1*, 38–54.

Jordan, M., Thrower, D., and Wilson L. (1992). Effects of vinblastine, podophyllotoxin and nocodazole on mitotic spindles. Implications for the role of microtubule dynamics in mitosis. J. Cell Sci. *102*, 401–416.

Kanemaru, K., Takio, K., Miura, R., Titani, K., and Ihara, Y. (1992). Fetal-type phosphorylation of the tau in paired helical filaments. J. Neurochem. *58*, 1667–1675.

Kenessey, A., and Yen, S.H. C. (1993). The extent of phosphorylation of fetal tau is comparable to that of PHF tau from Alzheimer paired helical filaments. Brain Res. *629*, 40–46.

Keryer, G., Luo, Z.J., Cavadore, J.C., Erlichman, J., and Bornens, M. (1993). Phosphorylation of the regulatory subunit of type-ii-beta cAMP-dependent protein kinase by cyclin B/p34(cdc2) kinase impairs its binding to microtubule-associated protein-2. Proc. Natl. Acad. Sci. USA *90*, 5418–5422.

King, K.L., and Cidlowski, J.A. (1995). Cell cycle and apoptosis: common pathways to life and death. J. Cell Biochem. *58*, 175–180.

Köpke, E., Tung, Y., Shaikh, S., Alonso, A., Iqbal, K., and Grundke-Iqbal, I. (1993). Microtubule-associated protein tau: abnormal phosphorylation of a non-paired helical filament pool in Alzheimer's disease. J. Biol. Chem. *268*, 24374–24384.

Kosik, K.S., and Greenberg, S.M. (1994). Tau protein and Alzheimer disease. In: Alzheimer Disease, ed. R. Terry, R. Katzman, and K. Bick, New York: Raven Press, 335–344.

Kosik, K.S., and McConlogue, L. (1994). Microtubule-associated protein function: lessons from expression in *Spodoptera frugiperda* cells. Cell Motil. Cytoskel. *28*, 195–198.

Ksiezak-Reding, H., Liu, W.K., and Yen, S.H. (1992). Phosphate analysis and dephosphorylation of modified tau associated with paired helical filaments. Brain Res. *597*, 209–219.

Lee, G., Cowan, N., and Kirschner, M. (1988). The primary structure and heterogeneity of tau protein from mouse brain. Science *239*, 285–288.

Leger, J., Kempf, M., Lee, G., and Brandt, R. (1997). Conversion of serine to aspartate imitates phosphorylation-induced changes in the structure and function of microtubule-associated protein tau. J. Biol. Chem. *272*, 8441–8446.

Lehrich, R.W., and Forrest, J.N. (1994). Protein-kinase C-zeta is associated with the mitotic apparatus in primary cell cultures of the shark rectal gland. J. Biol. Chem. *269*, 32446–32450.

Li, W.P., Chan, W.Y., Lai, H.W.L., and Yew, D.T. (1997). Terminal dUTP nick end labeling (TUNEL) positive cells in the different regions of the brain in normal aging and Alzheimer patients. J. Mol. Neurosci. *8*, 75–82.

Lichtenberg-Kraag, B., Mandelkow, E.-M., Biernat, J., Steiner, B., Schröter, C., Gustke, N., Meyer, H.E., and Mandelkow, E. (1992). Phosphorylation dependent interaction of neurofilament antibodies with tau protein: epitopes, phosphorylation sites, and relationship with Alzheimer tau. Proc. Natl. Acad. Sci. USA *89*, 5384–5388.

Lovestone, S. *et al.* (1994). Alzheimers disease-like phosphorylation of the microtubule-associated protein tau by glycogen-synthase kinase-3 in transfected mammalian-cells. Curr. Biol. *4*, 1077–1086.

Ludin, B., Doll, T., Meili, R., Kaech, S., and Matus, A. (1996). Application of novel vectors for GFP-tagging of proteins to study microtubule-associated proteins. Gene *173*, 107–111.

Mandelkow, E.-M., Biernat, J., Drewes, G., Gustke, N., Trinczek, B., and Mandelkow, E. (1995). Tau domains, phosphorylation, and interactions with microtubules. Neurobiol. Aging *16*, 355–362.

Mandelkow, E.-M., Drewes, G., Biernat, J., Gustke, N., Van Lint, J., Vandenheede, J.R., and Mandelkow, E. (1992). Glycogen synthase kinase-3 and the Alzheimer-like state of microtubule-associated protein tau. FEBS Lett. *314*, 315–321.

Matsuo, E.S., Shin, R.W., Billingsley, M.L., Vandevoorde, A., Oconnor, M., Trojanowski, J.Q., and Lee, V.M.Y. (1994). Biopsy-derived adult human brain tau is phosphorylated at many of the same sites as Alzheimer's disease paired helical filament tau. Neuron *13*, 989–1002.

Meikrantz, W., and Schlegel, R. (1996). Suppression of apoptosis by dominant-negative mutants of cyclin-dependent protein-kinases. J. Biol. Chem. *271*, 10205–10209.

Melan, M.A., and Sluder, G. (1992). Redistribution and differential extraction of soluble proteins in permeabilized cultured cells. Implications for immunofluorescence microscopy. J. Cell. Sci. *101*, 731–743.

Merrick, S, E., Demoise, D.C., and Lee, V.M. (1996). Site-specific dephosphorylation of tau protein at Ser202/Thr205 in response to microtubule depolymerization in cultured human neurons involves protein phosphatase 2A. J. Biol. Chem. *271*, 5589–5594.

Meyer, H.E., Eisermann, B., Heber, M., Hoffmann-Posorske, E., Korte, H., Weigt, C., Wegner, A., Hutton, T., Donella-Deana, A., Perich, J.W. (1993). Strategies for nonradioactive methods in the localization of phosphorylated amino-acids in proteins. FASEB J. *7*, 776–782.

Morishima-Kawashima, M., Hasegawa, M., Takio, K., Suzuki, M., Yoshida, H., Titani, K., and Ihara, Y. (1995). Proline-directed and non-proline-directed phosphorylation of PHF-tau. J. Biol. Chem. *270*, 823–829.

Morishima-Kawashima, M., and Kosik, K.S. (1996). The pool of MAP kinase associated with microtubules is small but constitutively active. Mol. Biol. Cell *7*, 893–905.

Obar, R.A., Dingus, J., Bayley, H., and Vallee, R.B. (1989). The RII subunit of cAMP-dependent protein-kinase binds to a common amino-terminal domain in microtubule-associated proteins 2a, 2b, and 2c. Neuron *3*, 639–645.

Olmsted, J.B., Stemple, D., Saxton, W., Neighbors, B., and Mcintosh, J.R. (1989). Cell cycle-dependent changes in the dynamics of MAP2 and MAP4 in cultured-cells. J. Cell Biol. *109*, 211–223.

Ookata, K., Hisanaga, S., Bulinski, J.C., Murofushi, H., Aizawa, H., Itoh, T.J., Hotani, H., Okumura, E., Tachibana, K., and Kishimoto, T. (1995). Cyclin-B interaction with microtubule-associated protein-4 (MAP4) targets p34(cdc2) kinase to microtubules and is a potential regulator of M-phase microtubule dynamics. J. Cell Biol. *128*, 849–862.

Otvos, L., Feiner, L., Lang, E., Szendrei, G., Goedert, M., and Lee, V.M. (1994). Monoclonal antibody PHF-1 recognizes tau protein phosphorylated at serine residue 396 and 404. J. Neurosci. Res. *39*, 669–673.

Pandey, S., and Wang, E. (1995). Cells en route to apoptosis are characterized by the upregulation of c-fos, c-myc, c-jun, cdc2, and RB phosphorylation, resembling events of early cell-cycle traverse. J. Cell Biochem. *58*, 135–150.

Park, D., Farinelli, S.E., and Greene, L.A. (1996). Inhibitors of cyclin-dependent kinases promote survival of post-mitotic neuronally differentiated PC12 cells and sympathetic neurons. J. Biol. Chem. *271*, 8161–8169.

Paudel, H., Lew, J., Ali, Z., and Wang, J. (1993). Brain proline-directed protein kinase phosphorylates tau on sites that are abnormally phosphorylated in tau associated with Alzheimer's paired helical filaments. J. Biol. Chem. *268*, 23512–23518.

Pope, W.B., Lambert, M.P., Leypold, B., Seupaul, R., Sletten, L., Krafft, G., and Klein, W.L. (1994). Microtubule-associated protein-tau is hyperphosphorylated during mitosis in the human neuroblastoma cell-line SH-SY5Y. Exp. Neurol. *126*, 185–194.

Preuss, U., Döring, F., Illenberger, S., and Mandelkow, E.-M. (1995). Cell cycle dependent phosphorylation and microtubule binding of tau protein stably transfected into Chinese hamster ovary cells. Mol. Biol. Cell *6*, 1397–1410.

Preuss, U., and Mandelkow, E.-M. (1998). Mitotic phosphorylation of tau protein in neuronal cell lines resembles phosphorylation in Alzheimer's disease. Eur. J. Cell Biol. *in press*).

Raghunandan, R., and Ingram, V.M. (1995). Hyperphosphorylation of the cytoskeletal protein tau by the MAP-kinase PK40 (ERK2): regulation by prior phosphorylation with cAMP-dependent protein kinase A. Biochem. Biophys. Res. Commun. *215*, 1056–1066.

Roder, H.M., Fracasso, R.P., Hoffman, F.J., Witowsky, J.A., Davis, G., and Pellegrino, C.B. (1997). Phosphorylation-dependent monoclonal tau antibodies do not reliably report phosphorylation by extracellular signal-regulated kinase-2 at specific sites. J. Biol. Chem. *272*, 4509–4515.

Sato-Harada, R., Okabe, S., Umeyama, T., Kanai, Y., and Hirokawa, N. (1996). Microtubule-associated proteins regulate microtubule function as the track for intracellular membrane organelle transports. Cell Struct. Funct. *21*, 283–295.

Schliwa, M., Euteneuer, U., Bulinski, J.C., and Izant, J.G. (1981). Calcium lability of cytoplasmic microtubules and its modulation by

microtubule-associated proteins. Proc. Natl. Acad. Sci. USA *78*, 1037–1041.

Schoenfeld, T.A., and Obar, R.A. (1994). Diverse distribution and function of fibrous microtubule-associated proteins in the nervous system. Int. Rev. Cytol. *151*, 67–137.

Scott, C., Spreen, R., Herman, J., Chow, F., Davison, M., Young, J., Caputo, C. (1993). Phosphorylation of recombinant tau by cAMP-dependent protein kinase: identification of phosphorylation sites and effect on microtubule assembly. J. Biol. Chem. *268*, 1166–1173.

Seeger, R., Danon, Y., Rayner, S., and Hoover, F. (1982). Definition of a Thy-1 determinant on human neuroblastoma, glioma, sarcoma, and teratoma cells with a monoclonal antibody. J. Immunol. *128*, 983–989.

Seubert, P. *et al.* (1995). Detection of phosphorylated Ser(262) in fetal tau, adult tau, and paired helical filament tau. J. Biol. Chem. *270*, 18917–18922.

Singh, T.J., Haque, N., Grundke-Iqbal, I., and Iqbal, K. (1995). Rapid Alzheimer-like phosphorylation of tau by the synergistic actions of non-proline-dependent protein-kinases and GSK-3. FEBS Lett. *358*, 267–272.

Smale, G., Nichols, N.R., Brady, D.R., Finch, C.E., and Horton, W.E. (1995). Evidence for apoptotic cell death in Alzheimer's disease. Exp. Neurol. *133*, 225–230.

Song, J.S., and Yang, S.D. (1995). Tau-protein kinase-1 (GSK-3-beta, kinase Fa) in heparin phosphorylates tau on Ser(199), Thr(231), Ser(235), Ser(262) Ser(369), and Ser(400) sites phosphorylated in Alzheimer-disease brain. J. Protein Chem. *14*, 95–105.

Steiner, B. *et al.* (1990). Phosphorylation of microtubule-associated protein tau: identification of the site for Ca++-calmodulin dependent kinase and relationship with tau phosphorylation in Alzheimer tangles. EMBO J. *9*, 3539–3544.

Stern, B., and Nurse, P. (1996). A quantitative model for the cdc2 control of S phase and mitosis in fission yeast. Trends Genet. *12*, 345–350.

Studier, W.F., Rosenberg, A.H., Dunn, J.J., and Dubendorff, J.W. (1990). Use of T7 RNA polymerase to direct the expression of cloned genes. Methods Enzymol. *185*, 60–89.

Thompson, L.J., and Fields, A.P. (1996). Beta(ii) protein kinase-C is required for the G2/M phase transition of the cell-cycle. J. Biol. Chem. *271*, 15045–15053.

Trinczek, B., Biernat, J., Baumann, K., Mandelkow, E.-M., and Mandelkow, E. (1995). Domains of tau protein, differential phosphorylation, and dynamic instability of microtubules. Mol. Biol. Cell *6*, 1887–1902.

Trojanowski, J., and Lee, V.M.Y. (1995). Phosphorylation of paired helical filament-tau in Alzheimers disease neurofibrillary lesions: focusing on phosphatases. FASEB J. *9*, 1570–1576.

Vandre, D., Centonze, V., Peloquin, J., Tombes, R., and Borisy, G.G. (1991). Proteins of the mammalian mitotic spindle: phosphorylation-dephosphorylation of MAP-4 during mitosis. J. Cell Sci. *98*, 577–588.

Verde, F., Dogterom, M., Stelzer, E., Karsenti, E., Leibler, S. (1992). Control of microtubule dynamics and length by cyclin A-dependent and cyclin B-dependent kinases in *Xenopus* egg extracts. J. Cell Biol. *118*, 1097–1108.

Vincent, I., Jicha, G., Rosado, M., and Dickson, D.W. (1997). Aberrant expression of mitotic cdc2/cyclin b1 kinase in degenerating neurons of Alzheimers-disease brain. J. Neurosci. *17*, 3588–3598.

Vincent, I., Rosado, M., and Davies, P. (1996). Mitotic mechanisms in Alzheimers disease. J. Cell Biol. *132*, 413–425.

Wang, Q.M., Fiol, C.J., DePaoli-Roach, A.A., and Roach, P.J. (1994). Glycogen synthase kinase-3β is a dual specificity kinase differentially regulated by tyrosine and serine/threonine phosphorylation. J. Biol. Chem. *269*, 14566–14574.

Wang, J.Z., Gong, C.X., Zaidi, T., Grundke-Iqbal, I., and Iqbal, K. (1995). Dephosphorylation of Alzheimer paired helical filaments by protein phosphatase-2a and phosphatase-2b. J. Biol. Chem. *270*, 4854–4860.

Watanabe, T., Ono, Y., Taniyama, Y., Hazama, K., Igarashi, K., Ogita, K., Kikkawa, U., and Nishizuka, Y. (1992). Cell-division arrest induced by phorbol ester in CHO cells overexpressing protein kinase-C-delta subspecies. Proc. Natl. Acad. Sci. USA *89*, 10159–10163.

Woodgett, J.R. (1991). A common denominator linking glycogen metabolism, nuclear oncogenes, and development. Trends Biochem. Sci. *16*, 177–181.

Yoshida, H., and Ihara, Y. (1993). Tau in paired helical filaments is functionally distinct from fetal tau: Assembly incompetence of paired helical filament tau. J. Neurochem. *61*, 1183–1186.

Zhai, Y., and Borisy, G.G. (1994). Quantitative determination of the proportion of microtubule polymer present during the mitosis-interphase transition. J. Cell Sci. *107*, 881–890.

Zheng-Fischhöfer, Q., Biernat, J., Mandelkow, E.-M., Illenberger, S., Godemann, R., and Mandelkow, E. (1998). Sequential phosphorylation of tau protein by GSK-3β and protein kinase A at Thr212 and Ser214 generates the Alzheimer-specific epitope of antibody AT100 and requires a paired helical filament-like conformation. Eur. J. Biochem. *252*, 542–552.

Exhibit B.

Vol. 215, No. 3, 1995
October 24, 1995

BIOCHEMICAL AND BIOPHYSICAL RESEARCH COMMUNICATIONS
Pages 1056-1066

Hyperphosphorylation of the Cytoskeletal Protein Tau by the MAP-Kinase $PK40^{erk2}$: Regulation by Prior Phosphorylation with cAMP-Dependent Protein Kinase A

Ramadevi Raghunandan and Vernon M. Ingram*

Department of Biology, Massachusetts Institute of Technology, Cambridge, MA 02139

Received September 13, 1995

$PK40^{erk2}$ is a MAP kinase which phosphorylates recombinant hTau40 up to 14 moles of phosphate/mole, markedly slowing its electrophoretic mobility. $PK40^{erk2}$ acting on TAU is expected to cause the appearance of Alzheimer's disease-specific phosphoepitopes, detectable by specific antibodies. Maximal phosphorylation in vitro of hTau40 by PKA_{cat} incorporates only 2-3 moles of phosphate/mole. Consequent, but smaller, reduction in electrophoretic mobility is seen, but not the formation of Alzheimer-specific or hyperphosphorylation-specific epitopes.

Phosphorylation of hTau40 by PKA_{cat} sharply reduces the number of phosphates that can now be introduced by $PK40^{erk2}$ to 5-6 moles/mole, instead of the expected 11 moles/mole. Thus, prior phosphorylation by PKA, a non-proline-directed protein kinase, regulates the conformation of the protein substrate Tau so as to make some sites very much less accessible to phosphorylation by the proline-directed kinase, $PK40^{erk2}$.

The microtubule associated protein Tau plays a crucial role in the assembly and stability of the microtubular cytoskeletal structure (1). There are 6 different isoforms of Tau present in the brain. These isoforms are formed by alternative splicing of the transcript from a single gene; the apparent molecular weights of the isoforms are between 50-68 kDa (2). Native adult Tau from normal brains has about 2 moles of phosphate (3,4). Tau-isoforms differ from each other in the number of repeat regions they carry, which varies between 3 and 4. They also differ in their

* To whom inquiries should be addressed at Department of Biology, M.I.T., 77 Massachusetts Avenue, Cambridge, MA 02139. Fax: 617.253.8699.

0006-291X/95 $12.00

phosphorylation status. The degree of phosphorylation of Tau affects its intrinsic structure (5), its interaction with other cytoskeletal proteins (6) and its susceptibility to proteolytic degradation (7).

Previous studies indicate that site specific phosphorylation, rather than the extent of phosphorylation, is necessary for the normal function of Tau (3). Tau from brains with Alzheimer disease is abnormally hyperphosphorylated (8); it is the major structural component of Paired Helical Filaments (PHF) which form the predominant component of neurofibrillary tangles (9,10). PHF-Tau has 6-8 molecules of phosphate (4), but the precise sites of phosphorylation are only approximately known. Tau present in PHFs does not bind tubulin effectively. It has been suggested that the aggregation of hyperphosphorylated Tau precedes the formation of NFT in AD diseased neurons (11).

Analysis of phosphorylation sites on PHF-Tau has led to the conclusion that proline directed protein kinase (PDPK) sites are phosphorylated, as are non-PDPK sites (12). Therefore, it is conceivable that more than one kinase is involved in hyperphosphorylating Tau. Of nine sites identified on PHF-Tau, seven could be phosphorylated by a MAP kinase (mitogen activated protein kinase). Protein kinase $PK40^{erk2}$ (13), glycogen synthase kinase-3 (GSK-3) (14), MAP kinase (15), Tau kinases (16) are the kinases which can phosphorylate Serine-proline/threonine-proline (SP/TP) sites specific for PDPK kinases. Non-PDPK kinases are CaMkinase II, PKA_{cat}, casein kinases, cyclin kinase, etc. (17). It is not known which are the kinases that hyperphosphorylate Tau in Alzheimer brain cells, but it is known that ERK2 (=$PK40^{erk2}$) is widely distributed in the brain.

Since both $PK40^{erk2}$ and PKA_{cat} can phosphorylate hTau40, we decided to see whether there was any site-specificity associated with either kinase. We used the two kinases sequentially, with unlabeled MgATP for the first reaction and γ-^{32}P-MgATP for the second. We could then study the resulting phosphopeptides and compare them with those produced by either kinase alone. Our results reveal that prior PKA_{cat} phosphorylation could act as a regulatory signal for further phosphorylation with $PK40^{erk2}$. It greatly reduces the rate and perhaps also the stoichiometry of $PK40^{erk2}$ phosphorylation, and still induces a hyperphosphorylated state of hTau40.

Materials and Methods

Recombinant hTau40 was purified from E.coli BL21 cells, containing the plasmid pRK172 as described by Goedert et al. (2), with minor modifications. Instead of CM-Sepharose chromatography, MonoS columns were used. Bovine brain $PK40^{erk2}$ was purified as described by Roder et al. (19). The catalytic subunit of protein kinase A, disodium ATP, and TPCK-treated trypsin were purchased from Sigma (St. Louis, MO).

Protein estimation was carried out either using the Coomassie Plus kit or the BCA protein assay kit from Pierce Co., using bovine serum albumin as the standard.

Phosphorylation of hTau40: Phosphorylation of hTau40 was performed as described by Roder et al. (19). A 30 µl reaction contained 20mM HEPES buffer pH 7.0, 2mM $MgCl_2$, 1mM ATP, 1mM DTT, 5µM okadaic acid (GIBCO BRL), 67 picomoles hTau40, 220cpm/picomole [γ-^{32}P]ATP, PKA_{cat} 5 units (as defined by Sigma) and/or $PK40^{erk2}$ 11.0 units [specific activity 4.8 nanomoles/min/mg of $PK40^{erk2}$ protein]; this was incubated at 37°C for the indicated time periods.

Preparation of unlabeled phosphorylated hTau40: Overnight phosphorylation of hTau40 by PKA_{cat} or by $PK40^{erk2}$ was carried out as described above, using unlabeled ATP and 300µg of hTau40. The reaction mixture was dialyzed against HEPES buffer and concentrated.

Hyperphosphorylation with γ-^{32}P-ATP of hTau40 previously phosphorylated by PKA_{cat}: PKA_{cat}-phosphorylated hTau40 was further phosphorylated by $PK40^{erk2}$, and $PK40^{erk2}$ phosphorylated hTau40 was further phosphorylated by PKA_{cat}. The second phosphorylation was done in the presence of γ-^{32}P-ATP and at low (1mM) unlabeled ATP. Phosphorylated hTau40 from all these different reactions was separated on 10% SDS PAGE and stained with Coomassie blue.

Phosphopeptide mapping: Samples of ^{32}P-labeled phosphorylated hTau40 from the above 2-step reactions were dried in a Speed Vac and oxidized with performic acid (20). The products were purified on G-50 Quick spin columns; the labeled proteins were concentrated in a Speed Vac and dissolved in 50mM ammonium bicarbonate buffer pH 8.0. Proteolytic digestion of the performic acid oxidized phosphorylated hTau40 preparations were carried out under conditions described in (20) at a trypsin to substrate ratio of 1:2. After 6 hours of digestion at 37°C another aliquot of fresh enzyme was added and the digestion continued for 16 hours. The digests were diluted in deionized water and concentrated in a Speed Vac. Separation of the peptides in the first dimension was on cellulose coated glass plates, Whatman (20x20cm), for 30 min at a constant voltage of 800V in a water cooled horizontal electrophoretic system. The electrophoresis buffer (pH4.5) contained butanol, acetic acid, pyridine, deionized water in a ratio of 1:0.5:0.5:18. TLC was carried out in the second dimension, using isobutyric acid, n-butanol, pyridine, glacial acetic acid, deionized water in a ratio of 12.5:0.38:0.96:0.58:5.58. TLC plates were dried and exposed to a preflashed NEN-Dupont X-ray film for 2-4 days (Fig. 4a-c).

Results

Phosphorylation of hTau40 by $PK40^{erk2}$ and by PKA_{cat}: Purified recombinant hTau40 was phosphorylated by $PK40^{erk2}$ for 4 hours, using γ-^{32}P-ATP; near-saturation was reached at 14.0±1.8 moles of

phosphate/mole hTau40 (Fig.1). Phosphorylation beyond four hours or increasing the enzyme concentration did not increase phosphorylation (data not shown). $PK40^{erk2}$ phosphorylation was dramatically inhibited by 6mM free ATP (data not shown) (13,18,19).

When recombinant hTau40 was phosphorylated by PKA_{cat} for 4 hours, using γ-^{32}P-ATP, near-saturation was reached at 3.1±0.96 moles of phosphate/mole hTau40 (Fig.1). The addition of a second aliquot of enzyme at 4 hours did not increase phosphorylation significantly; neither did phosphorylation beyond 6 hours. Previous experiments had shown that the PKA_{cat} reaction was completely blocked by the addition of the regulatory subunit of PKA (10 units per reaction mixture), but only partially by 6 mM free ATP in the reaction mixture (18).

To our surprise, ^{32}P-phosphorylation by $PK40^{erk2}$ of hTau40, previously phosphorylated with unlabeled ATP by PKA_{cat} as described

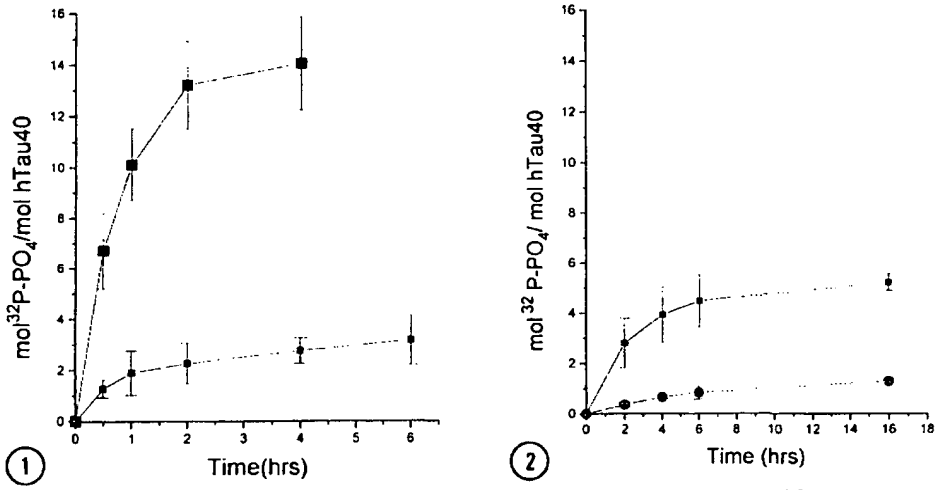

Fig. 1. Time course of Phosphorylation on hTau40 by $PK40^{erk2}$ and PKA_{cat}. Recombinant hTau40 67pmoles is phosphorylated to saturation by $PK40^{erk2}$ (11units; large closed squares) and PKA_{cat} (5 units; small closed squares) in presence of labeled ATP as described in materials and methods. Reactions are stopped at indicated time intervals. Incorporated counts on hTau40 are counted and the stoichiometry of phosphorylation is calculated. The average of three experiments is plotted with standard deviation as marked.

Fig. 2. Time course of phosphorylation on prior phosphorylated hTau40 by $PK40^{erk2}$ and PKA_{cat}. Phosphorylation of hTau40 by $PK40^{erk2}$ and PKA_{cat} is carried out to saturation in the absence of labeled ATP. PKA_{cat} phosphorylated hTau40 is further phosphorylated by $PK40^{erk2}$ (small closed squares) in presence of labeled ATP. $PK40^{erk2}$ phosphorylated hTau40 is further phosphorylated by PKA_{cat} (closed circle) in presence of labeled ATP. Stoichiometry of phosphorylation is calculated from 3 experiments for $PK40^{erk2}$ reaction and 2 experiments for PKA_{cat} reaction.

above, incorporated only 5.1±0.3 mol of phosphate after 16 hours of reaction. We had expected an incorporation of 11-14 moles of phosphate/mole protein, depending upon whether the 14 PO_4 residues incorporated by $PK40^{erk2}$ alone included any or all of the PKA-specific phosphates. In the reverse situation - unlabeled phosphorylation by $PK40^{erk2}$ first, followed by ^{32}P-phosphorylation by PKA_{cat} - incorporated only 1.3 mol of phosphate/mol of phosphorylated hTau40 after 16 hours. Phosphorylation of the substrate previously phosphorylated is very much slower and may not have reached saturation even after 16 hours (Fig. 2).

The products of the above two-stage reactions were separated on 10% SDS-PAGE and stained with Coomassie blue (Fig. 3). Unphosphorylated hTau40 protein in lane 1 is used as the control. Phosphorylation by $PK40^{erk2}$ alone resulted in the greatest retardation of mobility (lane 2), compared with phosphorylation by PKA_{cat} alone (lane 3). Near saturation phosphorylation by $PK40^{erk2}$ of hTau40 previously phosphorylated by PKA_{cat} had equally retarded mobility as hTau40 phosphorylated by $PK40^{erk2}$ alone, even though there are only 5.8 + 3 = 9 moles of phosphate/mole of protein instead of 14 (Table I).

hTau40 phosphorylated first by $PK40^{erk2}$ and then by PKA_{cat} showed the same mobility as hTau40 phosphorylated by $PK40^{erk2}$ alone. Apparent molecular weights were calculated: hTau40, 59 kDa;

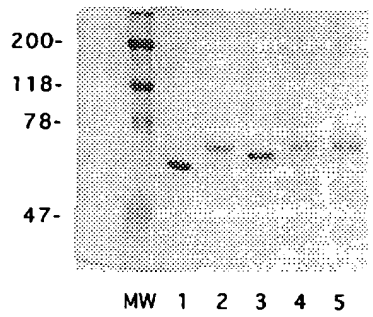

Fig. 3. Phosphorylation affects electrophoretic mobilities of hTau40. hTau40 is phosphorylated by $PK40^{erk2}$ or PKA_{cat} to saturation in the absence of labeled ATP. PKA_{cat} and $PK40^{erk2}$ phosphorylated hTau40 is further phosphorylated by $PK40^{erk2}$ or PKA_{cat}, respectively, for 16 hours under the conditions described in Materials and Methods. Phospho-hTau40 preparations from all four reactions are separated on 10% SDS PAGE and stained by Coomassie blue. Different lanes represented in the figure are lane(1) Unphosphorylated hTau40, lane(2) $PK40^{erk2}$ phosphorylated hTau40, lane(3) PKA_{cat} phosphorylated hTau40, lane(4) PKA_{cat} treatment of hTau40, followed by $PK40^{erk2}$, lane(5) $PK40^{erk2}$ treatment of hTau40, followed by PKA_{cat}.

Table I. Phosphorylation of hTau40 by PKA_{cat} & $PK40^{erk2}$

$PK40^{erk2}$, PKA_{cat} in sequence of kinase reaction	Stoichiometry of phosphorylation on hTau40 (moles/mole)
$PK40^{erk2}$	14.0 ± 1.8
PKA_{cat}	3.1 ± 0.96
PKA_{cat} followed by $PK40^{erk2}$	5.1 ± 0.33
$PK40^{erk2}$ followed by PKA_{cat}	1.3

Saturating phosphorylation with two kinases and a combination of the two kinases is carried out as described in Materials and Methods.

hTau40 phosphorylated by PKA_{cat}, 64 kDa; hTau40 phosphorylated by $PK40^{erk2}$, 69 kDa; hTau40 phosphorylated first by PKA_{cat} and then by $PK40^{erk2}$, or in the reverse order, also gave a molecular weight of 69 kDa.

We have at present no explanation for these results, except to suppose that the electrophoretic mobility of phosphorylated hTau40 is not just a function of the number of charged phosphate groups.

Phosphopeptide mapping: Tryptic digests of preparations of hTau40 labeled with γ-^{32}P-ATP by $PK40^{erk2}$ alone were examined by 2-dimensional TLC fingerprinting - electrophoresis at pH 4.5, followed by chromatography as described (Fig. 4a). Results of the radioactive fingerprints are summarized in Table II. Fig.4a represents the tryptic digest of hTau40 phosphorylated by PKA_{cat} alone, with a tracing of peptide spots below. Figure 4b is the phosphopeptide map obtained from hTau40 phosphorylated by $PK40^{erk2}$ alone. Figure 4c shows the phosphopeptide map obtained from hTau40 phosphorylated in sequence by PKA_{cat} (unlabeled) and $PK40^{erk2}$ (labeled with ^{32}P), as described in Materials and Methods. The intensity of different peptides on the fingerprints are different due to the extent of phosphorylation of a site, the presence of one or more sites phosphorylated in a peptide, and the yield of tryptic peptide cleavage. Amount of radioactivity loaded is approximately the same in each map. Peptides in good yield and present in well defined positions in the map are the only ones considered for this analysis.

Figures 4a-c: A prominent negatively charged tryptic peptide #1 appears to be present in all three reactions. It must contain

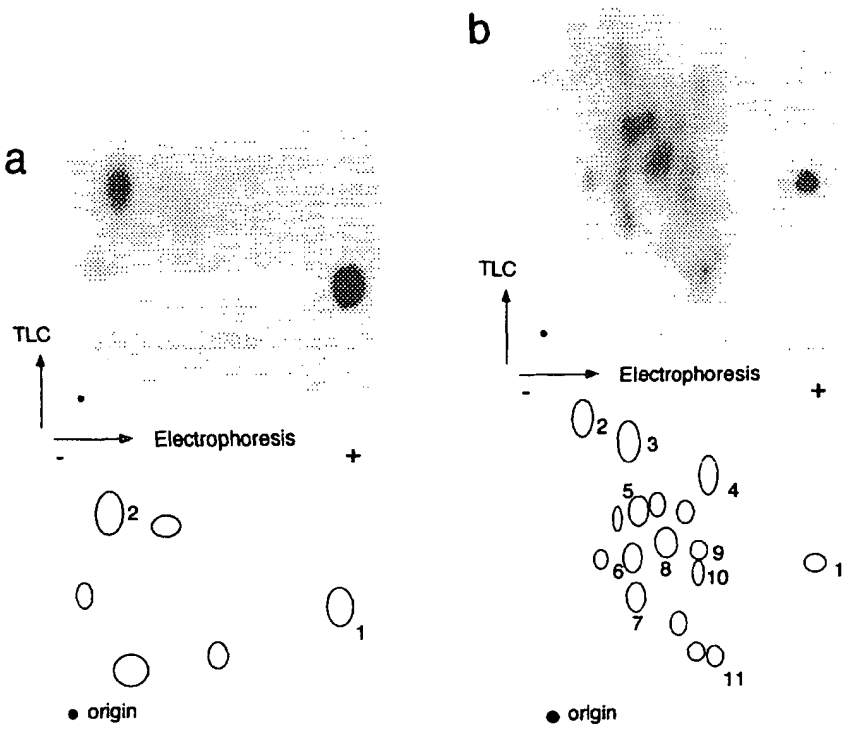

Fig. 4a. Autoradiograph of the two-dimensional phosphopeptide map of hTau40 phosphorylated by PKA_{cat} alone. Phosphorylation of hTau40 in presence of γ-^{32}P-ATP by PKA_{cat} is carried out for four hours. Phospho-hTau40 is fractionated in a G-50 quick spin column and performic acid oxidized. Phospho-hTau40 is then digested by trypsin and the peptides are separated as described in Methods. The lower panel is a tracing of the photograph.

Fig. 4b. Autoradiograph of the two-dimensional phosphopeptide map of hTau40 phosphorylated by $PK40^{erk2}$.alone. Phosphorylation of hTau40 in presence of γ-^{32}P-ATP by $PK40^{erk2}$ is carried out for four hours. Phospho-hTau40 is fractionated in a G-50 quick spin column and oxidized with performic acid. Phospho-hTau40 is then digested by trypsin and the peptides are separated as described in Methods. The lower panel is a tracing of the photograph.

ser/thr-pro sites for the proline-directed $PK40^{erk2}$ phosphorylation and other ser/thr sites for PKA_{cat}, a non-proline-directed kinase.

Peptide #2 is a favored site only when PKA_{cat} is used; it is poorly phosphorylated by $PK40^{erk2}$. The two strong peptides from PKA_{cat} phosphorylation correspond to the expected 2-3 moles of phosphate incorporated by PKA_{cat} reaction. The $PK40^{erk2}$-specific phosphopeptides 3-8 are variable in yield and apparently unaffected by previous phosphorylation by PKA_{cat}. Phosphopeptides c,d,e in Fig.4c are present in high yield only after phosphorylation by PKA_{cat}, followed by $PK40^{erk2}$ using γ-^{32}P-ATP.

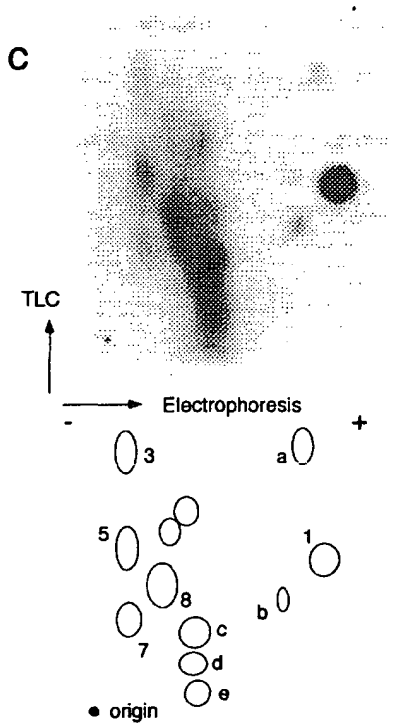

Fig. 4c. Autoradiograph of the two-dimensional phosphopeptide map of hTau40 phosphorylated by PKA_{cat} followed by $PK40^{erk2}$. Phosphorylation of hTau40 is carried out in the presence of unlabeled ATP by PKA_{cat}. Phospho-hTau40 from the cold reaction is further phosphorylated by $PK40^{erk2}$ in presence of γ-^{32}P-ATP. Phospho-hTau40 is fractionated in a G-50 quick spin column and oxidized with performic acid. Phospho-hTau40 is then digested by trypsin and the peptides are separated as described in Methods. The lower panel is a tracing of the photograph.

They are almost absent when hTau40 is phosphorylated by $PK40^{erk2}$ alone. These phosphopeptide spots are discussed below. This indicates that there is conformational change due to prior phosphorylation with PKA_{cat} which makes some sites much less available to phosphorylation by $PK40^{erk2}$.

Discussion

The combination of the two protein kinases PKA_{cat} and $PK40^{erk2}$ acting on recombinant hTau40 gave a very interesting result. The actions of these kinases on hTau40 are not independent of each other, but depend on the order in which Tau is exposed to the kinases. In the present study prior phosphorylation of hTau40 by PKA_{cat} sharply reduces the number of phosphates that can now be introduced by $PK40^{erk2}$ to 5-6 moles/mole, instead of the expected

Table II. Peptide classification* on phosphopeptide maps of hTau40 phosphorylated by PKA_{cat} alone (A), $PK40^{erk2}$ alone (B), and a combination of the two enzymes, $PK40^{erk2}$ after PKA_{cat} (C)

Peptide	Kinase	(A)	(B)	(C)
1	PKA_{cat} & $PK40^{erk2}$	++++	++++	++++
2#	PKA_{cat} & $PK40^{erk2}$	++	+	−
3	$PK40^{erk2}$	−	+	+
4	$PK40^{erk2}$	−	+	+
5	$PK40^{erk2}$	−	++	++
6	$PK40^{erk2}$	−	+	±
7	$PK40^{erk2}$	−	+	+
8	$PK40^{erk2}$	−	++	++
a	$PK40^{erk2}$ after PKA_{cat}	−	−	±
b	$PK40^{erk2}$ after PKA_{cat}	−	−	+
c	$PK40^{erk2}$ after PKA_{cat}	−	− †	++ √
d	PK40erk2 after PKA_{cat}	−	− †	+++ √
e	$PK40^{erk2}$ after PKA	−	− †	++ √

* Peptides appearing in the same position on these maps are numbered alike; letters are used for peptides appearing on only one map. Relative intensity of the peptides are scored with + symbols.

might be 2 different peptides or different sites on the same peptide.

† probably absent

√ These three strong tryptic peptides could be novel phosphorylation sites or could be due to incomplete tryptic digestion, caused by blocking of a trypsin digestion site.

11-14 moles/mole. Only some of the original $PK40^{erk2}$-specific phosphopeptides are still seen after prior reaction with PKA_{cat} (compare Figs. 4b & 4c). At the same time the rate of phosphorylation by $PK40^{erk2}$ is reduced (Fig. 2), as is the formation of the phosphorylated epitope detected by the mAb SMI-34 (18). This epitope is characteristic of those seen in the brains of Alzheimer patients. Our previous observation (18) that $PK40^{erk2}$ reaction is not complete when PKA_{cat}-phosphorylated hTau40 is used as the substrate confirms the same result. Thus, prior phosphorylation by PKA, a non-proline-directed protein kinase, regulates the conformation of the protein substrate Tau so as to make some expected sites much less accessible.

A prominent negatively charged peptide (#1) appears in all three maps. The number of peptides on the map from hTau40 phosphorylated by $PK40^{erk2}$ alone (Fig. 4b) is, as expected, much larger than the number on the hTau40 peptide map when PKA_{cat} alone is used (Fig. 4a). Figure 4c represents the phospho-peptide map of

hTau40 phosphorylated by PKA_{cat} with unlabeled ATP, followed by phosphorylation by $PK40^{erk2}$ with γ-^{32}P-ATP. There are quantitative as well as qualitative differences in the number of peptides seen. For example, peptides "c","d","e" are not seen in either of the other two peptide maps. This might be due to the prior phosphorylation by PKA_{cat} changing the conformation of the protein so as to make new additional sites available to $PK40^{erk2}$, or it might be explained by prior phosphorylation by PKA_{cat} of sites next to lysine or arginine, such as SK, which would make that lysine insensitive to trypsin digestion. There are 8 SK, 3 SR, 2 TR and 1 KS pairs, any one of which, if phosphorylated on S or T, might prevent tryptic cleavage at the expected basic amino acid. The apparently "new" phosphopeptide might in reality be an incompletely digested double peptide, of course in a new position, lower in chromatography than other peptides, because it is larger.

Studies of Singh et al. (17) indicate that a combination of different kinases on the same protein substrate can have a profound effect on the rate of reaction. These authors show the regulation of PDPK and non-PDPK kinases on bovine Tau, proving that prior phosphorylation of Tau by a non-PDPK kinase regulates further phosphorylation by a PDPK kinase depending on the type of non-PDPK kinase used (17).

Johnson (23) in a similar study with CaMKinase II and PKA_{cat} observes that prior phosphorylation of bovine Tau by CaMKinase II leads to reduced phosphorylation on the overlapping sites of PKA_{cat} and CaMKinase II, and increases the phosphorylation at PKA_{cat} specific sites.

These two studies are in agreement with our own observations that prior phosphorylation can be a regulatory step in the hyperphosphorylation of Tau.

Our findings suggest major changes in the conformation of at least the hTau40 form of Tau. The ability of Tau modified in this way to interact appropriately with microtubules may be compromised. It will be of great interest to determine which of these phosphorylation reactions - by PKA_{cat} or by $PK40^{erk2}$ or by both - is important *in vivo*.

References

1. Goedert, M., Spillantini, M.G., Jakes, R., Rutherford, D., and Crowther, R.A. (1989) Neuron 3, 519-526.
2. Goedert, M., and Jakes, R. (1990) EMBO J. 11, 4225-4230.

3. Garcia, J., Correas, I., and Avila, J. (1993) J. Biol. Chem. 109, 1643-1651.
4. Ksiezak-Reding, H., Leiu, W.K., and Yen, S.H. (1992) Brain Res. 597, 209-219.
5. Iqbal, K., Alonso, A., Gong, C., Khatoon, S., Kudo, T., Singh, T.J., and Grundke-Iqbal, I. (1993) Acta. Neuro. Biol. Exp. 53, 325-335.
6. Lindwall, G., and Cole, R.D. (1984) J. Biol. Chem. 259, 5301-5305.
7. Litersky, J.M., and Johnson, G.V.W. (1992) J. Biol. Chem. 267, 1563-1568.
8. Iqbal G, Iqbal K, Tung YC, Quinlan M, Wisniewski HM, Binder LI: Abnormal phosphorylation of the microtubule associated protein Tau in Alzheimer cytoskeletal pathology. Proc Natl Acad.Sci 83: 4913-4917, 1986.
9. Lee, V.M.Y., Balin, B.J., Otvos, L., and Trojanowsky, J.Q. (1991) Science 251, 675-678.
10. Iqbal, G., Iqbal, K., Tung, Y.C., Quinlan, M., Wisniewski, H.M., and Binder, L.I. (1986) Proc. Natl. Acad. Sci. USA 83, 4913-4917.
11. Bancher, C., Brunner, C., Lanman, H., Budka, H., Jellinger, K., Wiche, G., Seitelberger, F., Iqbal, G., Iqbal, K., and Wishniewski, H.M. (1989) Brain Res. 477, 90-99.
12. Hasegawa, M., Morishima, K.M., Takio, K., Sukuki, M., Titani, K., and Ihara, Y. (1992) J. Biol. Chem. 267: 17047-17054.
13. Roder, H.M., Eden, P.A., and Ingram, V.M. (1994) Biochem. Biophys. Res. Comm. 193, 639-647.
14. Mandelkow, E.M., Drewes, G., Biernet, J., Gustke, N., VanLint, J., Wandenheede, J.R., and Mandelkow, E. (1992) FEBS Lett. 314, 315-321.
15. Drewes, G., Litchenberg- Kragg, B., Doring, F., Mandelkow, E.M., Biernet, J., Goris, J., Doree, M., Mandelkow, E. (1992) EMBO J. 11, 2131-2138.
16. Ishiguro, K., Takamatsu, M., Tonizawa, K., Omori, A., Takashi, M., Arioka, M., Uchida, T., and Imahori K. (1992) J. Biol. Chem. 267, 10897-10901.
17. Singh, T.J., Iqbal, I.G., McDonald, B., and Iqbal, K. (1994) Mol. Cell Biochem. 131, 181-189.
18. Blanchard, B., Raghunandan, R., Roder, H.M., and Ingram, V.M. (1994) Biochem. Biophys. Res. Comm. 200, 187-194.
19. Roder, H.M., and Ingram, V.M. (1991) J. Neurosci. 11: 3325-3343.
20. Boyle, J.W., VanderGeer P., and Hunter, T. (1991) Meth. Enzymol. 201, 110-149.
21. Gustke, N., Triczek, B., Biernet, J., Mandelkow, E.M., and Mandelkow, E. (1994) Biol. Chem. 33, 9511-9522.
22. Scott, W.C., Spreen, C., Herman, L.J., Chow, P.F., Davison, D.M., Young, J., Caputo, B.C. (1993) J. Biol. Chem. 268, 1166-1173.
23. Johnson, G.W. (1992) J. Neurochem.59, 2056-2062.

Exhibit C

Molecular Neurobiology

ISSN0893-7648/98/16(1): 79–95/$12.25

Role of MAP Kinase in Neurons

Kohji Fukunaga* and Eishichi Miyamoto

Department of Pharmacology, Kumamoto University School of Medicine, Kumamoto 860, Japan

Abstract

Extracellular stimuli such as neurotransmitters, neurotrophins, and growth factors in the brain regulate critical cellular events, including synaptic transmission, neuronal plasticity, morphological differentiation and survival. Although many such stimuli trigger Ser/Thr-kinase and tyrosine-kinase cascades, the extracellular signal-regulated kinases, ERK1 and ERK2, prototypic members of the mitogen-activated protein (MAP) kinase family, are most attractive candidates among protein kinases that mediate morphological differentiation and promote survival in neurons. ERK1 and ERK2 are abundant in the central nervous system (CNS) and are activated during various physiological and pathological events such as brain ischemia and epilepsy. In cultured hippocampal neurons, simulation of glutamate receptors can activate ERK signaling, for which elevation of intracellular Ca^{2+} is required. In addition, brain-derived neurotrophic factor and growth factors also induce the ERK signaling and here, receptor-coupled tyrosine kinase activation has an association. We describe herein intracellular cascades of ERK signaling through neurotransmitters and neurotrophic factors. Putative functional implications of ERK and other MAP-kinase family members in the central nervous system are give attention.

Index Entries: MAP kinase; central nervous system; hippocampus; glutamate receptor; BDNF; calmodulin-dependent protein kinase; stress-activated protein kinase; synaptic plasticity; apoptosis.

Introduction

Mitogen-activated protein (MAP) kinase, also known as extracellular signal-regulated kinase (ERK), is a member of a family of serine/threonine protein kinases and has important roles in the regulation of cell growth and differentiation in response to stimulation with various growth factors. Effects of these growth factors are mediated by activation of cell-surface receptors with intrinsic protein-tyrosine kinase activity. The activation cascade of MAP kinase by stimulation with growth factors has been well documented (Blenis, 1993; Crews and Erikson, 1993; Davis, 1993; Nishida and Gotoh, 1993). The common pathway leading from the receptor tyrosine

*Author to whom all correspondence and reprint requests should be addressed.

kinase involves a small GTP-binding protein $p21^{ras}$ (RAS), which activates Raf-1, the c-raf-1 protooncogene product. Raf-1 phosphorylates MAP kinase/ERK kinase (MEK), which in turn phosphorylates and activates MAP kinase. In addition, numerous neurotransmitters and hormones also activate MAP kinase through stimulation of either of two classes of receptors, G protein-coupled receptors or ligand-gated ion channel-coupled receptors. Increase in intracellular Ca^{2+} is required to activate MAP kinase, as downstream signals from both kinds of receptor. The signaling of Ca^{2+}-dependent activation of MAP kinase is not fully understood.

The genes of MAP kinase are highly expressed in the CNS (Thomas and Hunt, 1993) and proteins of both ERK1 and ERK2 are widely but differently expressed in various regions of the rat brain (Ortiz et al., 1995). Accumulating evidence suggests physiological and pathological roles for MAP kinase in the CNS. MAP kinase in the rat brain was activated following electroconvulsive shock (Baraban et al., 1993), generalized seizure activity (Gass et al., 1993), or transient brain ischemia (Campos-González and Kindy, 1992). In the present article, we directed attention to regulation of MAP kinase activity by stimulation with neurotransmitters, neurotrophins, growth factors, or cytokines in the brain cells. Functional implications of the enzyme in the CNS are given attention.

Expression in the Central Nervous System

Three rat ERKs, ERK1, ERK2, and ERK3, have been purified and cloned (Boulton et al., 1991), and molecular and biochemical studies of MAP kinases have established that two homologous proteins, ERK1 and ERK2, correspond to the MAP-1 and MAP-2 kinase isozymes, respectively. Northern-blot analysis revealed that high levels of ERK1 and ERK2 mRNA are present in the nervous system of adult rats, in contrast to ERK3 mRNA, which is expressed at high levels early during development (Boulton et al., 1991). *In situ* hybridization histochemistry using specific oligonucleotide probes against ERK1 and ERK2 isoforms revealed the precise localization of these isoforms in the CNS of adult rats (Thomas and Hunt, 1993). The signal for ERK2 mRNA was more intense in many regions, including the cerebral cortex, olfactory bulb, hippocampus, amygdala, basal ganglia (except the globus pallidus and endopeduncular nucleus), basal nucleus, thalamus, hypothalamus, brain stem nuclei, cerebellum, and neurons in the spinal cord. In contrast, hybridization signals for ERK1 were relatively weak and were observed in restricted regions, in comparison to ERK2, including the olfactory bulb, cortex, regions of the hippocampus, amygdala, nucleus basalis of Maynert, substantia nigra, some hypothalamic and brain stem nuclei, and cerebellum, as well as neurons of the spinal cord (Thomas and Hunt, 1995). In the hippocampus, ERK1 was highly expressed in the dentate gyrus and was practically nil in the CA1 region, in contrast to expression of ERK2 in all regions of the hippocampus. In both cultured hippocampal neurons and cortical astrocytes, both ERK1 and ERK2 with molecular masses of 44 and 42 kDa were detected by immunoblotting analysis with antibodies prepared for the C-terminal peptide of ERK1, which recognized both ERK isoforms (Baraban et al., 1993; Kurino et al., 1995).

Expression of the upstream kinases of MAP kinase has been noted in the brain. MEK-1 and -2 are direct upstream kinases of MAP kinase and are derived from different genes. Northern-blot analysis indicates that MEK-2 is expressed at low levels in mouse adult brain and at higher levels in neonatal brain (Brott et al., 1993). This is in contrast to the high levels of MEK-1 expressed in the brain. In addition, a number of MEK-activating kinases have been reported, most notably c-Raf-1 and B-Raf. B-Raf is the most abundant Raf in the brain (Storm et al., 1990; Barnier et al., 1995). Consistent with these observations, the MEK-1 activating kinase was copurifed with B-raf in the bovine brain (Catling et al., 1994).

Activation of MAP Kinase by Stimulation of Glutamate Receptors

MAP kinase was activated following electroconvulsive shock (Baraban et al., 1993; Stratton et al., 1991) or generalized seizure activity (Gass et al., 1993) as well as transient brain ischemia (Campos-González and Kindy, 1992; Hu and Wieloch et al., 1994). These observations suggest that stimulation of glutamate receptors and/or depolarization results in activation of MAP kinase during these pathological events. Indeed, Bading and Greenberg (1991) reported that stimulation of the NMDA receptor leads to tyrosine phosphorylation of MAP kinase in cultured hippocampal neurons. In cultured cortical neurons, stimulation of the metabotropic glutamate and the kainate receptors, but not the NMDA receptor activated the 42-kDa MAP kinase. A burst of spontaneous synaptic activity in cultured cortical neurons was associated with activation of MAP kinase (Fiore et al., 1993). Treatment with a combination of tetrodotoxin, a voltage-dependent sodium-channel blocker and MK-801, a specific NMDA-receptor blocker, largely prevented MAP kinase activity as well as burst of spontaneous synaptic activity in cultured cortical neurons (Fiore et al., 1993).

Activation of MAP kinase by stimulation of glutamate receptors was evident in cultured hippocampal neurons (Kurino et al., 1995). Hippocampal neurons of 7–8 d in culture were stimulated with a short exposure to NMDA. After incubation for indicated times, the cells were frozen in liquid N_2. The MAP kinase activity was determined by in-gel kinase assay containing myelin basic protein as a substrate by SDS-PAGE. As shown in Fig. 1A, treatment with NMDA stimulated 42-kDa MAP kinase activity as well as the Ca^{2+}-independent form of CaM kinase II, as determined by SDS-PAGE. In the in-gel kinase assay, an increase of 400% in autonomous CaM kinase II (Ca^{2+}-independent activity) was evident after short exposure to NMDA and the activity reverted to near basal levels within 10 min (Fig. 1B). Likewise, a tran-

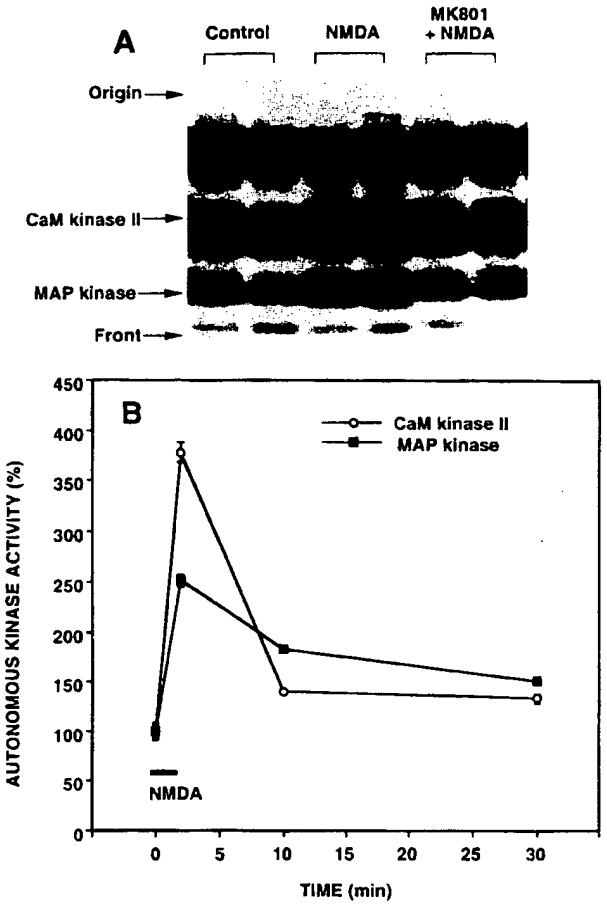

Fig. 1. Time course of MAP kinase and CaM kinase II activation by NMDA treatment in cultured rat hippocampal neurons. **(A)** In-gel kinase assay for MAP kinase and CaM kinase II. Hippocampal neurons of 7–8 d in culture were preincubated with Krebs-Ringer HEPES buffer (KRH) and exposed for 2 min to 100 μ*M* NMDA. After removal of NMDA by changing the medium, the cells were frozen at the indicated time. Cell extracts were prepared and subjected to SDS-PAGE containing myelin basic protein to assay autonomous CaM kinase II and MAP kinase. An autoradiograph shows the NMDA-induced activation of CaM kinase II and MAP kinase. The positions of the enzymes are indicated by arrows. **(B)** Time course of NMDA-induced activation of CaM kinase II and MAP kinase. The relative CaM kinase II and MAP kinase activities were measured using a Bio-Imaging analyzer (BA100 Fujifilm, Tokyo, Japan). The activity is expressed as a percentage of the control (without NMDA) at zero-time. Data are mean ± SE values (n = 6).

sient increase in MAP kinase was also found in the same gel. The NMDA-induced MAP kinase activation was totally prevented by inclusion of AP5 or MK-801 in the incubation medium. NMDA is a potent agonist used to induce MAP-kinase activation (Kurino et al., 1995). In addition to the NMDA receptor, the metabotropic-glutamate receptor, but not AMPA/kainate receptor is involved in glutamate-induced activation of MAP kinase (Kurino et al., 1995). This is in contrast to the observation of cultured cortical neurons in which the AMPA/kainate receptor was mainly involved in MAP kinase activation (Fiore et al., 1993). The signaling cascade of MAP-kinase activation through glutamate receptors was also investigated in the hippocampal neurons (Kurino et al., 1995). Because the glutamate-induced MAP-kinase activation was largely prevented in the presence of protein kinase C (PKC) inhibitor or prolonged incubation with phorbol ester to downregulate PKC (Fig. 2), PKC seemed to be mainly involved in MAP-kinase activation through glutamate receptors. However, a significant level of MAP-kinase activation through glutamate receptors remained after inhibition of PKC, but was totally abolished by removal of extracellular Ca^{2+}. In addition, ionomycin- induced MAP-kinase activation was independent of the PKC pathway. Interestingly, the ionomycin-induced MAP-kinase activation was abolished by inclusion of calmidazolium, a calmodulin antagonist as well as by KN93, a CaM kinase II inhibitor, in the incubation medium (Fukunaga et al., unpublished observation). We tested the effect of KN93 on MAP-kinase activation through various Ca^{2+}-dependent pathways. As shown in Fig. 3, KN93 has a small but significant inhibitory effect on the glutamate-induced MAP-kinase activation. The NMDA- and ionomycin- induced MAP- kinase activation was largely prevented by treatment with KN93, and Bay K8644 (an L-type voltage-dependent Ca^{2+} channel agonist)-induced MAP-kinase activation was abolished by the treatment. These results suggest that the pathways between the glutamate receptor and L-type voltage-dependent Ca^{2+} channel differ

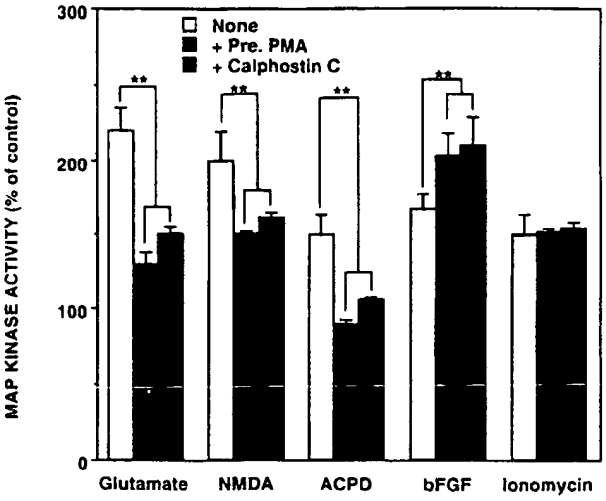

Fig. 2. Effects of protein kinase C downregulation and calphostin C on glutamate-induced activation of MAP kinase in cultured rat hippocampal neurons. For protein kinase C downregulation, hippocampal neurons of 7–8 d in culture were pretreated with 100 n*M* for 16 h (Pre. PMA) as indicated. The cells were then preincubated at 37°C for 30 min in Ca^{2+}-free KRH buffer and incubated for 10 min with 10 μ*M* glutamate, 100 μ*M* NMDA, 300 μ*M* ACPD, 10 ng/mL bFGF, or 5 μ*M* ionomycin in KRH buffer. 100 n*M* calphostin C was added during the last 10 min of preincubation and incubation with test agents. MAP-kinase activities in cell extracts were measured by in-gel kinase assay. Data are mean ± SE values (n = 6) and are expressed as percentages of the activity without glutamate, NMDA, ACPD, bFGF, or ionomycin, respectively. Changes in MAP-kinase activity were statistically significant: $^{**}p < 0.01$. From Kurino et al. (1995), with modifications.

with respect to the effects of KN93. Although the mechanism is unknown, the observations strongly indicate that calmodulin and CaM kinases are implicated in the Ca^{2+}-dependent and PKC-independent MAP-kinase activation through glutamate receptors and through the voltage-dependent Ca^{2+} channel. Finkbeiner and Greenberg (1996) proposed that the Ca^{2+}-sensitive Ras guanine nucleotide-releasing factor (Ras-GRF) is a candidate mediating Ca^{2+}-dependent Ras activation. Furthermore, the involvement of c-Raf-1 was not evident in case

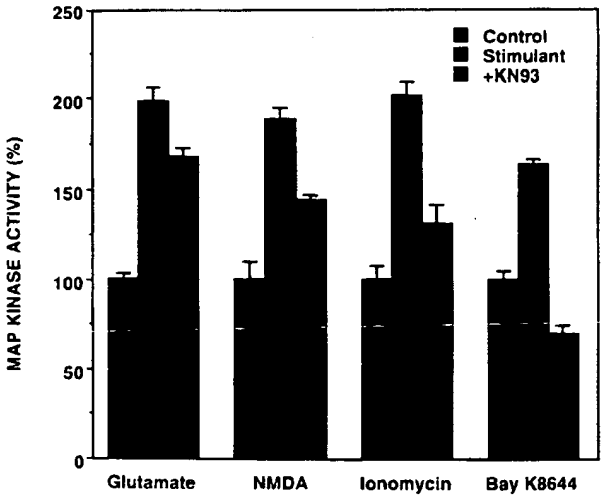

Fig. 3. Effects of KN93 on diverse Ca^{2+}-dependent MAP-kinase activation in cultured rat hippocampal neurons. Hippocampal neurons of 7–8 d in culture were preincubated for 30 min in the presence or absence of 10 μ*M* KN93. The cells were then incubated for 10 min with or without stimulants, including glutamate (10 μ*M*), NMDA (100 μ*M*), ionomycin (5 μ*M*) and Bay K8644 (5 μ*M*). MAP-kinase activities in cell extracts were measured by the in-gel kinase assay as shown in Fig. 1. From Fukunaga et al., unpublished data.

of glutamate-induced MAP kinase activation because of a lack of increased *in situ* phosphorylation of c-Raf-1 (Kurino et al., 1995). In contrast, increased phosphorylation of c-Raf-1 was noted following treatment of the hippocampal neurons with bFGF. The involvement of B-Raf should be tested in case of glutamate-induced activation, since the high expression and the association of B-Raf with MEK in the brain have been documented (Catling et al., 1994).

Activation of MAP Kinase by Stimulation of Neurotrophic and Growth-Factor Receptors

MAP-kinase activation by nerve-growth factor (NGF) has a central role in morphological differentiation of PC12 cells and sympathetic neurons (Marshall, 1995; Robbins et al., 1992; Cowley et al., 1994; Wood et al., 1992). Likewise, multiple neurotrophic factors regulate the development of the nervous system. Among neurotrophic factors, brain-derived neurotrophic factor (BDNF), neurotrophin-3 (NT-3), and NT-4/5 have been well characterized and were seen to have survival-promoting activity in certain types of neurons. For example, BDNF promotes survival and/or differentiation in rat septal cholinergic neurons, dopaminergic neurons in the substantia nigra, GABAergic neurons of the basal forebrain, and rat retinal ganglion cells (Alderson et al., 1990; Johnson et al., 1986; Hyman et al., 1991; Knusel et al., 1991). On the other hand, NT-3 exhibited neurotrophic effects on only neural crest- and nodose ganglion-derived sensory neurons (Knusel et al., 1991; Maisonpierre et al., 1990). In electrophysiological studies, application of BDNF, NT-3, or NT-4/5 potentiates glutamatergic synaptic transmission in cultured hippocampal neurons (Lessmann et al., 1994; Levine et al., 1995) as well as in hippocampal slices of adult rats (Kang and Schuman, 1995). A significant impairment of long-term potentiation (LTP) was observed in hippocampal slices of BDNF-knockout mice (Korte et al., 1995). Consistent with these observations, TrkB and TrkC, tyrosine kinase-coupled receptors specifically recognized by BDNF and NT-3, respectively, are highly expressed in the adult mouse brain (Klein et al., 1989, 1990a, b; Lamballe et al., 1994). Expression of BDNF is upregulated following LTP induction in rat hippocampal slices (Castren et al., 1993; Patterson et al., 1992). Taken together, these observations suggest important roles of neurotrophins in neuronal plasticity in the adult brain as well as developmental plasticity during synaptogenesis in the fetal brain. In both cases, the neurotrophins seem to act as specific retrograde messengers modulating synaptic transmission.

Extensive studies have been focused on intracellular signal transduction of neurotrophins to elucidate physiological functions in neuronal plasticity. Since MAP-kinase activa-

tion through the TrkA receptor, a tyrosine kinase-coupled receptor for nerve-growth factor (NGF) has been well documented concerning survival and morphological differentiation of PC12 cells, the central function of MAP kinase through TrkB and TrkC receptors is understood to be a signaling cascade to elicit modulating effects on neuronal plasticity. Marsh et al. (1993, 1996) reported a persistent activation of MAP kinase with exposure of BDNF to cultured hippocampal neurons. The BDNF-induced MAP kinase activation was also evident in cultured cortical astrocytes (Roback et al., 1995). In both neural cells, induction of c-Fos was closely associated with MAP-kinase activation by stimulation with BDNF. On the other hand, the TrkC receptor for NT-3 was highly expressed in pyramidal neurons but not in astrocytes (Marsh et al., 1996). The extent of the MAP-kinase activation by NT-3 was comparable to that with BDNF in hippocampal pyramidal neurons. Although BDNF and NT-3 have been known to promote neuronal survival on different types of neurons, the neurotrophins do not seem to promote survival of hippocampal pyramidal neurons (Marsh et al., 1996). In addition, BDNF had no apparent effect on mitotic activity in cortical glial cells, as determined by ^{3}H-thymidine incorporation under serum-free conditions. Taken together, BDNF-induced MAP kinase activation may not initiate a cascade that leads to survival promotion and mitogenesis, but may be involved in the modulation of synaptic transmission as a retrograde messenger in hippocampal LTP. This is consistent with the observation of an increased level of BDNF mRNA following the LTP induction (Castren et al., 1993; Patterson et al., 1992).

Application of exogenous neurotrophins such as NGF and BDNF has been seen to increase release of acetylcholine and glutamate in synaptosomal preparations of rat hippocampal neurons (Knipper et al., 1994a,b) and increase dopamine release in cell cultures of rat mesencephalic neurons (Blochl and Sirrenberg, 1996). In cultured hippocampal or cortical neurons, both neurotrophins stimulated phosphorylation of synapsin I, which is localized in presynaptic sites and is associated with synaptic vesicles and microfilaments (Knipper et al., 1994b; Jovanovic et al., 1996). In the case of cortical neurons, Jovanovic et al. (1996) clearly demonstrated that BDNF could stimulate the phosphorylation of synapsin I at sites for MAP kinase by using antibodies that recognize the phosphorylation site of synapsin I by MAP kinase. The phosphorylation by MAP kinase significantly reduced the potential of synapsin I to polymerize G-action and form the bundle of the actin filaments. The phosphorylation site for MAP kinase exists in both head and tail regions of synapsin I and just precedes the sites for CaM kinase II in the tail region. The MAP kinase-induced phosphorylation may account for acute effects on synaptic transmission in the cholinergic and glutamatergic neurons.

In addition to neurotrophins, bFGF and EGF have been seen to activate MAP kinase, in turn promote survival of various types of neurons, and increase the mitogenic activity of brain astrocytes. In cultured rat hippocampal neurons, bFGF promoted the bifurcation and growth of axonal branches without affecting the elongation rate of primary axons (Aoyagi et al., 1994), and resulted in increased complexity of axonal trees. Stimulation of the bFGF receptor associated with tyrosine kinase is coupled to activation of Ras and phospholipase Cγ, which induces activation of MAP kinase and PKC, respectively. Since the promotion of neurite branching activity by bFGF was not blocked by a PKC inhibitor and treatment with PMA, a PKC activator had no effect on the branching. MAP kinase may be involved in the morphological differentiation in cultured neurons. Similar to the neurotrophins, bFGF could modulate synaptic transmission by acting on GABAergic neurotransmission rather than glutamatergic neurotransmission (Tanaka et al., 1996). The molecular mechanisms underlying the synaptic potentiation by bFGF remain to be investigated.

In cultured cortical astrocytes and C6 glioma, bFGF produced a long-lasting increase in MAP-kinase activation (Tournier et al., 1994;

Kurino et al., 1996) and in turn promoted proliferation. The long-lasting increase in MAP-kinase activation was associated with translocation of the enzyme from the cytosol to the nucleus and/or increases in the perinucleus (Kurino et al., 1996) (Fig. 4). Traverse et al. (1992) suggested that the sustained activation of MAP kinase with nerve-growth factor might be required for translocation of the kinase to the nucleus and neuronal differentiation in PC12 cells. However, the transient activation with epidermal growth factor (EGF) was associated with no nuclear translocation of MAP kinase and only potentiated proliferation. Treatment with dibutyryl cyclic AMP or isoproterenol completely abolished the bFGF-induced MAP kinase activity (Kurino et al., 1996) as well as translocation into the nucleus as shown in Fig. 4. Similarly, the bFGF-induced stimulation of ^{3}H-thymidine uptake into astrocytes was abolished by treatment with dibutyryl cyclic AMP or isoproterenol (Kurino et al., 1996). Burgering et al. (1993) and Cook and McCormick (1993) reported that potentiation of DNA synthesis and activation of MAP kinase by stimulation with EGF in Rat 1 fibroblasts were inhibited by cyclic AMP accumulation that interfered in the MAP-kinase signaling cascade at the downstream site of Ras and the upstream site of Raf-1. Similarly, the bFGF-induced Raf-1 phosphorylation was inhibited by treatment with dibutyryl cyclic AMP in cultured astrocytes (Kurino et al., 1996). Häfner et al. (1994) reported that cyclic AMP-dependent protein kinase phosphorylated Raf-1 with concomitant inhibition of the activity. However, the precise molecular mechanisms of the inhibition of growth factor-induced MAP-kinase activation by cyclic AMP are not clear. In brain astrocytes, the cyclic AMP signaling cascade has been seen to promote differentiation rather than proliferation (Fahrig and Sommermeyer, 1993). Treatment of cultured astrocytes with dibutyryl cyclic AMP resulted in a morphological transformation from a flat, polygonal phenotype to a stellate-like cell shape. The differentiation by cyclic AMP elevation in cortical astrocytes was associated with increases in gene expression of different trophic factors and cytokines such as FGF-2 and interleukin-6 (Norris et al., 1994; Riva et al., 1996).

Activation of MAP kinase by the neurotrophins and growth factors has a common pathway leading from the receptor-tyrosine kinase that activates Ras, Raf-1 kinase, and MEKs, and in turn activates MAP kinase. Neurotrophins and growth factors are involved in morphological differentiation such as neurite branching and promote the cell survival. It is now questionable if both functions are elicited by activation of MAP kinase and whether target proteins for the enzyme locate in the neurons.

Activation of MAP Kinase by Stimulation of G-Protein-Coupled Receptors

Activation of MAP kinase through stimulation of neurotransmitter receptors that are coupled with heterotrimeric GTP-binding proteins is clearly evident in neuronal cells. MAP-kinase activation through the acetylcholine muscarinic M2 receptor coupled to G_i was found to be associated with Ras and Raf activation and was insensitive to genistein, a tyrosine-kinase inhibitor (Winitz et al., 1993). MAP-kinase activation mechanisms, through G_i- and G_q-coupled receptors, were further investigated in COS-7 cells that were transiently expressed by alpha-2A- and 1B-adrenergic receptors and muscarinic M1 receptor (Hawes et al., 1995; van et al., 1995). MAP kinase activation through G_i-coupled alpha-2A receptor was mediated by $\beta\gamma$ subunits of G_i and blocked by expression of dominant-negative $p21^{ras}$ as well as by dominant-negative Raf-1. This pathway was sensitive to a tyrosine-kinase inhibitor but was insensitive to PKC depletion by downregulation. In contrast, MAP-kinase activation through G_q-coupled alpha-1B and M1 receptors was not mediated by $\beta\gamma$ subunits and was not blocked by dominant-negative $p21^{ras}$ and tyrosine-kinase inhibitors. However, the

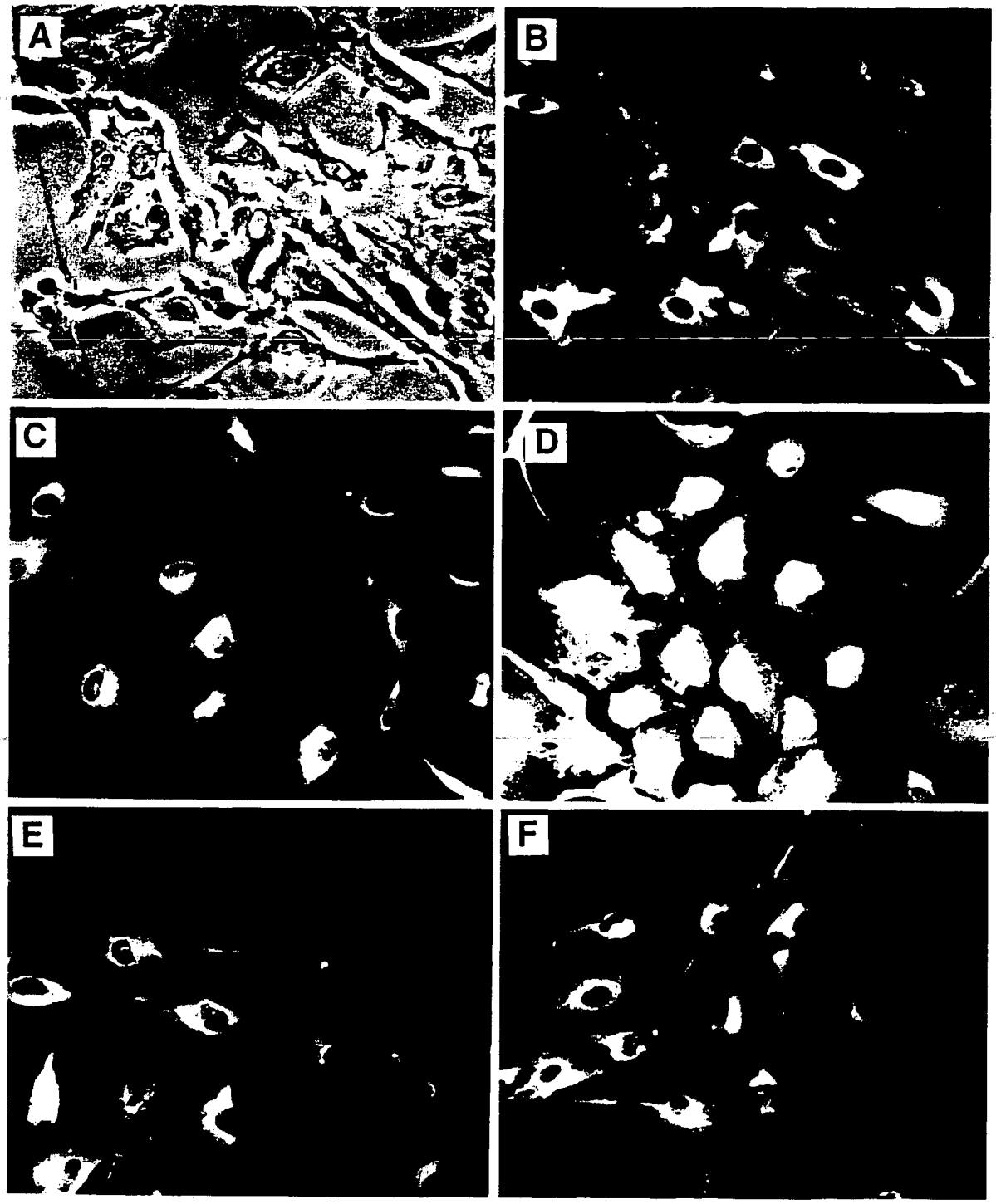

Fig. 4. Translocation of MAP kinase into the nuclei following treatments with bFGF and inhibition of this translocation by dbcAMP and isoproterenol. Indirect immunofluorescent localization of MAP kinase was investigated in cultured rat cortical astrocytes. The astrocytes were incubated for 1 h with no addition (**A** and **B**), 1 m dbc AMP (**C**), 10 ng/mL bFGF (**D**), 10 ng/mL bFGF plus 1 m*M* dbcAMP (**E**), or 10 ng/mL bFGF plus 10 μ*M* isproterenol (**F**) in serum-free culture medium. The cells were fixed in cold methanol, followed by treatment with 0.05% Triton X-100. Fixed cells were incubated with normal rabbit IgG of the rabbit anti-rat MAP-kinase R2 antibody (erk1-CT) (Upstate Biotechnology Inc., New York, NY) and processed to indirect immunofluorescence. The cells were examined by phase-contrast (**A**) and immunofluorescence (**B–F**). 200 X. From Kurino et al. (1996).

MAP-kinase activation was blocked by expression of dominant-negative Raf-1 and PKC depletion. Extensive studies using COS-7 cells with the expressed M2-muscarinic receptor demonstrated that the MAP kinase signaling pathway through βγ subunits was mediated through phosphoinositide 3-kinaseγ (PI3Kγ) and required a tyrosine kinase, probably Src-family kinase, as a downstream kinase (Lopez et al., 1997). Shc, Grab2, Sos, Ras, Raf-1, and MEK underlied in the signaling from the tyrosine kinase to MAP kinase activation, as a common pathway as seen in cases of growth-factor-receptor signaling. Although the PKC-dependent cascade in the activation of MAP kinase through G_q-coupled receptors is not fully understood, activation of Raf-1 through direct phosphorylation by PKC is possibly involved in the PKC-dependent pathway as described (Kolch et al., 1993; Carroll and May, 1994).

The heterogeneity of MAP-kinase signaling through G protein-coupled receptor also remains to be determined. Platelet-activating factor (PAF)-induced activation of MAP kinase is partly prevented by treatment with pertussis toxin (PTX), suggesting that it is G_i-coupled signal, but is not associated with $p21^{ras}$ activation (Honda et al., 1994). In cultured hippocampal neurons, PAF-induced MAP-kinase activation was weakly inhibited by PTX treatment but was abolished by a PKC inhibitor (Fukunaga et al., 1995). This would suggest that PAF-induced MAP-kinase activation in hippocampal neurons is mediated by G_q rather than G_i. Interestingly, in cultured neurons, stimulation of the PAF-receptor potentiated phosphorylation of synapsin I, probably because of activation of MAP kinase (Fukunaga et al., 1995) and in turn stimulated spontaneous excitatory synaptic activity through the AMPA receptor-ion channel (Tokutomi et al., 1997). These observations are consistent with those of BDNF-induced synapsin I phosphorylation and synaptic potentiation, as described above.

In addition to MAP-kinase activation through Gi- and Gq-coupled receptors, stimulation of Gs-coupled receptor may also activate MAP kinase in some cell types, including PC12 cells (Vossler et al., 1997). Accumulation of cyclic AMP does not antagonize the activation of MAP kinases by growth factors but activates MAP kinases (Frodin et al., 1994; Young et al., 1994). Potential role of Rap1, a member of small GTP-binding proteins from the Ras family, has been documented in vivo in the cAMP-mediated activation of B-Raf and in turn, MAP kinases. This is consistent with an observation that B-Raf can be activated by Rap1 in vitro (Ohtsuka et al., 1996).

Functional Implication of MAP Kinase in Physiological and Pathological Events in CNS

Initially, MAP kinase was identified as an insulin-stimulated serine/threonine kinase that phosphorylates microtubule-associated protein 2 (MAP2) and myelin basic protein. In PC12 cells, further characterization of MAP kinase stimulated by treatment with NGF and FGF was performed by using MAP2 as substrate. The *in situ* phosphorylation of MAP2 by MAP kinase was regulated by synaptic activity in both neonatal and adult hippocampal neurons (Quinlan and Halpain, 1996). Although the physiological relevance of MAP kinase-induced phosphorylation of cytoskeletal components such as MAP2 and synapsin I in the organization of the synapse has not been established in the developing nervous system, the phosphorylation of neuronal cytoskeletons are possibly involved in the neurotrophic factor-induced synaptic potentiation in the hippocampus (Lessmann et al., 1994; Levin et al., 1995; Kang and Schuman, 1995). The MAP kinase pathway may also function to regulate synaptic transmission through long-term changes in protein synthesis and gene expression at the nucleus. The stimulation of glutamate-, BDNF-, NT-3-, bFGF-, and PAF-receptors elicits an increase in immediate-early genes such as c-fos and zif-268 in cultured hippocampal neurons (Marsh et al., 1993, 1996; Bading et al., 1993; Ferhat et al., 1993; Bazan and

Allan, 1996). These immediate-early genes are expressed after various physiological and pathological events such as long-term potentiation, seizure, and brain ischemia. A central role of MAP kinase in the expression of the immediate-early genes has been well characterized. The signaling cascade of c-fos expression through glutamate receptors, especially the NMDA receptor, was extensively studied by Greenberg and colleagues (Bading et al., 1993; Miranti et al., 1995; Xia et al., 1996). The NMDA receptor mainly contributes to c-fos gene expression by glutamate stimulation. Elevation of Ca^{2+} through the NMDA receptor stimulates protein-tyrosine kinases including Src-family kinases and protein-tyrosine kinase 2 (PYK2) and in turn potentiates phosphorylation of Shc. The Shc/ Grab2/Sos complex stimulates Ras GDP/GTP-exchanging activity. The potential role of Ras-GRF (Ras-guanine-nucleotide-releasing factor), a member of GDP/GTP exchange factors was found to be involved in the Ca^{2+}-dependent pathway of Ras activation (Farnsworth et al., 1995). Ras-GRF may be related to the Ca^{2+}-dependent Ras activation by stimulation of L-type voltage-dependent Ca^{2+} channel by depolarization. Following the activation of Ras, activation of Raf-1/MEKK and MAP kinase seems to be a common pathway in different stimuli through BDNF, glutamate receptors and L-type voltage-dependent Ca^{2+} channel. However, the signaling cascades underlying c-fos-gene expression differ between NMDA receptor- and depolarization-induced activation, as summarized in Fig. 5. The NMDA-receptor-induced c-fos expression was mediated by transcription factors, including serum- response factor (SRF) and Elk-1, a member of the ternary-complex factors (TCFs). The phosphorylation of Elk-1 was directly mediated by MAP kinase, which in turn bound to serum response element in the promoter region of c-fos gene in combination with SRF as a dimer (Xia et al., 1996). Janknecht and Nordheim (1996) reported that cAMP-dependent protein-kinase can phosphorylate CBP, which binds to CREB and cooperatively potentiates the transcriptional activity of CREB. The regulation of CBP by MAP kinase may also be underlying in the potentiation of c-fos gene expression in cooperation with Elk-1 phosphorylation by MAP kinase (Janknecht and Nordheim, 1996). In contrast, c-fos expression through L-type Ca^{2+}-channel activation was mediated through CaM kinase II and/or CaM kinase IV. CREB is a target transcription factor for CaM kinases and activates c-fos-gene expression by binding to the cyclic AMP-responsive element (CRE) in its promoter region. As shown in Fig. 3, MAP-kinase activation through the L-type Ca^{2+}-channel was totally dependent on activation of CaM kinases because of inhibition by KN93, but the glutamate-induced activation was less well understood. Involvement of CaM kinase IV in MAP-kinase activation was reported by Enslen et al. (1996). In NG108 cells, the transient expression of CaM kinase IV increased activity of members of the MAP-kinase family, including ERK family kinase, c-Jun N-terminal kinase (JNK), and p38 MAP kinase. The mechanism of activation may be functional not only in neuronal cells but also in nonneuronal cells such as smooth muscle cells (Muthalif et al., 1996). Thus, in the depolarization-induced c-fos-gene expression, involvement of the MAP kinase/Elk-1 pathway through the voltage- dependent Ca^{2+} channel remains to be determined, because depolarization stimulates Ras activation through Ras-GRF (Farnsworth et al., 1995) and the depolarization-induced MAP-kinase activation is abolished by KN93 as described above.

In case of bFGF-induced MAP-kinase activation, the activated MAP kinase is translocated into the nucleus where many of the physiological targets for the MAP kinase are located. These substrates may include transcription factors such as c-Myc, c-Jun, and C/EBP beta (NF-IL6) that are known to be regulated by MAP-kinase phosphorylation. Further studies are needed to define the functional roles of transcription factors and their regulation by MAP-kinase phosphorylation in neuronal plasticity.

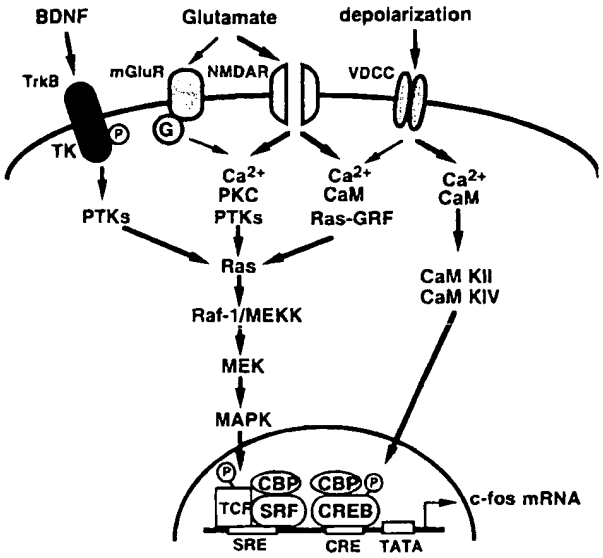

Fig. 5. Signaling pathways for activation of c-fos gene following stimulation with BDNF, glutamate, and depolarization. In cultured hippocampal neurons, stimulation with BDNF, glutamate, or depolarization activates the c-fos gene, through different pathways. The Ras/Raf-1/MAP-kinase pathway mainly contributes to activation of the c-fos gene by stimulation with glutamate and BDNF. In upstream pathways between receptor and Ras activation, the signaling from BDNF receptor, TrkB, has a common pathway with other growth factor receptors containing tyrosine kinase. The diversity of signaling through glutamate receptors to activate Ras has been documented. Both PKC-dependent and Ca^{2+}/calmodulin-dependent pathways have been proposed. Both pathways may share common regulators such as TCF and CBP to activate the c-fos gene. In contrast, stimulation by depolarization may induce the c-fos gene through activation of Ca^{2+}/calmodulin-dependent protein kinases which in turn phosphorylate CREB family proteins. VDCC, voltage-dependent calcium channel; TK, tyrosine kinase; PKC, protein kinase C; CaM, calmodulin; PTKs, protein tyrosine kinases; Ras-GRF, Ras-guanine nucleotide releasing factor; CaM KII and KIV, Ca^{2+}/calmodulin-dependent protein kinases II and IV; CBP, CREB-binding protein; TCF, ternary complex factor; SRF, serum response factor; CREB, cyclic AMP responsive element-binding protein.

Although MAP-kinase activation in pathological events in the brain has been documented, the target molecules of MAP kinase following the activation are not well understood. Phosphorylation of cytosolic phospholipase A2 (cPLA2) is mainly catalyzed by p42 and p44 MAP kinase (ERK1 and ERK2) as well as p38 MAP kinase and results in translocation of the enzyme to membranes and an increase in the intrinsic activity of the enzyme (Durstin et al., 1994; Kan et al., 1996; Kramer et al., 1996; Lin et al., 1993; Sa et al., 1995). cPLA2 is activated and/or induced during brain ischemia (Bazan et al., 1993; Lazarewicz et al., 1992; Owada et al., 1994), an observation consistent with activation of MAP kinase during brain ischemia (Campos-González and Kindy, 1992; Hu et al., 1994). However, activation of cPLA2 dose not always correlate with phosphorylation by MAP kinases (Kramer et al., 1996). The involvement of MAP kinase in phosphorylation of cPLA2 should be investigated during states of brain ischemia. Another possible target for MAP kinase is tau, a microtubule-associated protein, in the brain. Tau is a component of microtubules in soma and axons of neurons and a major component of paired helical filaments (PHFs) observed in brains of patients with Alzheimer's disease. The pathological tau is different from normal tau in its phosphorylation state, in which many Ser-Pro and Thr-Pro motifs in tau protein are highly phosphorylated (Pelech, 1995). Several studies supported the idea that MAP kinase as well as glycogen synthase kinase-3 is implicated in the phosphorylation of tau to produce PHFs (Drewes et al., 1992; Lu et al., 1993; Mandelkow et al., 1992). How the abnormally phosphorylated tau accumulates in PHFs in brains of subjects with Alzheimer's disease has yet to be clarified.

The potential role of MAP kinase in the promotion of neuronal survival seems functional during development of the brain as well as in neurodegenerative disorders. Various neurotrophic and growth factors promote survival as well as morphological differentiation in specific cell types in the brain ERK1 and ERK2, a subgroup of MAP kinase family, were mainly activated by trophic factors and seemed to me-

diate their neurotrophic actions. In addition, other subgroups of MAP-kinase family, c-Jun N-terminal kinase (JNK), and p38 MAP kinase family have been cloned and characterized. Both JNK and p38 MAP kinase have been considered to participate in cellular responses to environmental stresses, inflammatory cytokines, and apoptotic agents rather than mitogenic stimuli. JNK (also named stress-activated protein kinase, SAPK) and p38 MAP kinase are activated by tumor-necrosis factor (TNF), anisomycin, UV light, DNA-damaging agents, interleukin-1, endotoxin, osmotic stress, and heat shock. However, both kinase families have distinct upstream activators and different substrate specificities for transcription factors as target molecules c-Jun, a transcription factor, is a substrate of the JNK-signaling pathway, ATF2 is a target for p38 MAP kinase, and ELK-1 is phosphorylated by all three groups of MAP kinase family. Stimulation of cells with anisomycin and UV radiation induces c-fos and c-jun gene through potentiation of JNK-mediated phosphorylation of Elk-1 and of c-Jun or ATF2, respectively (Hazzalin et al., 1996). The induction of c-Jun is closely related to apoptosis in diverse cell types. Indeed, in case of Alzheimer's disease, the immunoreactivity for c-Jun is elevated in association with the pathological state of neurons (Cotman and Anderson, 1995; Anderson et al., 1994). Beta-amyloid-induced apoptosis was seen to be associated with sustained induction of c-Jun in cultured hippocampal neurons (Anderson et al., 1995). Furthermore, Xia et al. (1995) proposed that JNK and p38 MAP kinase-signaling pathways are implicated in neuronal programmed cell death. In differentiated PC12 cells, NGF withdrawal resulted in apoptosis, which is preceded by an increase in the p38 MAP-kinase activity. Reversibly, activation of ERK signaling by treatment with NGF could eliminate the apoptosis. These opposing effects of ERK and JNK/p38 MAP-kinase signaling were evident in cultured fetal neurons (Heidenreich and Kummer, 1996). The ERK signaling by stimulation with insulin inhibited p38 MAP-kinase activity in cultured neurons. Activation of MAP-kinase phosphatase may be underlying in the insulin-induced p38 MAP-kinase inhibition. This notion is consistent with findings that MAP-kinase phosphatases 1 and 2 (MKP1 and MKP2), dual-specific protein phosphatases, dephosphorylate and inactivate JNK1 and JNK2 that are expressed in COS7 cells in combination with MKP1 or MKP2. Furthermore, in PC12 cells, the UV-stimulated JNK activity is significantly reduced by pretreatment with NGF (Hirsch and Stork, 1997). The expression of MKP1 was reported to be stimulated following limbic epilepsy in the rat brain (Brondello et al., 1997). Another dual-specific phosphatase, PAC-1, was also transcriptionally induced in the rat brain following forebrain ischemia (Wiessner, 1995). Furthermore, the ERK signaling cascade may be directly underlying in the expression of MKP1 and MKP2 (Brondello et al., 1997). Taken together, the cross-talk between ERK signaling and JNK/p38 MAP-kinase signaling has a central role in apoptosis during synaptic elimination and in neurodegenerative disorder. To understand the molecular basis of apoptosis in both neuronal events, the precise signaling cascade of JNK/p38 MAP-kinase activation following apoptotic stimuli has to be established.

In the present article, attention was directed to activation of the MAP-kinase family following diverse stimuli to the brain. Acute effects of neurotrophic and growth factors as well as cytokines such as PAF on the synaptic transmission should be emphasized. MAP kinase is directly implicated in the modulation of synaptic transmission. Although several target proteins such as synapsin I and MAP2 have been proposed regarding substrate for MAP kinase in synapses, further studies are needed to define molecular mechanisms. In addition, MAP kinase activation through the NMDA receptor followed by induction of c-Fos is involved in the gene expression of synaptic components associated with LTP in the hippocampus and account for the long-lasting modification of synaptic transmission. It is an important observation that each of ERKs, JNKs, and p38 MAP kinase has preferential substrates such as NF-IL6, c-Jun, and ATF2, re-

spectively, in the nuclei. On the other hand, some transcription factors such as Elk-1 and CREB/ATF1 serve as a common target for ERKs and p38 MAP kinase (Tan et al., 1996). Taken together, these MAP-kinase family members may have respective specific functions related to survival, neural differentiation, and apoptosis but also have common functions such as neural plasticity, including stress-induced adaptations in the brain.

References

Alderson R. F., Alterman A. L., Barde Y. A., and Lindsay R. M. (1990) Brain-derived neurotrophic factor increases survival and differentiated functions of rat septal cholinergic neurons in culture. *Neuron* **5,** 297–306.

Anderson A. J., Cummings B. J., and Cotman C. W. (1994) Increased immunoreactivity for Jun- and Fos-related proteins in Alzheimer's disease: association with pathology. *Exp. Neurology* **125,** 286–295.

Anderson A. J., Pike C. J., and Cotman C. W. (1995) Differential induction of immediate early gene proteins in cultured neurons by beta-amyloid (A beta): association of c-Jun with A beta-induced apoptosis *J. Neurochem.* **65,** 1487–1498.

Aoyagi A., Nishikawa K., Saito H., and Abe K. (1994) Characterization of basic fibroblast growth factor-mediated acceleration of axonal branching in cultured rat hippocampal neurons. *Brain Res.* **661,** 117–126.

Bading H. and Greenberg M. E. (1991) Stimulation of protein tyrosine phosphorylation by NMDA receptor activation. *Science* **253,** 912–914.

Bading H., Ginty D. D., and Greenberg M. E. (1993) Regulation of gene expression in hippocampal neurons by distinct calcium signaling pathways. *Science* **260,** 181–186.

Baraban J. M., Fiore R. S., Sanghera J. S., Paddon H. B., and Pelech S. L. (1993) Identification of p42 mitogen-activated protein kinase as a tyrosine kinase substrate activated by maximal electroconvulsive shock in hippocampus. *J. Neurochem.* **60,** 330–336.

Barnier J. V., Papin C., Eychene A., Lecoq O., and Calothy G. (1995) The mouse B-Raf gene encodes multiple protein isoforms with tissue-specific expression. *J. Biol. Chem.* **270,** 23,381–23,389.

Bazan N. G. and Allan G. (1996) Platelet-activating factor in the modulation of excitatory amino acid neurotransmitter release and of gene expression. *J. Lipid Mediators Cell Signalling* **14,** 321–330.

Bazan N. G., Allan G., and Rodriguez de Turco E. B (1993) Role of phospholipase A2 and membrane-derived lipid second messengers in membrane function and transcriptional activation of genes: implications in cerebral ischemia and neuronal excitability. *Prog. Brain Res.* 247–257.

Blenis J. (1993) Signal transduction via the MAP kinases: proceed at your own RSK. *Proc. Natl Acad. Sci. USA* **90,** 5889–5892.

Blochl A. and Sirrenberg C. (1996) Neurotrophins stimulate the release of dopamine from rat mesencephalic neurons via Trk and p75Lntr receptors. *J. Biol. Chem.* **271,** 21,100–21,107.

Boulton T. G., Nye S. H., Robbins D. J., Ip N. Y., Radziejewska E., Morgenbesser S. D., De Pinho R. A., Panayotatos N., Cobb M. H., and Yancopoulos G. D. (1991) ERKs: a family of protein-serine/threonine kinases that are activated and tyrosine phosphorylated in response to insulin and NGF. *Cell* **65,** 663–675.

Brondello J. M., Brunet A., Pouyssegur J., and McKenzie F R. (1997) The dual specificity mitogen-activated protein kinase phosphatase-1 and -2 are induced by the p42/p44MAPK cascade. *J. Biol. Chem.* **272,** 1368–1376.

Brott B. K., Alessandrini A., Largaespada D. A., Copeland N. G., Jenkins N. A., Crews C. M., and Erikson R. L. (1993) MEK2 is a kinase related to MEK1 and is differentially expressed in murine tissues. *Cell Growth Differentiation* **4,** 921–929.

Burgering B. M., Pronk G. J., van W. P., Chardin P., and Bos J. L. (1993) cAMP antagonizes p21ras-directed activation of extracellular signal-regulated kinase 2 and phosphorylation of mSos nucleotide exchange factor. *EMBO J.* **12,** 4211–4220.

Campos-González R. and Kindy M. S. (1992) Tyrosine phosphorylation of microtubule-associated protein kinase after transient ischemia in the gerbil brain. *J. Neurochem.* **59,** 1955–1958.

Carroll M. P. and May W. S. (1994) Protein kinase C-mediated serine phosphorylation directly activates Raf-1 in murine hematopoietic cells. *J. Biol. Chem.* **269,** 1249–1256.

Castren E., Pitkanen M., Sirvio J., Parsadanian A., Lindholm D., Thoenen H., and Riekkinen P. J. (1993) The induction of LTP increases BDNF and NGF mRNA but decreases NT-3 mRNA in the dentate gyrus. *NeuroReport* **4,** 895–898.

Catling A. D., Reuter C. W., Cox M. E., Parsons S. J., and Weber M. J. (1994) Partial purification of a mitogen-activated protein kinase kinase activator from bovine brain. Identification as B-Raf or a B-Raf-associated activity. *J. Biol. Chem.* **269,** 30,014–30,021.

Cook S. J. and McCormick F. (1993) Inhibition by cAMP of Ras-dependent activation of Raf [*see* comments]. *Science* **262,** 1069–1072.

Cotman C. W. and Anderson A. J. (1995) A potential role for apoptosis in neurodegeneration and Alzheimer's disease. *Mol. Neurobiol.* **10,** 19–45.

Cowley S., Paterson H., Kemp P., and Marshall C. J. (1994) Activation of MAP kinase kinase is necessary and sufficient for PC12 differentiation and for transformation of NIH 3T3 cells. *Cell* **77,** 841–852.

Crews C. M. and Erikson R. L. (1993) Extracellular signals and reversible protein phosphorylation: what to Mek of it all. *Cell* **74,** 215–217.

Davis R. J. (1993) The mitogen-activated protein kinase signal transduction pathway. *J. Biol. Chem.* **268,** 14,553–14,556.

Drewes G., Lichtenberg K. B., Doring F., Mandelkow E. M., Biernat J., Goris J., Doree M., and Mandelkow E. (1992) Mitogen activated protein (MAP) kinase transforms tau protein into an Alzheimer-like state. *EMBO J.* **11,** 2131–2138.

Durstin M., Durstin S., Molski T. F., Becker E. L., and Sha'afi R. I. (1994) Cytoplasmic phospholipase A2 translocates to membrane fraction in human neutrophils activated by stimuli that phosphorylate mitogen-activated protein kinase. *Proc. Natl. Acad Sci. USA* **91,** 3142–3146.

Enslen H., Tokumitsu H., Stork P. J., Davis R. J., and Soderling T. R. (1996) Regulation of mitogen-activated protein kinases by a calcium/calmodulin-dependent protein kinase cascade. *Proc. Natl. Acad. Sci. USA* **93,** 10,803–10,808.

Fahrig T. and Sommermeyer H. (1993) Dibutyryl cyclic AMP-induced morphological differentiation of rat brain astrocytes increases alpha 1-adrenoceptor induced phosphoinositide breakdown by a mechanism involving protein synthesis. *Brain Res.* **602,** 318–324.

Farnsworth C. L., Freshney N. W., Rosen L. B., Ghosh A., Greenberg M. E., and Feig L. A. (1995) Calcium activation of Ras mediated by neuronal exchange factor Ras-GRF. *Nature* **376,** 524–527.

Ferhat L., Khrestchatisky M., Roisin M. P., and Barbin G. (1993) Basic fibroblast growth factor-induced increase in zif/268 and c-fos mRNA levels is Ca^{2+} dependent in primary cultures of hippocampal neurons. *J. Neurochem.* **61,** 1105–1112.

Finkbeiner S. and Greenberg M. E. (1996) Ca^{2+}-dependent routes to Ras. mechanisms for neuronal survival, differentiation, and plasticity? *Neuron* **16,** 233–236.

Fiore R. S., Murphy T. H., Sanghera J. S., Pelech S. L., and Baraban J. M. (1993) Activation of p42 mitogen-activated protein kinase by glutamate receptor stimulation in rat primary cortical cultures. *J. Neurochem.* **61,** 1626–1633.

Frodin M., Peraldi P., and Obberghen E. V. (1994) Cyclic AMP activates the mitogen-activated protein kinase cascade in PC12 cells. *J. Biol. Chem.* **269,** 6207–6214.

Fukunaga K., Ohmitsu M., and Miyamoto E. (1995) PAF-induced activation of CaM kinase II and MAP kinase in cultured rat hippocampal neurons. *Abs. Soc. Neurosc.*. **21,** 598.

Gass P., Kiessling M., and Bading H. (1993) Regionally selective stimulation of mitogen activated protein (MAP) kinase tyrosine phosphorylation after generalized seizures in the rat brain. *Neurosci. Lett.* **162,** 39–42.

Häfner S., Adler H. S., Mischak H., Janosch P., Heidecker G., Wolfman A., Pippig S., Lohse M., Ueffing M., and Kolch W. (1994) Mechanism of inhibition of Raf-1 by protein kinase A. *Mol. Cell. Biol.* **14,** 6696–6703.

Hawes B. E., van B. T., Koch W. J., Luttrell L. M., and Lefkowitz R. J. (1995) Distinct pathways of Gi- and Gq-mediated mitogen-activated protein kinase activation. *J. Biol. Chem.* **270,** 17,148–17,153.

Hazzalin C. A., Cano E., Cuenda A., Barratt M. J., Cohen P., and Mahadevan L. C. (1996) p38/RK is essential for stress-induced nuclear responses: JNK/SAPKs and c-Jun/ATF-2 phosphorylation are insufficient. *Current Biol.* **6,** 1028–1031.

Heidenreich K. A. and Kummer J. L. (1996) Inhibition of p38 mitogen-activated protein kinase by insulin in cultured fetal neurons *J.Biol. Chem* **271,** 9891–9894.

Hirsch D. D. and Stork P. J. (1997) Mitogen-activated protein kinase phosphatases inactivate stress-activated protein kinase pathways in vivo. *J. Biol. Chem.* **272,** 4568–4575.

Honda Z., Takano T., Gotoh Y., Nishida E., Ito K., and Shimizu T. (1994) Transfected platelet-activating factor receptor activates mitogen-activated protein (MAP) kinase and MAP kinase kinase in Chinese hamster ovary cells. *J. Biol. Chem.* **269,** 2307–2315.

Hu B. R. and Wieloch T. (1994) Tyrosine phosphorylation and activation of mitogen-activated protein kinase in the rat brain following transient cerebral ischemia *J. Neurochem.* **62,** 1357–1367.

Hyman C., Hofer M., Barde Y. A., Juhasz M., Yancopoulos G. D., Squinto S. P., and Lindsay R. M. (1991) BDNF is a neurotrophic factor for dopaminergic neurons of the substantia nigra. *Nature* **350,** 230–232.

Janknecht R. and Nordheim A. (1996) Regulation of the c-fos promoter by the ternary complex factor Sap-1a and its coactivator CBP. *Oncogene* **12,** 1961–1969.

Johnson J. E., Barde Y. A., Schwab M., and Thoenen H. (1986) Brain-derived neurotrophic factor supports the survival of cultured rat retinal ganglion cells. *J. Neurosci.* **6,** 3031–3038.

Jovanovic J. N., Benfenati F., Siow Y. L., Sihra T. S., Sanghera J. S., Pelech S. L., Greengard P., and Czernik A. J. (1996) Neurotrophins stimulate phosphorylation of synapsin I by MAP kinase and regulate synapsin I-actin interactions. *Proc. Natl. Acad. Sci. USA* **93,** 3679–3683.

Kan H., Ruan Y., and Malik K. U. (1996) Involvement of mitogen-activated protein kinase and translocation of cytosolic phospholipase A2 to the nuclear envelope in acetylcholine-induced prostacyclin synthesis in rabbit coronary endothelial cells. *Mol. Pharmacol.* **50,** 1139–1147.

Kang H. and Schuman E. M. (1995) Long-lasting neurotrophin-induced enhancement of synaptic transmission in the adult hippocampus. *Science* **267,** 1658–1662.

Klein R., Parada L. F., Coulier F., and Barbacid M. (1989) trkB, a novel tyrosine protein kinase receptor expressed during mouse neural development. *EMBO J.* **8,** 3701–3709.

Klein R., Martin Z. D., Barbacid M., and Parada L. F. (1990a) Expression of the tyrosine kinase receptor gene trkB is confined to the murine embryonic and adult nervous system. *Development* **109,** 845–850.

Klein R., Conway D., Parada L. F., and Barbacid M. (1990b) The trkB tyrosine protein kinase gene codes for a second neurogenic receptor that lacks the catalytic kinase domain. *Cell* **61,** 647–656.

Knipper M, da, Penha, Berzaghi, M., Blochl A., Breer H., Thoenen H., and Lindholm D. (1994a) Positive feedback between acetylcholine and the neurotrophins nerve growth factor and brain-derived neurotrophic factor in the rat hippocampus. *Eur. J. Neurosci.* **6,** 668–671.

Knipper M., Leung L. S., Zhao D., and Rylett R. J. (1994b) Short-term modulation of glutamatergic synapses in adult rathippo campus by NGF. *NeuroReport* **5,** 2433–2436.

Knusel B., Winslow J. W., Rosenthal A., Burton L. E., Seid D. P., Nikolics K., and Hefti F. (1991) Promotion of central cholinergic and dopaminergic neuron differentiation by brain-derived neurotrophic factor but not neurotrophin 3. *Proc. Natl. Acad. Sci. USA* **88,** 961–965.

Kolch W., Heidecher G., Kochs G., Hummel R., Vahidi H., Mischak H., Finkenzeller G., Marmé D., and Rapp U. R. (1993) Protein kinase Cα activates RAF-1 by direct phosphorylation. *Nature* **364,** 249–252.

Korte M., Carroll P., Wolf E., Brem G., Thoenen H., and Bonhoeffer T. (1995) Hippocampal long-term potentiation is impaired in mice lacking brain-derived neurotrophic factor. *Proc. Natl. Acad Sci. USA* **92,** 8856–8860.

Kramer R M., Roberts E. F., Um S. L., Borsch H. A., Watson S. P., Fisher M. J., and Jakubowski J. A. (1996) p38 mitogen-activated protein kinase phosphorylates cytosolic phospholipase A2 (cPLA2) in thrombin-stimulated platelets. Evidence that proline-directed phosphorylation is not required for mobilization of arachidonic acid by cPLA2. *J. Biol. Chem.* **271,** 27,723–27, 729.

Kurino M., Fukunaga K., Ushio Y., and Miyamoto E. (1995) Activation of mitogen-activated protein kinase in cultured rat hippocampal neurons by stimulation of glutamate receptors. *J. Neurochem.* **65,** 1282–1289.

Kurino M., Fukunaga K., Ushio Y., and Miyamoto E. (1996) Cyclic AMP inhibits activation of mitogen-activated protein kinase and cell proliferation in response to growth factors in cultured rat cortical astrocytes. *J. Neurochem.* **67,** 2246–2255.

Lamballe F., Smeyne R. J., and Barbacid M. (1994) Developmental expression of trkC, the neurotrophin-3 receptor, in the mammalian nervous system. *J. Neurosci.* **14,** 14–28.

Lazarewicz J. W., Salinska E., and Wroblewski J. T. (1992) NMDA receptor-mediated arachidonic acid release in neurons: role in signal transduction and pathological aspects. *Adv. Exp. Med. Biol.* 73–89.

Lessmann V., Gottmann K., and Heumann R. (1994) BDNF and NT-4/5 enhance glutamatergic synaptic transmission in cultured hippocampal neurones. *NeuroReport* **6,** 21–25.

Levine E. S., Dreyfus C. F., Black I. B., and Plummer M. R. (1995) Brain-derived neurotrophic factor rapidly enhances synaptic transmission in hippocampal neurons via postsynaptic tyrosine kinase receptors. *Proc. Natl. Acad. Sci. USA* **92,** 8074–8077.

Lin L. L., Wartmann M., Lin A. Y., Knopf J. L., Seth A., and Davis R. J. (1993) cPLA2 is phosphorylated and activated by MAP kinase. *Cell* **72,** 269–278.

Lopez I. M., Crespo P., Pellici P. G., Gutkind J. S., and Wetzker R. (1997) Linkage of G protein-coupled receptors to the MAPK signaling pathway through PI 3-kinase gamma. *Science* **275,** 394–397.

Lu Q., Soria J. P., and Wood J. G. (1993) p44mpk MAP kinase induces Alzheimer type alterations in tau function and in primary hippocampal neurons. *J. Neurosci. Res.* **35,** 439–444.

Maisonpierre P. C., Belluscio L., Squinto S., Ip N. Y., Furth M. E., Lindsay R. M., and Yancopoulos G. D. (1990) Neurotrophin-3: a neurotrophic factor related to NGF and BDNF. *Science* **247,** 1446–1451.

Mandelkow E. M., Drewes G., Biernat J., Gustke N., Van L. J., Vandenheede J. R., and Mandelkow E. (1992) Glycogen synthase kinase-3 and the Alzheimer-like state of microtubule-associated protein tau. *FEBS Lett.* **314,** 315–321.

Marsh H. N. and Palfrey H. C. (1996) Neurotrophin-3 and brain-derived neurotrophic factor activate multiple signal transduction events but are not survival factors for hippocampal pyramidal neurons. *J. Neurochem.* **67,** 952–963.

Marsh H. N., Scholz W. K., Lamballe F., Klein R., Nanduri V., Barbacid M., and Palfrey H. C. (1993) Signal transduction events mediated by the BDNF receptor gp 145trkB in primary hippocampal pyramidal cell culture. *J. Neurosci.* **13,** 4281–4292

Marshall C. J. (1995) Specificity of receptor tyrosine kinase signaling transient versus sustained extracellular signal-regulated kinase activation. *Cell* **80,** 179–185.

Miranti C. K., Ginty D. D., Huang G., Chatila T., and Greenberg M. E. (1995) Calcium activates serum response factor-dependent transcription by a Ras- and Elk-1-independent mechanism that involves a Ca^{2+}/calmodulin-dependent kinase. *Mol. Cell Biol.* **15,** 3672–3684.

Muthalif M. M., Benter I. F., Uddin M. R., and Malik K. U. (1996) Calcium/calmodulin-dependent protein kinase IIalpha mediates activation of mitogen-activated protein kinase and cytosolic phospholipase A2 in norepinephrine-induced arachidonic acid release in rabbit aortic smooth muscle cells. *J. Biol. Chem.* **271,** 30,149–30,157.

Nishida E. and Gotoh Y. (1993) The MAP kinase cascade is essential for diverse signal transduction pathways. *Trends Biochem. Sci.* **18,** 128–131.

Norris J. G., Tang L. P., Sparacio S. M., and Benveniste E. N. (1994) Signal transduction pathways mediating astrocyte IL-6 induction by IL-1 beta and tumor necrosis factor-alpha. *J. Immunol.* **152,** 841–50.

Ohtsuka T., Shimizu K., Yamamori B., Kuroda S., and Takai Y. (1996) Activation of brain B-Raf protein kinase by Rap1B small GTP-binding protein. *J. Biol. Chem.* **271,** 1258–1261.

Ortiz J., Harris H. W., Guitart X., Terwilliger R. Z., Haycock J. W., and Nestler E. J. (1995) Extracellular signal-regulated protein kinases (ERKs) and ERK kinase (MEK) in brain: regional distribution and regulation by chronic morphine. *J. Neurosci.* **15,** 1285–1297.

Owada Y., Tominaga T., Yoshimoto T., and Kondo H. (1994) Molecular cloning of rat cDNA for cytosolic phospholipase A2 and the increased gene expression in the dentate gyrus following transient forebrain ischemia. *Brain Res. Mol. Brain Res.* **25,** 364–368.

Patterson S. L., Grover L. M., Schwartzkroin P. A., and Bothwell M. (1992) Neurotropin expression in rat hippocampal slices, a stimulus paradigm inducing LTP in CA1 evokes increases in BDNF and NT-3 mRNAs. *Neuron* **9,** 1081–1088.

Pelech S. L. (1995) Networking with proline-directed protein kinases implicated in tau phosphorylation. *Neurobiol. Aging* **16,** 247–256.

Quinlan E. M. and Halpain S. (1996) Emergence of activity-dependent, bidirectional control of microtubule-associated protein MAP2 phosphorylation during postnatal development. *J. Neurosci.* **16,** 7629–7637.

Riva M. A., Molteni R., Lovati E., Fumagalli F., Rusnati M., and Racagni G. (1996) Cyclic AMP-dependent regulation of fibroblast growth factor-2 messenger RNA levels in rat cortical astrocytes.: comparison with fibroblast growth factor-1 and ciliary neurotrophic factor. *Mol. Pharmacol.* **49,** 699–706.

Roback J. D., Marsh H. N., Downen M., Palfrey H. C., and Wainer B. H. (1995) BDNF-activated signal transduction in rat cortical glial cells. *Eur. J. Neurosci.* **7,** 849–862.

Robbins D. J., Cheng M., Zhen E., Vanderbilt C. A., Feig L. A., and Cobb M. H. (1992) Evidence for a Ras-dependent extracellular signal-regulated

protein kinase (ERK) cascade. *Proc. Natl. Acad. Sci. USA* **89,** 6924–6928.

Sa G., Murugesan G., Jaye M., Ivashchenko Y., and Fox P. L. (1995) Activation of cytosolic phospholipase A2 by basic fibroblast growth factor via a p42 mitogen-activated protein kinase-dependent phosphorylation pathway in endothelial cells. *J. Biol. Chem.* **270,** 2360–2366.

Storm S. M., Cleveland J. L., and Rapp U. R. (1990) Expression of raf family protooncogenes in normal mouse tissues. *Oncogene* **5,** 345–351.

Stratton K. R., Worley P. F., Litz J. S., Parsons S. J., Huganir R. L., and Baraban J. M. (1991) Electroconvulsive treatment induces a rapid and transient increase in tyrosine phosphorylation of a 40-kilodalton protein associated with microtubule-associated protein 2 kinase activity. *J. Neurochem.* **56,** 147–152.

Tan Y., Rouse J., Zhang A., Cariati S., Cohen P., and Comb M. J. (1996) FGF and stress regulate CREB and ATF-1 via pathway involving p38 MAP kinase and MAPKAP kinase-2 *EMBO J.* **15,** 462–4642.

Tanaka T., Saito H. and Matsuki N. (1996) Basic fibroblast growth factor modulates synaptic transmission in cultured rat hippocampal neurons. *Brain Res.* **723,** 190–195.

Thomas K. L. and Hunt S. P. (1993) The regional distribution of extracellularly regulated kinase-1 and -2 messenger RNA in the adult rat central nervous system. *Neuroscience* **56,** 741–757.

Tokutomi N., Fukunaga K., Tokutomi Y., Miyamoto E., and Nishi K. (1997) Platelet-activating factor, a dual modulation of excitatory synaptic transmission in the rat hippocampus. *Japan J. Pharmacol.* **73,** 176P.

Tournier C., Pomerance M., Gavaret J. M., and Pierre M. (1994) MAP kinase cascade in astrocytes. *Glia* **10,** 81–88.

Traverse S., Gomez N., Paterson H., Marshall C., and Cohen P. (1992) Sustained activation of the mitogen-activated protein (MAP) kinase cascade may be required for differentiation of PC12 cells. Comparison of the effects of nerve growth factor and epidermal growth factor. *Biochem. J.* **288,** 351–355.

van B. T., Hawes B. E., Luttrell D. K., Krueger K. M., Touhara K., Porfiri E., Sakaue M., Luttrell L. M., and Lefkowitz R. J. (1995) Receptor-tyrosine-kinase- and G beta gamma-mediated MAP kinase activation by a common signalling pathway. *Nature* **376,** 781–784.

Vossler M. R., Yao H., York R. D., Pan M.-G., Rim C. S., and Stork P. J. S. (1997) cAMP activates MAP kinase and Elk-1 through a B-Raf- and Rap1-dependent pathway. *Cell* **89,** 73–82.

Wiessner C. (1995) The dual specificity phosphatase PAC-1 is transcriptionally induced in the rat brain following transient forebrain ischemia. *Brain Res. Mol. Brain Res.* **28,** 353–356.

Winitz S., Russell M., Qian N. X., Gardner A., Dwyer L., and Johnson G. L. (1993) Involvement of Ras and Raf in the Gi-coupled acetylcholine muscarinic m2 receptor activation of mitogen-activated protein (MAP) kinase kinase and MAP kinase. *J. Biol. Chem.* **268,** 19,196–19,199.

Wood K. W., Sarnecki C., Roberts T. M., and Blenis J. (1992) ras mediates nerve growth factor receptor modulation of three signal-transducing protein kinases: MAP kinase, Raf-1, and RSK. *Cell* **68,** 1041–1050.

Xia Z., Dickens M., Raingeaud J., Davis R. J., and Greenberg M. E. (1995) Opposing effects of ERK and JNK-p38 MAP kinases on apoptosis. *Science* **270,** 1326–1331.

Xia Z., Dudek H., Miranti C. K., and Greenberg M. E. (1996) Calcium influx via the NMDA receptor induces immediate early gene transcription by a MAP kinase/ERK-dependent mechanism. *J. Neurosci.* **16,** 5425–5436.

Young S. W., Dickens, M., and Tavaré J. M. (1994) Differentiation of PC12 cells in response to a cAMP analogue is accompanied by sustained activation of mitogen-activated protein kinase. Comparison with the effects of insulin, growth factors and phorbol esters. *FEBS Lett.* **338,** 212–216.

Exhibit D

Cellular Immunology 203, 29–38 (2000)
doi:10.1006/cimm.2000.1668, available online at http://www.idealibrary.com on IDEAL®

Role of cAMP-Dependent Pathway in Eosinophil Apoptosis and Survival

Hun Soo Chang,* Ki Won Jeon, Young Hoon Kim, Il Yup Chung,* and Choon Sik Park

*Division of Allergy and Respiratory Medicine, Department of Internal Medicine, Soonchunhyang University Hospital, and *Department of Biochemistry and Molecular Biology, Hanyang University, Seoul, Korea*

Received February 1, 2000; accepted May 18, 2000

The survival and apoptosis of eosinophils is of pivotal importance for controlling allergic diseases such as asthma and rhinitis. In this study we have investigated the role for cAMP in regulating eosinophil survival and apoptosis in the absence of eosinophil-active cytokines. The treatment with dibutyryl cyclic AMP (dbcAMP) increased eosinophil survival with a concomitant decrease of apoptosis in a dose-dependent manner. The pretreatment with a protein kinase A (PKA) inhibitor blocked the effects of dbcAMP on survival and apoptosis of eosinophils. The catalytic subunit of PKA was translocated to nucleus in parallel with a robust increase of intracellular cAMP levels upon exposure to dbcAMP but not IL-5, suggesting the separation of PKA activation from the IL-5-induced suppression of eosinophil apoptosis. When eosinophils were treated with pharmacological inhibitors of protein kinases prior to exposure to dbcAMP or IL-5, only the mitogen-activating protein kinase (MAPK) inhibitor, PD098059, was partly able to block dbcAMP-induced augmentation of eosinophil viability, whereas both Janus kinase 2 and MAPK inhibitors effectively interrupted the IL-5-induced prolongation of eosinophil survival. The effects of dbcAMP and these protein kinase inhibitors on eosinophil apoptosis were confirmed by morphologic analysis. We propose that a cAMP-dependent pathway may constitute an important component for regulating eosinophil survival/apoptosis and that cAMP may inhibit eosinophil apoptosis through the activation of PKA and of subsequent MAPK in part. © 2000 Academic Press

INTRODUCTION

Eosinophils are the major effector cells in damaging airway tissues by releasing toxic mediators into target sites, and thus play an important role in the development of allergic diseases such as asthma and rhinitis (1–3). Because of such destructive property in the allergic state, the eosinophil survival should be strictly regulated *in vivo*. The inhibition of eosinophil apoptosis may be a principal mechanism by which eosinophil survival is maintained and prolonged, thereby sustaining the effector functions of eosinophils in allergic inflammation (4, 5; see review in 6). The initiation of apoptosis, therefore, is of therapeutic interest for resolving the eosinophilic inflammation of respiratory allergy. Interleukin-5 (IL-5) is the most potent cytokine that regulates the differentiation and activation of eosinophils and is thought to be responsible for blood and tissue eosinophilia (4, 7–9). IL-5 binding to its receptor has recently been shown to activate a number of protein tyrosine kinases including Lyn (10, 11), Janus kinase 2 (Jak2) (10), Fyn (12), and Syk (11, 13). The activation of the tyrosine kinases subsequently leads to the activation of a Ras-Raf-1-mitogen-activating protein kinase (MAPK) pathway for eosinophil survival (14, 15). Jak2 directly phosphorylates signal transducer and activator of transcription (STAT)1 to suppress eosinophil apoptosis (16, 17).

Other pathways for the inhibition of eosinophil apoptosis besides the tyrosine kinases-mediated signal transductions have not been clearly demonstrated. The increase of the intracellular cAMP concentration by using cAMP analogs or agents that cause to enhance intracellular cAMP level is shown to prevent eosinophils from spontaneous apoptosis (18) and Fas-induced apoptosis (19). Similarly, the elevation of intracellular cAMP is also observed to inhibit apoptosis in some cell types when they are deprived of growth factors (20), and exposed to cytokines (21), nitric oxide (22), and cycloheximide (23). The major intracellular receptor for cAMP is a regulatory (R) subunit of protein kinase A (PKA). Binding of cAMP to the R subunit releases a catalytic (C) subunit from the R subunit, leading to nuclear localization and subsequent activation of downstream signaling and transcription events (24), which are likely to account for recognized roles for cAMP in certain functions. Among the downstream signalings, the cAMP-dependent pathway may have cross-talk-type interactions with early transmembrane signaling mechanisms. Most notably, PKA activation has been shown to uncouple heterogeneous receptors to

0008-8749/00 $35.00

phosphoinositide-specific phospholipases C (25), resulting in the inhibition of agonist-dependent increases in intracellular Ca^{2+} concentration (26).

Although the increase of intracellular cAMP is shown to suppress eosinophil apoptosis, it is not known whether the resulting PKA activation is essential for eosinophil survival. Moreover, the interaction of the cAMP-dependent pathway with Jak2 and components of a MAP kinase cascade remains unclear in the process of eosinophil apoptosis. In the present study, we examined the role for cAMP in regulating apoptosis/survival of human eosinophils, whether the nuclear localization of PKA occurs in inducing cAMP-mediated suppression of eosinophil apoptosis, and whether Jak2 and MAP kinase pathways influence the cAMP-induced alteration of eosinophil apoptosis.

MATERIALS AND METHODS

Reagents

Human serum albumin and RPMI1640 medium were purchased from GIBCO BRL (Gaithersburg, MD). CD16 monoclonal antibody-conjugated microbeads were purchased from Miltenyi Biotec (Belgisch-Gladbach, Germany). Dibutyryl cyclic AMP (dbcAMP, N^6,2′-*O*-dibutytyladenosine 3′,5′-cyclic monophosphate), propidium iodide (PI), and RNase A were purchased from Sigma Chemical Co. (St. Louis, MO). *N*-[2-(*p*-bromocinnamylamino)ethyl]-5-isoquinoline sulfonamide (H89), a specific inhibitor of PKA, was obtained from Biomol Research Laboratories, Inc. (Plymouth Meeting, PA). An inhibitor of Jak2 kinase, AG-490 (tyrphostins B42 [2-cyano-3-(3,4-dihydroxyphenyl)-*N*-(benzyl)-2-propenamide]), and an inhibitor of MAPK kinase, PD 098059 ([2-(2-amino-3-methoxyphenyl)-oxanaphthalen-4-one]), were obtained from RBI (Natick, MA). Recombinant human IL-5 was purchased from R&D Systems (Minneapolis, MN). Diff-Quik solution was obtained from American Scientific Products (McGaw Park, IL). Rabbit polyclonal anti-human PKAα cat (C-20) antibody was purchased from Santa Cruz Biotechnology, Inc. (Santa Cruz, CA). Peroxidase-conjugated goat IgG anti-rabbit IgG was purchased from Cappel Research Products (Durham, NC). Enhanced chemiluminescence (ECL) and cAMP enzyme immunoassay system (Biotrak) was obtained from Amersham Pharmacia Biotech (Piscataway, NJ). Nitrocellulose filter (Protran) was purchased from Schleicher & Schuell Co. (Keene, NH).

Eosinophil Purification

Eosinophils were isolated from peripheral blood of atopic subjects as previously described (27). Briefly, after the removal of erythrocytes, a leukocyte-rich layer was centrifuged at 300*g* for 10 min and then washed twice in [piperazinebis (ethanesulfonic acid)] (Pipes) buffer (25 nM Pipes, 110 mM NaCl, 5 mM KCl, 40 mM NaOH, and 5.4 mM glucose). Percoll and Pipes buffer were mixed and layered at the indicated volumes in 140 × 10-mm polystyrene tubes. The leukocyte-rich suspension in 2 ml of the Percoll solution (1.070 g/ml) was layered on top of the gradients and centrifuged at 1600*g* for 30 min at 4°C. The enriched eosinophil fractions were incubated with CD16 monoclonal antibody-conjugated microbeads (Miltenyi Biotec), and negative selection was carried out with a magnetic cell separator (MACS system; Becton-Dickinson, Mountain View, CA) to remove the contaminated neutrophils. The purity of eosinophils was more than 98% as determined on the microscopic examination of cytocentrifuge slides prepared by Diff-Quik stain. The viability was more than 98% at the beginning of culture.

Eosinophil Cultures

Purified eosinophils were suspended at a concentration of 1×10^6 cells/ml in tissue culture medium (TCM), which includes RPMI 1640 medium containing 2-mercaptoethanol (50 mM), garamycin (10 μg/ml), and 1% human serum albumin. A 100-μl volume of the eosinophil suspension was added to each well of 96-well microplates and incubated at 37°C in 5% CO_2 incubator in the presence of varying concentrations of the reagents such as dbcAMP (5×10^{-6}–5×10^{-4} M), H89, AG-490, and PD 098059. To determine whether the activation of PKA is involved in the dbcAMP-induced enhancement of eosinophil survival, eosinophils were incubated in the presence of dbcAMP for 72 h with or without pretreatment with H89 for 15 min. The same procedures were employed to examine the effects of dbcAMP on apoptosis except for 24 h incubation period in place of 72 h. To determine whether the activation of MAP kinase and Jak2 is involved in the dbcAMP-induced enhancement of eosinophil survival, eosinophils were pretreated with either 30 μM AG-490 or 100 μM PD 98059 for 15 min and then exposed to dbcAMP (5×10^{-4} M) for the additional 72 h. TCM and IL-5 (0.1 ng/ml) were used as negative and positive controls, respectively, in each experiment. Triplicate cultures were set up for each sample.

Assessment of Viability and Apoptosis

Both viability and apoptosis of eosinophils were determined by measuring propidium iodide (PI)-stained cells with a flow cytometer (FACscan, Becton-Dickinson). For the measurement of cell viability, eosinophils were incubated with reagents for 72 h and stained with PI (2 μg/ml). The viability of cultured eosinophils was accessed by PI exclusion. The PI-excluded eosinophils were considered viable cells. At least 1×10^4 cells were analyzed. Red fluorescence of PI-stained, dead cells was measured with FL2 detector as previously de-

scribed (28). The percentage of viability was calculated as [(the number of viable cells/the number of total cells) × 100]. On the other hand, the quantitative analysis of eosinophil apoptosis was carried out by measuring the amount of DNA of PI-stained eosinophils (29). Briefly, eosinophils (100 μl) cultured for 24 h were centrifuged, resuspended in 2 ml of cold 70% ethanol, and incubated at 4°C for 1 h. The cell suspension was washed with phosphate-buffered saline (PBS) by centrifugation and resuspended in 0.5 ml PBS. The cell suspension was treated with 0.5 ml RNase A (100 μg/ml) and was followed by the addition of 1 ml of PI (100 μg/ml) in PBS. The cells were incubated in the dark at room temperature for 15 min and kept at 4°C until measurement. Ten thousand cells from each sample were analyzed in triplicate.

Measurement of Intracellular cAMP Levels

Intracellular cAMP concentrations were determined using a cAMP enzyme immunoassay kit (Amersham) according to the manufacturer's instructions. Briefly, eosinophils (1×10^4 cells) were treated with dbcAMP (4×10^{-4} M) or IL-5 (0.1 ng/ml) for different time intervals, harvested, lysed by the addition of 65% (v/v) ethanol, and centrifuged at 2000*g* at 4°C. The supernatant was dried and solubilized in 100 μl of the assay buffer. Each 100 μl of samples and standards were added to each well of 96-well microplates that had been coated with donkey anti-rabbit IgG and reacted with 100 μl of a rabbit anti-cAMP antibody at 4°C for 2 h. Fifty microliters of cAMP-conjugated peroxidase was added to the reaction mixture and incubated at 4°C for 1 h. After aspiration and washing of wells, 150 μl of substrate (diaminobenzidine) solution was added, and then the microplate was shaken for 60 min at room temperature until color was developed. The reactions was stopped by the addition of 100 μl of 1 M sulfuric acid, and the plates were read on MAXline microplate readers (Molecular Devices Corp., Menlo Park, CA) using a wavelength of 450 nm. The absolute concentration of cAMP was determined by extrapolation from the standard curve that was generated by using known amounts of cAMP, and expressed as fmol/10^4 cells. Duplicate measurements were set up for each sample and standard.

Morphologic Analysis of Apoptosis

Eosinophil apoptosis was also analyzed by light microscopic examination as follows. Fifty microliters of cultured eosinophils was diluted to thirds with Ca^{2+}- and Mg^{2+}-free PBS and cytocentrifuged at 500*g* for 5 min using a Cytospin II (Shandon Southerland, Sewickley, PA). After air drying, the applied cells were stained with Diff-Quik, dried, and examined under a light microscopy at 400× magnification. The morphologic criteria of apoptosis include (a) reduced cell volume containing a densely stained nuclear lobe, (b) the absence of chromatin within nuclear fragments, and (c) a cellular fragment containing a densely stained nuclear fragment.

Immunoblot Analysis of Catalytic Component of PKA

Cultured eosinophils (3×10^6 cells) that had been treated with dbcAMP (5×10^{-4} M) or IL-5 (0.1 ng/ml) were washed with PBS twice, lysed mechanically in buffer AT (15 mM Hepes, pH 7.9, 60 nM KCl, 15 mM NaCl, 14 mM 2-mercaptoethanol, 2 mM EDTA, 0.3 M sucrose, 5 μg/ml aprotinin, 10 μg/ml leupeptin, 2 μg/ml pepstatin, 0.1 mM phenylmethylsulfonyl fluoride (PMSF), and 0.1% Triton X-100) with a tuberculin syringe and incubated for 5 min on ice. The cell lysate was layered on 1 vol of a sucrose cushion containing 1 M sucrose in AT buffer and centrifuged at 10,000*g* for 5 min. The pellet and the supernatant represent nuclear and cytoplasmic fractions, respectively. Protein (200 μg) was resolved by sodium dodecyl sulfate (SDS)–polyacrylamide gel (12%) electrophoresis and electrophoretically transferred to nitrocellulose filter. The nitrocellulose paper was rinsed in Tris-buffered saline with Tween 20 (TBST) (10 mM Tris–HCl, pH 8, 150 mM NaCl, 0.05% Tween 20) and blocked with 5% nonfat dry milk in TBST for 1 h. The membrane was probed with a rabbit polyclonal antibody (1:1000 dilution) raised against alpha catalytic subunit of human PKA (Santa Cruz, CAL) for 2 h. After washing three times with TBST for 15 min, the membrane was incubated with a peroxidase-conjugated anti rabbit IgG (1:20,000 dilution) (Cappel Research Product; Durham, NC) in TBST for 1 h and developed by enhanced chemiluminescence (ECL) (Amersham Pharmacia Biotech.) according to the manufacturer's instruction.

Statistics

Wilcoxon signed rank test was applied to the changes of apoptosis and viability by treatment with agents used in the study. The difference was considered significant when the *P* value was less than 0.05. The results were expressed as mean ± standard error of the mean (SEM) unless otherwise stated.

RESULTS

Effects of dbcAMP on the Survival and Apoptosis of Eosinophils

To examine whether intracellular cAMP levels could affect the eosinophil survival and apoptosis, freshly isolated eosinophils (1.0×10^5 cells/0.1 ml) were treated with different concentrations of dbcAMP (5×10^{-6}–5×10^{-4} M), an cAMP analog, and their viability and apoptosis were determined by measuring PI exclusion and PI-incorporated DNA amount, respectively. As shown in Fig. 1a, only 21.9±2.2% of unstimulated eosinophils survived after culture for 72 h (the average

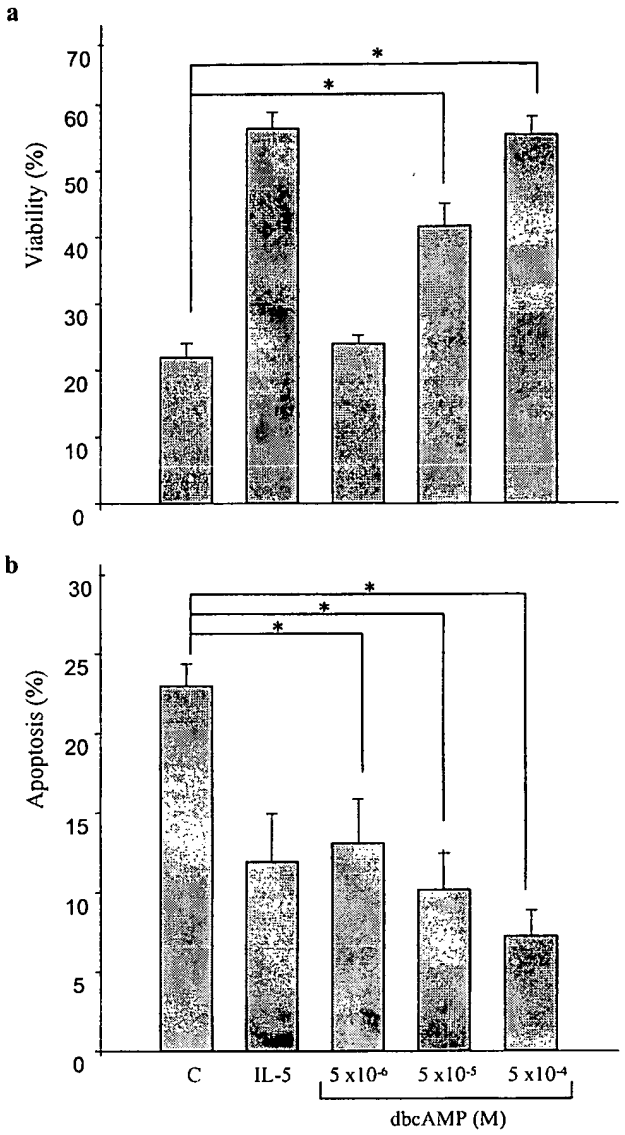

FIG. 1. The effect of dbcAMP on eosinophil survival (a) and apoptosis (b). Eosinophils (1×10^5 cells) on 96-well microplate were incubated in the presence of varying concentrations of dbcAMP or IL-5 (0.1 ng/ml). Eosinophil viability and apoptosis were determined after 72- and 24-h incubation, respectively, as described under Materials and Methods. The data presented are the mean ± SEM of six independent experiments done in triplicate. Statistical analysis was performed comparing medium (C) alone values to those obtained with dbcAMP. $^*P < 0.05$.

of six independent experiments, $n = 6$). IL-5 stimulation increased eosinophil survival (56.4 ± 2.5%), as expected. When eosinophils were cultured in the presence of dbcAMP (5×10^{-4} M), the viability was significantly increased up to a comparable level to that induced by IL-5 (0.1 ng/ml). The fold increase over medium value was 2.2 and 2.8 at 5×10^{-5} and 5×10^{-4} M dbcAMP, respectively. To determine the effect of dbcAMP on eosinophil apoptosis, similar experiments were carried out in which eosinophils were treated with varying concentrations of dbcAMP for 24 h in place of 72 h (Fig. 1b). DbcAMP significantly reduced eosinophil apoptosis in a dose-dependent manner. Thus the increased survival of eosinophils by dbcAMP parallels the decreased apoptosis. These data also support previous findings of dbcAMP effects on eosinophil survival (18) and apoptosis (19).

Effect of dbcAMP and IL-5 on the Concentration of Intracellular cAMP

To examine whether dbcAMP and IL-5 increase the intracellular levels of cAMP in eosinophils, we measured cAMP levels in eosinophils treated with dbcAMP or IL-5 for 15 min and 1, 4, 8, and 24 h. The intracellular cAMP concentration of unstimulated eosinophils was not changed until 24 h of culture (Table 1). The level of intracellular cAMP was significantly increased at 15 min in eosinophils treated with 5×10^{-4} M dbcAMP compared with that in unstimulated eosinophils ($n = 5$, 3602 ± 62 *vs* 66 ± 35 fmol/10^4 cells) and was maintained at high levels until 24 h. On the contrary, IL-5 treatment did not increase the cAMP levels during 24 h.

Nuclear Translocation of PKA by dbcAMP and IL-5

DbcAMP is a cell permeable cAMP analog which preferentially activates PKA (30, 31). The translocation of catalytic subunit of PKA from cytosol to nucleus was used as a marker for PKA activation in our study. To investigate whether dbcAMP and IL-5 could activate PKA, we determined the subcellular localization of a catalytic subunit of PKA in eosinophils. At the beginning of culture of eosinophils, a substantial fraction of the catalytic component, which appeared as a 40-kDa protein, was found in the cytosol with modest amount in the nuclear extract. The ratio of cytosolic over nuclear localization of PKA in unstimulated eosinophils remained unchanged until 4 h (Fig. 2). It should also be noted that IL-5 stimulation caused little translocation of PKA to nucleus. After stimulation with 5×10^{-4} M dbcAMP, however, the increased nuclear localization of PKA with a concomitant decrease in the cytosolic fraction was observed at 1 h and persisted at least for 4 h. Thus PKA translocation to nucleus is achieved by dbcAMP but not IL-5. This data was also consistent with the fact that IL-5 did not increase the intracellular levels of cAMP in eosinophils as described above.

Effect of a PKA Inhibitor on dbcAMP-Treated Eosinophil Survival and Apoptosis

To determine whether dbcAMP reduces eosinophil apoptosis through PKA activation, eosinophils were pretreated for 15 min with different concentrations of H89, a selective PKA inhibitor which is known to com-

TABLE 1

The Accumulation of cAMP in Eosinophils Stimulated with dbcAMP and IL-5

	cAMP (fmol/10^4 cells)[b]					
Treatment[a]	0 h	15 min	1 h	4 h	8 h	24 h
—	54.1 ± 32.6	66.0 ± 34.6	81.0 ± 56.8	85.1 ± 57.2	62.0 ± 34.9	69.4 ± 46.3
IL-5	—	117.8 ± 53.2	75.5 ± 52.9	80.1 ± 55.7	186.5 ± 108.9	66.3 ± 40.4
dbcAMP	—	3602.0 ± 62.6*	3614.2 ± 56.3*	3622.7 ± 42.5*	3607.2 ± 46.6*	3676.8 ± 35.0*

[a] Eosinophils (1×10^4 cells) were treated with dbcAMP (5×10^{-4} M) or IL-5 (0.1 ng/ml) for indicated time intervals.
[b] cAMP concentrations were determined by a competitive binding method with a cAMP assay kit. The results represent the average of five experiments.
* $P < 0.001$ vs untreated or IL-5-treated eosinophils.

pete ATP for binding to the catalytic subunit of PKA (32), and incubated with dbcAMP (5×10^{-4} M) for an additional 24 h or 72 h depending upon the measurement of eosinophil apoptosis and survival, respectively. H89 attenuated the ability of dbcAMP to inhibit eosinophil apoptosis in a dose-dependent fashion (Fig. 3a). The pretreatment with 5 μM H89 significantly increased eosinophil apoptosis compared with that with dbcAMP alone ($n = 5$, 22.0 ± 4.6 vs 14.3 ± 5.3%, $P < 0.05$) while H89 (5 μM) by itself had little effect on the apoptosis of unstimulated eosinophils (data not shown). These results indicate that the suppression of eosinophil apoptosis by the elevated intracellular cAMP is largely, if not all, operated through a PKA-dependent pathway. A similar result was obtained from H89 effect on eosinophil viability. H89 (5 μM) pretreatment reduced dbcAMP-mediated increase of survival (46.1 ± 4.4 vs 60.1 ± 5.2%, $P < 0.05$) (Fig. 3b). These results indicate that the survival of unstimulated eosinophils appears to be independent from the basal activity of PKA. Conversely, PKA activation may play a certain role in the apoptosis of eosinophils only when they are stimulated.

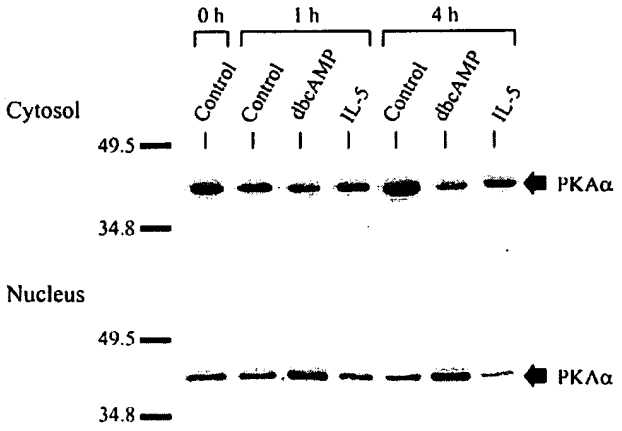

FIG. 2. Immunoblot analysis of PKA translocation. Eosinophils (3×10^6 cells) were incubated without or with dbcAMP (5×10^{-4} M) or IL-5 (0.1 ng/ml) for 0, 1, and 4 h. 200 μg of cell lysate was subjected to Western blot analysis with an anti-human PKAα-cat antibody. Controls mean unstimulated eosinophils. Proteins were size-fractioned on SDS–polyacrylamide gel (12%) electrophoresis. Molecular mass markers are shown on the left. Representative of two experiments.

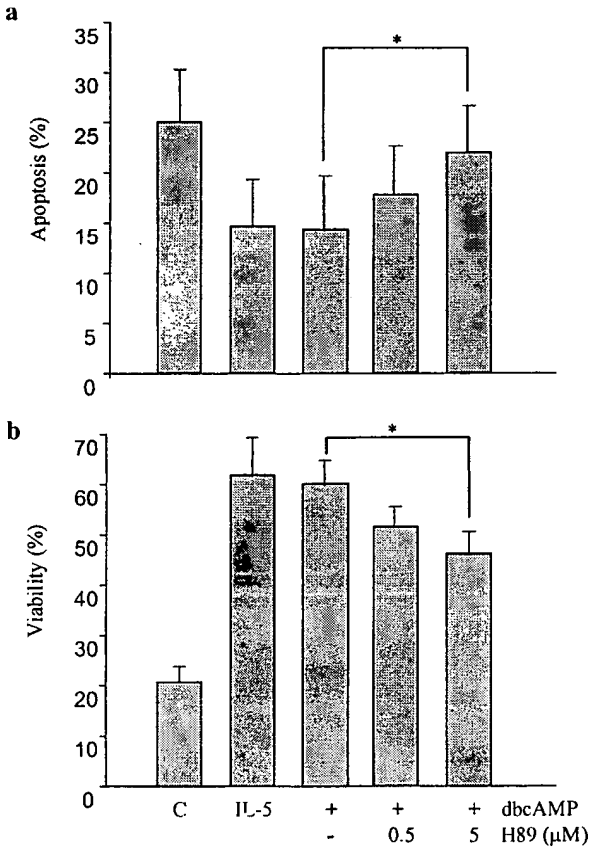

FIG. 3. The effect of PKA inhibitor (H89) on apoptosis (a) and survival (b) of eosinophils in the presence of dbcAMP. Eosinophils were preincubated with or without H89 (0.5 and 5.0 μM) for 15 min, at which point dbcAMP (5×10^{-4} M) or IL-5 (0.1 ng/ml) was added for an additional 24 h (a) and 72 h (b). Apoptosis and viability were measured as described under Materials and Methods. The data presented are the mean ± SEM of five independent experiments done in triplicate. Statistical analysis was performed comparing dbcAMP alone to H89. *$P < 0.05$.

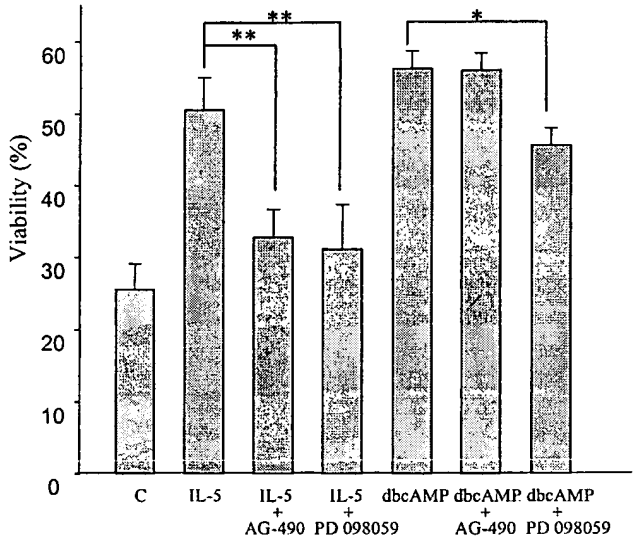

FIG. 4. The effect of Jak2 (AG-490) and MAPK kinase inhibitors (PD 098059) on dbcAMP-mediated viability of eosinophils. Eosinophils were preincubated with AG-490 (30 μM) or PD098059 (100 μM) for 15 min before the addition of dbcAMP (5×10^{-4} M) for 72 h. Eosinophil viability was determined as described under Materials and Methods. The data presented are the mean ± SEM of seven independent experiments done in triplicate. Statistical analysis was performed comparing dbcAMP or IL-5 alone to AG-490 and PD098059. $^{*}P < 0.05$; $^{**}P < 0.01$.

Effect of MAP Kinase and Jak2 Inhibitors on Eosinophil Survival

The functional relevance of Lyn, Jak2, and Raf-1 kinases in eosinophil survival and degranulation have recently been investigated using specific inhibitors of protein kinase (33) and anti-sense probes (34). All these three kinases are required for the suppression of eosinophil apoptosis by IL-5 and GM-CSF, whereas Lyn and Jak2 are not important for the upregulation of CD11b and the secretion of eosinophil cationic proteins (34). To investigate whether the activation of either MAP kinase or Jak2 is involved in dbcAMP-induced prolongation of eosinophil survival, eosinophils were pretreated with 100 μM PD 098059 (35), a MAPK kinase inhibitor, or 30 μM AG-490 (36), a Jak2 inhibitor, for 15 min, cultured in the presence of either dbcAMP (5×10^{-4} M) or IL-5 (0.1 ng/ml) for 72 h, and then followed by the measurement of viability. The spontaneous survival of eosinophils ($n = 7$, 24.7±4.7%) was not affected by the pretreatment with PD 098059 (23.3±4.6%, $P > 0.05$) or AG-490 (23.3±3.8%, $P > 0.05$). PD 098059 and AG-490 dramatically reduced the IL-5-induced prolongation of eosinophil survival ($n = 7$, 50.5±4.6%) to 31.1 ± 6.2 and 32.8 ± 3.9%, respectively ($n = 7$, $P < 0.01$) (Fig. 4), ensuring that both MAPK kinase and Jak2 are required for the signaling pathway of IL-5-induced prolongation of eosinophil survival as previously reported (10, 14–17). In contrast, PD 098059 significantly reduced dbcAMP-induced prolongation of eosinophil viability (45.5 ± 2.5% vs 56.2 ± 2.5%, $n = 5$, $P < 0.05$), whereas AG-490 had little effect (55.9 ± 2.5%) on the survival of eosinophils in the presence of dbcAMP. This result indicates that the dbcAMP-induced enhancement of eosinophil survival is partly mediated by the activation of MAPK kinase but not of Jak2. These observations were confirmed by morphologic analyses of apoptotic eosinophils that had been incubated for 24 h with the kinase inhibitors in the presence of dbcAMP (Fig. 5). Eosinophils underwent spontaneous apoptosis in the absence of any reagents (Fig. 5a), and dbcAMP (5×10^{-4} M) markedly reduced eosinophils displaying apoptotic features (Fig. 5b). The pretreatment with 5×10^{-6} M H89 (Fig. 5c) or 100 μM PD 098059 (Fig. 5e) but not with 30 μM AG-490 (Fig. 5d) increased apoptotic eosinophils in the presence of dbcAMP. The morphologic features of eosinophils on the posttreatment with dbcAMP (Fig. 5e) were comparable to those with 0.1 ng/ml IL-5 (Fig. 5f) in the presence of PD 098059.

DISCUSSION

In this study the effects of dbcAMP on eosinophil survival and apoptosis were investigated. We demonstrate that dbcAMP prolongs the survival of eosinophils with the concomitant inhibition of their apoptosis in the absence of IL-5 (Figs. 1 and 5), indicating that a cAMP-dependent pathway appears to be involved in survival/apoptosis of eosinophils. Our results are in excellent agreement with the previous findings where dbcAMP treatment augments the survival of eosinophils in the absence of granulocyte-macrophage colony-stimulating factor (GM-CSF) (18) and decreases spontaneous (19) or Fas-mediated apoptosis (37). The inhibitory effects of cAMP on eosinophil apoptosis were also observed in other cell types: cAMP is shown to prevent neuronal cells from apoptosis (38) and to inhibit Fas-induced apoptosis of hepatocytes (39) and neutrophils (19). Nonetheless, controversy remains as to the effect of dbcAMP on eosinophil apoptosis. DbcAMP was demonstrated to shorten the survival of eosinophils stimulated with GM-CSF (18) and abolish the IL-5-induced prevention of DNA fragmentation (40). The agents that increase an intracellular cAMP level, such as cholera toxin (18) and specific phosphodiesterase inhibitors (IBMX and rolipram) (19), were also shown to produce the exact same patterns in eosinophil apoptosis/survival depending upon the presence of IL-5 and GM-CSF. Thus the dual effects of cAMP seem to be related to the presence of these cytokines. However, it is not still clear, at this moment, what the nature of cAMP-dependent pathway is that either inhibits the spontaneous apoptosis of eosinophils or antagonizes the anti-apoptotic effects of these cytokines. We speculate that although eosinophils receive an anti-apoptotic signal

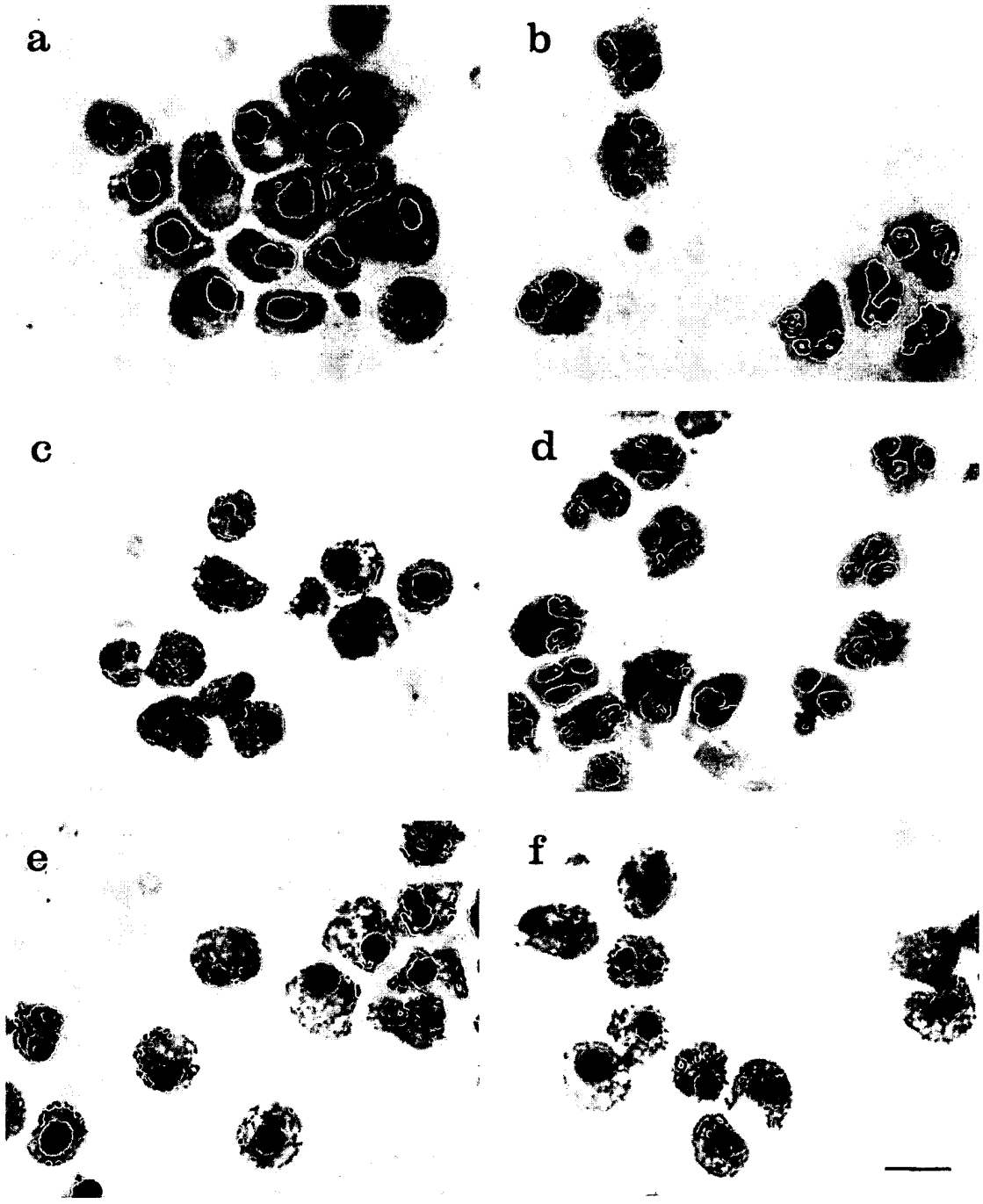

FIG. 5. Morphologic features of cultured eosinophils in the presence of protein kinase inhibitors, dbcAMP and IL-5. Eosinophils were preincubated for 15 min in the presence of 5 μM H89 (c), 30 μM AG-490 (d), or 100 μM PD098058 (e), and then treated with 5×10^{-4} M dbcAMP for an additional 24 h. In the same set of experiments, eosinophils were incubated in the absence (a) or presence of dbcAMP (b) for 24 h without pretreatment. For comparison, 100 μM PD 098059 was pretreated before exposure to IL-5 (0.1 ng/ml) for 24 h (f). The cultured eosinophils were microscopically visualized by staining with Diff-Quik. Scale bars = 10 μm.

induced by these cytokines, the subsequent increase of cAMP level appears to override the anti-apoptotic signal, thereby suppressing the prolonged survival of eosinophils. Conversely, in the absence of the activation of these cytokine receptors the cAMP-dependent pathway alone is likely to sufficiently direct eosinophils to favor survival. In the latter case it is noteworthy that a nonspecific phosphodiesterase inhibitor theophylline is able to accelerate eosinophil apoptosis even in the absence of these cytokines, unlike dbcAMP (19). The au-

thors in the report claim that the effect of theophylline on granulocyte apoptosis is independent of its cAMP-increasing capability. Alternatively, there is a possibility that theophylline would exert its function by elevating intracellular cAMP level in the presence of the eosinophil-active cytokines while factor(s) other than cAMP, which is inducible or activated by theophylline, could be dominant to overcome the inhibitory effect of cAMP on apoptosis of unstimulated eosinophils. Whatever mechanism is operating to produce this consequence, the opposing effects of dbcAMP depending upon the presence of these cytokines must be considered within the context of therapeutic strategy for eosinophilic inflammation in patients with respiratory allergy. Corticosteroids have been used for therapeutic trials of patients with asthma due to their activity to inhibit allergic inflammation (41). The corticosteroids are also able to increase the apoptosis not only of unstimulated eosinophils but also of eosinophils stimulated with cytokines such as interleukin-3 (IL-3), IL-5, and GM-CSF (42). In the case of patients with moderate to severe asthma who have the increased expression of these cytokines in the bronchial tree, the introduction of a high dose of β-agonists or cAMP-elevating agents with corticosteroids might induce eosinophil apoptosis more than corticosteroid alone. After the allergic inflammation is declined, however, the combined use of β-agonists with corticosteroids could exert a harmful effect by preventing the unprimed eosinophils from apoptosis or by reducing the apoptotic effect of corticosteroids as seen in *in vitro* study (43). Thus the potential effects of β-agonist therapy might be related to the presence or absence of *in vivo* IL-5 expression.

Our results show that the treatment with dbcAMP but not with IL-5 resulted in the elevation of intracellular cAMP levels (Table 1). In accordance with this result, it is also observed that the catalytic component of PKA was translocated to nucleus after stimulation with dbcAMP as evidenced by Western blot analysis (Fig. 2). IL-5 was not able to induce the nuclear localization of PKA. It is noticeable that the event of PKA translocation is not shared in signal transduction pathways for eosinophil survival mediated by the two reagents. This result suggests that the activation of PKA is not, if at all, directly involved in the prolonged survival of eosinophils by IL-5. Our data also reveal that H89 (5 μM) attenuated dbcAMP-induced decrease of eosinophil apoptosis with inhibitory effect on eosinophil survival (Fig. 3), indicating that the activation and possibly subsequent nuclear localization of PKA are necessary to inhibit apoptotic pathways as well as to prolong eosinophil survival and that the deactivation of PKA may nullify the dbcAMP-mediated effects.

Since it was shown that MAP kinase and Jak2 are required for eosinophil survival, we investigated whether these two protein kinases are involved in the dbcAMP-induced inhibition of eosinophil survival. Our results reveal that the prolongation of eosinophil survival by dbcAMP was partly prevented by a MAPK inhibitor (PD098059) but not a Jak2 inhibitor while both inhibitors blocked IL-5-mediated survival of eosinophils (Figs. 4 and 5). These data suggest that the signal transduction for eosinophil survival by dbcAMP and IL-5 constitute overlapping but distinct components. PD098059 is shown to selectively inhibit MAPK/ERK kinase (MEKs) without affecting PKA activity in several cell lines (35). These MEKs are activated by Ras proteins via Raf family members (44). Since PD098059 reverses the positive effect of dbcAMP on eosinophil survival, the target of PKA could be located upstream to MAP kinase in propagating an anti-apoptotic signal. The effects of PKA on Raf-1/MAP kinase pathway have been reported, which are either inhibitory or stimulatory depending upon cell types: PKA mediates the inhibition of the Raf-1/MAP kinase in smooth muscle cells (45, 46), vascular endothelial cells (47), and astrocytes (48). In contrast, PKA stimulates the Raf-1/MAP kinase in cardiac myocytes (49) and neuronal cells (50). Our data supports the stimulatory role of PKA in MAP kinase-mediated eosinophil survival, and provides evidence for a cross-talk between PKA and MAP kinase pathway in respect to eosinophil survival/apoptosis.

It is also possible that a transcriptional mechanism accounts for the prevention of eosinophil apoptosis via the expression of anti-death genes induced by dbcAMP since both transcription and translation inhibitors are shown to abolish the enhancing effects of IL-5 and GM-CSF on eosinophil viability (5, 51). One of such candidates is Bcl-2, the product of protooncogene. However, it was shown that dbcAMP does not induce or augment Bcl-2 expression in eosinophils as reported in other (19) and our studies (unpublished observation). Another possibility is the involvement of other transcription factors since the activated PKA is known to directly phosphorylate transcription factors such as CREB and CREM (52) and to modulate NF-κ B (53) and NF-AT (54) in other cell types. It remains to be clarified whether these transcription factors are involved in the prevention of eosinophil apoptosis and what is a major target of PKA activation at a transcription level for eosinophil survival.

In summary, the increase of intracellular cAMP is able to prolong the survival of eosinophils and to inhibit spontaneous apoptosis. These processes require the activation and subsequent nuclear localization of PKA. DbcAMP-initiated survival of eosinophils may be mediated partly through the activation of MAP kinase but not of Jak2.

ACKNOWLEDGMENTS

This work was supported by KOSEF 96-0403-07-01-3, Korea. The authors thank Ms. Myung Ran Lee and Eun Young Kim for assistance with eosinophil isolation.

REFERENCES

1. Bousquet, J., Chanez, P., Lacoste, J. Y., Barneon, G., Ghavanian, N., Enander, I., Venge, P., Ahlstedt, S., Simony-Lafontaine, J., Godard, P., and Michel, F., Eosinophilic inflammation in asthma. *N. Engl. J. Med.* **323,** 1033–1039, 1990.
2. Takafugi, S., Ohtoshi, T., Takizawa, H., Tadokoro, K., and Ito, K., Eosinophil degranulation in the presence of bronchial epithelial cells. *J. Immunol.* **156,** 3980–3985, 1996.
3. Flavahan, N. A., Slifman, N. R., Gleich, G. J., and Vanhoutte, P. M., Human eosinophil major basic protein causes hyperreactivity of respiratory smooth muscle: Role of the epithelium. *Am. Rev. Respir. Dis.* **138,** 685–688, 1988.
4. Simon, H. U., Yousefi, S., Schranz, C., Schapowal, A., Bachert, C., and Blaser, K., Direct demonstration of delayed eosinophil apoptosis as a mechanism causing tissue eosinophilia in nasal polyps. *J. Immunol.* **158,** 3902–3908, 1997.
5. Yamaguchi, Y., Suda, T., Ohta, S., Tominaga, K., Miura, Y., and Kasahara, T., Analysis of the survival of mature human eosinophils: Interleukin-5 prevents apoptosis in mature human eosinophils. *Blood* **78,** 2542–2547, 1991.
6. Simon, H. U., and Blaser, K., Inhibition of programmed eosinophil death: A key pathogenic event for eosinophilia. *Immunol. Today* **16,** 53–55, 1995.
7. Dent, L. A., Strath, M., Mellor, A. L., and Sanderson, C. J., Eosinophilia in transgenic mice expressing interleukin-5. *J. Exp. Med.* **172,** 1425–1431, 1990.
8. Mould, A. W., Matthaei, K. I., Young, I. G., and Foster, P. S., Relationship between interleukin-5 and eotaxin in regulating blood and tissue eosinophilia in mice. *J. Clin. Invest.* **99,** 1064–1071, 1997.
9. Ohnishi, T., Kita, H., and Weiler, D., IL-5 is the predominant eosinophil-active cytokine in the antigen-induced pulmonary late reaction. *Am. Rev. Respir. Dis.* **147,** 901–907, 1993.
10. Alam, R., Pazdrak, K., Stafford, S., and Forsythe, P., The interleukin-5/receptor interaction activates Lyn and Jak2 tyrosine kinases and propagates signals via the Ras-Raf-1-MAP kinase and the Jak-STAT pathways in eosinophils. *Int. Arch. Allergy Immunol.* **107,** 226–227, 1995.
11. Yousefi, S., Hoessli, D. C., Blaser, K., Mils, G. B., and Simon, H. U., Requirement of Lyn and Syk tyrosine kinases for the prevention of apoptosis by cytokine in human eosinophils. *J. Exp. Med.* **183,** 1407–1414, 1996.
12. Appleby, M. W., Kerner, J. D., Chien, S., Maliszewski, C. R., Bondada, S., and Perlmutter, R. M., Involvement of p59fynT in interleukin-5 receptor signaling. *J. Exp. Med.* **182,** 811–820, 1995.
13. Dorsch, M., Hock, H., and Diamantstein, T., Tyrosine phosphorylation of Shc is induced by IL-3, IL-5 and GM-CSF. *Biochem. Biophys. Res. Commun.* **200,** 562–568, 1994.
14. Pazdrak, K., Schreiber, D., Forsythe, P., Justement, L., and Alam, R., The intracellular signal transduction mechanism of interleukin-5 in eosinophils: The involvement of lyn tyrosine kinase and the Ras-Raf-1-MEK-microtubule-associated protein kinase pathway. *J. Exp. Med.* **181,** 1827–1834, 1995.
15. Bates, M. E., Bertics, P. J., and Busse, W. W., IL-5 activates a 45-kilodalton mitogen-activated protein (MAP) kinase and Jak-2 tyrosine kinase in human eosinophils. *J. Immunol.* **156,** 711–718, 1996.
16. Pazdrak, K., Stafford, S., and Alam, R., The activation of the Jak-STAT 1 signaling pathway by IL-5 in eosinophils. *J. Immunol.* **155,** 397–402, 1995.
17. van der Bruggen, T., Caldenhoven, E., Kanters, D., Coffer, P., Raaijmakers, J. A., Lammers, J. W., and Koenderman, L., Interleukin-5 signaling in human eosinophils involves JAK2 tyrosine kinase and Stat1 alpha. *Blood* **85,** 1442–1448, 1995.
18. Hallsworth, M. P., Giembycz, M. A., Barnes, P. J., and Lee, T. H., Cyclic AMP-elevating agents prolong or inhibit eosinophil survival depending on prior exposure to GM-CSF. *Br. J. Pharmacol.* **117,** 79–86, 1996.
19. Yasui, K., Nakazawa, T., Agematsu, K., and Komiyama, A., Theophylline accelerates granulocyte apoptosis not via phosphodiesterase inhibition. *J. Clin. Invest.* **100,** 1677–1684, 1997.
20. Xia, Z., Dickens, M., Raingeaud, J., Davis, R. J., and Greenberg, M., Opposing effects of ERK and JNK-p38 MAP kinases on apoptosis. *Science* **270,** 1326–1331, 1995.
21. Nobes, C. D., and Tolkovsky, A. M., Neutralizing anti-p21ras Fabs suppress rat sympathetic neuron survival induced by NGF, LIF, CNTF and cAMP. *Eur. J. Neurosci.* **7,** 344–350, 1995.
22. Messmer, U. K., Lapetina, E. G., and Brune, B., Nitric oxide-induced apoptosis in RAW 264.7 macrophages is antagonized by protein kinase C- and protein kinase A-activating compounds. *Mol. Pharmacol.* **47,** 757–765, 1995.
23. Geier, A., Weiss, C., Beery, R., Haimsohn, M., Hemi, R., Malik, Z., and Karasik, A., Multiple pathways are involved in protection of MCF-7 cells against death due to protein synthesis inhibition. *J. Cell. Physiol.* **163,** 570–576, 1995.
24. Cassano, S., Gallo, A., Buccigross, V., Porcellini, A., Cerillo, R., Gottesman, M. E., and Avvedimento, E. V., Membrane localization of cAMP-dependent protein kinase amplifies cAMP signaling to the nucleus in PC12 cells. *J. Biol. Chem.* **271,** 29870–29875, 1996.
25. Ahmed, M. U., Hazeki, K., Hazeki, O., Katada, T., and Ui, M., Cyclic AMP-increasing agents with chemoattractant-induced respiratory burst in neutrophils as a result of the inhibition of phosphatidylinositol 3-kinase rather than receptor-operated Ca2+ influx. *J. Biol. Chem.* **270,** 23816–23822, 1995.
26. Rasmussen, H., Kelley, G., and Douglas, J. S., Interactions between Ca2+ and cAMP messenger system in regulation of airway smooth muscle contraction. *Am. J. Physiol.* **258,** L279–L288, 1990.
27. Gartner, I., Separation of human eosinophils in density gradients of polyvinylpyrrolidone-coated silica gel (Percoll). *Immunology* **40,** 113–136, 1980.
28. Park, C. S., Choi, Y. S., Ki, S. Y., Moon, S. H., Jeong, S. W., Uh, S. T., and Lim, Y. H., Granulocyte-macrophage colony-stimulating factor is the main cytokine enhancing survival of eosinophil. *Eur. Respir. J.* **12,** 872–879, 1998.
29. Nicolletti, I., Migliorati, G., Pagliacci, M. C., Grignani, F., and Richardi, C., A rapid and simple method for measuring thymocyte apoptosis by propidium iodide staining and flow cytometry. *J. Immunol. Methods* **139,** 271–279, 1991.
30. Meyer, R. B., Jr., and Miller, J. P., Analogs of cyclic AMP and cyclic GMP: General methods of synthesis and the relationship of structure to enzymic activity. *Life Sci.* **14,** 1019–1040, 1974.
31. Hei, Y. J., MacDonell, K. L., McNeill, J. H., and Diamond, J., Lack of correlation between activation of cyclic AMP-dependent protein kinase and inhibition of contraction of rat vas deferens by cyclic AMP analogs. *Mol. Pharmacol.* **39,** 233–238, 1991.
32. Engh, R. A., Girod, A., Kinzel, V., Huber, R., and Bossemeyer, D., Crystal structures of catalytic subunit of cAMP-dependent protein kinase in complex with isoquinolinesulfonyl protein

kinase inhibitors H7, H8, and H89. Structural implications for selectivity. *J. Biol. Chem.* **271,** 26157–26164, 1996.

33. Simon, H.-U., Yousefi, S., Dibbert, B., Levi-Schaffer, F., and Blaser, K., Anti-apoptotic signals of granulocyte-macrophage colony-stimulating factor are transduced via Jak2 tyrosine kinase in eosinophils. *Eur. J. Immunol.* **27,** 3536–3539, 1995.
34. Pazdrak, K., Olszewska-Pazdrak, B., Stafford, S., Garofalo, P. R., and Alam, R., Lyn, Jak2, and Raf-1 kinases are critical for the antiapoptotic effect of interleukin-5, whereas only Raf-1 kinase is essential for eosinophil activation and degranulation. *J. Exp. Med.* **188,** 421–429, 1998.
35. Dudley, D. T., Pang, L., Decker, S. J., Bridges, A. J., and Saltiel, A. R., A synthetic inhibitor of the mitogen-activated protein kinase cascade. *Proc. Natl. Acad. Sci. USA* **92,** 7686–7689, 1995.
36. Meydan, N., Grunberger, T., Dadi, H., Shahar, M., Arpaia, E., Lapidot, Z., Leeder, J. S., Freedman, M., Cohen, A., Gazit, A., Levitzki, A., and Roifman, C. M., Inhibition of acute lymphoblastic leukemia by a Jak-2 inhibitor. *Nature* **379,** 645–648, 1996.
37. Hebestreit, H., Dibbert, B., Balatti, I., Braun, D., Schapowal, A., Blaser, K., and Simon, H.-U., Disruption of Fas receptor signaling by nitric oxide in eosinophils. *J. Exp. Med.* **187,** 415–425, 1998.
38. Tanaka, J., Koshimura, K., Murakama, Y., Sohmiya, M., Yanaihara, N., and Kato, Y., Neuronal protection from apoptosis by pituitary adenylate cyclase-activating polypeptide. *Regul. Pept.* **72,** 1–8, 1997.
39. Fladmark, K. E., Gjertsen, B. T., Doskeland, S. O., and Vintermyr, O. K., Fas/APO-1(CD95)-induced apoptosis of primary hepatocytes is inhibited by cAMP. *Biochem. Biophys. Res. Commun.* **232,** 20–25, 1997.
40. Ohta, K., Sawamoto, S., Nakajima, M., Kubota, S., Tanaka, Y., Miyasaka, T., Nagai, A., Hirai, K., Mano, K., and Miyashita, H., The prolonged survival of human eosinophils with interleukin-5 and its inhibition by theophylline via apoptosis. *Clin. Exp. Allergy* **26 Suppl 2,** 10–15, 1996.
41. Stellato, C., Schwiebert, L. M., and Schleimer, R. P., *In* "Asthma" (P. J. Barnes, M. M. Grunstein, A. R. Leff, and A. J. Woolcock, Eds.), Vol. 2, pp. 1569–1596, Lippincott-Raven, New York, 1997.
42. Wallen, N., Kita, H., Weiler, D., and Gleich, G. J., Glucocorticoids inhibits cytokine-mediated eosinophil survival. *J. Immunol.* **147,** 3490–3495, 1991.
43. Nielson, C. P., and Hadjokas, N. E., Beta-adrenoceptor agonists block corticosteroid inhibition in eosinophils. *Am. J. Respir. Crit. Care Med.* **157,** 184–191, 1998.
44. Freshney, N. W., Rawlinson, L., Guesdon, F., Jones, E., Cowley, S., Hsuan, J., and Saklatvala, J., Interleukin-1 activates a novel protein kinase cascade that results in the phosphorylation of Hsp27. *Cell* **78,** 1039–1049, 1994.
45. Bonisch, D., Weber, A. A., Wittpoth, M., Osinski, M., and Schror, K., Antimitogenic effects of trapidil in coronary artery smooth muscle cells by direct activation of protein kinase A. *Mol. Pharmacol.* **54,** 241–248, 1998.
46. Pelvin, R., Malarkey, K., Aidulis, D., Mclees, A., and Gould, G. W., Cyclic AMP inhibitors inhibit PDGF-stimulated mitogen-activated protein kinase activity in rat aortic smooth muscle cells via inactivation of c-Raf-1 kinase and induction of MAP kinase phosphatase-1. *Cell. Signal* **9,** 323–328, 1997.
47. D'Angelo, G., Lee, H., and Weiner, R. I., cAMP-dependent protein kinase inhibits the mitogenic action of vascular endothelial growth factor and fibroblast growth factor in capillary endothelial cells by blocking Raf activation. *J. Cell. Biochem.* **67,** 353–366, 1997.
48. Kurino, M., Fukunaga, K., Ushio, Y., and Miyamoto, E., Cyclic AMP inhibits activation of mitogen-activated protein kinase and cell proliferation in response to growth factors in cultured rat cortical astrocytes. *J. Neurochem.* **67,** 2246–2255, 1996.
49. Yamazaki, T., Komuro, I., Zou, Y., Kudoh, S., Mizuno, T., Hiroi, Y., Shiojima, I., Takano, H., Kinurawa, K., Kohmoto, Y., Takahashi, T., and Yazaki, Y., Protein kinase A and protein kinase C synergistically activate the Raf-1 kinase/mitogen-activated protein kinase cascade in neonatal rat cardiomyocytes. *J. Mol. Cell. Cardiol.* **29,** 2491–2501, 1997.
50. Vossler, M. R., Yao, H., York, R. D., Pan, M. G., Rim, C. S., and Stork, P. J., cAMP activates MAP kinase and Elk-1 through a B-Raf- and Rap1-dependent pathway. *Cell* **89,** 73–82, 1997.
51. Tai, P.-C., Sun, L., and Spry, C. J., Effects of IL-5, granulocyte/macrophage colony-stimulating factor (GM-CSF) and IL-3 on the survival of human blood eosinophils in vitro. *Clin. Exp. Immunol.* **85,** 312–316, 1991.
52. Ruchaud, S., Seite, P., Foulkes, N. S., Sassone-Corsi, P., and Lanotte, M., The transcriptional repressor ICER and cAMP-induced programmed cell death. *Oncogene* **15,** 827–836, 1997.
53. Neumann, M., Grieshammer, T., Chuvpilo, S., Kneitz, B., Lohoff, M., Schimpl, A., Franza, B. R., Jr., and Serfling, E., RelA/p65 is a molecular target for the immunosuppressive action of protein kinase A. *EMBO J.* **14,** 1991–2004, 1995.
54. Lacour, M., Arrighi, J. F., Muller, K. M., Carlberg, C., Saurat, J. H., and Hauser, C., cAMP up-regulates IL-4 and IL-5 production from activated CD4+ T cells while decreasing IL-2 release and NF-AT induction. *Int. Immunol.* **6,** 1333–1343, 1994.

Exhibit E

Activation of MAP kinase (ERK-1/ERK-2), tyrosine kinase and VEGF in the human brain following acute ischaemic stroke

M. Slevin,[CA] J. Krupinski,[1] A. Slowik,[1] F. Rubio,[2] A. Szczudlik[1] and J. Gaffney

Department of Biological Sciences, Manchester Metropolitan University, Chester St., Manchester M6 5GD, UK; [1]Department of Neurology, Collegium Medicum, Jagiellonian University, Cracow, Poland; [2]Department of Neurology, Hospital Princeps d'Espanya, Ciutat Sanitaria i Universitaria de Bellvitge, Barcelona, Spain

[CA]Corresponding Author

Received 31 May 2000; accepted 14 June 2000

We examined expression of vascular endothelial growth factor (VEGF), phosphorylation of mitogen activated protein kinase (MAP) kinase (ERK1 and ERK2) and tyrosine phosphorylation in 19 patients (aged 58–90 years; mean 75) who died 1–44 days after acute ischaemic stroke. In the grey matter penumbra, 13 of 19 patients showed an increase in MAP kinase tyrosine phosphorylation (ERK1; 2.0- to 8-fold, ERK2; 2.2- to 11-fold) compared with normal contralateral tissue. In almost all cases, ERK-2 phosphorylation was higher than ERK1. Of these 13 patients, 11 also showed a general increase in tyrosine kinase phosphorylation, and eight expressed increased levels of VEGF protein (2.5- to 5-fold). In tissue examined directly from the infarct core, activation of the above proteins was not observed in the, majority of patients. In the white matter, seven of 19 patients (penumbra), and nine of 19 patients (stroke) had an increase in MAP kinase tyrosine phosphorylation (ERK1; 2.0- to 4.6-fold and ERK-2; 2.3- to 5.4-fold respectively) compared with normal contralateral tissue. There was no relationship between activation of MAP kinase and expression of VEGF. Examination of phosphorylated MAP kinase by immunohistochemistry revealed an increase in immunoreactivity in neurones, astroglial cells, reactive microglia and endothelial cells in areas surrounding infarcts, especially in areas with the highest density of microvessels. In conclusion, chronic activation of tyrosine phosphorylated events, in particular redistribution and phosphorylation of MAP kinase (ERK1/ERK2) occurs consistently in the grey matter penumbra of brain tissue following ischaemic stroke, and may be associated with increase in expression of VEGF. These signal transduction events could be important determinants of the extent of neuronal survival and/or angiogenic activity in the recovering brain tissue. *NeuroReport* 11:2759–2764 © 2000 Lippincott Williams & Wilkins.

Key words: Ischaemic stroke; MAP kinase; Tyrosine phosphorylation; VEGF

INTRODUCTION

Activation of intracellular signal transduction pathways after ischaemic stroke is probably a crucial event determining cell survival following cytokine and growth factor activation [1]. Transcriptional regulation involves activation of tyrosine phosphorylation cascades and NFkB, leading to either protection or programmed cell death [2]. Similarly, new microvessel growth (angiogenesis) following ischaemia is regulated by diffusable growth factors, cytokines and extracellular components generated by both parenchymal (astrocytes, microglia, oligodendrocytes and endothelial cells), and infiltrating cells (monocytes, macrophages and leukocytes) [3]. During tissue repair, wound healing and possibly in ischaemic penumbra, angiogenesis helps to restore the function of damaged tissue [4]. We have shown that angiogenesis correlates with patient survival [5] and that survival of neurones was greatest in areas of tissue undergoing angiogenesis [6], suggesting that angiogenic factors might also be neuroprotective determinants of neuronal survival. *In vitro* studies have shown that epidermal growth factor, basic fibroblast growth factor, transforming growth factor beta, neurotrophin and vascular endothelial growth factor (VEGF), are neuroprotective and antiapoptotic [7]. Therefore the synthesis and expression of one or more angiogenic molecules immediately after the onset of stroke as well as during reperfusion may be an important factor in determining recovery. In particular, we have recently shown increased expression of VEGF in both the serum [8] and tissue penumbra [9] of patients following acute ischaemic stroke.

Activation of signal transduction pathways follows binding of cytokines or growth factors to cell surface receptors. Tyrosine autophosphorylation sites within the catalytic domain of the receptor can regulate tyrosine kinase activity of associated down-stream signalling molecules (eg PLC-γ, shc and P13- kinase) following binding to their src homology-2 (sh2) domains [10]. Tyrosine phosphorylation of the 44 and 42 kDa MAP kinase proteins (ERK1 and ERK2)

causes them to undergo nuclear translocation resulting in activation of early response genes (Elk-1, c-fos, c-jun), which culminates in cell transcription [11]. Stimulation of these kinases is of key importance in regulation of cell mitogenesis, differentiation, synaptic transmission and neuro-protective mechanisms [12,13].

It is important to establish any relationship between constitutively activated signal transduction pathways, associated expression of mitogenic and neurotrophic factors, and recovery of neurones/angiogenesis particularly in penumbra tissue surrounding the ischaemic infarct. In this paper we have examined tyrosine phosphorylation, MAP kinase tyrosine phosphorylation and VEGF protein expression in the penumbra, infarct and normal contralateral tissue from 19 patients who died following acute ischaemic stroke.

MATERIALS AND METHODS

Patients and tissue samples: Brain tissue samples from human atherothrombotic or cardioembolic stroke were obtained from 19 patients (12 male, seven female), with permission of the ethics committee from the Department of Neuropathology, Jagiellonian university, Krakow, Poland and from seven patients (three male, four female) from the Department of Neurology, Hospital Princeps d'Espanya, Barcelona, Spain (Table 1). Patients were aged 58–90 years (mean 75) and lived for 1–44 days following ischaemic stroke. All routine blood parameters including peripheral leukocytosis, cholesterol, fibrinogen, urea and glucose levels were determined at the time of admission. Full clinical examination was also carried out on admission and where possible, after 24 h, 7, 14 and 30 days. The examinations were scored according to the 58-point Scandinavian Stroke Scale (SSS) [14]. Immediately following death, the body was placed in a cold chamber for 2–12 h before tissue dissection.

Brain tissue was separated into stroke-affected areas and penumbra (area of tissue immediately surrounding infarct), together with normal contralateral tissue for both grey and white matter. After dissection, tissue was immediately snap frozen, and stored in liquid nitrogen until use. A portion of each dissected sample was processed for histology and stained with haematoxylin and eosin to confirm tissue morphology.

Extraction of protein from tissue samples/Western blotting: Tissue samples (500 mg) were washed in ice-cold PBS and homogenized with a Teflon homogenizer at 4°C in 1.5 ml buffer containing 10 mM Tris–HCl (pH 7.5), 50 mM NaCl, 0.5% sodium deoxycholate, 0.5% Nonidet P40, 0.1% SDS, 1 mM sodium vanadate and 5 μg/ml aprotinin [12]. Extracts were sonicated, centrifuged (twice at 33 000 × *g*, 15 min) and the supernatant containing the soluble enzymes stored at −70°C. Protein concentrations were determined by the Bradford assay. Equal concentrations of protein (10 μg) from each lysate were mixed with 2× Laemmli buffer, vortex mixed and boiled for 15 min before application and separation along with pre-stained mol. wt markers by 12% SDS–PAGE. The proteins were electroblotted onto nitrocellulose filters (Hoefer, San Francisco, CA) and the filters blocked overnight with 1% BSA in TBS–Tween (50 mM Tris–HCl, pH 7.4; 200 mM NaCl and 1% Tween 20). After blocking, filters were stained for 4 h at room temperature with antiphosphotyrosine, anti-phosphorylated ERK-1/ERK-2 monoclonal or anti-α-actin polyclonal antibodies (Autogen Bioclear, Ca, USA; 1:1000 in blocking buffer). Filters were washed in TBS–Tween (5 × 3 min) before staining with the appropriate peroxidase-conjugated secondary antibody (anti-rabbit or anti-mouse, 1:1000) for 1 h at room temperature. After washing in TBS–Tween (5 × 3 min) blots were developed using the ECL Western-blotting detection system (Amersham, Aylesbury, UK).

The amounts of protein/phosphorylated protein relative to α-actin staining recovered after Western blotting, were measured on an LKB densitometer. VEGF bands were observed sometimes at 21 kDa and 42 kDa (the dimeric form). In these cases, the sum of the two bands was determined. Results are semi-quantitative, and are given as a numerical (fold) increase or decrease compared with control untreated cells, assigned an arbitrary value of one. ECL development times varied between experiments and therefore the intensity of staining is not directly comparable.

Immunohistochemistry: For morphological studies and immunohistochemistry, human samples were fixed in 4% paraformaldehyde in PBS for 24 h at 4°C. Fixed brains were cryoprotected and stored at −70°C. For immunohistochemistry, 10 μm serial sections were cut with a cryostat. The avidin–biotin–peroxidase method was used for immunohistochemistry (ABC kit, Vectastain, Vector). After blocking endogenous peroxidase, the sections were incubated with normal serum and then incubated at 4°C overnight with the primary antibody to phosphorylated MAP-kinase. Following incubation with the primary antibody, sections were incubated for 1 h with biotinylated anti-mouse IgG antibodies diluted 1:100, and finally with ABC at a dilution of 1:100 for 1 h at room temperature. The peroxidase reaction was visualized with 0.05% diaminobenzidine (DAB) and 0.001% hydrogen peroxide.

RESULTS

Protein expression in grey matter: The majority of patients (13 of 19) showed increased MAP kinase (ERK1 and ERK2) tyrosine phosphorylation in the penumbra (> 2-fold; Fig. 1a) compared with control contralateral tissue. The range of increase was 2.0- to 8.5-fold (ERK1) and 2.2- to 11.0-fold (ERK2; Table 1). In 11 of these 13 patients there was a concomitant increase in expression of tyrosine phosphorylated proteins of Mr 38–200 kDa (Fig. 1b, Table 1). VEGF (Mr 21 and 42 kDa) was raised in eight of these patients (range of increase 2.2- to 5.5-fold; Fig. 1c, Table 1). In all figures the α-actin controls are shown.

In stroke tissue only five out of 19 patients showed increased MAP kinase tyrosine phosphorylation (range, ERK1; 2.0–9.2; ERK2; 2.9–8.4; Table 1) compared with normal contralateral tissue. These five patients also expressed higher MAP kinase phosphorylation in the penumbra. Of these five, only one patient also exhibited increased protein tyrosine phosphorylation and three had increased VEGF. Only four of 19 patients had an overall increase in protein tyrosine phosphorylation and no pattern was seen between this and expression of other proteins.

Table 1. Patient details and protein expression

Patient	Age (years)/Sex	Survival (days)	Hemisphere	Grey Matter								White matter							
				Penumbra				Stroke				Penumbra				Stroke			
				ERK1	ERK2	TP	VEGF	ERK1	ERK2	TP	VEGF	ERK1	ERK2	TP	VEGF	ERK1	ERK2	TP	VEGF
1	77/M	25	L	3.1	6.0	++	2.2	NC	NC	+	NC	1.4	1.7	NC	NC	1.9	2.1	+	NC
2	90/M	12	L	1.5	2.6	+	3.1	NC	NC	+	3.1	1.5	1.1	NC	NC	1.7	1.2	NC	1.5
3	68/M	6	L	NC	NC	NC	NC	NC	NC	+	NC	NC	NC	NC	3.1	NC	NC	NC	0.8
4	81/F	44	R	0.9	0.6	++	NC	0.7	0.7	NC	NC	0.8	0.7	NC	2.3	0.7	0.5	NC	2.3
5	67/F	3	PIEN	5.0	3.5	+	NC	0.5	0.8	+	NC	NC	NC	NC	NC	2.4	1.2	NC	NC
6	85/F	4	L	1.6	1.5	+	4.0	1.5	1.5	+	2.5	2.8	3.2	++	0.7	2.5	3.5	NC	1.8
7	60/F	31	R	4.1	7.0	++	3.4	2.0	3.0	NC	NC	NC	NC	NC	NC	NC	NC	NC	NC
8	63/F	2	R	1.5	2.6	++	NC	1.5	3.1	NC	NC	NC	NC	++	2.2	NC	NC	+	NC
9	74/M	15	L	6.1	2.2	++	NC	0.9	0.7	+	NC	2.0	5.4	NC	NC	2.2	4.1	NC	NC
10	75/M	29	R	NC	NC	NC	NC	NC	NC	+	NC	NC	NC	NC	NC	NC	NC	NC	NC
11	71/M	5	R	2.0	4.3	+	2.1	1.2	1.5	NC	0.6	1.2	3.2	−	NC	1.1	2.1	NC	NC
12	84/M	9	R	2.0	4.2	NC	2.6	1.1	4.5	NC	3.5	1.7	4.4	++	1.7	1.5	3.6	+	1.9
13	86/M	15	R/L	NC	NC	NC	NC	0.4	0.5	++	3.0	1.3	2.3	++	1.4	0.8	0.6	+	2.9
14	84/M	3	R	8.5	11.0	++	5.5	9.2	8.4	+	3.1	4.6	5.4	++	2.1	3.9	2.9	+	NC
15	68/M	3	L	NC	NC	NC	NC	NC	NC	+	NC	NC	NC	ND	NC	2.1	2.3	NC	NC
16	69/F	37	R	4.1	7.3	++	3.0	3.0	2.9	NC	NC	NC	NC	++	NC	0.5	0.7	+	0.7
17	73/M	26	R	1.5	3.5	+	NC	NC	NC	++	1.6	NC	NC	NC	NC	0.4	0.8	−	0.5
18	84/F	29	R	2.2	8.1	NC	2.8	NC	NC	−	NC	NC	NC	−	NC	NC	NC	NC	NC
19	58/M	17	R	1.6	2.5	−	NC	0.8	0.7	NC	NC	3.1	3.5	NC	NC	2.0	2.1	NC	3.2

Tp, tyrosine phosphorylase; NC, no change; +,++ small or large increase compared with control; − small decrease.

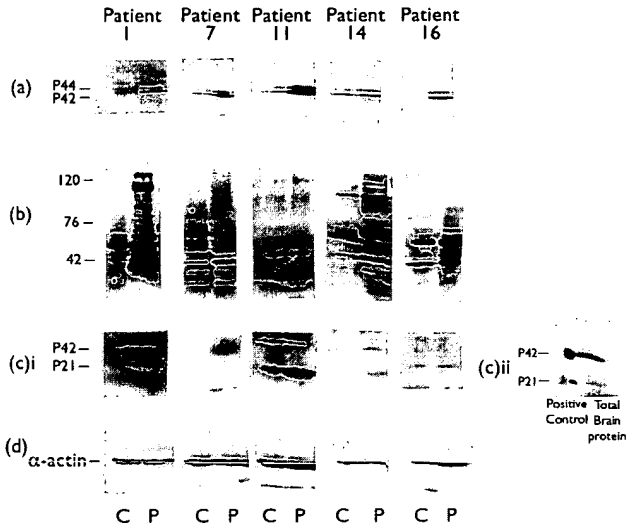

Fig. 1. (a) Expression of phosphorylated ERK-1 (p44) and ERK-2 (p42). (b) Expression of tyrosine phosphorylated proteins, and (ci) Expression of VEGF (p21 and p42 dimer) in the grey matter penumbra of patients following ischaemic stroke. (cii) VEGF positive control. (d) α-actin controls.

Protein expression in white matter: MAP kinase tyrosine phosphorylation was increased in seven of 19 patients in the penumbra compared with normal contralateral tissue. The range of increase was 2.0- to 4.6-fold (ERK1) and 2.3- to 5.4-fold (ERK2). Of these seven, four also had increased protein tyrosine phosphorylation (Table 1). VEGF protein expression was increased in eight of 19 patients (range 2.1- to 5.5-fold) although there was no relationship between this and either MAP kinase or tyrosine kinase phosphorylation in the same patients.

In stroke tissue, MAP kinase tyrosine phosphorylation was increased in nine of 19 patients compared to normal contralateral tissue. The range of expression was 2.0- to 3.9-fold (ERK-1) and 2-1- to 4.1-fold (ERK-2; Table 1). Of these, only three showed an increase in VEGF (range 2.3- to 3.2-fold. Patients showed similar expression of all parameters excluding MAP kinase tyrosine phosphorylation compared to normal contralateral tissue.

Immunohistochemistry: Samples from seven patients were used for immunohistochemistry. Increased immunoreactivity was observed in the areas surrounding infarcted core. This increase was observed in the majority of cells i.e. neurones, astroglial cells, reactive microglia as well as endothelial cells. Both white and grey matter showed higher immunoreactivity than contralateral or control normal tissue. Increase in reactivity was associated with significant redistribution of MAP kinase localization. Neurones of the penumbra were homogenously stained in all the cortical layers. In the areas with higher density of microvessels there was significant increase in the immunoreactivity. Within the penumbra tissue and especially in the white matter small islands of highly stained reactive astroglia and microglia/macrophages were visible, as well as projecting axons of cortical neurones. In the infarcted core immunohistochemistry dramatically decreased especially in the patients who survived longer after stroke. In the contralateral hemisphere we observed a very regular pattern of staining. Neurones within the grey matter layers I, III and V were notably stained. In other cells immunostaining was very weak. This pattern was homogenous. In the white matter only single cells, especially astrocytes or blood derived cells were stained (Table 2, Fig. 2a–d).

Relationship to patient clinical information: Expression of MAP kinase, tyrosine phosphorylated proteins and VEGF, were not influenced by patient age, sex, time of survival after stroke, stroke sub-types, associated clinical pathologies or any measured blood parameters (data not included).

DISCUSSION

Studies of ischaemic brain injury in animal models have demonstrated activation of intra- and intercellular signalling pathways by growth factors and cytokines which increase neuronal resistance to degeneration and death [1]. Recovery from the debilitating effects of acute ischaemic stroke depend in part on recovery of the damaged area (reduction in stroke volume) particularly in the penumbra. We have shown that recovery of this tissue correlates with the extent of angiogenic activity [5,6]. Consequently, an increase in activation of signal transducing intermediates in the area of diseased tissue could be of importance in stimulating endothelial cell growth and delaying or preventing neuronal apoptosis [15]. Critical cellular events including synaptic transmission, neuronal differentiation and survival are probably regulated through signal transduction pathways involving MAP kinase and receptor coupled tyrosine kinase activity [13]. Tyrosine kinase and MAP kinase activity is increased following cell receptor binding with an array of mitogenic growth factors and cytokines [16] and also following stress and exposure to hormones and neurotransmitters [17]. ERK1 and ERK2 are abundant in the central nervous system and are activated during various physiological and pathological events including brain ischaemia, especially in the presence of neurotrophic/growth factors. In this study we show increased MAP kinase (ERK1 and ERK2) tyrosine phosphorylation in the grey matter of 13 of 19 subjects following ischaemic stroke compared with normal contralateral tissue. ERK-2 was increased to a greater degree than ERK-1, possibly due to its more widespread localization throughout the CNS [13]. Eleven of these 13 also showed a general increase in expression of tyrosine phosphorylated proteins. In contrast, tissue taken from within the infarcted zone did not show an increase in these activities in the majority of patients compared to normal contralateral tissue. We have shown by immunohistochemistry, an increase in immunoreactivity in the penumbra areas in most of the cells, but a decrease in the infarcted core. Areas of tissue with high blood vessel density also expressed increased MAP kinase immunoreactivity. Chronic activation of tyrosine phosphorylated proteins was apparent, since patients surviving for several weeks after the initial insult, maintained elevated expression. Recently, human reactive astrocytes were shown to chronically express increased amounts of tyrosine phosphorylated MAP kinase following infarction, trauma and

Table 2. IHC showing phosphorylated ERK-1/ERK-2 localization

No.	Sex	Age	Stroke distribution /type	Survival (days)	Infarcted zone	Penumbra	Contralateral
1	M	71	MCA	5	Neurones + Astrocytes ++ Microglia/macrophages ++ Endothelial cells +	Neurones +++ Astrocytes +++ Microglia/macrophages +++ Endothelial cells +++	Neurones ++ Astrocytes + Microglia/macrophages +/− Endothelial cells +/−
2	F	84	MCA	57	Neurones +/− Astrocytes + Microglia/macrophages +++ Endothelial cells ++	Neurones + Astrocytes ++ Microglia/macrophages ++ Endothelial cells +	Neurones + Astrocytes + Microglia/macrophages − Endothelial cells +/−
3	F	78	MCA	3	Neurones +/− Astrocytes +/− Microglia/macrophages ++ Endothelial cells ++	Neurones + Astrocytes ++ Microglia/macrophages ++ Endothelial cells +	Neurones + Astrocytes + Microglia/macrophages + Endothelial cells +/−
4	M	54	PCA	1	Neurones + Astrocytes + Microglia/macrophages + Endothelial cells +	Neurones + Astrocytes ++ Microglia/macrophages ++ Endothelial cells +	Neurones + Astrocytes + Microglia/macrophages − Endothelial cells +/−
5	F	73	MCA	3	Neurones + Astrocytes + Microglia/macrophages + Endothelial cells +	Neurones +++ Astrocytes +++ Microglia/macrophages +++ Endothelial cells +++	Neurones ++ Astrocytes + Microglia/macrophages +/− Endothelial cells +/−
6	F	76	MCA	2	Neurones +/− Astrocytes + Microglia/macrophages +++ Endothelial cells ++	Neurones + Astrocytes ++ Microglia/macrophages ++ Endothelial cells ++	Neurones + Astrocytes + Microglia/macrophages +/− Endothelial cells +/−
7	F	72	MCA	4	Neurones +/− Astrocytes ++ Microglia/macrophages ++ Endothelial cells +	Neurones ++ Astrocytes ++ Microglia/macrophages +++ Endothelial cells +++	Neurones ++ Astrocytes + Microglia/macrophages +/− Endothelial cells +/−

+, weak staining; ++, moderate staining; +++, strong staining.

chronic epilepsy [18], suggesting its importance in persistence of astrogliosis. Interestingly, activation of MAP kinase was shown in mice following cerebral ischaemia, however pretreatment with the MEK-1 inhibitor PD98059 reduced focal infarct volume by 55% at 22 h after ischaemia [19], suggesting that at least short-term activation of the MAP kinase pathway could contribute to brain injury after stroke. Immunohistochemistry demonstrated strong staining of phosphorylated MAP kinase associated with neurones in deeper cortical layers in the penumbra region. ERK-2 activation was previously shown in neurones in association with spontaneous synaptic activity and following stimulation of glutamate receptors [13]. Other studies have demonstrated the importance of MAP kinase activation in regulation of synaptic transmission [20] and axonal growth [21]. Recently, increased expression of the Tie-1 transmembrane receptor kinase was shown associated with microvessels bordering pan necrotic tissue, in rat brain following ischaemic stroke [22], suggesting its involvement in vascular remodelling after embolic stroke. Whilst it may be beneficial to inhibit activation of tyrosine kinase/MAP kinase activity immediately following the onset of stroke, most data points towards a beneficial effect of long-term, constitutional activity of these pathways in the functional recovery of damaged tissue.

Analysis of protein expression in the white matter showed a similar pattern of activation of MAP kinase and tyrosine kinase in penumbra although levels were not as high, and occurred in a smaller number of patients. This may be due to the lower concentration of neurones as well as weaker inflammatory response (observed in tissue sections) [23].

We have previously reported an increase in expression of VEGF protein in both the tissue penumbra, associated with neurones, endothelial cells and astrocytes [9] and in serum [8] of patients following ischaemic stroke. Our study shows that in the grey matter penumbra of the 13 patients expressing increased MAP kinase tyrosine phosphorylation, eight also expressed higher levels of VEGF protein. These patients also showed an increase in general tyrosine phosphorylation compared to normal contralateral tissue. VEGF is mitogenic for endothelial cells and its expression could be linked to activation of the tyrosine kinase and MAP kinase signal transduction cascade. Both astroglia [24] and monocyte derived macrophages [25] can synthesise and express VEGF, a process which is up-regulated in hypoxic conditions. In human glioma cells seeded at high density, increased expression of VEGF MRNA occurred concurrently with tyrosine phosphorylation of several proteins including MAP kinase [26]. Incubation of these cells with genistein (a specific tyrosine kinase inhibitor) significantly reduced VEGF mRNA expression suggesting, in agreement with our own findings, a possible link between the two processes. In the rat model of cerebral ischaemia, VEGF produced by microglial cells and macrophages binds to its receptors on nearby vascular endothelial cells, initiating an angiogenic response which counterbalances tissue hypoxia [27]. Constitutive activation

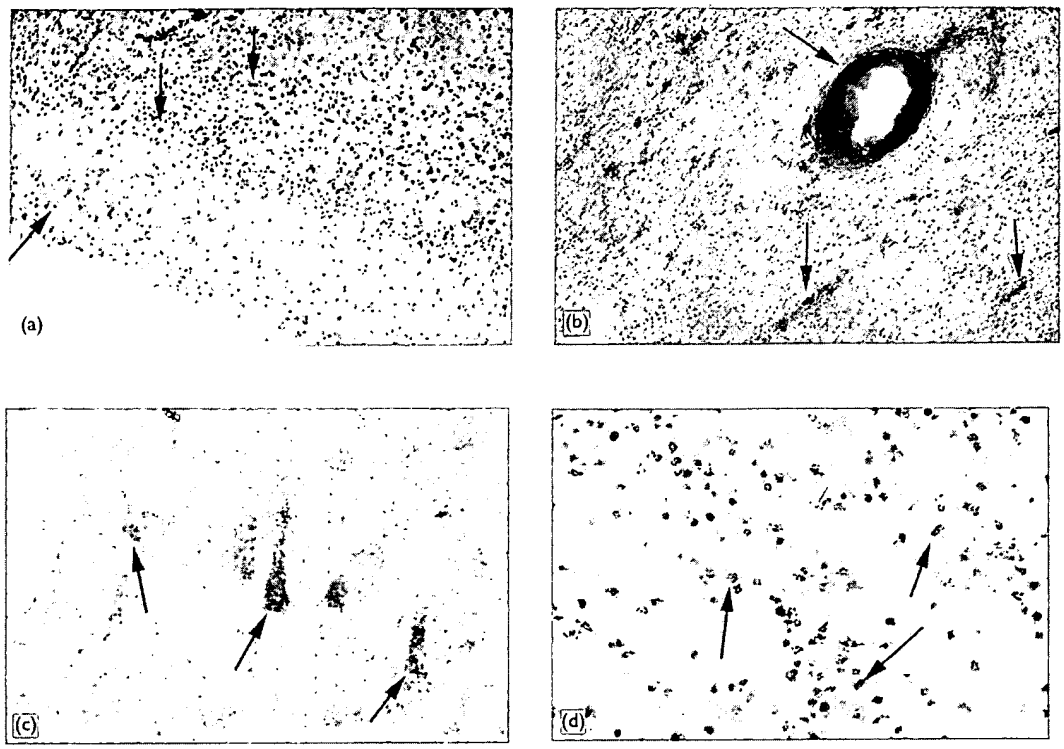

Fig. 2. IHC analysis of cellular distribution of tyrosine phosphorylated MAP kinase (ERK-1 and ERK-2) in patients following ischaemic stroke. **(a)** Normal control tissue with strong but homogenous staining in the grey matter. Mainly neurones in cortical layers I, III, and V are stained (arrows) (×200) **(b)** In penumbra tissue, most of the microvascular endothelial cells were strongly stained (arrows) (×400). **(c)** There was intensive staining in neurones in the grey matter penumbra areas. This immunostaining was mainly preserved in neurones localised within deeper cortical layers ie. V, VI. Mainly neuronal cell body was stained and only very weak staining was present in projections (arrows) (×400). **(d)** Section taken from the infarcted core of the patient who survived 44 days after ischaemic stroke. Dead neurones are weakly stained and most of the immunoreaction is present within the infiltrating astroglia and microglia/macrophages (arrows) (×200).

of these enzymes in glial cells may indirectly help to maintain VEGF protein expression thus sustaining angiogenesis in the penumbra region of damaged tissue.

CONCLUSION

Recent work using rat stroke models and other *in vitro* studies, suggest the initial cellular response to ischaemia involving tyrosine kinase, MAP kinase and VEGF activation/expression, may in fact contribute to tissue damage and increase in stroke volume. However longer term studies suggest that recovery of neuronal function in ischaemic border zones could benefit from a constitutively activated pathway, which stimulates angiogenesis and tissue reorganisation. Our findings of chronic activation of MAP kinase and tyrosine phosphorylation, together with upregulation of VEGF protein, may help to explain the mechanism of neuronal protection in penumbra tissue undergoing angiogenesis, and could be of relevance when considering clinical management of patients to maximize recovery after acute ischaemic stroke.

REFERENCES

1. Mattson MP. *Neurosci Biobehav Rev* **21**, 193–206 (1997).
2. Porter AC and Vaillancourt RR. *Oncogene* **17**, 1343–1352 (1998).
3. Schoft RJ and Morrow LA. *Cardiovascular Res* **27**, 1155–1161 (1993).
4. Wynendaele W, van Oosterom AT, Pawinski A *et al. Pharm World Sci* **20**, 225–235 (1998).
5. Krupinski J, Kaluza J, Kumar P *et al. Lancet* **342**, 742 (1993).
6. Krupinski J, Kaluza J, Kumar P *et al. Stroke* **25**, 642–649 (1994).
7. Silverman WF, Krum JM and Rosenstein JM. *Neuroscience* **90**,1529–1541 (1999).
8. Slevin M, Slowik A, Kumar P *et al. Stroke*, In Press (2000).
9. Issa R, Krupinski J, Bujny T *et al. Lab Invest* **79**, 417–425 (1999).
10. Lemmon MA and Schlessinger J. *Trends Biol Sci* **19**, 459–464 (1994).
11. Mielke K, Brecht S, Dorst A *et al. Neuroscience* **91**, 471–483 (1999).
12. Slevin M, Krupinski J, Kumar S *et al. Lab Invest* **78**, 987–1003 (1998).
13. Fukunaga K and Miyamoto E. *Mol Neurobiol* **16**, 79–95 (1998).
14. Scandanavian Stroke Study Group. *Stroke* **16**, 885–890 (1985).
15. Walton M, MacGibbon G, Joung D *et al. J Neurosci Res* **53**, 330–342 (1998).
16. Tallquist MD, Soriano P and Klinghoffer RA. *Oncogene* **18**, 7917–7932 (1999).
17. Girault JA, Costa A, Derkinderen P *et al. Trends Neurosci* **22**, 257–263 (1999).
18. Mandell JW and Vandenberg SR. *Neuroreport* **10**, 3567–3572 (1999).
19. Alessandrini A, Namura S, Moskowitz MA *et al. Proc Natl Acad Sci USA* **96**, 12866–12869 (1999).
20. Suzuki T, Mitake S and Murata S. *Brain Res* **840**, 36–44 (1999).
21. Perron JC and Bixby JL. *Mol Cell Neurosci* **13**, 362–378 (1999).
22. Zhang ZG, Chopp M, Lu D *et al. Brain Res* **847**, 338–342 (1999).
23. Schnell L, Fearn S, Klassen H *et al. Eur J Neurosci* **11**, 3648–3658 (1999).
24. Behzadian MA, Wang XL, Shabrawey M *et al. Glia* **24**, 216–225 (1998).
25. Harmey JH, Dimitriadis E, Kay E *et al. Ann Surg Oncol* **5**, 271–278 (1998).
26. Mukhopadhyay D, Tsiokas L and Sukhatme VP. *Gene Expression* **7**, 53–60 (1998).
27. Plate KH, Beck H, Danner S *et al. J Neuropathol Exp Neurol* **58**, 654–666 (1999).

Exhibit F

Intravenous administration of MEK inhibitor U0126 affords brain protection against forebrain ischemia and focal cerebral ischemia

Shobu Namura*†, Koji Iihara*, Shinya Takami*, Izumi Nagata*, Haruhiko Kikuchi*, Koji Matsushita‡, Michael A. Moskowitz‡, Joseph V. Bonventre§, and Alessandro Alessandrini§

*Stroke and Brain Protection, Research Institute, and Department of Neurosurgery, National Cardiovascular Center, 5-7-1 Fujishirodai, Suita, Osaka 565-8565, Japan; and ‡Stroke and Neurovascular Regulation, and §Renal Unit, Massachusetts General Hospital, Harvard Medical School, Charlestown, MA 02129

Edited by L. L. Iversen, University of Oxford, Oxford, United Kingdom, and approved July 6, 2001 (received for review May 1, 2001)

Brain subjected to acute ischemic attack caused by an arterial blockage needs immediate arterial recanalization. However, restoration of cerebral blood flow can cause tissue injury, which is termed reperfusion injury. It is important to inhibit reperfusion injury to achieve greater brain protection. Because oxidative stress has been shown to activate mitogen-activated protein kinases (MAPKs), and because oxidative stress contributes to reperfusion injury, MAPK may be a potential target to inhibit reperfusion injury after brain ischemia. Here, we demonstrate that reperfusion after forebrain ischemia dramatically increases phosphorylation level of extracellular signal-regulated kinase 2 (ERK2) in the gerbil hippocampus. In addition, i.v. administration of U0126 (100–200 mg/kg), a specific inhibitor of MEK (MAPK/ERK kinase), protects the hippocampus against forebrain ischemia. Moreover, treatment with U0126 at 3 h after ischemia significantly reduces infarct volume after transient (3 h) focal cerebral ischemia in mice. This protection is accompanied by reduced phosphorylation level of ERK2, substrates for MEK, in the damaged brain areas. Furthermore, U0126 protects mouse primary cultured cortical neurons against oxygen deprivation for 9 h as well as nitric oxide toxicity. These results provide further evidence for the role of MEK/ERK activation in brain injury resulting from ischemia/reperfusion, and indicate that MEK inhibition may increase the resistance of tissue to ischemic injury.

Cardiac arrest or cerebral arterial occlusion can cause a brain attack. Quickly restoring the cerebral blood flow is needed to stop brain injury. The most exciting new development in the field of stroke research is the recent approval of i.v. injection of tissue plasminogen activator that dissolves the blood clot (1, 2). Restoration of blood flow not only brings oxygen and nutrients into the damaged brain, but also produces free radicals such as reactive oxygen and reactive nitrogen species. These free radicals have been shown to contribute to oxidative injury. The tissue damage by the restoration of blood flow is termed reperfusion injury (3, 4). Thus, inhibition of reperfusion injury may be important to achieve greater brain protection.

Mitogen-activated protein kinase (MAPK) family members, including extracellular signal-regulated kinases (ERK1/2), p38 MAPK, and c-Jun N-terminal kinase (JNK), respond to various extracellular stimuli, thereby transmitting extracellular signals into the nucleus. ERK1/2 are activated by MAPK/ERK kinase1/2 (MEK1/2) by phosphorylating these MAPKs (5). The MEK/ERK pathway plays a crucial role in cell growth and differentiation (6, 7). ERK1/2 are constitutively expressed in the adult brain (8); however, little is known about the function of ERK1/2 in postmitotic, terminally differentiated neurons. The MEK/ERK pathway is also activated by reactive oxygen and reactive nitrogen species (9–11). Several *in vivo* studies showed that ERK1/2 are phosphorylated in the damaged brain after ischemia, hypoglycemia, and kainate-induced seizure (12–15). We previously reported that intraventricular administration of MEK1 inhibitor PD98059 (16) decreased infarct volume after focal cerebral ischemia (17). This work suggests that the MEK/ERK pathway plays a crucial role in ischemic brain injury.

Recently, a novel and more potent MEK-specific inhibitor U0126 was developed (18, 19). Whereas U0126 inhibits the enzymatic activity of MEK1/2, PD98059 blocks the phosphorylation of MEK1, but cannot efficiently inhibit the activity of MEK1 once it is phosphorylated (16). In this study, we investigated whether U0126 enhances the neuronal survivability after ischemia and reperfusion in experimental models.

Methods

Ischemia Model. Forebrain ischemia was induced by bilateral carotid artery occlusion (BCAO) in male gerbils (50–70 g) under anesthesia with 1.0% halothane in 70% N_2O and 30% O_2. Focal cerebral ischemia was induced by middle cerebral artery occlusion (MCAO) using silicon-coated 8-0 nylon filament in male ICR or ddY mice (20–22 g; Japan SLC, Hamamatsu, Japan) as described (20). Regional cerebral blood flow was monitored by laser-Doppler flowmetry (FLO-C1, Omegawave, Tokyo, Japan). U0126 (Promega) or vehicle (0.1 M PBS containing 0.4% dimethyl sulfoxide) was injected into the femoral vein. Animal protocols followed the National Cardiovascular Center's guidelines for animal care and experiments.

Evaluation of Hippocampal Injury. Seven days after reperfusion, coronal brain sections of 40 μm thickness were made by using a freezing microtome, and stained with 0.1% cresyl violet. The CA1 pyramidal cells were counted and expressed as cells per millimeter.

Evaluation of Brain Infarction. Brains were cut into coronal slices, and incubated with 2% 2,3,5-triphenyltetrazolium chloride, as described (21). The infarcted areas were measured on each section by an image analysis system (Olympus, Tokyo, Japan), and infarction volume was calculated by summing the infarct areas. Evaluation of brain atrophy volume was done by calculating using the following formula: (contralateral volume − ipsilateral volume) × 100/contralateral volume.

Primary Culture. Mixed cortical cell cultures containing both neurons and glia were prepared from ICR mouse embryos at 15

This paper was submitted directly (Track II) to the PNAS office.

Abbreviations: BCAO, bilateral carotid artery occlusion; JNK, c-Jun N-terminal kinase; MAPK, mitogen-activated protein kinase; ERK, extracellular-signal regulated kinase; MEK, MAPK/ERK kinase; MCAO, middle cerebral artery occlusion; NMDA, *N*-methyl-D-aspartic acid; NO, nitric oxide; SNP, sodium nitroprusside; CS, control solution.

See commentary on page 10989.

†To whom reprint requests should be addressed. E-mail: namura@ri.ncvc.go.jp.

The publication costs of this article were defrayed in part by page charge payment. This article must therefore be hereby marked "*advertisement*" in accordance with 18 U.S.C. §1734 solely to indicate this fact.

MEDICAL SCIENCES

days of gestation as described (22). The cultures were used at 15 days *in vitro*. For oxygen deprivation, the cultures were transferred to an anaerobic chamber (Forma Scientific, Marietta, OH) containing a gas mixture of 5% CO_2, 10% H_2, and 85% N_2. The culture media were replaced with deoxygenated, glucose free or glucose (20 mM) containing Earle's balanced salt solution (BSS), and the cultures were placed in the chamber at 37°C. Oxygen deprivation was terminated by replacing the medium with oxygenated BSS containing 20 mM glucose, and cultures were returned to the normoxic incubator. For toxicity experiments, the culture media were replaced with Hepes-buffered control solution (CS, pH 7.4) containing toxin. For glutamate, *N*-methyl-D-aspartic acid (NMDA) and sodium nitropruside (SNP) toxicity experiments, the culture was exposed to Hepes-buffered CS containing 300 μM of these compounds for 5 min, and then the culture media were replaced with CS for 24 h. For kainic acid toxicity, the culture was exposed to CS containing 30 μM of kainic acid for 24 h.

Evaluation of Cell Death. Cell death was determined by measuring propidium iodide (PI) fluorescence by using a multiwell plate fluorescence scanner (Cytofluor, Series 4000, PerSeptive Biosystems, Framingham, MA; ref. 23). Data were expressed as percentage of PI fluorescence in sister cultures exposed to 1 mM NMDA for 24 h.

Western Blot Analysis. Western blotting was performed as described previously (17) by using phospho-specific antibodies for the protein kinases (1:1,000; New England Biolabs). To analyze protein levels of ERK1/2, the immunoblots were stripped and reprobed with anti-ERK1 and anti-ERK2 antibodies (1:2,000, respectively; Santa Cruz Biotechnology).

Immunostaining. Immunostaining was done as described previously (24). The dilution of primary antibody was 1:100 for phospho-ERK1/2 and 1:500 for total-ERK2, respectively. For double immunostaining, the sections were also treated with NeuN monoclonal antibody (1:1,000; Chemicon), and then phospho-ERK1/2 and NeuN immunoreactivities were respectively labeled with Alexa Fluor 546 and Alexa Fluor 488 (Molecular Probes). The sections were observed by using an Olympus confocal laser microscope (FLUOVIEW, Tokyo, Japan).

Statistics. Data are presented as mean ± SEM. Data were analyzed by Student *t* test or one-way ANOVA followed by Bonferroni's post hoc test. For neurological score, Mann–Whitney *U* test was used. $P < 0.05$ was considered statistically significant.

Results

Reperfusion After Forebrain Ischemia Phosphorylates ERK1/2 in the Hippocampus. First we asked whether ERK1/2 are involved in hippocampal injury after forebrain ischemia in the gerbil. We examined the changes in phosphorylation of ERK1/2 in the hippocampus by using a phospho-ERK1/2 antibody. ERK1/2 were dephosphorylated by BCAO. The longer duration of BCAO resulted in the greater dephosphorylation of ERK1/2 (Fig. 1*A Top*). This may be a result of decreased ATP production during ischemia. Significant increase in phosphorylation of ERK1/2 was observed by 5 min after reperfusion after 3.5 min of BCAO, and persisted until 1 h, compared with sham control (Fig. 1*A Middle*). However, the total ERK1/2 protein levels did not change during reperfusion period (Fig. 1*A Bottom*). These results indicate that ERK1/2 are activated by reperfusion after BCAO. We next examined changes in phosphorylation levels of other protein kinases. We found a very weak increase in phospho-p38 MAPK at 1 to 5 min after reperfusion; however, we found no significant increase in phospho-JNK and phospho-p70^{S6} kinase over sham (Fig. 1*B*). These results suggest that MEK/ERK pathway is a major MAPK cascade activated in the hippocampus after forebrain ischemia and reperfusion.

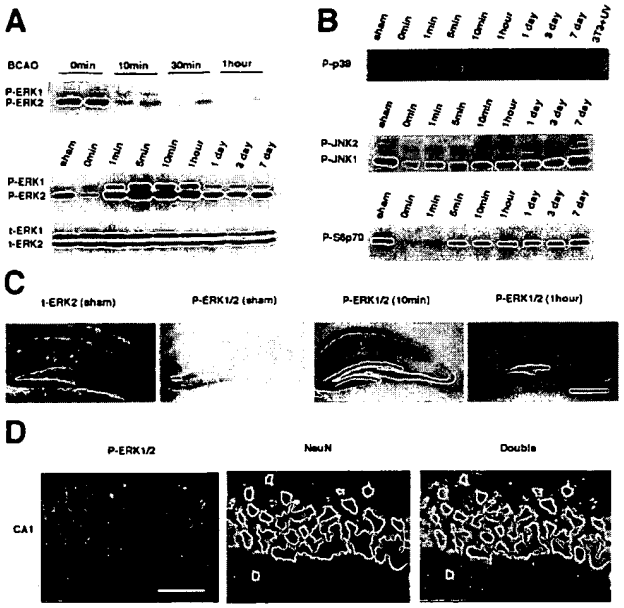

Fig. 1. Reperfusion after forebrain ischemia increases phosphorylation of ERK1/2 in hippocampus. (*A*) Ischemia alone by BCAO dephosphorylates ERK1/2 (*Top*), whereas reperfusion after 3.5 min BCAO increases phosphorylation levels of ERK1/2 (*Middle*). Total protein levels of ERK1/2 are not affected by 3.5 min BCAO and reperfusion (*Bottom*). Data were reproduced by five independent experiments. (*B*) Time-dependent changes in phospho-p38 MAPK (*Top*), phospho-JNK (*Middle*), and phospho-p70^{S6} kinase (*Bottom*) in the hippocampus after 3.5 min BCAO. UV-treated NIH 3T3 cell lysate (3T3 + UV) was used as a control for p38 MAPK phosphorylation. Data were reproduced by five independent experiments. (*C*) Immunostaining of sham-control or ischemic brains after 10 min or 1 h of reperfusion by using total ERK2 (t-ERK2) or phospho-ERK1/2 (P-ERK1/2) antibodies. Scale bar = 1 mm. (*D*) Confocal microscopic images document the localization of phospho-ERK1/2 immunoreactivity (red) and NeuN (CNS neuronal specific marker) immunoreactivity (green) in single tissue section from subfield CA1 after 10 min reperfusion after 3.5 min BCAO. Scale bar = 100 μm.

To determine the cell type in which ERK1/2 are phosphorylated, we did immunostaining using phospho-ERK1/2 antibody on brain sections. Total-ERK2 immunostained cells were found throughout the hippocampus, whereas little phospho-ERK1/2 immunoreactivity was detected in the sham-operated animals. After 10 min of reperfusion, intense phospho-ERK1/2 immunostaining was detected in the CA1, dentate gyrus, and mossy fibers, but not in the pyramidal cell layer of CA3 that survives 3.5 min BCAO (Fig. 1*C*). Closer analysis of CA1 pyramidal cells revealed phospho-ERK1/2 immunostaining in both cytoplasm and nucleus (Fig. 1*D*). Phospho-ERK1/2 immunostaining returned to the basal levels in these areas by 1 h after reperfusion, with some phospho-ERK1/2 immunostaining persisting in neurons in the hilar region (Fig. 1*C*).

U0126 Attenuates Hippocampal Injury After Forebrain Ischemia. To examine whether inhibition of MEK1/2 protects the hippocampus, we tested i.v. administration of U0126 in gerbils subjected to 3.5 min BCAO. U0126 reduced phospho-ERK1/2 immunoreactivity on immunoblots as well as phospho-ERK1/2 immunostaining in the CA1 pyramidal cells 10 min after reperfusion in a dose-dependent manner (Fig. 2*A* and *B*). Moreover, U0126 pretreatment decreased the loss of CA1 pyramidal cells at 7 days

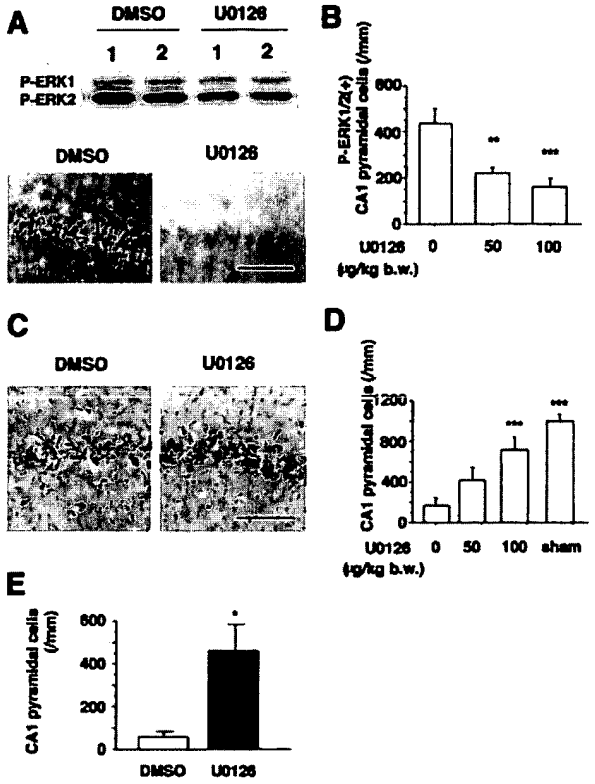

Fig. 2. U0126 reduces phosphorylation of ERK1/2 and subsequent neuronal death in the CA1 after forebrain ischemia. (*A*) Western blot analysis and immunostaining by using phospho-ERK1/2 antibody demonstrating that i.v. injection of U0126 (100 μg/kg) reduces phosphorylation level of ERK1/2 in the hippocampus after 10 min of reperfusion after 3.5 min BCAO. Photomicrographs of phospho-ERK1/2 immunostaining were taken from the subfield CA1. Scale bar = 200 μm. (*B*) The number of phospho-ERK1/2 immunoreactive CA1 pyramidal cells. U0126 was injected i.v. 10 min before 3.5 min BCAO. **, $P < 0.01$; ***, $P < 0.001$, compared with the DMSO-injected group (ANOVA). Data are presented as mean + SEM ($n = 6$–8). (*C*) Photomicrographs of the subfield CA1 stained with 0.1% cresyl violet from DMSO- and U0126-administrated gerbils. DMSO or U0126 was injected i.v. 10 min before 3.5 min BCAO, and the brains were evaluated 7 days after reperfusion. Scale bar = 200 μm. (*D*) Dose-dependent protective effect by injection of U0126 10 min before ischemia. The brains were examined 7 days after reperfusion. ***, $P < 0.001$, compared with the DMSO-injected group (ANOVA). Data are presented as mean + SEM ($n = 5$–8). (*E*) Neuroprotection by i.v. injection of U0126 (100 μg/kg) during ischemia (3 min after BCAO). The brains were examined 7 days after reperfusion. *, $P < 0.05$ (unpaired Student *t* test). Data are presented as mean + SEM ($n = 5$ and 6 in DMSO and U0126 group).

(Fig. 2 *C* and *D*). At the doses used, U0126 did not affect the rectal temperature during ischemia and after reperfusion (Table 1). Mean arterial blood pressure, partial oxygen (pO_2) and carbon dioxide (pCO_2) tensions, blood pH, and glucose levels were not affected by U0126 when compared with vehicle injection (Table 2). Furthermore, injection of U0126 at 3 min after BCAO was protective in the CA1 when evaluated at 7 days (Fig. 2*E*).

U0126 Protects Brain in Stroke Models. We next tested U0126 in mouse ischemic stroke models. Pretreatment with i.v. administration of U0126 dramatically decreased infarct volume 24 h after permanent MCAO. Maximum protection was achieved with 200 μg/kg of U0126, with a 42% ($P < 0.001$) reduction in infarct volume (Fig. 3*A*). Neurological deficits 24 h after ischemia were improved by U0126 (Table 3). U0126 administration 1 h after MCAO was protective, but not when given 3 h after MCAO in the permanent focal ischemia model (Fig. 3*A*). U0126 did not affect regional cerebral blood flow, core temperature, and body weight after MCAO (Table 3).

We next examined whether delayed injection of U0126 during ischemia protects brain against 3 h reversible MCAO. U0126 (200 μg/kg) injected 10 min before reperfusion significantly decreased infarct volume by 40% ($P < 0.01$) at 24 h after reperfusion (Fig. 3*B*). Densitometric analysis of phospho-ERK2 immunoblots demonstrated that the level of phosphorylation after U0126 was significantly reduced by 27% in the ischemic hemisphere ($P = 0.026$, $n = 3$; Fig. 3*C*). Phospho-ERK1/2 was also reduced in the damaged brain areas in U0126-injected mice by immunostaining (Fig. 3*D*). This brain protection was sustained for 35 days. In U0126-injected animals, there was a 41% decrease in brain atrophy compared with vehicle-injected animals ($P < 0.05$; Fig. 3*E*). U0126 did not affect regional cerebral blood flow and core temperature during and after MCAO (data not shown). Thus, these data suggest that administration of U0126 after onset of ischemic stroke inhibits brain injury.

U0126 Protects Cortical Cultures Against Oxygen Deprivation as Well as Nitric Oxide (NO) Toxicity. Finally, to study the protective effect of U0126 at the cellular level, we examined the drug effect in mouse primary cultured cortical neurons. First, we tested U0126 in cortical neurons subjected to hypoxia. Nine hours of oxygen deprivation followed by 24 h reoxygenation caused death in 80–90% of neuronal cells, which could be inhibited by U0126. NMDA antagonist dizocilpine (MK-801; 10 μM) was also protective as reported previously (ref. 25; Fig. 4*A*). The protection

Table 1. Changes in rectal temperature (°C) after 3.5 min BCAO in the gerbil

	U0126, μg/kg		
	0 ($n = 6$)	50 ($n = 7$)	100 ($n = 7$)
BCAO	37.4 ± 0.1	37.4 ± 0.2	37.5 ± 0.1
Reperfusion	37.8 ± 0.2	38.0 ± 0.2	38.0 ± 0.3
1 hr	38.6 ± 0.2	39.0 ± 0.3	39.1 ± 0.5
3 hr	37.9 ± 0.2	37.6 ± 0.3	38.3 ± 0.4
6 hr	38.4 ± 0.3	38.4 ± 0.2	38.5 ± 0.1

Table 2. Effects of i.v. injection of U0126 on physiological parameters in the gerbil

	DMSO	U0126 (100 μg/kg)
MABP, mmHg		
Before	74.8 ± 7.5 ($n = 5$)	74.6 ± 8.5 ($n = 5$)
15 min	81.2 ± 5.1 ($n = 5$)	75.0 ± 5.6 ($n = 5$)
pH		
Before	7.38 ± 0.01 ($n = 10$)	7.35 ± 0.02 ($n = 10$)
15 min	7.39 ± 0.02 ($n = 10$)	7.35 ± 0.02 ($n = 10$)
pCO_2, mmHg		
Before	42.6 ± 2.2 ($n = 10$)	40.6 ± 1.8 ($n = 10$)
15 min	40.8 ± 1.6 ($n = 10$)	38.0 ± 2.0 ($n = 10$)
pO_2, mmHg		
Before	147.2 ± 4.8 ($n = 10$)	145.9 ± 8.1 ($n = 10$)
15 min	156.5 ± 5.5 ($n = 10$)	152.2 ± 6.2 ($n = 10$)
Glucose, mg/dl		
Before	97.5 ± 4.9 ($n = 10$)	108.3 ± 6.8 ($n = 10$)
15 min	111.1 ± 7.9 ($n = 10$)	115.4 ± 15.6 ($n = 10$)
30 min	116.2 ± 5.0 ($n = 5$)	105.0 ± 12.6 ($n = 5$)

MABP, mean arterial blood pressure. Results are mean ± SEM.

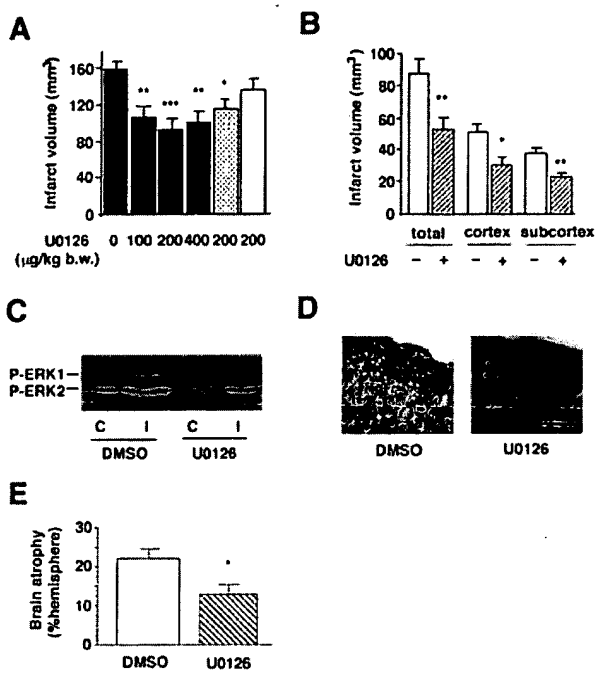

Fig. 3. U0126 protects brain against damage resulting from ischemic stroke in mice. (*A*) Infarct volume after 24 h of MCAO. U0126 was injected 10 min before (filled columns), 1 h (dotted column), or 3 h (open column) after MCAO. *, $P < 0.05$; **, $P < 0.01$; ***, $P < 0.001$, compared with the vehicle-injected group (ANOVA). Data are presented as mean + SEM (n = 8–11). (*B*) Infarct volume 24 h after reperfusion after 3 h of reversible MCAO. DMSO (open columns) or U0126 (200 μg/kg; hatched columns) was injected i.v. at 2 h and 50 min after induction of MCAO (i.e., 10 min before reperfusion). Data are presented as mean + SEM (n = 12 in each group). *, $P < 0.05$; **, $P < 0.01$ (unpaired Student t test). (*C* and *D*) Immunoblotting (*C*) and immunostaining (*D*) using phospho-ERK1/2 antibody show that i.v. injection of U0126 (200 μg/kg) during ischemia diminishes phospho-ERK1/2 immunoreactivity in the damaged brain 5 min after reperfusion after 3 h of MCAO. C, contralateral; I, ipsilateral. Scale bar = 200 μm. (*E*) Brain atrophy volume 35 days after reperfusion after 3 h of MCAO. Single injection of DMSO or U0126 (200 μg/kg) was given 10 min before reperfusion. Data are presented as mean + SEM (n = 8 and 10 in DMSO and U0126 group, respectively). *, $P < 0.05$ (unpaired Student t test).

by U0126 was dose dependent (Fig. 4*B*). Ten micromolar of U0126 afforded a 40% reduction in cell death. We also tested U0126 in cortical neurons subjected to combined oxygen and glucose deprivation. Although MK-801 protected against oxygen/glucose deprivation consistently with previous reports (26), U0126 was not effective (Fig. 4*C*).

We next examined the phosphorylation levels of ERK1/2 in cortical neurons subjected to oxygen deprivation. Nine hours of oxygen deprivation resulted in a concomitant increase and decrease in phosphorylated ERK1 and ERK2, respectively (Fig. 4*D Top*). At 2 h after reoxygenation, the levels of phosphorylation in both ERK1 and ERK2 were increased, and sustained until 3 h. U0126 inhibited phosphorylation of ERK2 in a dose-dependent manner, but interestingly did not affect the phosphorylation level of ERK1. Total protein levels of ERK1/2 did not change after oxygen deprivation and reoxygenation (Fig. 4*D Middle*). We also studied the phosphorylation levels of MEK1/2, direct activators of ERK1/2. U0126 blocks activity but not phosphorylation of MEK1/2 (18). The phosphorylation of MEK1/2 was greater in U0126 treated cultures at all time points (Fig. 4*D Bottom*). This finding may result from inhibition of MEK1/2 turnover, or the lack of activation of downstream molecules, such as phosphatases, that ordinarily play a negative feedback role. To further verify the specificity of U0126, we examined the effects of U0126 on phosphorylation of other protein kinases. U0126, at concentrations up to 10 μM, did not affect phosphorylation levels in p38 MAPK, JNK, and $p70^{S6}$ kinase (Fig. 4*E*).

Both excessive excitation of the glutamate receptors and overproduction of free radicals have been implicated in neuronal cell death resulting from ischemia (27, 28). In addition, glutamate receptor stimulation and NO have been shown to phosphorylate ERK2 in cultured cortical neurons (11, 29). We next asked whether U0126 is protective under these specific toxic conditions. We tested U0126 in primary cultured cortical neurons exposed to glutamate, NMDA, or kainic acid. U0126 was not protective against these excitotoxins (Fig. 4*F*). Rather, 10 μM U0126 enhanced cell death by NMDA. In contrast, U0126 dramatically inhibited neuronal cell death by exposure for 5 min to the NO donor, SNP, in a dose-dependent manner, with a maximum inhibition at 10 μM (Fig. 4*G*). Another MEK1 inhibitor, PD98059 (25 μM), also attenuated neuronal cell death by SNP at 12 h; however, this protection was not found at 24 h (data not shown). p38 MAPK inhibitor SB203580 (10 μM) was not protective against SNP (Fig. 4*H*).

Table 3. Physiological parameters and neurological deficit score after permanent MCAO

	U0126, μg/kg			
	0 (n = 8)	100 (n = 9)	200 (n = 9)	400 (n = 11)
Core temp., °C	37.0 ± 0.1	37.0 ± 0.0	36.9 ± 0.1	37.0 ± 0.1
TM temp., °C	37.3 ± 0.2	37.1 ± 0.1	37.5 ± 0.2	37.3 ± 0.1
rCBF, %	15.0 ± 2.0	13.5 ± 1.1	17.0 ± 1.4	17.4 ± 0.7
Neurological score	1.5 ± 0.3	0.6 ± 0.2*	0.6 ± 0.2*	0.5 ± 0.2*
BW loss, %	21.8 ± 1.6	18.2 ± 0.9	20.8 ± 0.9	14.5 ± 1.7

Results are mean ± SEM. Temp., temperature; TM, Temporal muscle; BW, body weight. Data for temperatures and rCBF were collected at 30 min after induction of MCAO. rCBF is expressed as a percentage of the value before MCAO. Neurological scoring was determined according to Hara *et al.* (20) and done at 24 hr after MCAO. Body weight loss (%) was calculated as 100 × [body weight (before) − body weight (24 h)]/body weight (before). *, $P < 0.05$ by Mann–Whitney U test, compared with 0 μg/kg group.

Discussion

We demonstrated that i.v. administration of U0126, a MEK1/2 inhibitor, protects brain against damage after forebrain as well as focal cerebral ischemia. In addition, we clearly demonstrated that U0126 provides protection in primary cultured cortical neurons against SNP, as well as oxygen deprivation.

Ischemia and reperfusion enhanced phospho-ERK1/2 immunostaining not only in the CA1 pyramidal cells but also in dentate granule cells that escape damage under the current ischemic condition. These results indicate that MEK/ERK activation results in damage or survival in a cell type-specific manner. Different outcomes after MEK/ERK activation in these two neuronal cell types may be explained by other signaling pathways, such as phosphatidylinositol 3-kinase (PI3-kinase)/Akt. PI3-kinase/Akt have been implicated in cell survival and are differentially regulated and/or activated in a neuronal cell type-specific manner. We demonstrated that Akt activation is more dramatic and prolonged in the dentate gyrus than CA1 after forebrain ischemia in the gerbil (30). Hence, these signaling pathways need to be investigated in specific cell types in any given experimental model.

The mechanisms by which ERK activation leads to neuronal cell death remain unclear. However, the evidence that ERK activation contributes to cell death is accumulating. A critical role for ERK in hydrogen peroxide-induced cell death was

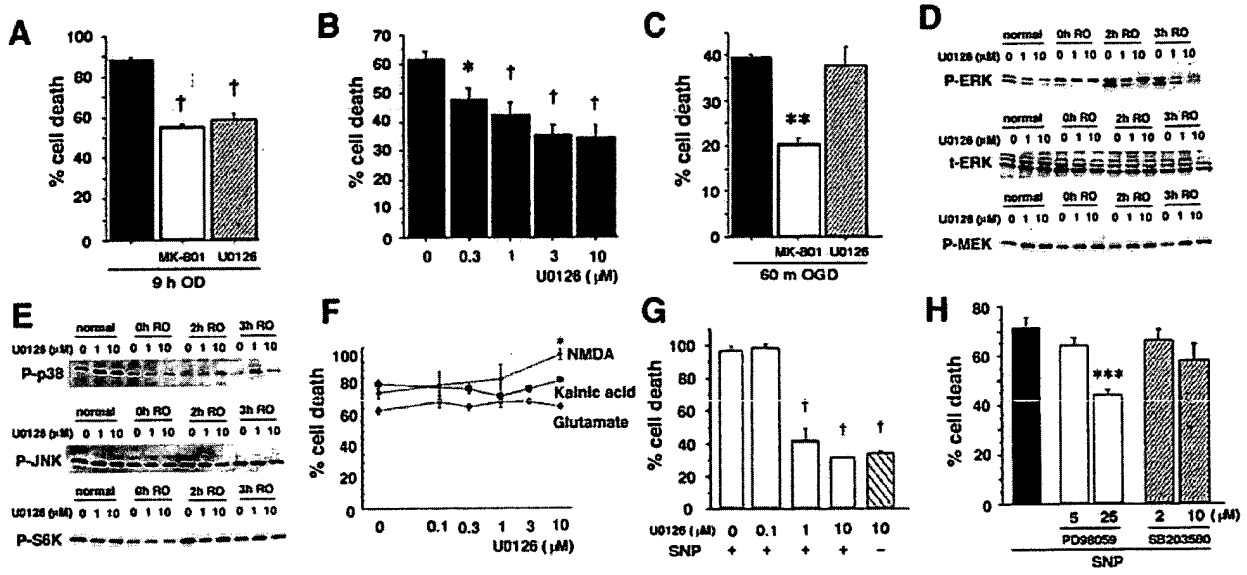

Fig. 4. U0126 protects cortical cultures against oxygen deprivation and SNP. (*A*) Protection by MK-801 (10 μM) and U0126 (10 μM) against neuronal death resulting from 9 h of oxygen deprivation followed by 24 h reoxygenation. †, $P < 0.0001$, compared with oxygen deprivation alone (ANOVA). Data are presented as mean ± SEM ($n = 16$). (*B*) Dose-dependent protective efficacy of U0126 in primary cultured cortical neurons exposed to 9 h of oxygen deprivation followed by 24 h reoxygenation. *, $P < 0.05$; †, $P < 0.0001$, compared with 0 μM (ANOVA). Data are presented as mean ± SEM ($n = 12$). (*C*) U0126 is not protective against 60 min of oxygen/glucose deprivation. **, $P < 0.01$, compared with control (ANOVA). Data are presented as mean ± SEM ($n = 4$). (*D*) Dose-dependent effects of U0126 on phosphorylation of ERK and MEK in primary cultured cortical neurons exposed to 9 h of oxygen deprivation and reoxygenation (RO) for the indicated time. (*E*) U0126 does not affect phosphorylation levels of p38 MAPK, JNK, and $p70^{S6}$ kinase in primary cultured cortical neurons exposed to 9 h of oxygen deprivation and reoxygenation (RO) for the indicated time. (*F*) U0126 does not protect primary cultured cortical neurons exposed for 5 min to 300 μM glutamate (filled circle) or 300 μM NMDA (diamond). U0126 is not protective against exposure to 30 μM kainic acid (square) for 24 h. *, $P < 0.05$, compared with 0 μM (ANOVA). Data are presented as mean ± SEM ($n = 8$). (*G*) Dose-dependent efficacy of U0126 in primary cultured cortical neurons exposed to 300 μM SNP for 5 min. Cell death was determined at 24 h after exposure. †, $P < 0.0001$, compared with 0 μM (ANOVA). Data are presented as mean ± SEM ($n = 8$). (*H*) Another MEK1 inhibitor, PD98059, but not p38 MAPK inhibitor SB203580 attenuates neuronal death by exposure to SNP (300 μM) for 5 min. Cell death was determined at 12 h. Data are presented as mean ± SEM ($n = 8$). *, $P < 0.05$, compared with control (ANOVA).

demonstrated in an oligodendrocyte cell line (31). Another study provides evidence that ERK activation contributes to zinc toxicity in cortical neurons (32). Our laboratory and Stanciu *et al.* independently demonstrated that MEK inhibitors block oxidative glutamate toxicity in cortical neurons (33, 34). Enhancement by brain-derived neurotrophic factor (BDNF) in NO-induced neuronal apoptosis has been shown to be mediated by ERK activation (35). Recently, it has been shown that cisplatin-induced apoptosis in HeLa cells requires ERK activation (36).

We observed that U0126 up to 10 μM does not affect p38 MAPK, JNK, and $p70^{S6}$ kinase in primary cultured cortical neurons. In addition, p38 MAPK inhibitor SB203580 was not protective against SNP. Therefore, we can exclude the possibility that U0126 protected by nonspecific inhibition of these proapoptotic molecules. We found that U0126 did not reduce the phosphorylation levels of MEK1/2 in cortical neurons exposed to oxygen deprivation. Rather, U0126 was associated with an increase of MEK1/2 phosphorylation levels. These results suggest that U0126 does not affect upstream components of MEK1/2. Furthermore, the protection afforded by U0126 is not due to scavenging of free radicals because NO elicits phosphorylation of ERK2 by direct activation of Ras, an upstream effector of the MEK/ERK pathway (11). Another MEK inhibitor, PD98059, also attenuated SNP-induced neuronal death. Hence, we believe that the neuroprotective efficacy of U0126 results from its inhibition of MEK1/2.

U0126 inhibited phosphorylation of ERK2 in a dose-dependent manner; however, U0126 had no effect on phosphorylation of ERK1 during 2 h after reoxygenation after 9 h of oxygen deprivation. The inhibition of ERK2 phosphorylation was correlated with inhibition of neuronal death. These findings suggest that ERK1 and ERK2 play differential roles in cell survival and cell death, respectively. Sutherland *et al.* have shown that activation of ERK2 but not ERK1 is associated with B cell antigen receptor-induced apoptosis in B lymphoma cells (37). We cannot presently explain this differential effect of U0126 on the phosphorylation states of ERK1 and ERK2. It is possible that phosphorylated ERK1 may be more stable than phosphorylated ERK2 in cortical neurons during these reoxygenation periods.

In conclusion, we demonstrated brain protection against ischemia by i.v. injection of MEK inhibitor U0126. These results constitute further evidence for the crucial role of MEK/ERK in brain injury resulting from ischemia and reperfusion in experimental models. In addition, as demonstrated in our animal models, phosphorylation of ERK2 was dramatically increased in the brain by reperfusion after ischemia. These data, together with accumulating evidence that the MEK/ERK pathway contributes to oxidative injury (31, 33, 34, 36), suggest that U0126 may protect brain from reperfusion injury.

This work was supported by Special Coordination Funds for Promoting Science and Technology, STA, Japan (S.N. and I.N.), The Japan Society for the Promotion of Science Fellowship (S.N. and A.A.), Japan Research Foundation for Clinical Pharmacology (S.N.), Grants-in-Aid for Scientific Research, the Ministry of Education, Science, Sports and Culture, Japan (S.N.), and a Massachusetts General Hospital Interdepartmental Stroke Project Grant from the National Institutes of Health (M.A.M., J.V.B., and A.A.).

1. The National Institute of Neurological Disorders and Stroke rt-PA Stroke Study Group. (1995) *N. Engl. J. Med.* **333,** 1581–1587.
2. Hacke, E. C., Kaste, M., Fieschi, C., Toni, D., Lesaffre, E., von Kummer, R., Boysen, G., Bluhmki, E., Hàxter, G., Mahagne, M.-H., *et al.* (1995) *J. Am. Med. Assoc.* **274,** 1017–1025.
3. Birnbaum, Y., Leor, J. & Kloner, R. A. (1997) *J. Thromb. Thrombolysis* **4,** 185–195.
4. Kontos, H. A. (1985) *Circ. Res.* **57,** 508–516.
5. Seger, R. & Krebs, E. G. (1995) *FASEB J.* **9,** 726–735.
6. Boulton, T. G., Nye, S. H., Robbins, D. J., Ip, N. Y., Radziejewska, E., Morgenbesser, S. D., DePinho, R. A., Panayotatos, N., Cobb, M. H. & Yancopoulos, G. D. (1991) *Cell* **65,** 663–675.
7. Segal, R. A. & Greenberg, M. E. (1996) *Annu. Rev. Neurosci.* **19,** 463–472.
8. Fiore, R. S., Bayer, V. E., Pelech, S. L., Posada, J., Cooper, J. A. & Baraban, J. M. (1993) *Neuroscience* **55,** 463–472.
9. Baas, A. S. & Berk, B.C (1995) *Circ. Res.* **77,** 29–36.
10. Guyton, K. Z., Liu, Y., Gorospe, M., Xu, Q. & Holbrook, N. J. (1996) *J. Biol. Chem.* **271,** 4138–4142.
11. Yun, H. Y., Gonzalez-Zulueta, M., Dawson, V. L. & Dawson, T. M. (1998) *Proc. Natl. Acad. Sci. USA* **95,** 5773–5778.
12. Campos-González, R. & Kindy, M. (1992) *J. Neurochem.* **59,** 1955–1958.
13. Kindy, M. S. (1993) *J. Cereb. Blood Flow Metab.* **13,** 372–377.
14. Hu, B.-R. & Wieloch, T. (1994) *J. Neurochem.* **62,** 1357–1367.
15. Ohtsuki, T., Matsumoto, M., Kitagawa, K., Mabuchi, T., Mandai, K., Matsushita, K., Kuwabara, K., Tagaya, M., Ogawa, S., Ueda, H., Kamada, T. & Yanagihara, T. (1996) *Am. J. Physiol.* **271,** C1085–C1097.
16. Alessi, D. R., Cuenda, A., Cohen, P., Dudley, D. T. & Saltiel, A. R. (1995) *J. Biol. Chem.* **270,** 27489–27494.
17. Alessandrini, A., Namura, S., Moskowitz, M. A. & Bonventre, J. V. (1999) *Proc. Natl. Acad. Sci. USA* **95,** 12866–12869.
18. Favata, M. F., Horiuchi, K. Y., Manos, E. J., Daulerio, A. J., Stradley, D. A., Feeser, W. S., Van Dyk, D. E., Pitts, W. J., Earl, R. A., Hobbs, F., *et al.* (1998) *J. Biol. Chem.* **273,** 18623–18632.
19. DeSilva, D. R., Jones, E. A., Favata, M. F., Jaffee, B. D., Magolda, R. L., Trzaskos, J. M. & Scherle, P. A. (1998) *J. Immunol.* **160,** 4175–4181.
20. Hara, H., Haung, P. L., Panahian, N., Fishman, M. C. & Moskowitz, M. A. (1996) *J. Cereb. Blood Flow Metab.* **16,** 605–611.
21. Bederson, J. B., Pitts, L. H., Germano, S. M., Nishimura, M. C., Davis, R. L. & Bartkowski, H. M. (1986) *Stroke* **17,** 1304–1308.
22. Hertz, E., Yu, Ach., Hertz, L., Juurlink, B. H. J. & Schousboe, A. (1989) in *A Dissection and Tissue Culture Manual of the Nervous System,* eds. Shahar, A., de Vellis, J., Vernadakis, A. & Haber, B. (Liss, New York), pp. 183–186.
23. Sattler, R., Charlton, M. P., Hafner, M. & Tymianski, M. (1997) *J. Cereb. Blood Flow Metab.* **17,** 455–463.
24. Namura, S., Zhu, J., Fink, K., Endres, M., Srinivasan, A., Tomaselli, K. J., Yuan, J. & Moskowitz, M. A. (1998) *J. Neurosci.* **18,** 3659–3668.
25. Goldberg, M. P., Weiss, J. H., Pham, P.-C. & Choi, D. (1987) *J. Pharmacol. Exp. Ther.* **243,** 784–791.
26. Goldberg, M. P. & Choi, D. (1993) *J. Neurosci.* **13,** 3510–3524.
27. Choi, D. W. (1988) *Neuron* **1,** 623–634.
28. Beckman, J. S. (1991) *J. Dev. Physiol.* **15,** 53–59.
29. Fiore, R. S., Murphy, T. H., Sanghera, J. S., Pelech, S. L. & Baraban, J. M. (1993) *J. Neurochem.* **61,** 1626–1633.
30. Namura, S., Nagata, I., Kikuchi, H., Andreucci, M. & Alessandrini, A. (2000) *J. Cereb. Blood Flow Metab.* **20,** 1301–1305.
31. Bhat, N. R. & Zhang, P. (1999) *J. Neurochem.* **72,** 112–119.
32. Park, J. A. & Koh, J. Y. (1999) *J. Neurochem.* **73,** 450–456.
33. Satoh, T., Nakatsuka, D., Watanabe, Y., Nagata, I., Kikuchi, H. & Namura, S. (2000) *Neurosci. Lett.* **288,** 163–166.
34. Stanciu, M., Wang, Y., Kentor, R., Burke, N., Watkins, S., Kress, G., Reynolds, I., Klann, E., Angiolieri, M. R., Johnson, J. W., *et al.* (2000) *J. Biol. Chem.* **275,** 12200–12206.
35. Ishikawa, Y., Ikeuchi, T. & Hatanaka, H. (2000) *J. Neurochem.* **75,** 494–502.
36. Wang, X., Martindale, J. L. & Holbrook, N. J. (2000) *J. Biol. Chem.* **275,** 39435–39443.
37. Sutherland, C. L., Heath, A. W., Pelech, S. L., Young, P. R. & Gold, M. R. (1996) *J. Immunol.* **157,** 3381–3390.

Exhibit G

Archives of Biochemistry and Biophysics
Vol. 396, No. 1, December 1, pp. 133–137, 2001
doi:10.1006/abbi.2001.2578, available online at http://www.idealibrary.com on IDEAL®

RESEARCH REPORT

Injury-Induced Osteopontin Gene Expression in Rat Arterial Smooth Muscle Cells Is Dependent on Mitogen-Activated Protein Kinases ERK1/ERK2

Sara Moses,[1] Ahnders Franzén, Cecilia Lövdahl,[2] and Anna Hultgårdh-Nilsson
Department of Cell and Molecular Biology, Section for Connective Tissue Biology, Lund University, Lund, Sweden

Received August 16, 2001; published online November 9, 2001

Previous work shows that osteopontin has a role during matrix reorganization after tissue injury including vascular conditions such as atherosclerosis and restenosis following angioplasty. *In vitro,* osteopontin promotes activities such as adhesion and migration but the mechanisms that regulate the expression of this matrix protein remain essentially unknown. This study examined if the ERK signaling pathway is involved in injury-induced osteopontin expression in cultured rat aortic smooth muscle cells. Northern and Western blotting demonstrated a marked activation of osteopontin expression in response to injury. Treating the cells with PD98059, a specific MEK1 inhibitor, prior to injury, blocked this upregulation. MEK1 phosphorylates ERK1/ERK2, which belong to the family of mitogen-activated protein kinases. We conclude that ERK1/ERK2 are involved in the regulation of osteopontin expression in cultured vascular smooth muscle cells. © 2001 Elsevier Science

Key Words: **SMC; osteopontin; ERK1/ERK2; *in vitro* injury.**

Tissue remodeling and repair require communication between cells and the extracellular matrix (ECM)[3] (1). Interaction of cells with the ECM, or purified ECM molecules, appears to mediate not only attachment but also proliferation, migration, and differentiation. The expression of ECM molecules and their assembly into a more abundant, but less functional, ECM have also been shown to occur during pathological conditions including diseases of the vessel wall such as atherosclerosis and restenosis after angioplasty (2, 3). Osteopontin is a glycoprotein in the ECM mediating cell binding via $\alpha_v\beta_3$ and other integrins (4, 5). Most studies have focused on the role of osteopontin in bone tissue but it is now evident that it is a common component also in response to vessel wall injury (6). In primary cultures of rat arterial smooth muscle cells (SMC) we have shown that osteopontin mRNA is strongly upregulated during the change from contractile to synthetic phenotype (7). Since phenotypic modulation and subsequent migration and proliferation of vascular SMC are important features in the development of atherosclerosis and restenosis (8, 9) this result adds further support for osteopontin as an important factor in injury-induced alterations of SMC structure and functions. Other *in vitro* studies suggest that osteopontin may be functionally important for migration of SMC (10). Recently, integrin antagonists and a neutralizing osteopontin antibody have been reported to inhibit intimal thickening in animal models. Accordingly, it is likely that osteopontin stimulates migration of SMC from the media to the intima. In previous investigations it was shown that migration of SMC from the media to the intima is stimulated by osteopontin (11, 12) and that osteopontin expression increases in response to injury in several tissues including heart (13, 14). Furthermore, osteopontin gene expression is stimulated by angiotensin II in cardiac microvascular endothelial cells, and is suggested to be dependent on reactive oxygen spieces and mitogen-activated protein kinase (MAPK) (15).

Intracellular signaling pathways that mediate biological effects upon mechanical stimulation include the mitogen-activated protein kinases. These enzymes include the extracellular signal-regulated kinases 1 and 2 (ERK1/ERK2) which are activated by the cytoplasmic protein cascade con-

This article was originally submitted to *Molecular Cell Biology Research Communications* and was accepted for publication by the MCBRC editorial board. As MCBRC is no longer published under its own cover, this work is now appearing as a research report in ABB with the approval of the authors and the *Archives of Biochemistry and Biophysics* executive board.

[1] To whom correspondence should be addressed at Lund University, Department of Cell and Molecular Biology, Section for Connective Tissue Biology, BMC, C12, S-221 84 Lund, Sweden. Fax: +46 46 211 3417. E-mail: sara.moses@medkem.lu.se.

[2] Present address: Department of Physiology and Pharmacology, Karolinska Institutet, Stockholm, Sweden.

[3] Abbreviations used: ECM, extracellular matrix; MAPK mitogen-activated protein kinase; ERK, extracellular signal-regulated kinase; MEK, MAPK kinase; JNK, c-jun N-terminal kinase; OPN, osteopontin; MMP, metalloproteinase; SMC, smooth muscle cells; NCS, newborn calf serum; BSA, bovine serum albumin; PBS, phosphate-buffered saline; PMA, phorbol myristoyl.

0003-9861/01 $35.00

sisting of ras, raf, and MEK1 (16–18). ERK1/ERK2 have also been shown to be a major intracellular pathway involved in the regulation of SMC growth *in vitro* as well as *in vivo*. Recent studies demonstrate that mitogenic concentrations of oxidized low-density lipoprotein and free radicals both activate ERK1/ERK2 leading to proliferation of SMC (19, 20). Furthermore, mechanical stretch activates ERK2 and c-Jun N-terminal kinase (JNK1) in cardiac fibroblasts (21), cyclic strain stress induces MAPKs in rat vascular SMC (22), and integrins may act as mechanotransducers (23). Balloon injury of the rat carotid artery induces activation of ERK1/ERK2 within 30 min (24) and it has been suggested that ERK1/ERK2 activation promotes medial but not intimal cell replication (25). *In vitro,* it has been shown that PDGF BB stimulation of SMC leads to a rapid activation of MAPK and that protein kinase A inhibits this activation (26). Furthermore, the chemotactic response of rat SMC toward PDGF BB appears to be coupled to activation of ERK1/ERK2 (27).

In this study we have used rat SMC in an *in vitro* model of mechanical injury to identify the role of ERK1/ERK2 in osteopontin expression.

MATERIAL AND METHODS

Materials. Ham's medium F-12, newborn calf serum (NCS), and collagenase were obtained from Gibco Bri (Paisley, UK); bovine serum albumin (BSA) from Sigma Chemical Co. (St. Louis, MO); trypsin from Difco (Detroit, MI); and cell culture plastics from Falcon (Lincoln Park, NJ). [6-^{3}H]Thymidine was purchased from DuPont NEN (Boston, MA), and glutaraldehyde from TAAB. All other chemicals were obtained from Sigma Chemical Co.

The MEK1 inhibitor (PD98059) and the phospho-specific ERK1/ERK2 MAPK antibody were purchased from New England BioLabs (Beverly, MA). The total anti-MAPK (ERK1+ERK2) antibody was from Zymed (San Francisco, CA). The anti-SMC α-actin antibody was from Sigma Chemical Co. The Osteopontin monoclonal antibody MPIII10$_1$ [developed by M. Solursh and A. Franzén] was obtained from the Developmental Studies Hybridoma Bank developed under the auspices of the NICHD and maintained by the University of Iowa, Department of Biological Sciences, Iowa City, Iowa. Peroxidase-conjungated secondary antibodies (anti-rabbit IgG and anti-mouse IgG) were purchased from BioSource International (Camarillo, CA).

Cell culture. SMC were isolated by collagenase digestion of the aortic media of 350–400 g male Sprague-Dawley rats (B & K Universal, Sollentuna, Sweden) (28). Ham's medium F-12 was supplemented with 10 mM Hepes, 10 mM TES (pH 7.3), 50 mg/L L-ascorbic acid, and 50 mg/L gentamycin sulfate (referred to as medium F-12), and 10% NCS. Cells were grown at 37°C in a humidified atmosphere of 5% CO_2 in air. Cells used in all experiments were in their second passage.

In vitro injury. Cells were allowed to grow to confluence in the presence of 10% NCS. Growth arrest was achieved by incubation with serum-free F-12 medium containing 0.1% endotoxin-free BSA for 48 h. Fresh medium, with the addition of 20 μM PD98059 or 2 μL DMSO/ml (solvent), was added 1 h prior to the injury, made by gentle pressure with a 3-mm-wide soft plastic tube to the bottom of the cell culture dish for 5 s (29). The cells were harvested for extraction of RNA and protein at indicated time points.

RNA isolation and Northern blot analysis. RNA from injured confluent cultures was extracted essentially according to Chirgwin *et al.* (30). SMC were lysed by the use of 4 M guanidine isothiocyanate supplemented with 25 mM sodium acetate (pH 6.0) and 1% β-mercaptoethanol and lysates were gradient-centrifuged in 5.7 M cesium chloride. Soluble RNA was precipitated in sodium acetate (pH 6.0) and ethanol at −70°C and quantity and purity were determined by spectrophotometry at 260 and 280 nm.

After agarose gel electrophoresis of RNA and transfer to Hybond-N membranes (Amersham), filters were hybridized in a buffer containing 50% formamide, for 20 h at 42°C with ^{32}P-labeled cDNA probe (osteopontin (31)). After hybridization and washing, the filters were exposed to Fuji RX-L film.

RT-PCR. RNA from injured confluent cultures were extracted using Rneasy Mini total RNA kit (Qiagen GmbH, Hilden, Germany) according to the manufacturer's instructions. Average yield from one confluent plate was 20 μg total RNA and 5 μg was used for reverse transcription to produce first-strand cDNA. Super Script II RNAse H reverse transcriptase (Life Technologies) and oligo(dT)$_{15}$ primers (Promega Corporation, Madison, WI) were used in accordiance with the manufacturer's protocol.

The transcripts were amplified from the cDNA by the standard polymerase chain reaction technique using *Taq* polymerase (one cycle of 1.5 min at 92°C, followed by 33 cycles of 0.5 min at 92°C, 0.5 min at 60°C, and 1 min at 72°C followed by 3 min at 72°C). The RT-PCR amplicons were separated by electrophoresis on a 1.5% agarose gel containing ethidium bromide. The primer sequences for up- and downstream primers, respectively, were for rat osteopontin, 5′-tgactcatggctggtcttcc-3′ and 5′-agatgctgtagccacttggc-3′, and for rat β-actin, which was used as an internal standard, 5′-tgtatgcctctggtcgtacca-3′ and 5′-cagcactgtttggcatagag-3′. The intensity of the bands was analyzed with a laser denitometer (FujiFilm Laser 1000) and Image Gauge software.

Protein isolation and Western blot analysis. Cells from control and injured cultures were washed twice with ice-cold PBS and harvested in 150 μl lysis buffer (32) (2% (w/v) SDS was included in the lysis buffer for osteopontin analyses). Equal amounts of proteins, 20 μg assessed according to the Bradford method, were separated in 10% SDS-polyacrylamide gels (33) under reducing conditions. After electrophoresis, proteins were transferred onto Hybond-C extranitrocellulose membrane (Amersham Life Science, Buckinghamshire, UK). After blocking, the membranes were incubated overnight at 4°C with 1:1000 dilution of primary antibodies in TBS-T (0.1% (v/v) Tween-20) containing 1% (w/v) nonfat milk powder. After washing, the blots were incubated with horseradish peroxidase-linked secondary antibodies (1:10 000 dilution in TBS-T containing 1% (w/v) nonfat milk powder for 2 h at room temperature). The blots were washed and bound antibody was detected using chemiluminescense.

Statistical analysis. Results for each group are given as mean ± SD. The significance of the differences between indicated groups was determined using the unpaired t test with Welch correction. A $P < 0.05$ was considered significant.

Ethical considerations. The investigation was performed with permission from the local ethical committee and conforms to the *Guide for the Care and Use of Laboratory Animals* published by the U.S. National Institutes of Health (NIH Publication No. 85-23, revised 1985).

RESULTS

Mechanical Injury Induces Phosphorylation of ERK1/ERK2 in Smooth Muscle Cells

Phosphorylation of ERK1/ERK2 was analyzed by Western blotting using a phospho-specific ERK1/ERK2 antibody. Detectable levels of the phosphorylated form of ERK1/ERK2 were present in low amounts in protein extracts from uninjured cells (Fig. 1). Injury caused a rapid increase in ERK1/ERK2 phosphorylation, which began to decline after 10 min to reach basal level 60 min after injury. Treatment with 20 μM PD98059, a selective inhibitor of MEK1 activation and the MAPK cascade, decrease injury-induced ERK1/ERK2

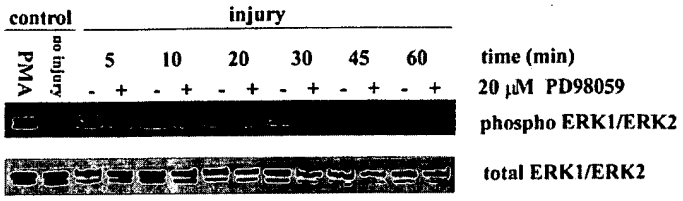

FIG. 1. ERK1/ERK2 phosphorylation after *in vitro* injury. Effect of the MEK1 inhibitor PD98059 on injury-induced ERK1/ERK2 phosphorylation. Proteins were extracted at indicated time points as described under Materials and Methods, and the lysates were then analyzed by Western blotting using a phospho-specific anti-ERK1/ERK2 antibody and a total ERK1/ERK2 antibody. Confluent serum-starved cultures were used as a negative control and PMA-treated (5 μM, 10 min) SMC as a positive control. The figure shows a representative blot.

phosphorylation in a dose-dependent manner. The antibody detecting total ERK1/ERK2 levels was used as loading control. A 5 μM phorbol myristoyl acetate (PMA)-treated SMC served as a positive control of ERK1/ERK2 phosphorylation.

Effect of PD98059 on Injury-Induced Osteopontin Expression

To analyze the effect of PD98059 on injury-induced osteopontin expression, protein and RNA were extracted from injured cultures and analyzed by Western and Northern blotting. Injury to serum-starved SMC cultures induced an evident increase in osteopontin protein levels at Day 2 postinjury, which was markedly suppressed by pretreating the cells with PD98059 (Fig. 2). Neither injury nor PD98059 affected OPN protein levels at time points before 24 h. Furthermore, the minute amounts of OPN detected in the uninjured control cultures were suppressed by PD98059.

OPN mRNA were present in uninjured cultures and injury induced a strong upregulation of in the amounts of these transcripts at 2 and 6 h detected by Northern blotting (Fig. 3A). Preincubating the cells with PD98059 blocked the injury-induced upregulation. Addition of PD98059 did not affect transcription of OPN mRNA in uninjured SMC or in cells harvested 0.5 h after injury (Fig. 3A). The finding that PD98059 blocked injury-induced OPN mRNA was further confirmed by RT-PCR. Figure 3B demonstrates a significant

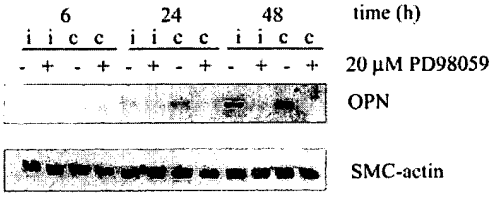

FIG. 2. Effects of PD98059 on injury-induced osteopontin protein expression. A 20 μM PD98059 or solvent (2 μl DMSO/ml) serum-free was added 60 min before injury. Proteins were extracted at indicated time points, and the lysates were then analyzed by Western blotting using an anti-osteopontin antibody. As controls, uninjured cultures ± PD98059 were used. An anti-SMC α-actin antibody was used as loading control. The figure shows a representative blot. i, injured cultures; and c, uninjured control cultures.

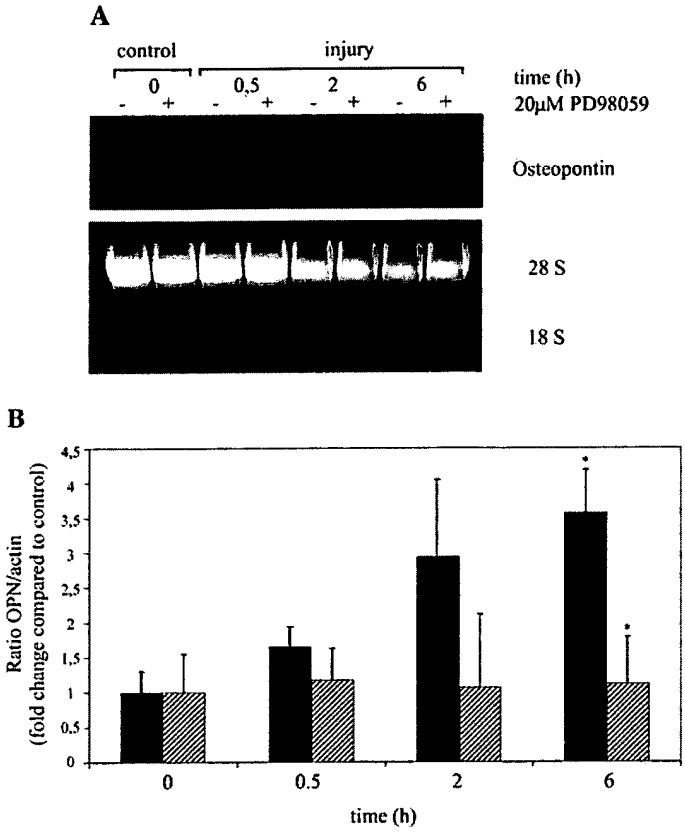

FIG. 3. Effects of PD98059 on injury-induced osteopontin mRNA expression. Confluent, serum-starved cultures of rat SMC were pretreated with 20 μM PD98059 or solvent (2 μl DMSO/ml), and total RNA was extracted at indicated time points after *in vitro* injury as described under Materials and Methods. (A) Northern blot for OPN mRNA (15 μg of total RNA/lane). Ethidium bromide staining of ribosomal RNA (28 and 18 S) was used as loading control. (B) Expression of OPN and β-actin mRNA detected by RT-PCR. Black bars represent the solvent-treated cultures and striped bars represent the PD98059-treated cultures. The graph shows mean values ± SD ($n = 3$), and the expression in control cultures (Time 0) was set to 1. The difference in OPN mRNA expression between the uninjured control culture and the 6-h time point, as well as the difference at the 6-h time point between PD98059 and solvent treatment, was statistically significant (* $P < 0.05$).

injury-induced increase in levels of OPN transcripts at the 6-h time points as compared to controls (Fig. 3B).

DISCUSSION

The specific aim of this study was to analyze a possible involvement of ERK1/ERK2 in injury-induced activation of the osteopontin gene. Briefly, our data suggest that activation of the osteopontin gene in cultured SMC can be induced by mechanical injury and that this activation is dependent on a prior activation of the mitogen-activated protein kinase ERK1/ERK2. Several previous reports have demonstrated, in different cell types, that the MAPK signaling cascades are activated as a result of mechanical stimuli (16, 18). Cyclic strain stretch activates all three members of the MAPKs, i.e.,

ERK1/ERK2, JNK1, and p38 in rat aortic smooth muscle cells (22). Balloon injury to the rat carotid artery has also been shown to activate ERK1/ERK2 kinases within 15 min after balloon injury (24). Koyama *et al.* also observed a marked increase in ERK1/ERK2 activity in response to arterial injury. Furthermore, a reduction, but not complete inhibition, of both DNA replication and ERK1/ERK2 activity was observed when the MEK1 inhibitor PD98059 was added (25). We have demonstrated that *in vitro* injury to cultures of SMC induced proliferation as well as migration of cells into the wounded area. These activities were shown to partly be dependent on intracellular Ca^{2+} release and ERK1/ERK2 phosphorylation (34). Here, we confirm the ERK1/ERK2 phosphorylation in SMC as a response to mechanical injury (Fig. 1).

Osteopontin expression is common during a number of different responses to injury of the vessel wall including neointima formation and atherosclerosis (35). These responses range from controlling functions in smooth muscle and endothelial cells such as adhesion, migration, proliferation and regulation of calcification within the damaged artery (6). The expression of osteopontin is regulated by developmental and tissue-specific mechanisms. Recently, it has been shown that osteopontin gene expression in osteoblasts could be induced by increased phosphate levels (36) as well as by oscillatory fluid flow via ERK1/ERK2 and p38 activation (37). Xie *et al.* demonstrate that angiotensin II activates osteopontin gene expression, involving ERK1/ERK2 activation, in cardiac microvascular endothelial cells (15).

The finding that PD98059 blocked injury-induced expression of the osteopontin gene (Figs. 2 and 3) indicates that activation of this gene can be coupled to the ERK1/ERK2 pathway. The initial factor(s) starting this signaling cascade after injury is still unknown but may originate from either the injured cells or the matrix. Koyama *et al.* were able to block ERK1/ERK2 activity after balloon injury in rat arteries with anti-fibroblast growth factor 2 antibodies (25), a factor known to be released both from injured SMC and from the matrix (38, 39). Furthermore, a study by Wilson *et al.* further points out that integrin-ECM interactions are important for stretch-induced mitotic responses in SMC. They demonstrate that stretch increases DNA synthesis in SMC cultured on collagen, fibronectin, or vitronectin (40). By using specific matrix substrates and inhibitors of specific integrins the authors demonstrate a role for MAP kinases and integrins as transducers of mechanical stimuli (12). Experiments with conditioned media from the stretched cultures suggest that the integrin-mediated activation of ERK is a direct effect of the stretch and not induced in an autocrine/paracrine manner (21). Data from our laboratory, obtained from experiments using conditioned media from injured SMC cultures, indicate that the activation of the osteopontin gene and ERK1/ERK2 is dependent on an autocrine/paracrine stimulation (unpublished data). The use of different cell types and/or passage number may explain the divergence in these results.

OPN mRNA as well as protein is present in small amounts also in uninjured cultures (Figs. 2 and 3). From our data it is obvious that this basal OPN expression is dependent on ERK1/ERK2 phosphorylation. When studying alterations in the presence of different matrix components the balance between production and degradation must be considered. It has been shown that matrix metalloproteinases (MMPs) are active in cultures of SMC, and data from our laboratory demonstrate that stromelysin is activated as a response to *in vitro* injury (41, 42). A hypothesis for alterations in OPN protein levels as a response to injury is that the injury induces MMP activity, which causes degradation of existing matrix. This will activate synthesis of new matrix, where OPN is one important component, allowing migration and proliferation of SMC into the injured area. Indeed, it has been shown that the composition of the matrix is important for proliferation of smooth muscle cells. These cells respond to stretch with proliferation as long as they are grown on a substrate of collagen, fibronectin, or vitronectin. The mitotic response was not achieved when cells were cultured on elastin or laminin (40).

In summary, we report that ostepontin expression is upregulated on both mRNA and protein level in response to mechanical injury of SMC in culture. Furthermore, by using a specific MEK1 inhibitor, PD98059, we have shown that injury-induced osteopontin expression is dependent on a concurrent activation of the ERK1/ERK2 signaling pathway.

ACKNOWLEDGMENTS

This work was supported from the Fund of Lars Hiertas Minne, the Fund of Sigurd and Elsa Golje, the King Gustaf V 80th Birthday Fund, the Swedish Medical research Council, the Swedish Heart Lung Foundation, the Magn. Bergvall Foundation, the Fund Lund University, the Alfred Österlunds Foundation, Swedish Match, the Craford Foundation, and the Bergqvist Foundation.

REFERENCES

1. Gailit, J., and Clark, R. A. (1994) *Curr. Opin. Cell. Biol.* **6,** 717–725.
2. Libby, P., Schwartz, D., Brogi, E., Tanaka, H., and Clinton, S. K. (1992) *Circulation* **88,** III47–III52.
3. Ferns, G. A., Stewart-Lee, A. L., and Anggard, E. E. (1992) *Atherosclerosis* **92,** 89–104.
4. Franzén, A., and Heinegård, D. (1985) *Biochem. J.* **232,** 715–724.
5. Liaw, L., Skinner, M. P., Raines, E. W., Ross, R., Cheresh, D. A., Schwartz, S. M., and Giachelli, C. M. (1995) *J. Clin. Invest.* **95,** 713–724.
6. Giachelli, C. M., Schwartz, S. M., and Liaw, L. (1995) *Trends Cardiovasc. Med.* **5,** 88–95.
7. Hultgardh-Nilsson, A., Lovdahl, C., Blomgren, K., Kallin, B., and Thyberg, J. (1997) *Cardiovasc. Res.* **34,** 418–430.
8. Ross, R. (1993) *Nature* **362,** 801–809.
9. Thyberg, J., Blomgren, K., Roy, J., Tran, P. K., and Hedin, U. (1997) *J. Histochem. Cytochem.* **45,** 837–846.
10. Liaw, L., Almeida, M., Hart, C. E., Schwartz, S. M., and Giachelli, C. M. (1994) *Circ. Res.* **74,** 214–224.
11. Liaw, L., Lombardi, D. M., Almeida, M. M., Schwartz, S. M. deBlois, D., and Giachelli, C. M. (1997) *Arterioscler. Thromb. Vasc. Biol.* **17,** 188–193.
12. Panda, D., Kundu, G. C., Lee, B. I., Peri, A., Fohl, D., Chackalaparampil, I., Mukherjee, B. B., Li, X. D., Mukherjee, D. C., Seides, S., Rosenberg, J., Stark, K., and Mukherjee, A. B. (1997) *Proc. Natl. Acad. Sci. USA* **94,** 9308–9313.
13. Murry, C. E., Giachelli, C. M., Schwartz, S. M., and Vracko, R. (1994) *Am. J. Pathol.* **145,** 1450–1462.

14. Liaw, L., Birk, D. E., Ballas, C. B., Whitsitt, J. S., Davidson, J. M., and Hogan, B. L. (1998) *J. Clin. Invest.* **101,** 1468–1478.
15. Xie, Z., Pimental, D. R., Lohan, S., Vasertriger, A., Pligavko, C., Colucci, W. S., and Singh, K. (2001) *J. Cell. Physiol.* **188,** 132–138.
16. Sadoshima, J., and Izumo, S. (1993) *EMBO J.* **12,** 1681–1692.
17. Komuro, I., Kudo, S., Yamazaki, T., Zou, Y., Shiojima, I., and Yazaki, Y. (1996) *FASEB J.* **10,** 631–636.
18. Li, Y. S., Shyy, J. Y., Li, S., Lee, J., Su, B., Karin, M., and Chien, S. (1996) *Mol. Cell. Biol.* **16,** 5947–5954.
19. Augé, N., Escargueil-Blanc, I., Lajoie-Mazenc, I., Suc, I., Andrieu-Abadie, N., Pieraggi, M. T., Chatelut, M., Thiers, J. C., Jaffrezou, J. P., Laurent, G., Levade, T., Negre-Salvayre, A., and Salvayre, R. (1998) *J. Biol. Chem.* **273,** 12893–12900.
20. Baas, A. S., and Berk, B. C. (1995) *Circ. Res.* **77,** 29–36.
21. MacKenna, D. A., Dolfi, F., Vuori, K., and Ruoslahti, E. (1998) *J. Clin. Invest.* **101,** 301–310.
22. Li, C., Hu, Y., Mayr, M., and Xu, Q. (1999) *J. Biol. Chem.* **274,** 25273–25280.
23. Shyy, J. Y., and Chien, S. (1997) *Curr. Opin. Cell. Biol.* **9,** 707–713.
24. Lille, S., Daum, G., Clowes, M. M., and Clowes, A. W. (1997) *J. Surg. Res.* **70,** 178–186.
25. Koyama, H., Olson, N. E., Dastvan, F. F., and Reidy, M. A. (1998) *Circ. Res.* **82,** 713–721.
26. Graves, L. M., Bornfeldt, K. E., Raines, E. W., Potts, B. C., Macdonald, S. G., Ross, R., and Krebs, E. G. (1993) *Proc. Natl. Acad. Sci. USA* **90,** 10300–10304.
27. Graf, K., Xi, X. P., Yang, D., Fleck, E., Hsueh, W. A., and Law, R. E. (1997) *Hypertension* **29,** 334–339.
28. Thyberg, J., Hedin, U., and Bottger, B.A. (1990) *in* Cell Culture Techniques in Heart and Vessel Research (H. M. Piper, Ed.), pp. 315–333, Springer-Verlag, Berlin.
29. Calara, F., Ameli, S., Hultgardh-Nilsson, A., Cercek, B., Kupfer, J., Hedin, U., Forrester, J., Shah, P. K., and Nilsson, J. (1996) *Arterioscler. Thromb. Vasc. Biol.* **16,** 187–193.
30. Chirgwin, J. M., Przybyla, A. E., MacDonald, R. J., and Rutter, W. J. (1979) *Biochemistry* **18,** 5294–5299.
31. Kiefer, M. C., Bauer, D. M., and Barr, P. J. (1989) *Nucleic. Acids. Res.* **17,** 3306.
32. Ares, M. P., Porn-Ares, M. I., Moses, S., Thyberg, J., Juntti-Berggren, L., Berggren, P., Hultgardh-Nilsson, A., Kallin, B., and Nilsson, J. (2000) *Atherosclerosis* **153,** 23–35.
33. Laemmli, U. K. (1970) *Nature* **227,** 680–685.
34. Moses, S., Dreja, K., Lindqvist, A., Lövdahl, C., Hellstrand, P., and Hultgårdh-Nilsson, A. (2001) *Exp. Cell Res.,* in press doi: 10.1006/excr.2001.5308.
35. Giachelli, C. M., Bae, N., Almeida, M., Denhardt, D. T., Alpers, C. E., and Schwartz, S. M. (1993) *J. Clin. Invest.* **92,** 1686–1696.
36. Beck, G. R., Jr., Zerler, B., and Moran, E. (2000) *Proc. Natl. Acad. Sci. USA* **97,** 8352–8357.
37. You, J., Reilly, G. C., Zhen, X., Yellowley, C. E., Chen, Q., Donahue, H. J., and Jacobs, C. R. (2001) *J. Biol. Chem.* **276,** 13365–13371.
38. Klagsbrun, M., and Edelman, E. R. (1989) *Arteriosclerosis* **9,** 269–278.
39. Schmidt, A., Skaletz-Rorowski, A., Breithardt, G., and Buddecke, E. (1995) *Eur. J. Cell. Biol.* **67,** 130–135.
40. Wilson, E., Sudhir, K., and Ives, H. E. (1995) *J. Clin. Invest.* **96,** 2364–2372.
41. Lovdahl, C., Thyberg, J., Cercek, B., Blomgren, K., Dimayuga, P., Kallin, B., and Hultgardh-Nilsson, A. (1999) *Histol. Histopathol.* **14,** 1101–1112.
42. Lovdahl, C., Thyberg, J., and Hultgardh-Nilsson, A. (2000) *J. Vasc. Res.* **37,** 345–354.

Exhibit H

Lack of ERK activation and cell migration in FGF-2-deficient endothelial cells[1]

GIUSEPPE PINTUCCI,*,† DAVID MOSCATELLI,§ FIORELLA SAPONARA,*,† PETER R. BIERNACKI,*,† F. GREGORY BAUMANN,*,† COSTAS BIZEKIS,† AUBREY C. GALLOWAY,*,† CLAUDIO BASILICO,‡ AND PAOLO MIGNATTI*,†,§,[2]

*The Seymour Cohn Cardiovascular Surgical Research Laboratory, Division of Cardiothoracic Surgery, †The John H. C. Ranson Basic Science Research Laboratory, Department of Surgery, ‡Department of Microbiology, and §Department of Cell Biology, New York University School of Medicine, New York, New York, USA

SPECIFIC AIMS

We tested the hypothesis that fibroblast growth factor 2 (FGF-2) -induced activation of ERK1/2 is required for endothelial cell migration. We used endothelial cells from mice genetically deficient in FGF-2 to test ERK1/2 activation and cell migration in response to mechanical damage.

PRINCIPAL FINDINGS

1. Lack of ERK1/2 activation and migration in wounded FGF-2 −/− endothelial cells

Exogenous FGF-2 induces a variety of endothelial cell responses through activation of the ERK pathway. To study the role of endogenous FGF-2, we characterized cell migration and ERK-1/2 activation in FGF-2 −/− and wild-type (wt) endothelial cells. By the in vitro wound assay, wt endothelial cells showed high motility; in contrast, wounded FGF-2 −/− endothelial cells migrated very poorly. Neutralizing antibody to FGF-2 greatly reduced wt cell migration; conversely, addition of human recombinant FGF-2 (hrFGF-2) restored normal migration in FGF-2 −/− cells, showing that impaired migration resulted from the genetic deficiency of this growth factor. Analysis of ERK activation showed that FGF-2 −/− endothelial cells had lower levels of active ERK-1/2 than their wt counterpart (**Fig. 1**). Addition of hrFGF-2 resulted in dramatic activation of ERK-1/2 in both cell types. Conversely, wounding of the cell monolayer caused increased ERK-1/2 activation in wt but not FGF-2 −/− cells (Fig. 1). UO126, a synthetic inhibitor of MEK (MAPK kinase) -1/2, dramatically down-regulated cell migration and abolished ERK1/2 activation in wt and FGF-2 −/− cells; anti-FGF-2 antibody reduced ERK activation only in wt cells. These results show that endogenous FGF-2 controls endothelial cell migration through activation of the ERK pathway.

2. ERK activation occurs at the wound edge

To understand whether ERK is activated in all the cells of a wounded monolayer or only in those cells at the wound edge that participate in the repair response, we characterized ERK activation in situ by immunostaining with antibody to active ERK-1/2. As expected, addition of hrFGF-2 resulted in ERK-1/2 activation in virtually all cells of wt and FGF-2 −/− monolayers. In contrast, wounding induced ERK activation only in wt cells, where active ERK was detected exclusively in cells located at the wound edge. Thus, FGF-2-mediated ERK-1/2 activation after wounding occurs exclusively at the wound edge.

3. FGF-2 induces endothelial cell migration but not proliferation

FGF-2 induces endothelial cell migration and proliferation. To test whether under our wound assay conditions FGF-2 also affected cell proliferation, we characterized FGF-2 −/− endothelial cell migration in the presence of either 0.5% fetal calf serum (FCS) or 10% FCS. With 10% FCS, the number of migrating cells was considerably higher than in the presence of 0.5% FCS. UO126 abolished FGF-2-induced cell migration but had a much lower effect on 10% FCS-stimulated cells. BrdU incorporation experiments showed that 10% FCS induced proliferation among both cells in the monolayer and cells migrated into the wound space. In contrast, hrFGF-2 had no effect on the contact-inhibited cells of the monolayer but induced BrdU incorporation in only a few cells migrated into the wounded area (**Fig. 2**). Migrating wt cells also showed little or no increase in DNA synthesis. Thus, FGF-2 controls endothelial cell migration through ERK activation without affecting proliferation.

[1] To read the full text of this article, go to http://www.fasebj.org/cgi/doi/10.1096/fj.01-0815fje; to cite this article, use *FASEB J.* (February 25, 2002) 10.1096/fj.01-0815fje

[2] Correspondence: Department of Cell Biology, NYU School of Medicine, 550 First Ave., New York, NY 10016, USA. E-mail: mignap01@med.nyu.edu

0892-6638/02/0016-0598 © FASEB

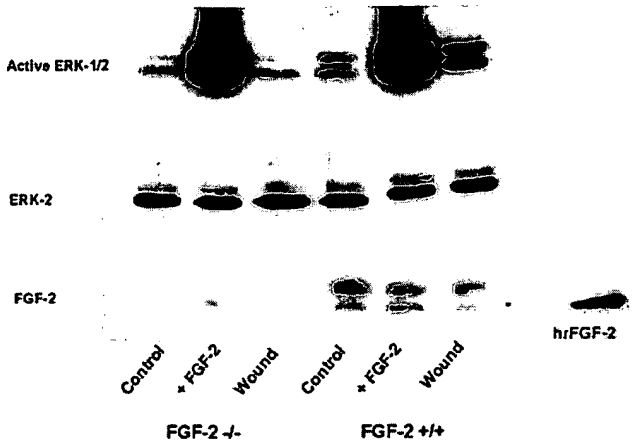

Figure 1. Wounding activates ERK-1/2 in wild-type but not FGF-2 −/− endothelial cells. Western blotting analysis of ERK-1/2 activation in FGF-2 −/− or FGF-2+/+ endothelial cells either wounded (Wound) or treated with 10 ng/ml of hrFGF-2 (+FGF-2) or untreated (Control). The cells were harvested 20 min after growth factor addition or wounding and active ERK was characterized with a phosphospecific antibody. The membrane used for active ERK analysis was stripped and reprobed with anti-ERK-2 antibody to control for equal loading and transfer of cell extract protein. Cell extracts were also analyzed by Western blotting with FGF-2 antibody. High (21.5–22 kDa) and low (18 kDa) molecular mass FGF-2 are present in wt endothelial cells. In contrast, FGF-2 (18 kDa) can be seen only in extracts of FGF-2 −/− cells to which hrFGF-2 was added (+FGF-2). hrFGF-2 (18 kDa) is shown as a control in the rightmost lane. This experiment was repeated 3 times with comparable results.

CONCLUSIONS AND SIGNIFICANCE

Endothelial cell repair of mechanical damage is fundamental for the reconstitution of vessel integrity. FGF-2 controls a variety of endothelial cell functions, and its expression levels in vascular endothelial cells correlate with the efficiency of wound repair in vitro. Here we show that *1)* mechanical damage of FGF-2 −/− endothelial cells does not result in ERK activation; *2)* wound-induced cell migration is strongly decreased in FGF-2−/− endothelial cells; *3)* upon mechanical damage, endogenous FGF-2 induces ERK activation only in the cells lining the wound edge; *4)* FGF-2-induced ERK activation controls endothelial cell migration without a significant effect on proliferation. Because FGF-2 −/− cells respond to exogenous FGF-2, these findings unequivocally demonstrate a link between FGF-2-induced ERK activation and cell migration (**Fig. 3**).

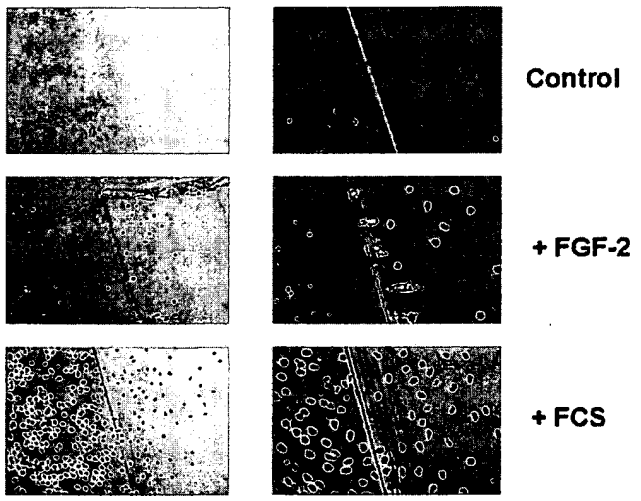

Figure 2. FGF-2 stimulates cell migration without affecting proliferation. BrdU incorporation in wounded FGF-2 −/− endothelial cells. Wounded cells were incubated with either hrFGF-2 (10 ng/ml) or FCS (10%) or no addition (Control) for 24 h. BrdU uptake was analyzed by immunocytochemistry. Two magnifications of the same fields are shown (left panels, ob 10×; right panels, ob 20×). This experiment was repeated twice with comparable results.

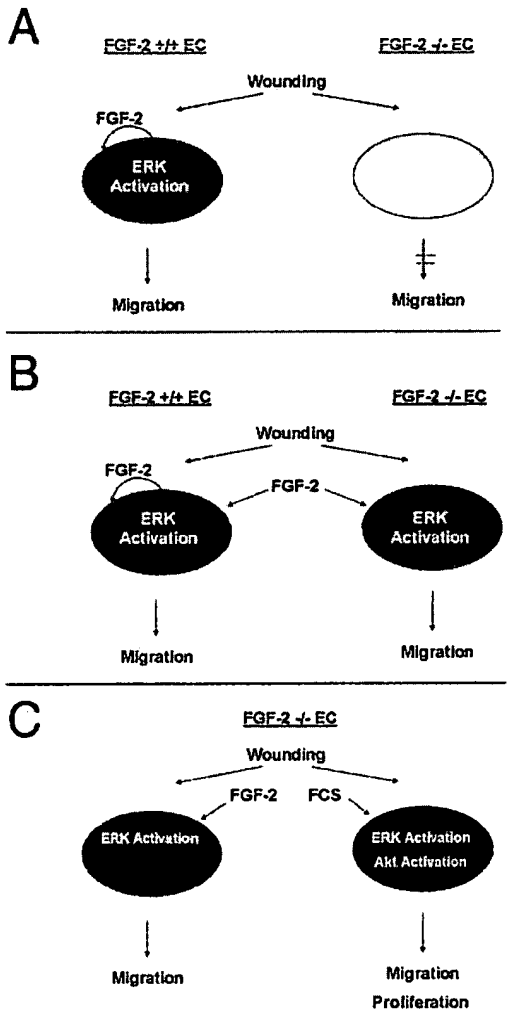

Figure 3. FGF-2-induced ERK activation controls cell migration without affecting proliferation. *A)* FGF-2-expressing endothelial cells respond to wounding with increased ERK activation, which prompts them to migrate. In contrast, the absence of endogenous FGF-2 results in lack of ERK activation and migration. *B)* Exogenous FGF-2 restores ERK activation and migration in wounded FGF-2-deficient endothelial cells. *C)* FGF-2 addition to wounded FGF-2-deficient endothelial cells induces migration via ERK activation without affecting cell proliferation. Serum factors induce activation of a variety of signaling pathways, including ERK activation, with an increase in cell proliferation.

In light of the number of growth factors produced by cultured endothelial cells and the redundancy of FGFs, it is remarkable that FGF-2 alone regulates endothelial wound repair. ERK activation in wounded wt endothelial cells is localized at the wound edge. This effect may be mediated by FGF-2 derived from extracellular matrix or released from damaged cells at the wound edge. ERK activation induced by this growth factor in an autocrine or paracrine manner mediates the intracellular signaling for cell migration.

FGF-2 $-/-$ mice are viable, fertile, and have no gross abnormalities. However, they show neuronal defects in certain brain areas and a delayed repair of excisional skin wounds. No other FGFs appear to compensate for this defect. Because mice deficient in FGF-7, a potent keratinocyte growth factor, have normal excisional skin wound repair, the delayed wound healing observed in FGF-2 $-/-$ mice suggests the involvement of cells other than epidermal keratinocytes. Endothelial cells are key candidates, as new vessel formation is required for the repair of deep skin wounds. Our results indicate a major mechanism to explain the wound repair defect of FGF-2$-/-$ mice.

Most growth factors exert their biological effects mostly by activating the ERK and the phosphoinositide 3 kinase (PI-3K) signaling pathways. These pathways have been implicated in cell proliferation, migration, differentiation, and survival in a variety of cell types. Our results show that endothelial cell migration in response to injury is mediated by FGF-2-induced activation of the ERK pathway. FGF-mediated control of endothelial cell migration but not proliferation represents an efficient mechanism to achieve a rapid angiogenic response. A separate control of proliferation and migration has been described in several systems, including the control of *C. elegans* myoblast migration by egl-17, a member of the FGF family. Similarly, inhibition of the ERK pathway decreases PDGF-BB-induced migration of vascular smooth muscle cells without inhibition of focal adhesion kinase phosphorylation. However, endothelial cell proliferation requires activation of the ras/ERK and PI-3K/Akt pathways. In our experimental model, FGF-2 strongly activated ERK-1/2, but its effect on Akt activation was much lower than that of serum (Fig. 3). This mechanism could explain the differential effect of FGF-2 on cell migration and proliferation we observed.

In conclusion, our data establish a link between FGF-2 expression, activation of the ERK pathway, and endothelial cell migration and may provide indications for the development of tools aimed to either block or promote endothelial cell migration in a variety of pathophysiological settings that involve new vessel formation. FJ

Exhibit I

Am J Physiol Heart Circ Physiol
279: H1635–H1644, 2000.

Significance of ERK cascade compared with JAK/STAT and PI3-K pathway in gp130-mediated cardiac hypertrophy

HIROAKI KODAMA, KEIICHI FUKUDA, JING PAN, MOTOAKI SANO, TOSHIYUKI TAKAHASHI, TAKAHIRO KATO, SHINJI MAKINO, TOMOHIRO MANABE, MITSUSHIGE MURATA, AND SATOSHI OGAWA
Cardiopulmonary Division, Department of Internal Medicine, Keio University School of Medicine, Tokyo 160-8582, Japan

Received 30 July 1999; accepted in final form 19 April 2000

Kodama, Hiroaki, Keiichi Fukuda, Jing Pan, Motoaki Sano, Toshiyuki Takahashi, Takahiro Kato, Shinji Makino, Tomohiro Manabe, Mitsushige Murata, and Satoshi Ogawa. Significance of ERK cascade compared with JAK/STAT and PI3-K pathway in gp130-mediated cardiac hypertrophy. *Am J Physiol Heart Circ Physiol* 279: H1635–H1644, 2000.—We compared the role of the Raf-1/mitogen-activated protein kinase/extracellular signal-regulated protein kinase (MEK)/extracellular signal-regulated protein kinase (ERK)/p90^{RSK} cascade in gp130-mediated cardiac hypertrophy with the contribution of the Janus kinase (JAK)/signal transduction and activation of transcription (STAT) and phosphatidylinositide 3-kinase (PI3-K) pathways. Primary cultured neonatal rat cardiomyocytes were stimulated with leukemia inhibitory factor (LIF). LIF sequentially activated Raf-1, MEK1/2, ERK1/2, and p90^{RSK}. We used PD-98059 (a specific MEK inhibitor), AG-490 (a JAK2 inhibitor), and wortmannin (a PI3-K inhibitor) to confirm that this cascade was independent of the JAK/STAT and PI3-K/p70 S6 kinase (S6K) pathways. PD-98059, AG-490, and wortmannin suppressed the LIF-induced increase in [^{3}H]phenylalanine uptake by 54.7, 21.5, and 25.6%, respectively, and inhibited the increase in cell area by 61.2, 42.8, and 39.2%, respectively. Reorganization of myofilaments was predominantly suppressed by AG-490. LIF-induced expression of c-*fos*, brain natriuretic peptide, and skeletal α-actin mRNA was markedly suppressed by PD-98059 and moderately suppressed by wortmannin and AG-490. Atrial natriuretic peptide was significantly suppressed by AG-490. These findings indicate that this pathway is critically involved in protein synthesis, induction of c-*fos*, brain natriuretic peptide, and skeletal α-actin expression and is partially involved in myofilament reorganization and atrial natriuretic peptide induction in gp130-mediated cardiac hypertrophy.

leukemia inhibitory factor; mitogen-activated protein kinase; cardiomyocyte

TARGETED DISRUPTION of the gp130 gene, a common signal transducer for the interleukin (IL)-6 family of cytokines [IL-6, IL-11, oncostatin M, leukemia inhibitory factor (LIF), ciliary neurotrophic factor, and cardiotrophin-1] (10, 24), led to failure of the myocardium to mature (1, 42) and suggested that members of this cytokine family may be important cardiac hypertrophic growth factors. Transgenic mice expressing IL-6 and IL-6 receptor displayed constitutive tyrosine phosphorylation of gp130 in the myocardium and cardiac hypertrophy (9). Chen (4) and Hirota et al. (8) demonstrated that aortic pressure overload in ventricle-restricted gp130 knockout mice displays the rapid onset of dilated cardiomyopathy and massive induction of myocyte apoptosis compared with the control mice, which exhibit compensatory hypertrophy. Pennica et al. (23) recently cloned a novel IL-6 family cDNA for cardiotrophin-1 from an ES cell library that had a potent hypertrophic effect on cardiomyocytes. These findings indicated that a gp130-dependent signaling pathway might be critically involved in the hypertrophic response of cardiomyocytes.

We (13) and Kunisada et al. (16) previously demonstrated that LIF causes cardiac hypertrophy and activates the Janus kinase (JAK)/signal transduction and activation of transcription (STAT) pathway, and Kunisada et al. (17) reported that overexpression of constitutively active STAT3 augmented the LIF-induced increase in [^{3}H]leucine uptake and hypertrophy marker gene expression, whereas overexpression of a dominant-negative STAT3 decreased these events. Oh et al. (22) reported that LIF activated phosphatidylinositide 3-kinase (PI3-K) and that PI3-K stimulated protein kinase B and p70 S6 kinase (S6K) in cardiomyocytes. PI3-K activates Akt kinase (15) and other serine-threonine kinases and plays an important role not only in activation of glucose transport and glycogenesis (5, 38) but also in protein synthesis via p70 S6K. Insulin-like growth factor-I (11) and ANG II, well-known hypertrophic growth factors for cardiomyocytes, have been shown to activate the PI3-K pathway (26, 27). These findings confirmed the significance of the JAK/STAT and the PI3-K pathways in gp130-mediated cardiac hypertrophy.

Kunisada et al. (16) reported that the signaling pathway downstream of gp130 also activated an extracel-

Address for reprint requests and other correspondence: K. Fukuda, Cardiopulmonary Div., Dept. of Internal Medicine, Keio University School of Medicine, 35 Shinanomachi, Shinjuku-ku, Tokyo 160-8582, Japan (E-mail: kfukuda@mc.med.keio.ac.jp).

The costs of publication of this article were defrayed in part by the payment of page charges. The article must therefore be hereby marked "*advertisement*" in accordance with 18 U.S.C. Section 1734 solely to indicate this fact.

lular signal-regulated protein kinase (ERK) in cardiomyocytes. However, they did not address the significance of this cascade and upstream signaling of ERK in gp130-mediated cardiac hypertrophy. ERK, or mitogen-activated protein kinase (MAPK), is one of a family of serine/threonine kinases thought to play a central role in the signaling events leading to cell proliferation or differentiation in a variety of cell types (21, 31). The ERK cascade may transduce signals from diverse receptor types, including receptor protein tyrosine kinases, G protein-coupled receptors, and cytokine receptors, to produce growth responses. In cultured cardiomyocytes, the well-known cardiac hypertrophic growth factors phenylephrine, endothelin-1, ANG II, and fibroblast growth factor activate p42 and p44 isoforms of ERK (2, 5, 29). However, the contribution of the ERK cascade to the induction of cardiac hypertrophy remains controversial. Glennon et al. (7) demonstrated that antisense oligodeoxynucleotides against the ERK isoforms p42 and p44 inhibited the morphological changes of hypertrophy in cardiomyocytes exposed to phenylephrine. Post et al. (25) demonstrated that dominant-interfering mutants of ERK p42 and p44 as well as the use of PD-98059, an inhibitor of MAPK/ERK (MEK), failed to block phenylephrine-induced atrial natriuretic peptide (ANP) expression. Interestingly, neither carbachol nor ATP, which activate ERK, can induce cardiac hypertrophy (25). Thus it would be of interest to characterize the role of this pathway in gp130-mediated cardiac hypertrophy.

To address the significance of this cascade in gp130-mediated cardiac hypertrophy, we compared the role of this pathway with that of the JAK/STAT and PI3-K/p70 S6K pathways by analyzing their contribution to protein synthesis, gene expression, and myofilament reorganization.

METHODS

Cell culture. Primary cultures of cardiomyocytes were prepared from the ventricles of 1-day-old neonate Wistar rats, as described previously (13, 14). Cells were seeded at a density of $1–5 \times 10^5$ cells/cm^2 on gelatin-coated dishes. The nonmyocyte population was <5%, as determined by immunofluorescence staining with monoclonal antisarcomeric myosin antibody (MF20). Recombinant murine LIF was purchased from Genzyme. After 24 h of serum depletion, cardiomyocytes were stimulated with LIF (1,000 U/ml) in the presence or absence of MEK inhibitor (PD-98059, 30 μM), PI3-K inhibitor (wortmannin, 10 nM), and JAK2 inhibitor (AG-490, 20 μM) (20).

Immunoprecipitation and Western blot analysis. Cell lysates were prepared with lysis buffer containing 50 mM Tris·HCl (pH 7.4), 150 mM NaCl, 5 mM EDTA, 1.0% Triton X-100, 0.25% sodium deoxycholate, 50 mM NaF, 10 mM $Na_3P_2O_7$, 1 mM Na_3VO_4, 1 mM phenylmethylsulfonyl fluoride, 10 μg/ml aprotinin, and 10 μg/ml leupeptin. Lysates were immunoprecipitated using anti-STAT3, Raf-1, ERK1/2, p70 S6K, and p90^{RSK} polyclonal antibody (Santa Cruz) at 4°C for 12 h and then protein G-Sepharose (Sigma Chemical) for 1 h. Proteins were separated on 7.5–12.5% SDS-polyacrylamide gels. Western blot analysis was performed as described previously (13, 14). Anti-phospho-ERK, phospho-MEK polyclonal antibody (New England Biolab), or anti-phosphotyrosine antibody (4G10) was used as a primary antibody. A peroxidase-conjugated goat anti-rabbit IgG or a peroxidase-conjugated rabbit anti-mouse IgG was used as a secondary antibody. Signals were visualized with enhanced chemiluminescence (Amersham).

Kinase activity assays for Raf-1 and ribosomal S6 kinases. Immunoprecipitates were washed three times with lysis buffer and three times with kinase buffer containing 25 mM Tris·HCl (pH 7.4), 10 mM $MgCl_2$, 1 mM dithiothreitol, and 0.5 mM EGTA and 2 μM protein kinase inhibitor peptide and then incubated with 2.5 nmol of syntide-2, a synthetic Raf-1-specific substrate (Santa Cruz), or 2.5 nmol of S6 peptide (UBI) in the presence of 40 μM ATP and 2 μCi of [γ-^{32}P]ATP. After a 20-min incubation at 25°C, aliquots of supernatant were spotted on P81 paper (Whatman), washed five times in 0.75% phosphoric acid, dried, and counted by the Cerenkov technique.

Kinase assay in myelin basic protein-containing gel. Activities of ERKs were assayed by the "in-gel" method with use of myelin basic protein (MBP)-containing gels, as described previously (41). Cell lysates were separated on an SDS-polyacrylamide gel containing 0.5 g/l MBP (Sigma Chemical). ERKs in the gels were denatured in 6 M guanidine HCl and renatured in 50 mM Tris·HCl (pH 8.0) containing 0.04% Tween 20 and 5 mM 2-mercaptoethanol. The phophorylative activity of ERKs was assayed by incubating the gel with [γ-^{32}P]ATP at 30°C for 1 h. After incubation, the gel was extensively washed, dried, and subjected to autoradiography.

Gel mobility shift assay. Cardiomyocytes were rinsed with PBS at 0°C and scraped into the same buffer. Nuclear extracts were prepared according to standard methods described previously (13, 14). Five micrograms of nuclear extract were incubated with 1 μg of poly(dI-dC)-poly(dI-dC) (Pharmacia Biotech) with or without competitor oligonucleotide in 20 μl of 10 mM HEPES (pH 7.9), 50 mM NaCl, 1 mM EDTA, and 10% glycerol for 20 min at 25°C. The samples were incubated with 1 or 2 fmol of radiolabeled probes (~5,000 cpm) for 10 min at 25°C. The probes were purchased from Santa Cruz Biotechnology, and their sequences have been described (SIE-DNA, 5′-CAGTTCCCGTCAATC-3′). Binding reactions were resolved by a 4% native PAGE.

Immunofluorescence photography and cell-sizing protocol. Cells grown on glass coverslips were permeabilized in 1% formaldehyde-PBS for 10 min. After fixation, cells were stained with antisarcomeric myosin antibodies (MF20), as described previously (13). The sizes (surface area and perimeter) of the cardiomyocytes were measured using enlarged, calibrated fluorescent photomicrographs and quantitated and validated with a Power Macintosh computer (model G4) and an Epson scanner (model GT-9000) with Adobe Photoshop version 5.0J and NIH image version 1.56 software.

Incorporation of [^{3}H]phenylalanine. The effects of LIF on [^{3}H]phenylalanine uptake were determined in gelatin-coated 24-well plates. Serum-starved cardiomyocytes were stimulated with LIF (1,000 U/ml) in the presence or absence of PD-98059, wortmannin, and AG-490. After 48 h of LIF stimulation, [^{3}H]phenylalanine uptake was measured as described previously (13). The results were expressed as disintegrations per minute per well. Each data point was the mean of six separate experiments.

RNA extraction and Northern blot analysis. Total RNA was isolated using TRIzol reagent. Rat ANP cDNA was obtained by RT-PCR from the heart RNA and cloned into the pCR II plasmid. PCR fragments of the rat skeletal α-actin cDNA were kindly provided by Hiroshi Ito. Rat glyceraldehyde 3-phosphate dehydrogenase cDNA was used as an internal control. Inserts were labeled with [γ-^{32}P]dCTP by the

random priming technique. A 20-μg sample of total RNA was run on a 1% MOPS-formaldehyde-agarose gel, and Northern blots were performed as described previously (13).

Statistical analysis. Values are means ± SD. Statistical significance among mean values was evaluated with an ANOVA. Student's *t*-test was used when two values were compared. Differences were considered significant when $P < 0.05$.

RESULTS

LIF activates the Raf-1/MEK/ERK/p90^{RSK} cascade in cardiomyocytes. To demonstrate the signal transduction pathways involved in LIF-induced cardiac hypertrophy, we elucidated the protein kinase pathway of phosphorylation by examining the time course of activation of Raf-1, MEK1/2, and ERK1/2. We initially observed a rapid increase in the MAPKKK activity of Raf-1 from 2 min after LIF stimulation and a gradual decrease thereafter (Fig. 1). We confirmed that equal amounts of Raf-1 proteins were immunoprecipitated in each reaction.

We next observed LIF-induced activation of MEK1/2. Because activation of MEK1/2 occurs through phosphorylation of serine residues 217 and 221, Western blot analysis was performed using anti-phospho-MEK antibody. Serine phosphorylation of MEK1/2 increased at 2 min, peaked at 5 min, and returned to the control level at 30 min (Fig. 2*A*). The MAPKK activity of MEK was also increased. MAPKK activity of MEK led to maximal levels at 5 min (data not shown).

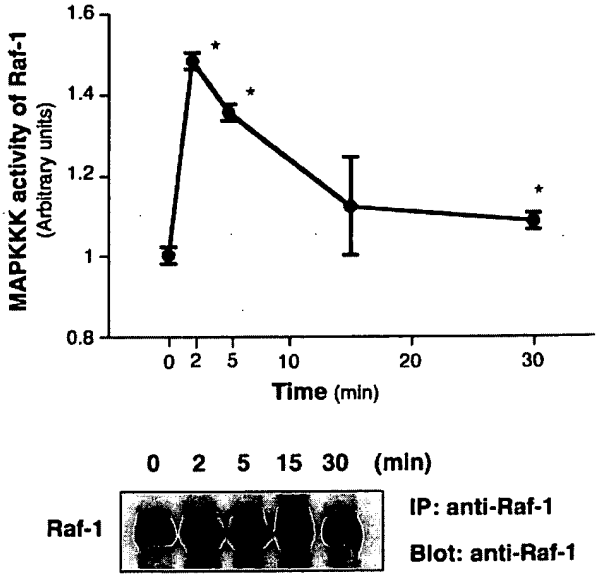

Fig. 1. Leukemia inhibitory factor (LIF) stimulated mitogen-activated protein kinase kinase kinase (MAPKKK) activity of Raf-1 in cardiomyocytes. Confluent, serum-starved cardiomyocytes were stimulated with LIF (1,000 U/ml) for 2–30 min. Cell lysates were immunoprecipitated with an anti-Raf-1 antibody and incubated with Raf-1-specific substrate and [γ-^{32}P]ATP. Results are means of 4 separate experiments, in which each experiment showed similar results. *$P < 0.01$. To confirm that equal amounts of protein were immunoprecipitated in each reaction, aliquots of the samples were also immunoprecipitated and subjected to Western blot analysis with anti-Raf-1 antibody (*bottom*). IP, immunoprecipitation.

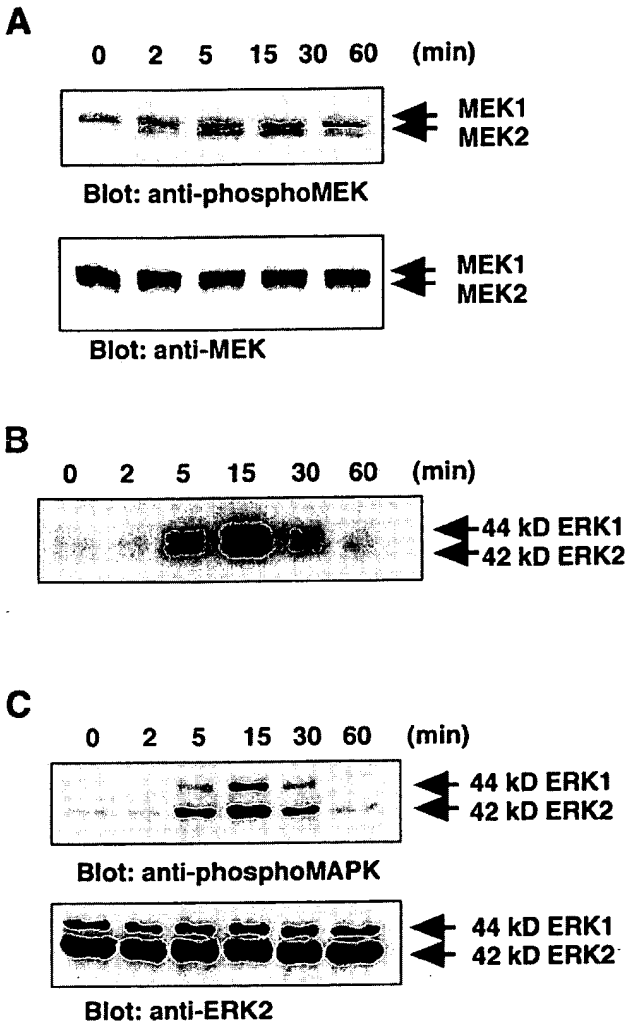

Fig. 2. LIF sequentially activates mitogen-activated protein kinase (MAPK)/extracellular signal-regulated protein kinase (MEK1/2) and extracellular signal-regulated protein kinase (ERK1/2) in cardiomyocytes. *A*: LIF phosphorylated and activated MEK1/2 in cardiomyocytes. Confluent, serum-starved cardiomyocytes were stimulated with LIF (1,000 U/ml) for 2–60 min. Cell lysates were separated and blotted with anti-phospho-MEK antibody (*top*) and anti-MEK antibody (*bottom*). Positions of MEKs are indicated by arrows at *right*. Serine phosphorylation of MEK1/2 increased after 2 min and peaked at 5 min. Each lane contained equal amounts of MEK1 and MEK2 (*bottom*). *B*: LIF stimulated myelin basic protein (MBP) kinase activity of ERK1/2 in cardiomyocytes. Cell lysates were resolved on a 10% SDS-polyacrylamide gel containing MBP (0.5 g/l). After denaturation and renaturation, phosphorylative activities of ERKs were assayed by incubating the gel with [γ-^{32}P]ATP. MBP kinase activity of ERK increased at 5 min after LIF stimulation and peaked at 15 min. A representative autoradiogram from 3 independent experiments is shown. *C*: LIF induced tyrosine phosphorylation of ERK1/2 in cardiomyocytes. Cell lysates were separated and blotted with anti-phospho-ERK antibody (*top*) and anti-ERK antibody (*bottom*). Positions of ERKs are indicated by arrows at *right*. Tyrosine-phosphorylated ERK1 and ERK2 increased after 5 min and peaked at 15 min. Each lane contained equal amounts of ERK1 and ERK2 (*bottom*).

We measured the activities of ERKs using the in-gel method. MBP kinase activity migrating at 42 and 44 kDa increased after LIF stimulation, reached a maximum level at 15 min, and gradually decreased there-

after (Fig. 2*B*). Western blot analysis with anti-phospho-ERK antibody showed that ERK1/2 were unphosphorylated in unstimulated cells (Fig. 2*C*). Tyrosine phosphorylation of ERK1/2 increased at 5 min, peaked at 15 min, and returned to the control level at 30 min. This observation is consistent with the notion that phosphorylation of ERKs reflects their activation (21).

Ribosomal S6 kinases (p70 S6K and $p90^{RSK}$) have been thought to be key enzymes in protein synthesis and are related to the ERK or PI3-K signal transduction pathways (12, 19). There is accumulating evidence to suggest that p70 S6K (3, 28) and $p90^{RSK}$ (29) were critically involved in cardiac hypertrophy. However, the localization and the precise role of ribosomal S6 kinases in cardiac hypertrophy are not well understood. To verify that $p90^{RSK}$ is activated by LIF and is downstream of ERK, but not of JAK/STAT or PI3-K, in cardiomyocytes, S6 kinase activity was measured in the presence and absence of PD-98059, wortmannin, or AG-490. The S6 kinase activity of $p90^{RSK}$ increased as early as 5 min and peaked at 15 min. LIF-induced activation of $p90^{RSK}$ was significantly inhibited by PD-98059 ($n = 5$, $P < 0.01$), but not by wortmannin or AG-490 (Fig. 3). Taken together, these results indicate that LIF activated the Raf-1/MEK/ERK/$p90^{RSK}$ cascade and that $p90^{RSK}$ is independent of the JAK/STAT and PI3-K pathways.

LIF-induced activation of PI3-K/p70 S6K pathway was independent of the JAK/STAT or Raf-1/MEK/ERK/$p90^{RSK}$ pathway. A previous report showed that LIF activated the PI3-K/p70 S6K pathway in rat cardiomyocytes (22). To confirm that this pathway was

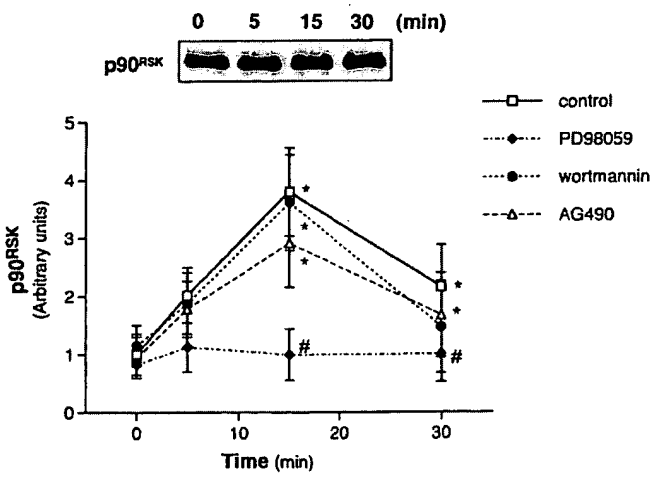

Fig. 3. LIF-induced activation of $p90^{RSK}$ was mediated by MEK/ERK pathway, but not by phosphatidylinositide 3-kinase (PI3-K) or JAK/STAT pathway. S6 kinase activity was measured as described in METHODS. S6 kinase activity of $p90^{RSK}$ was increased by LIF as early as 5 min and peaked at 15 min (control). Equal amounts of $p90^{RSK}$ were immunoprecipitated in each reaction (control; *top*). To determine the upstream signal of $p90^{RSK}$, S6 kinase activity was measured in the presence and absence of PD-98059 or wortmannin. LIF-induced activation of $p90^{RSK}$ was significantly inhibited by PD-98059, but not by AG-490 or wortmannin. $^*P < 0.01$ vs. *time 0*; $^\#P < 0.01$ vs. LIF stimulation ($n = 5$).

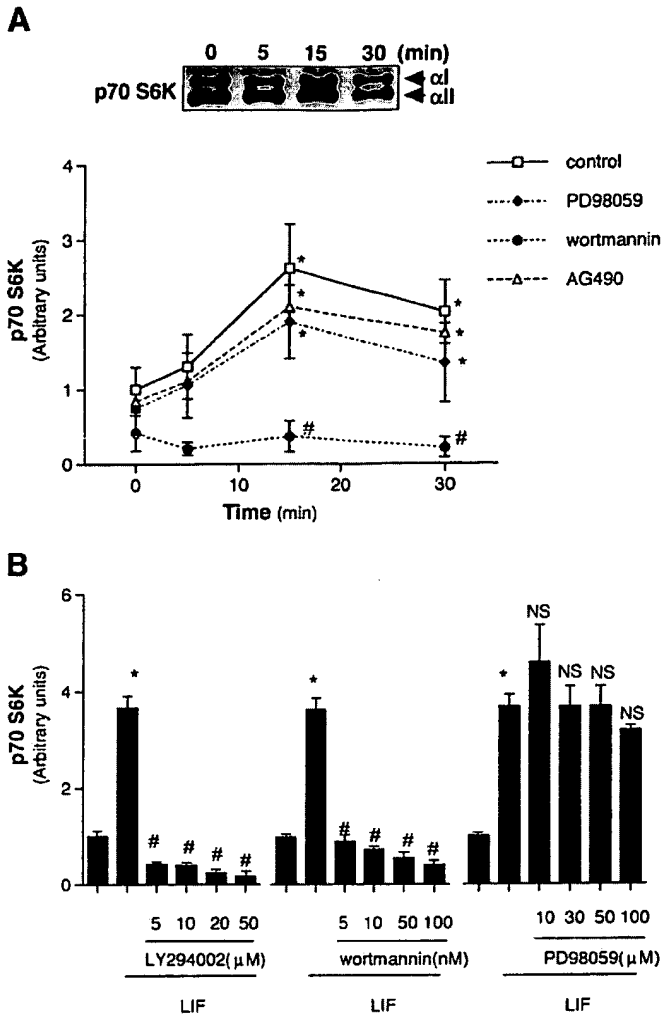

Fig. 4. LIF-induced activation of p70 S6K was mediated by PI3-K, but not by the MEK/ERK pathway or JAK/STAT pathways. *A*: time course of the kinase activity of p70 S6K and the effect of wortmannin, AG-490, and PD-98059 on LIF-stimulated cardiomyocytes. p70 S6K kinase activity was increased by LIF as early as 5 min and peaked at 15 min (control). Equal amounts of p70 S6K were immunoprecipitated in each reaction (control; *top*). The positions of the 85-kDa form (αI) and the 70-kDa form (αII) of p70 S6K are indicated. To determine the upstream signal of p70 S6K, S6 kinase activity was measured in the presence and absence of PD-98059 or wortmannin. LIF-induced activation of p70 S6K was significantly inhibited by wortmannin, but not by AG-490 or PD-98059. Results are means of 5 separate experiments. $^*P < 0.01$ vs. *time 0*; $^\#P < 0.01$ vs. LIF stimulation. *B*: dose-inhibitory relationship between wortmannin, LY-294002, and PD-98059 and p70 S6K activity in LIF-stimulated cardiomyocytes. Cells were preincubated with various concentrations of these inhibitors and stimulated with LIF, and the kinase activity of p70 S6K was measured 15 min after the stimulation. NS, not significant.

independent of the JAK/STAT or the Raf-1/MEK/ERK/$p90^{RSK}$ pathway, we performed a kinase activity assay for p70 S6K under various concentrations of wortmannin, LY-294002, AG-490, and PD-98059. LIF activated p70 S6K as early as 5 min, and activation peaked at 15 min (Fig. 4*A*). LIF-induced activation of p70 S6K was significantly inhibited by wortmannin, but not by PD-98059 or AG-490. Figure 4*B* shows the effect of various

concentrations of LY-294002, wortmannin, and PD-98059 on p70 S6K in LIF-stimulated cells. LY-294002 and wortmannin completely blocked p70 S6K even at a lower concentration. Neither PD-98059 nor AG-490 (data not shown) attenuated p70 S6K activity even at a higher concentration. These findings indicated that the PI3-K/p70 S6K pathway was independent of the other two pathways.

Independence of the Raf-1/MEK/ERK/p90^{RSK}, JAK/STAT, and PI3-K/p70 S6K pathways. Because this study is based on the effect of inhibitors of each pathway, it was important to clarify the specificity of the inhibitors and independence of these three pathways. To demonstrate that PD-98059, wortmannin, and AG-490 (20) work as specific inhibitors of the Raf-1/MEK/ERK/p90^{RSK}, PI3-K/p70 S6K, and JAK/STAT pathways, respectively, we preincubated the cells with these inhibitors before LIF stimulation and detected in-gel phosphorylation of MBP by ERK, tyrosine phosphorylation of STAT3, and p70 S6K activity and performed a gel mobility shift assay.

AG-490 inhibited the tyrosine phosphorylation of STAT3, whereas PD-98059 or wortmannin did not (Fig. 5*A*). Densitometric analysis revealed that AG-490 inhibited LIF-induced phosphorylation of STAT3 in cardiomyocytes by 88.4 ± 7.8%. Gel mobility shift assay revealed that STAT3 activated by LIF bound to its consensus SIE site and that AG-490 almost completely inhibited this process, whereas wortmannin and PD-98059 did not (Fig. 5*B*). Figure 5*C* shows the in-gel phosphorylation of MBP by ERK after preincubation with these inhibitors in LIF-stimulated cells. Figure 5*D* shows the dose dependency of the inhibitors. PD-98059 at 10 μM clearly inhibited the LIF-induced MBP phosphorylation by ERK, whereas AG-490 did not. Previous reports showed that wortmannin at lower concentrations (5–10 nM) specifically inhibited PI3-K (18), but wortmannin at higher concentrations (50–100 nM) also inhibited ERK in various cell types (33). Figure 5*D* revealed that 10 nM wortmannin had no effect on MBP phosphorylation, whereas 100 nM wortmannin attenuated MBP phosphorylation in LIF-stimulated cardiomyocytes. These findings indicated that PD-98059, wortmannin (5–10 nM), and AG-490 could be used as specific inhibitors of the Raf-1/MEK/ERK/p90^{RSK}, PI3-K/p70 S6K, and JAK/STAT pathways, respectively.

LIF-induced increase in [^{3}H]phenylalanine uptake is predominantly mediated by the Raf-1/MEK/ERK/p90^{RSK} cascade. We tried to determine which of these pathways plays an important role in LIF-induced cardiac hypertrophy. The effect of PD-98059, wortmannin, or AG-490 on LIF-induced protein synthesis was investigated by measuring [^{3}H]phenylalanine uptake. LIF caused a 67% increase in [^{3}H]phenylalanine uptake compared with the control (Fig. 6). PD-98059, wortmannin, and AG-490 inhibited the LIF-induced [^{3}H]phenylalanine uptake by 54.7, 21.5, and 25.6%, respectively, whereas these inhibitors at this concentration had minimal effects on the basal [^{3}H]phenylalanine uptake. The results were fully reproducible and indicated that the LIF-induced increase in protein synthesis in cardiomyocytes was mediated by all these pathways and that the Raf-1/MEK/ERK/p90^{RSK} pathway plays the most important role in protein synthesis among these three pathways.

Effect of PD-98059, wortmannin, and AG-490 on LIF-induced increase in cell size. Morphometric analysis was used to evaluate any effect of the signal transduction inhibitors on the LIF-induced increase in cardiomyocytes. LIF caused a 35 and 43% increase in cell area and perimeter compared with the control cells, respectively. PD-98059, wortmannin, and AG-490 significantly decreased the increase in cell area by 61.2, 42.8, and 39.2%, respectively (Fig. 7*A*). PD-98059, wortmannin, and AG-490 significantly decreased the LIF-induced increase in perimeter of the cells by 38.8, 31.0, and 34.6%, respectively (Fig. 7*B*). These inhibitors at this concentration did not have any substantial effects on the basal size of the unstimulated cells. These results indicated that all these pathways were involved in the induction of cardiac hypertrophy and that, again, the Raf-1/MEK/ERK/p90^{RSK} cascade plays the most important role in cell size increase.

Figure 8 shows representative immunofluorescence photographs of cardiomyocytes stimulated with LIF for 48 h in the presence of the various signal transduction inhibitors. LIF clearly caused reorganization of the myofilaments. AG-490 strongly inhibited the reorganization of myofilaments, whereas PD-98059 and wortmannin also inhibited reorganization, but to a lesser extent.

Differential regulation of hypertrophic marker gene expression in gp130-mediated signaling. To determine which pathway may mediate activation of hypertrophic marker genes such as c-*fos*, brain natriuretic peptide (BNP), skeletal α-actin, and ANP, we performed Northern blot analysis on LIF-stimulated cells in the presence and absence of PD-98059, wortmannin, and AG-490. LIF activated c-*fos* (30 min), BNP (1 h), skeletal α-actin (24 h), and ANP (24 h; Fig. 9). Expression of c-*fos* was strongly inhibited by PD-98059 and moderately inhibited by wortmannin and AG-490. BNP expression was markedly inhibited by PD-98059 but was only slightly inhibited by wortmannin and AG-490. Skeletal α-actin expression was strongly inhibited by PD-98059 and wortmannin and was not affected by AG-490. In contrast, ANP expression was significantly inhibited by AG-490 but was not affected by PD-98059 or wortmannin. These findings indicated that various hypertrophic marker genes were differentially regulated by these three pathways in gp130-mediated cardiac hypertrophy.

DISCUSSION

The relay system that transmits signals from gp130 to the nucleus involves at least three distinct pathways of protein phosphorylation: the JAK/STAT (13, 16), PI3-K/p70 S6K (22, 30) and ERK pathways (16, 30). We investigated the role of the ERK pathway in gp130-mediated cardiac hypertrophy and found that *1*) LIF

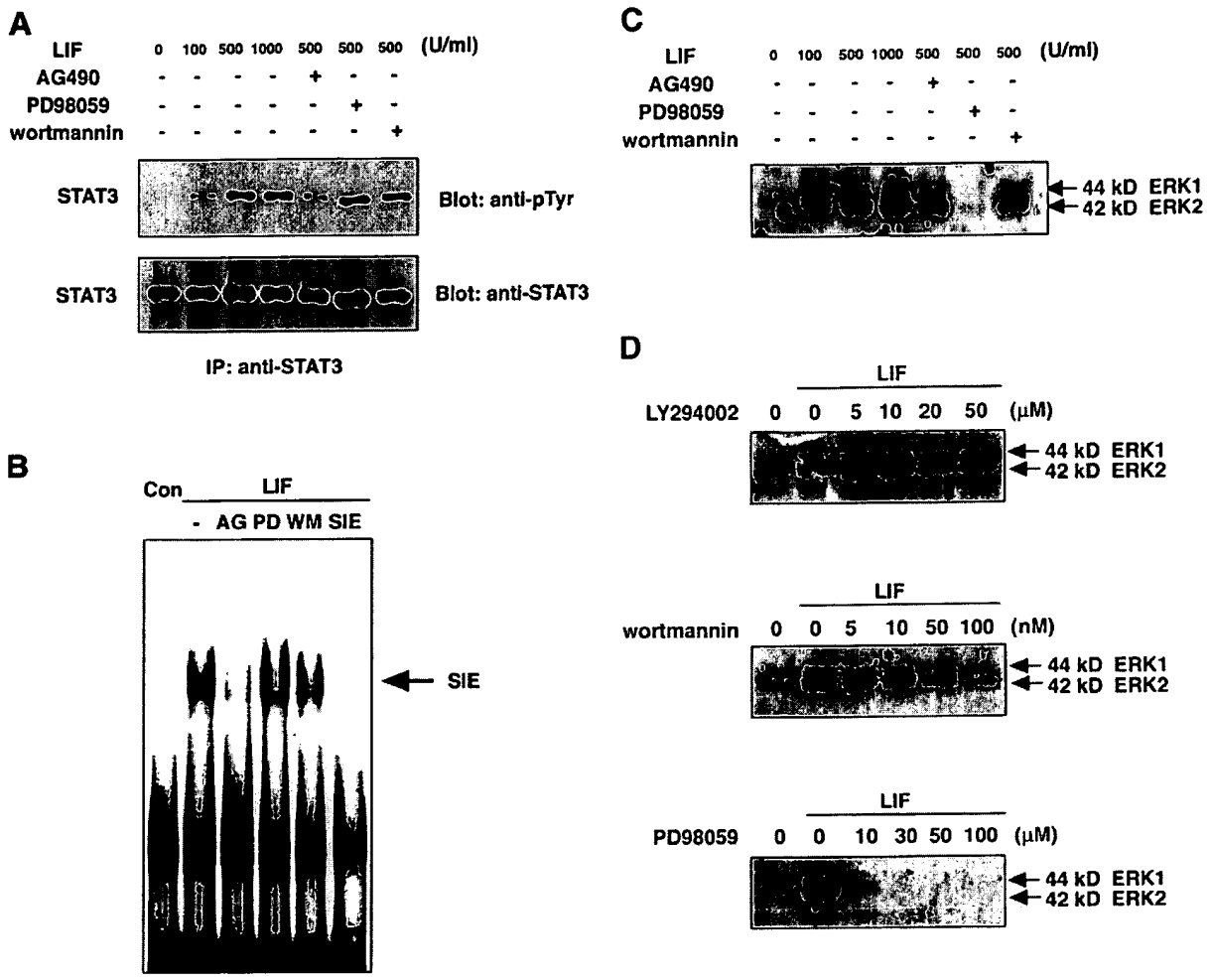

Fig. 5. Inhibitory effects of AG-490 (AG), PD-98059 (PD), and wortmannin (WM) on activation of signal transduction and activation of transcription (STAT3) and ERK1/2. *A*: tyrosine phosphorylation of STAT3 was inhibited by AG-490, but not by PD-98059 or wortmannin. Confluent, serum-starved cardiomyocytes were stimulated with LIF (100–1,000 U/ml) for 5 min in the presence and absence of AG-490, PD-98059, or wortmannin. Tyrosine phosphorylation of STAT3 was investigated by IP-Western blot analysis. AG-490 decreased LIF-induced phosphorylation of STAT3 by 88.4 ± 7.8%, whereas PD-98059 or wortmannin did not affect the phosphorylation of STAT3. To confirm that equal amounts of STAT3 were immunoprecipitated in each reaction, the same membranes were reprobed with anti-STAT3 antibody. Similar results were obtained from 3 independent experiments. *B*: LIF-induced gel mobility shift of SIE was inhibited by AG-490, but not by PD-98059 or wortmannin. Gel mobility shift assay was performed on cells that had been preincubated with or without AG-490 (20 μM), wortmannin (10 nM), or PD-98059 (30 μM) and stimulated with LIF. *Right lane,* competition by unlabeled SIE probe to demonstrate that this band was specific. *C*: ERK1/2 activity was inhibited by PD-98059, but not by wortmannin or AG-490. Confluent, serum-starved cardiomyocytes were stimulated with LIF (100–1,000 U/ml) for 15 min in the presence and absence of AG-490, PD-98059, or wortmannin. Activities of ERK1/2 were assayed by the "in-gel" method. PD-98059 clearly inhibited the LIF-induced activation of ERK1/2, whereas AG-490 and wortmannin did not significantly affect the activation of ERK1/2. A representative autoradiogram from 3 independent experiments is shown. *D*: dose-inhibitory relationship between wortmannin and LY-294002 and ERK. In-gel MBP phosphorylation activity was measured under various concentrations of wortmannin, LY-294002 and PD-98059. A low dose of wortmannin (5–10 nM) had no effect on LIF-induced ERK activation; a high dose (100 nM) inhibited ERK activation. LY-294002 did not attenuate this activation. PD-98059 at 10 μM was sufficient to inhibit ERK in LIF-stimulated cardiomyocytes.

sequentially activates the Raf-1/MEK/ERK-p90^{RSK} cascade in rat cardiomyocytes, *2*) activation of these three pathways was basically independent, *3*) PD-98059, wortmannin, and AG-490 inhibited LIF-induced increase in [^{3}H]phenylalanine uptake and cell area, *4*) LIF-induced reorganization of the myofilament was apparently suppressed by AG-490, but PD-98059 or wortmannin only had a minimal effect, and *5*) LIF-induced expression of c-*fos*, BNP, and skeletal α-actin was markedly suppressed by PD-98059 and was moderately suppressed by wortmannin and AG-490, but, in contrast, LIF-induced expression of ANP was significantly suppressed by AG-490 but was not suppressed by PD-98059 or wortmannin. These findings indicated

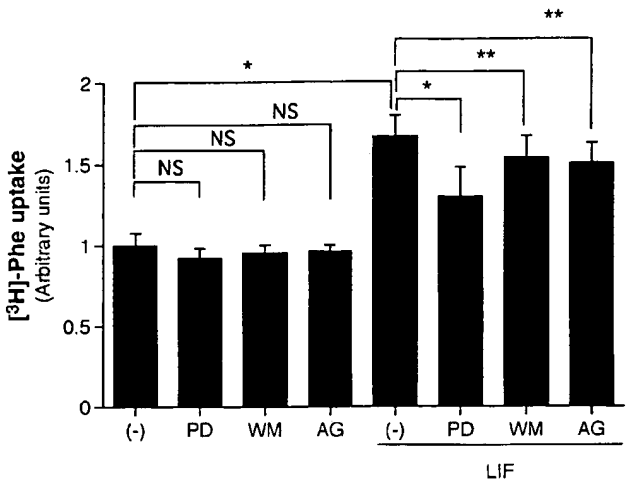

Fig. 6. Effects of PD-98059 (PD), wortmannin (WM), and AG-490 (AG) on LIF-induced increase in [^{3}H]phenylalanine uptake. Serum-starved cardiomyocytes were stimulated with LIF (1,000 U/ml) in the presence and absence of PD-98059, wortmannin, and AG-490, and [^{3}H]phenylalanine uptake was measured at 48 h after stimulation. The LIF-induced increase in [^{3}H]phenylalanine uptake was inhibited by PD-98059, wortmannin, and AG-490 by 54.7, 21.5, and 25.6%, respectively. Each bar represents mean of 6 separate experiments. $*P < 0.01$; $**P < 0.05$.

that the Raf-1/MEK/ERK-p90^{RSK} pathway was critically involved in the progression of gp130-mediated cardiac hypertrophy in addition to the other two pathways and that each pathway induces different hypertrophic marker genes.

There is conflicting evidence on the role of the ERK cascade in the development of cardiac hypertrophy. The Raf-1/MEK/ERK cascade, also known as the ERK module, can be activated by various hypertrophic stimuli, including phenylephrine, endothelin-1, ANG II, and mechanical stress (2, 5, 29, 40, 41), and has been shown to play an important role in cardiac hypertrophy. Transfection of constructs encoding active Ras, Raf-1, or MEK can induce ANP, β-myosin heavy chain, skeletal α-actin, and myosin light chain-2v promoter activities (34, 36, 37). Dominant-negative Ras or Raf-1 can inhibit phenylephrine-induced ERK and cardiac hypertrophic gene promoter activities (34, 36). These findings suggested that the Raf-1/MEK/ERK pathway was critical to the development of cardiac hypertrophy.

In contrast, Thorburn et al. (35) reported that overexpression of the active forms of Raf-1 or ERK does not cause the sarcomeric organization typical of hypertrophic growth, and Post et al. (25) reported that inhibition of MEK by PD-98059 did not suppress phenylephrine-induced sarcomeric organization or ANP gene expression. Moreover, they showed that ATP and carbachol activated the Raf-1/MEK/ERK cascade, although neither of these reagents could cause cardiac hypertrophy. These findings suggested that the activation of ERK alone was not sufficient for the induction of cardiac hypertrophy and hypertrophic gene expression and suggested that the role of this pathway was distinct from ligand to ligand.

The present study compared the roles of these three pathways in LIF-induced cardiac hypertrophy with use of specific inhibitors. We previously observed that AG-490, wortmannin (10 nM), and PD-98059 specifically blocked the JAK/STAT, PI3-K/p70 S6K, and Raf-1/MEK/ERK/p90^{RSK} pathways, respectively, but did not attenuate other pathways. These findings suggested that these three pathways were mutually independent. However, the findings that all these pathways attenuated hypertrophic marker gene expression indicated that these pathways cooperatively regulated hypertrophic gene expression.

The present data indicated that inhibition of Raf-1/MEK/ERK/p90^{RSK} cascade in gp130-mediated cardiac hypertrophy suppressed protein synthesis and induction of c-*fos*, BNP, and skeletal-α-actin, whereas it had a minimal effect on ANP gene expression and myofil-

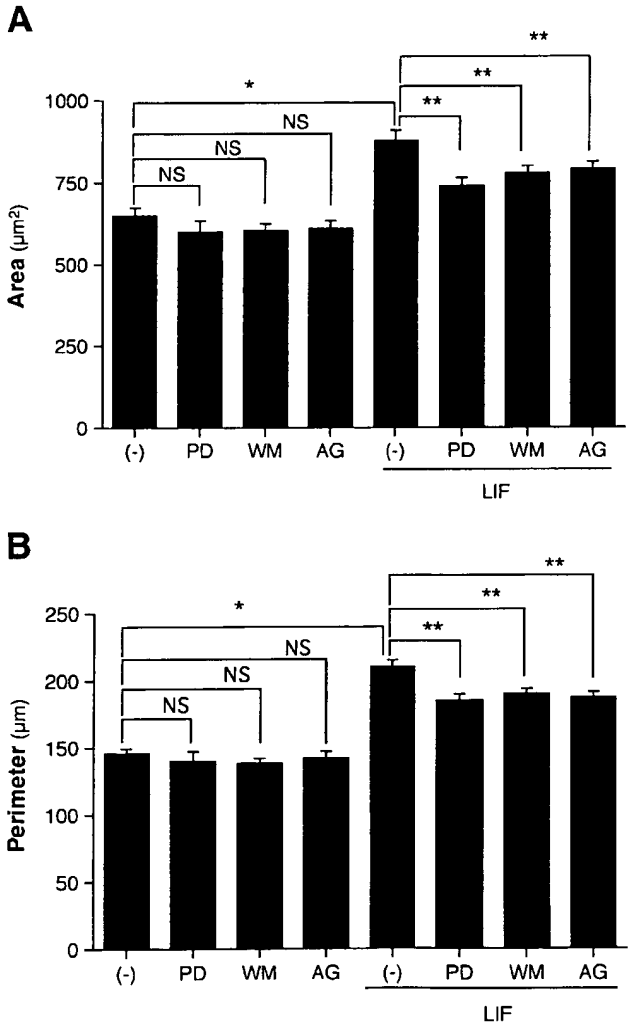

Fig. 7. Effect of PD-98059 (PD), wortmannin (WM), and AG-490 (AG) on LIF-induced increase in cell area (*A*) and perimeter (*B*). Cardiomyocytes were stimulated with LIF for 48 h in the presence and absence of PD-098059, wortmannin, and AG-490. Surface area and perimeter of the cardiomyocytes were measured using calibrated fluorescent photomicrographs of the sarcomeric myosin, which were quantitated and validated. $*P < 0.01$; $**P < 0.05$.

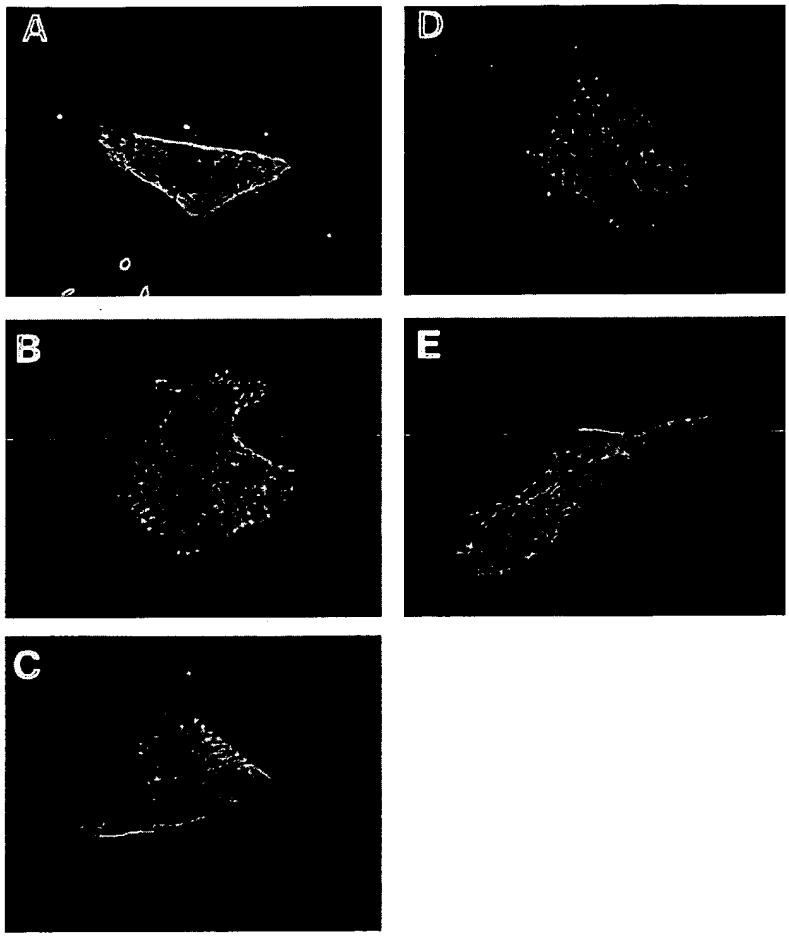

Fig. 8. Effect of PD-98059, wortmannin, and AG-490 on LIF-induced increase in myofilament reorganization. Representative immunofluorescent photographs of cardiomyocytes stained with antisarcomeric myosin are shown. Serum-starved cardiomyocytes were stimulated with LIF (1,000 U/ml) for 48 h in the presence and absence of PD-98059, wortmannin, and AG-490. LIF caused an increase in cell size and reorganization of myofilaments. *A*: control; *B*: LIF; *C*: LIF + PD-98059; *D*: LIF + wortmannin; *E*: LIF + AG-490.

ament reorganization. The finding that the inhibition of this cascade did not affect myofilament reorganization or ANP gene induction in gp130-mediated cardiac hypertrophy is in accordance with results obtained in phenylephrine-induced cardiac hypertrophy (25, 35). However, the finding that inhibition of this cascade suppressed protein synthesis and induction of c-*fos*, BNP, and skeletal-α-actin strongly indicates that this pathway was critically involved in gp130-mediated cardiac hypertrophy. Together, these results suggest that this cascade plays a crucial role in gp130-mediated cardiac hypertrophy, although this pathway alone may

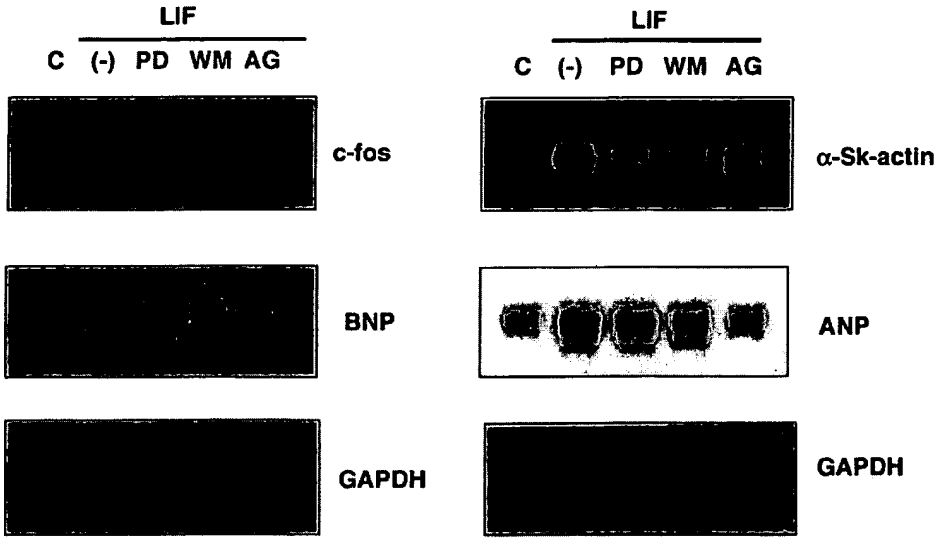

Fig. 9. Effect of PD-98059 (PD), wortmannin (WM), and AG-490 (AG) on LIF-induced gene expression. Cardiomyocytes were stimulated with LIF in the presence and absence of PD-98059, wortmannin, and AG-490, and total RNA was extracted at 30 min (c-*fos*), 1 h [brain natriuretic peptide (BNP)], or 24 h [skeletal α-actin and atrial natriuretic peptide (ANP)] after stimulation. LIF-induced c-*fos* and skeletal α-actin expression was strongly inhibited by PD-98059 and moderately by wortmannin and AG-490. BNP expression was strongly inhibited by PD-98059, but only slightly by wortmannin and AG-490. In contrast, LIF-induced expression of ANP was strongly inhibited by AG-490. GAPDH, glyceraldehyde 3-phosphate dehydrogenase.

not be sufficient for the development of cardiac hypertrophy. Recent studies demonstrated that gp130-mediated cardiac hypertrophy has a phenotype distinct from that for phenylephrine-induced cardiac hypertrophy (39). It was interesting that the inhibition of this cascade caused a similar response, although these two ligands caused quite distinctive hypertrophic phenotypes.

In the present study we observed a role for the PI3-K and JAK/STAT pathways in hypertrophic marker gene induction. Oh et al. (22) revealed that inhibition of PI3-K resulted in suppression of protein synthesis and partial inhibition of c-*fos* induction in LIF-mediated cardiac hypertrophy, but they did not find a role for this pathway in induction of other hypertrophic marker genes. The present study revealed that inhibition of the PI3-K/p70 S6K pathway caused partial inhibition of BNP, skeletal α-actin, and ANP. Kunisada et al. (17) showed that adenovirus-mediated transfer of dominant-negative mutants of STAT3 partially attenuated c-*fos* and ANP expression in cardiomocytes. We have observed the effect of a JAK2 inhibitor on hypertrophic marker gene induction. It was quite interesting that expression of ANP was more strongly inhibited by a JAK2 inhibitor than MEK or PI3-K inhibitors, whereas expression of other hypertrophic marker genes such as c-*fos*, BNP, and skeletal α-actin was strongly inhibited by a MEK inhibitor. Because the rat ANP promoter region does not contain an SIE consensus sequence (32), AG-490 did not directly inhibit the transcription of ANP. Furthermore, myofilament reorganization induced by LIF was more strongly disrupted by AG-490 than by PD-98059. These findings indicated that the JAK/STAT pathway and the Raf-1/MEK/ERK pathway play different roles in gp130-mediated cardiac hypertrophy, but further studies are needed to clarify the precise role of each pathway.

The authors acknowledge the technical assistance of Kio Nakamaru.

This study was supported in part by Japan Society for the Promotion of Science "Research for the Future" Program Grant JSPS-RFTF97I00201, a research grant from the Ministry of Education, Science, and Culture, Japan, and a Health Science Research Grant for Advanced Medical Technology from the Ministry of Welfare, Japan.

REFERENCES

1. **Akira S, Yoshida K, Tanaka T, Taga T, and Kishimoto T.** Targeted disruption of the IL-6 related genes: gp130 and NF-IL-6. *Immunol Rev* 148: 221–253, 1995.
2. **Bogoyevitch MA, Glennon PE, Anderson MB, Clerk A, Lazou A, Marshall CJ, Parker PJ, and Sugden PH.** Endothelin-1 and fibroblast growth factors stimulate the mitogen-activated protein kinase cascade in cardiac myocytes. *J Biol Chem* 269: 1110–1119, 1994.
3. **Boluyt MO, Zheng JS, Younes A, Long X, O'Neill L, Silverman H, Lakatta EG, and Crow MT.** Rapamycin inhibits α_1-adrenergic receptor-stimulated cardiac myocyte hypertrophy but not activation of hypertrophy-associated genes. Evidence for involvement of p70 S6 kinase. *Circ Res* 81: 176–186, 1997.
4. **Chien KR.** Stress pathways and heart failure. *Cell* 98: 555–558, 1999.
5. **Clerk A, Bogoyevitch MA, Anderson MB, and Sugden PH.** Differential activation of protein kinase C isoforms by endothelin-1 and phenylephrine and subsequent stimulation of p42 and p44 mitogen-activated protein kinases in ventricular myocytes cultured from neonatal rat hearts. *J Biol Chem* 269: 32848–32857, 1994.
6. **Frevert EU and Kahn BB.** Differential effects of constitutively active phosphatidylinositol 3-kinase on glucose transport, glycogen synthase activity, and DNA synthesis in 3T3-L1 adipocytes. *Mol Cell Biol* 17: 190–198, 1997.
7. **Glennon PE, Kaddoura S, Sale EM, Sale GJ, Fuller SJ, and Sugden PH.** Depletion of mitogen-activated protein kinase using an antisense oligodeoxynucleotide approach downregulates the phenylephrine-induced hypertrophic response in rat cardiac myocytes. *Circ Res* 78: 954–961, 1996.
8. **Hirota H, Chen J, Betz UA, Rajewsky K, Gu Y, Ross J Jr, Muller W, and Chien KR.** Loss of a gp130 cardiac muscle cell survival pathway is a critical event in the onset of heart failure during biomechanical stress. *Cell* 97: 189–198, 1999.
9. **Hirota, H, Yoshida K, Kishimoto T, and Taga T.** Continuous activation of gp130, a signal-transducing receptor component for interleukin 6-related cytokines, causes myocardial hypertrophy in mice. *Proc Natl Acad Sci USA* 92: 4862–4866, 1995.
10. **Ip NY, Nye S, Boulton TG, Davis S, Taga T, Li Y, Birren SJ, Yasukawa K, Kishimoto T, Anderson DJ, Stahl N, and Yancopoulous GD.** CNTF and LIF act on neuronal cells via shared signaling pathways that involve the IL-6 signal transducing receptor component gp130. *Cell* 69: 1121–1132, 1192.
11. **Ito H, Hiroe M, Hirata Y, Tsujino M, Adachi S, Shichiri M, Koike A, Nogami A, and Marumo F.** Insulin-like growth factor-I induces hypertrophy with enhanced expression of muscle specific genes in cultured rat cardiomyocytes. *Circulation* 87: 1715–1721, 1993.
12. **Jaster R, Bittorf T, and Brock J.** Involvement of phosphatidylinositol 3-kinase in the mediation of erythropoietin-induced activation of $p70^{S6k}$. *Cell Signal* 9: 175–179, 1997.
13. **Kodama H, Fukuda K, Pan J, Makino S, Baba A, Hori S, and Ogawa S.** Leukemia inhibitory factor, a potent cardiac hypertrophic cytokine, activates the JAK/STAT pathway in rat cardiomyocytes. *Circ Res* 81: 656–663, 1997.
14. **Kodama H, Fukuda K, Pan J, Makino S, Sano M, Takahashi T, Hori S, and Ogawa S.** Biphasic activation of the JAK/STAT pathway by angiotensin II in rat cardiomyocytes. *Circ Res* 82: 244–250, 1998.
15. **Kohn AD, Takeuchi F, and Roth RA.** Akt, a pleckstrin homology domain containing kinase, is activated primarily by phosphorylation. *J Biol Chem* 271: 21920–21926, 1996.
16. **Kunisada K, Hirota H, Fujio Y, Matsui H, Tani Y, Yamauchi-Takihara K, and Kishimoto T.** Activation of JAK-STAT and MAP kinases by leukemia inhibitory factor through gp130 in cardiac myocytes. *Circulation* 94: 2626–2632, 1996.
17. **Kunisada K, Tone E, Fujio Y, Matsui H, Yamauchi-Takihara K, and Kishimoto T.** Activation of gp130 transduces hypertrophic signals via STAT3 in cardiac myocytes. *Circulation* 98: 346–352, 1998.
18. **Nakanishi S, Kakita S, Takahashi I, Kawahara K, Tsukuda E, Sano T, Yamada K, Yoshida M, Kase H, and Matsuda Y.** Wortmannin, a microbial product inhibitor of myosin light chain kinase. *J Biol Chem* 267: 2157–2163, 1992.
19. **Nguyen TT, Scimeca JC, Filloux C, Peraldi P, Carpentier JL, and Van Obberghen E.** Co-regulation of the mitogen-activated protein kinase, extracellular signal-regulated kinase 1, and the 90-kDa ribosomal S6 kinase in PC12 cells. Distinct effects of the neurotrophic factor, nerve growth factor, and the mitogenic factor, epidermal growth factor. *J Biol Chem* 268: 9803–9810, 1993.
20. **Nielsen M, Kaltoft K, Nordahl M, Ropke C, Geisler C, Mustelin T, Dobson P, Svejgaard A, and Odum N.** Constitutive activation of a slowly migrating isoform of Stat3 in mycosis fungoides: tyrphostin AG490 inhibits Stat3 activation and growth of mycosis fungoides tumor cell lines. *Proc Natl Acad Sci USA* 94: 6764–6769, 1997.

21. **Nishida E and Gotoh Y.** The MAP kinase cascade is essential for diverse signal transduction pathways. *Trends Biochem Sci* 18: 128–131, 1993.
22. **Oh H, Fujio Y, Kunisada K, Hirota H, Matsui H, and Kishimoto T, and Yamauchi-Takihara K.** Activation of phosphatidylinositol 3-kinase through glycoprotein 130 induces protein kinase B and p70 S6 kinase phosphorylation in cardiac myocytes. *J Biol Chem* 273: 9703–9710, 1998.
23. **Pennica D, King KL, Shaw KJ, Luis E, Rullamas E, Luoh SM, Decabonne WC, Knutzon DS, Yen R, Chien KR, and Baker JB, and Wood WI.** Expression cloning of cardiotrophin-1, a cytokine that induces cardiac hypertrophy. *Proc Natl Acad Sci USA* 92: 1142–1146, 1995.
24. **Pennica D, Shaw KJ, Swanson TA, Moore MW, Shelton DL, Zioncheck KA, Rosenthal A, Taga T, Paoni NF, and Wood WI.** Cardiotrophin-1. *J Biol Chem* 270: 10915–10922, 1995.
25. **Post GR, Goldstein D, Thuerauf DJ, Glembotski CC, and Brown JH.** Dissociation of p44 and p42 mitogen-activated protein kinase activation from receptor-induced hypertrophy in neonatal rat ventricular myocytes. *J Biol Chem* 271: 8452–8457, 1996.
26. **Poyner DR, Jackson TR, and Hawkins PT.** Stimulation of phosphatidylinositol-3-kinase by insulin-like growth factor 1 and other agonists (Abstract). *Biochem Soc Trans* 20: 140S, 1992.
27. **Rabkin SW, Goutsouliak V, and Kong JY.** Angiotensin II induces activation of phosphatidylinositol 3-kinase in cardiomyocytes. *J Hypertens* 15: 891–899, 1992.
28. **Sadoshima J and Izumo S.** Rapamycin selectively inhibits angiotensin II-induced increase in protein synthesis in cardiac myocytes in vitro. Potential role of 70-kD S6 kinase in angiotensin II-induced cardiac hypertrophy. *Circ Res* 77: 1040–1052, 1995.
29. **Sadoshima J, Qiu Z, Morgan JP, and Izumo S.** Angiotensin II and other hypertrophic stimuli mediated by G protein-coupled receptors activate tyrosine kinase, mitogen-activated protein kinase, and 90-kD S6 kinase in cardiac myocytes. *Circ Res* 76: 1–15, 1995.
30. **Schiemann WP and Nathanson NM.** Involvement of protein kinase C during activation of the mitogen-activated protein kinase pathway by leukemia inhibitory factor. Evidence for participation of multiple signaling pathways. *J Biol Chem* 269: 6376–6382, 1994.
31. **Seger R and Krebs EG.** The MAPK signaling cascade. *FASEB J* 9: 726–735, 1995.
32. **Seidman CE, Wong DW, Jarcho JA, Bloch KD, and Seidman JG.** *Cis*-acting sequences that modulate atrial natriuretic factor gene expression. *Proc Natl Acad Sci USA* 85: 4104–4108, 1998.
33. **Sue-A-Quan AK, Fialkow L, Vlahos CJ, Schelm JA, Grinstein S, Butler J, and Downey GP.** Inhibition of neutrophil oxidative burst and granule secretion by wortmannin: potential role of MAP kinase and renaturable kinases. *J Cell Physiol* 172: 94–108, 1997.
34. **Thorburn A, Thorburn J, Chen SY, Powers S, Shubeita HE, Feramisco JR, and Chien KR.** H-*ras*-dependent pathways can activate morphological and genetic markers of cardiac muscle cell hypertrophy. *J Biol Chem* 268: 2244–2249, 1993.
35. **Thorburn J, Frost JA, and Thorburn A.** Mitogen-activated protein kinases mediate changes in gene expression, but not cytoskeletal organization associated with cardiac muscle cell hypertrophy. *J Cell Biol* 126: 1565–1572, 1994.
36. **Thorburn J, McMahon M, and Thorburn A.** Raf-1 kinase activity is necessary and sufficient for gene expression changes but not sufficient for cellular morphology changes associated with cardiac myocyte hypertrophy. *J Biol Chem* 269: 30580–30586, 1994.
37. **Thuerauf DJ and Glembotski CC.** Differential effects of protein kinase C, Ras, and Raf-1 kinase on the induction of the cardiac B-type natriuretic peptide gene through a critical promoter-proximal M-CAT element. *J Biol Chem* 272: 7464–7472, 1997.
38. **Vanhaesebroeck B, Leevers SJ, Panayotou G, and Waterfield MD.** Phosphoinositide 3-kinases: a conserved family of signal transducers. *Trends Biochem Sci* 22: 267–277, 1997.
39. **Wollert KC, Taga T, Saito M, Narazaki M, Kishimoto T, Glembotski CC, Vernallis AB, Heath JK, Pennica D, Wood WI, and Chien KR.** Cardiotrophin 1 activates a distinct form of cardiac muscle cell hypertrophy. *J Biol Chem* 271: 9535–9545, 1996.
40. **Yamazaki T, Komuro I, Kudoh S, Zou Y, Shiojima I, Mizuno T, Takano H, Hiroi Y, Ueki K, Tobe K, and Yazaki Y.** Mechanical stress activates protein kinase cascade of phosphorylation in neonatal rat cardiac myocytes. *J Clin Invest* 96: 438–446, 1995.
41. **Yamazaki T, Tobe K, Hoh E, Maemura K, Kaida T, Komuro I, Tamemoto H, Kadowaki T, Nagai R, and Yazaki Y.** Mechanical loading activates mitogen-activated protein kinase and S6 peptide kinase in cultured rat cardiac myocytes. *J Biol Chem* 268: 12069–12076, 1993.
42. **Yoshida K, Taga T, Saito M, Suematsu S, Kumanogoh A, Tanaka T, Fujiwara H, Hirata M, Yamagami T, Nakahata T, Hirabayashi T, Yoneda Y, Tanaka K, Wang WZ, Mori C, Shiota K, Yoshida N, and Kishimoto T.** Targeted disruption of gp130, a common signal transducer for the interleukin 6 family of cytokines, leads to myocardial and hematologic disorders. *Proc Natl Acad Sci USA* 93: 407–411, 1996.

Exhibit J

ELSEVIER

Cardiovascular Research 53 (2002) 131–137

Cardiovascular Research

www.elsevier.com/locate/cardiores

Activation of mitogen-activated protein kinases and p90 ribosomal S6 kinase in failing human hearts with dilated cardiomyopathy

Yasuchika Takeishi[a,*,1], Qunhua Huang[b,1], Jun-ichi Abe[b,1], Wenyi Che[b], Jiing-Dwan Lee[c], Hisaaki Kawakatsu[d], Brian D. Hoit[a], Bradford.C. Berk[b], Richard A. Walsh[a]

[a]*Department of Medicine, Case Western Reserve University, Cleveland, OH 44106-5029, USA*
[b]*Center for Cardiovascular Research, University of Rochester, Rochester, NY 14642, USA*
[c]*Department of Immunology, The Scripps Research Institute, La Jolla, CA 92037, USA*
[d]*Lung Biology Center, University of California at San Francisco, San Francisco, CA 94143, USA*

Received 19 March 2001; accepted 2 August 2001

Abstract

Objective: A new member of the MAP kinase family, big MAP kinase-1 (BMK1), has been recently identified to promote cell growth and attenuate apoptosis. P90 ribosomal S6 kinase (p90RSK), one of the potentially important substrates of extracellular signal regulated kinase (ERK), regulates gene expression in part via phosphorylation of CREB and the Na^+/H^+ exchanger. Recently, we have demonstrated that the activity of BMK1, Src (the upstream regulator of BMK1) and p90RSK was increased in hypertrophied myocardium induced by pressure-overload in the guinea pig. However, the abundance and activity of these kinases in human hearts are unknown. **Methods:** In addition to the three classical MAP kinases (ERK, p38 kinase, and c-Jun NH_2-terminal kinase (JNK)), we examined the protein expression and activity of Src, BMK1, and p90RSK in explanted hearts from patients with dilated cardiomyopathy ($n=9$). Normal donor hearts, which were not suitable for transplant for technical reasons, were used as controls ($n=5$). **Results:** There were no significant differences in the levels of protein expression of these kinases between normal and failing hearts. ERK1/2 and p90RSK were activated in heart failure compared to control ($P<0.01$ and $P<0.03$, respectively), while the activity of p38 kinase was decreased ($P<0.05$) and the activity of JNK was unchanged in heart failure. By contrast, the activities of Src and BMK1 were significantly reduced in end-stage heart failure compared to normal donor hearts ($P<0.05$). **Conclusion:** These data suggest that multiple MAP kinases, p90RSK, and Src are differentially regulated in human failing myocardium of patients with idiopathic dilated cardiomyopathy and may be involved in the pathogenesis of this complex disease.

Keywords: Cardiomyopathy; Heart failure; Protein kinases; Signal transduction

1. Introduction

Heart failure is an increasingly important public health problem with a high mortality rate. Although a variety of metabolic and/or neurohumoral factors are implicated in the progression of this syndrome, the precise mechanisms responsible for this complex condition are poorly understood. Activation of the Gαq signaling pathway, which includes protein kinase C (PKC), appears to play a critical role in the progression of heart failure [1]. Recently, we found that translocation of PKC isoforms from cytosolic to membranous fractions were increased in a conventional animal model of heart failure that was induced by pressure-overload [2,3] and in myocardium from patients with end-stage heart failure [4]. As downstream phosphorylation targets of PKC activation, the mitogen-activated protein (MAP) kinase family plays an important role in cardiac hypertrophy and failure [5]. Four subfamilies of

*Corresponding author. Present address: The First Department of Internal Medicine, Yamagata University School of Medicine, 2-2-2 Iida-Nishi, Yamagata 990-9585, Japan. Tel.: +81-23-628-5302; fax: +81-23-628-5305.

E-mail address: takeishi@med.id.yamagata-u.ac.jp (Y. Takeishi).

[1]Yasuchika Takeishi, Qunhua Huang, and Jun-ichi Abe contributed equally to this work.

Time for primary review 29 days.

0008-6363/02/$ – see front matter
PII: S0008-6363(01)00438-2

MAP kinases have been identified, including extracellular signal-regulated kinase (ERK1/2), c-Jun NH_2 terminal kinase (JNK), p38 kinase, and big MAP kinase 1 (BMK1 or ERK5) [5]. BMK1 is a recently identified MAP kinase family member, which shares the TEY activation motif with ERK1/2 but is activated by MEK5 [6]. It has been reported that oxidative stress using H_2O_2 activates ERK1/2, JNK and p38 kinase in neonatal rat cardiomyocytes [7], and ischemia followed by reperfusion activates JNK and p38 kinase in isolated coronary-perfused rat hearts [8]. In addition, we recently showed that oxidative stress activates ERK1/2 and BMK1 in coronary-perfused isolated adult guinea pig hearts [9]. Each MAP kinase subfamily may be regulated by different signal transduction pathways that modulate specific cell functions [10]. A potentially important downstream effector of ERK1/2 is p90 ribosomal S6 kinase (p90RSK), which plays a pivotal role in cell growth by activating several transcription factors as well as the Na^+/H^+ exchanger (NHE-1) [11].

Although there are considerable data pertaining to MAP kinases in animal models of cardiac hypertrophy and heart failure, data regarding these kinases in the failing human heart are limited, particularly for p90RSK and BMK1. Accordingly, the purpose of this study was to characterize the activity of multiple MAP kinases including BMK1 and p90RSK in explanted failing hearts from patients with idiopathic dilated cardiomyopathy. Of note, we excluded patients with ischemic cardiomyopathy from the present study, since it is known that ischemia itself activates several MAP kinases.

2. Material and methods

2.1. Patient population

Left ventricular myocardium was obtained from nine hearts explanted from patients with end-stage heart failure who were undergoing orthotopic cardiac transplantation (all men, mean age 41±15 years). All patients were diagnosed with New York Heart Association class IV congestive heart failure secondary to idiopathic dilated cardiomyopathy. Non-failing human myocardium was obtained from five donors (four men and one woman, mean age 44±19 years), who had sustained traumatic brain death; these donors had normal cardiac function (as assessed echocardiographically) and had not been prescribed cardiovascular medications. The normal donor hearts were not used for transplantation because of technical reasons, such as death of the recipient, logistic problems, signs of chest trauma after explantation, etc. The investigation conforms with the principles outlined in the Declaration of Helsinki (*Cardiovascular Research* 1997;35:2–3).

2.2. Protein preparation

Myocardial samples were immediately frozen in liquid nitrogen after dissection and were stored at −80°C until use [4,12]. The sampling conditions were identical for both failing and non-failing hearts. Fibrotic or adipose tissue, endocardium, epicardium, or great vessels were carefully excised, and remaining tissue was homogenized with 4 vols of ice-cold lysis buffer (50 mM sodium pyrophosphate, 50 mM NaF, 50 mM NaCl, 5 mM EDTA, 5 mM EGTA, 100 μM Na_3VO_4, 10 mM HEPES, pH 7.4, 1% Triton X-100, 0.1% SDS, 500 μM phenylmethanesulfonyl fluoride (PMSF), and 10 μg/ml leupeptin). The heart homogenates were centrifuged at 14 000×*g* (4°C for 30 min), and protein concentration was determined using the Bradford protein assay (Bio-Rad, Hercules, CA, USA) [2,9,12]. The protein expression and activity of the following kinases were examined in both failing and non-failing human myocardium: ERK1/2, P38 kinase, JNK, p90RSK, Src, and BMK1.

2.3. Immunoprecipitation and Western blot analysis

For immunoprecipitation, cell lysates were incubated with rabbit anti-human BMK1 antibody (J.D. Lee, The Scripps Research Institute, La Jolla, CA, USA) for 12 h at 4°C and then incubated with 20 μl of protein A-Sepharose CL-4B (Pharmacia Biotech, Piscataway, NJ, USA) for 1 h on a roller system (RT-50, Taitec, Koshigaya, Saitama, Japan) at 4°C [9,13]. The beads were washed two times with 1 ml lysis buffer, two times with 1 ml LiCl wash buffer (500 mM LiCl, 100 mM Tris–HCl, pH 7.6, 0.1% Triton X-100, 1 mM DTT) and two times in 1 ml washing buffer (HEPES 20 mM, pH 7.2, 2 mM EGTA, 10 mM $MgCl_2$, 1 mM DTT, 0.1% Triton X-100). For Western blot analysis, cell lysates or immunoprecipitates were subjected to SDS–PAGE and proteins were transferred to nitrocellulose membranes (Amersham Life Science, Arlington Heights, IL, USA) as previously described [9,13]. The membrane was blocked for 1 h at room temperature with a commercially available blocking buffer from Gibco BRL (Life Technologies, Rockville, MD, USA). To examine the protein expression, the blots were then incubated for 1 h at room temperature with anti-BMK1, ERK1, ERK2 (rabbit anti-rat, cross-reactive with human; Santa Cruz Biotechnology, Santa Cruz, CA, USA), p38 kinase (rabbit anti-human; Santa Cruz Biotechnology), JNK1, JNK2 (rabbit anti-human; Santa Cruz Biotechnology), p90RSK (goat anti-human; Santa Cruz Biotechnology), or Src (rabbit anti-human; Santa Cruz Biotechnology), followed by incubation for 1 h with secondary antibody conjugated with horse radish peroxidase (KPL laboratories, Gaithesburg, MD, USA). Immunoreactive bands were visualized using enhanced chemiluminescence (ECL, Amersham Life Science).

2.4. Activity for ERK1/2, p38 kinase and Src

To examine phosphorylation of ERK1/2 and p38 kinase, the blots were incubated for 12 h with anti phospho-specific ERK1/2 (mouse anti-human; New England Biolabs, Beverly, MA, USA) and phospho-specific p38 kinase (mouse anti-human; New England Biolabs) antibodies, respectively. We and other investigators have previously reported that immunoblotting with phospho-specific ERK1/2 antibody has a good correlation with an immune complex kinase assay [14,15]. Activity of Src was measured using anti activated-Src antibody clone 28 (H. Kawakatsu, University of California San Francisco, San Francisco, CA, USA), which recognizes only the activated form of Src [9,13].

2.5. p90RSK, JNK, and BMK1 kinase assays

p90RSK kinase activity was measured by glutathione *S*-transferase (GST)-NHE-1 phosphorylation and BMK1 kinase activity was measured by autophosphorylation as described previously [9]. JNK activity was measured with a commercially available kit (New England Biolabs, Beverly, MA, USA) based on phosphorylation of recombinant c-Jun [9]. We could not detect ERK1/2, p38, p90RSK, or BMK1 in c-Jun fusion protein beads immunoprecipitates, indicating that JNK is the dominant c-Jun kinase present (data not shown).

2.6. Statistical analysis

Data are reported as mean±S.D. Statistical analysis was performed with the StatView 4.0 package (Abacus Concepts, Berkeley, CA, USA). Differences between failing and non-failing hearts were analyzed by un-paired *t*-test. *P* values less than 0.05 were considered significant.

3. Results

3.1. ERK1/2 expression and activity: comparison with p90RSK

As determined by quantitative immunoblotting, there were no significant differences in the level of ERK1/2 protein expression between failing human hearts with end-stage dilated cardiomyopathy and non-failing human hearts (Fig. 1A). By contrast, the activity of ERK1/2 was increased in failing hearts with dilated cardiomyopathy compared to non-failing control hearts (4.2±0.1-fold, $P<0.01$).

We also evaluated p90RSK activation in the same samples, since p90RSK is one of the important downstream substrates of ERK1/2. As shown in Fig. 1B, there was no significant difference in p90RSK protein expression between failing and non-failing hearts. However, p90RSK activity was significantly increased (2.1±0.7-fold, $P<0.03$) in failing myocardium.

3.2. Determination of p38 kinase and JNK expression and activity

It has been reported that cellular stresses such as hyperosmotic shock, protein synthesis inhibitors (e.g. anisomycin), hypoxia/reoxygenation, and reactive oxygen species activate p38 kinase and JNK in cultured cardiomyocytes [5]. To determine the role of p38 kinase and JNK in failing human hearts with idiopathic dilated cardiomyopathy, we examined the protein expression and activity of p38 kinase and JNK. As shown in Fig. 2, although neither the protein expression of p38 kinase, JNK1, and JNK2 nor the activity of JNK were significantly different in normal and failing myocardium, the p38 kinase activity (0.4±0.3-fold, $P<0.05$) was significantly reduced in myocardium from failing hearts.

3.3. Src and BMK1 expression and activity in human failing hearts

We previously demonstrated that Src kinase regulates BMK1 activity in part by oxidative stress in adult guinea pig hearts [8]. Since reactive oxygen species are known to be increased in failing myocardium, we also examined here Src and BMK1 kinases activity. As shown in Fig. 3, Src and BMK1 protein expression was not different between failing and non-failing myocardium. Src activity, which was evaluated by anti-activated Src-clone 28 antibody, was decreased significantly in failing human hearts (0.7±0.2-fold, $P<0.05$). As shown in Fig. 3B, BMK1 activity was also decreased in failing human hearts compared to non-failing hearts (0.4±0.2-fold, $P<0.05$).

4. Discussion

In the present study, we examined whether the expression and activity of multiple MAP kinases, p90RSK, and Src were altered in ventricular tissue from failed human hearts with end-stage dilated cardiomyopathy. We found no differences in protein abundance of these kinases between failing and non-failing human hearts. The mean activities of ERK1/2 and p90RSK were significantly greater in failing hearts compared to non-failing donor hearts. In contrast, p38 kinase, Src, and BMK1 activities were reduced in human myocardium with end-stage heart failure. We could not detect any significant changes in JNK activity between failing and non-failing hearts. These data suggest that the MAP kinase family activity is differentially regulated in human dilated cardiomyopathy without any alterations in protein abundance.

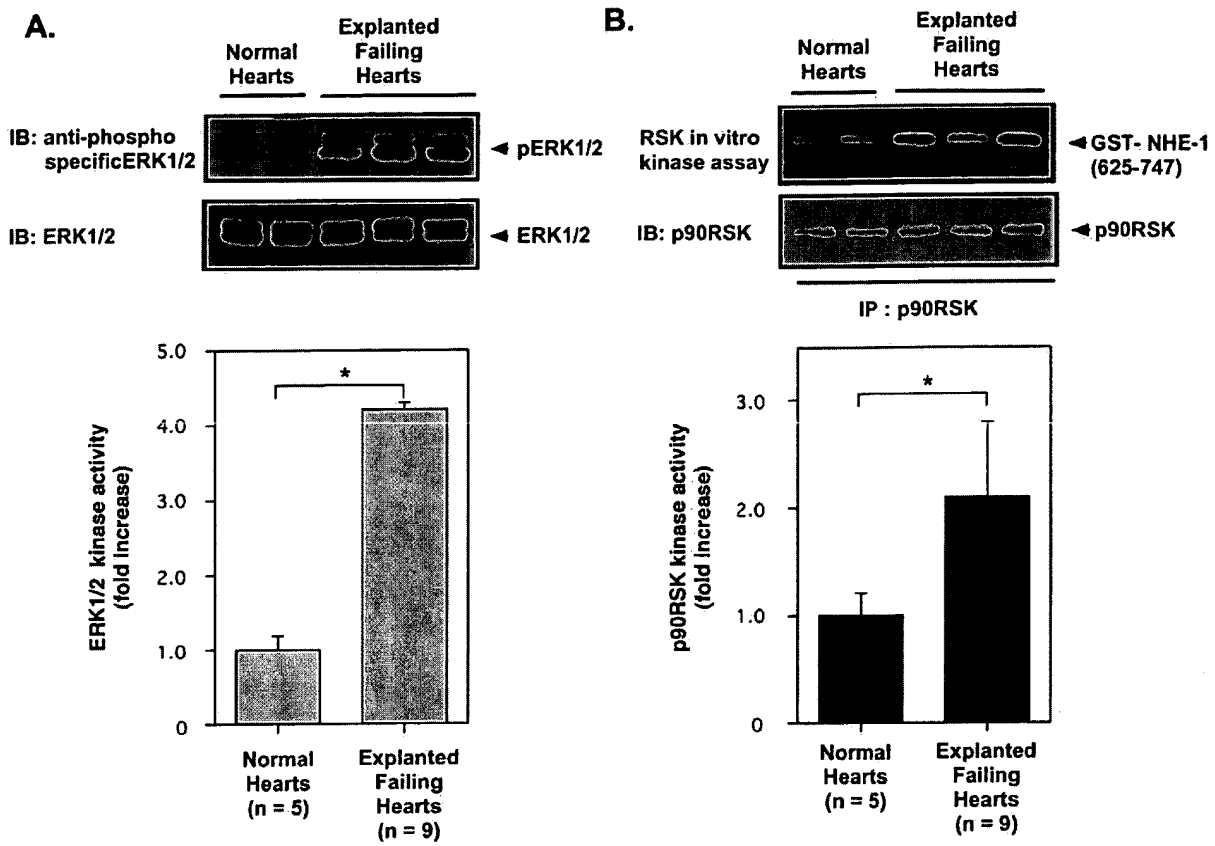

Fig. 1. ERK1/2 and p90RSK in failing and non-failing human hearts. (A) ERK1/2 activity in whole heart extracts was measured by Western blot analysis with a phospho-specific ERK antibody (upper). No difference in the amount of ERK1/2 protein was observed in lysates from any of the heart samples by Western blot analysis with anti-ERK1/2 (lower). For densitometric analysis of ERK1/2 activity, results were normalized for all experiments by arbitrarily setting the densitometry of control heart samples (non-failing hearts) to 1.0 (shown is mean±S.D.). (B) p90RSK activity was measured by an in vitro kinase assay using GST-NHE-1 (625–747) as a substrate. p90RSK protein level was examined by Western blot analysis with anti-p90RSK antibody. Representative autoradiogram showing p90RSK kinase activity (upper panel) and Western blot analysis showing p90RSK protein levels (lower panel). Densitometric analysis revealed that kinase activity of ERK1/2 and p90RSK was significantly increased in explanted human failing hearts compared to normal control hearts. IB, immuno-blotting; * $P<0.05$.

Cook et al. [16] have reported that ERK1/2 activity was unchanged and p38 kinase activity was increased in failing human hearts secondary to ischemic cardiomyopathy. In our study, the patients were diagnosed as idiopathic dilated cardiomyopathy, while in that study they selected patients with heart failure secondary to ischemic cardiomyopathy. It has been reported that ischemia and ischemia/reperfusion induced multiple MAP kinase activation [5,8,9]. Therefore, it is likely that the presence of ischemia itself, in addition to LV dysfunction and heart failure, modulates the activity of multiple MAP kinases in these patients.

To our knowledge, this is the first report of p90RSK, Src and BMK1 activity in human tissues. We have reported that protein expression and activity of PKC isoforms are elevated in guinea pig model of heart failure by chronic pressure-overload [2,3] and in human explanted hearts with end-stage heart failure [4,12]. We and others have reported that ERK1/2 and p90RSK activation are at least in part PKC-dependent [17]. ERK1/2 were the first MAP kinases described and it has been reported that ERK1/2 activation protects against apoptotic cell death [18,19]. Among the substrates of ERK, p90RSK is a versatile mediator of ERK signal transduction [11,17]. These include: (1) regulation of gene expression via phosphorylation of transcription factors including c-fos, cAMP-response element-binding protein (CREB) and CREB-binding protein, (2) regulation of protein synthesis by phosphorylation of polyribosomal proteins and glycogen synthase kinase-3, and (3) stimulation of the Na^+/H^+ exchanger by phosphorylating serine 703 of NHE-1 [10]. Recently Bonni et al. [19] and Tan et al. [20] reported that p90RSK phosphorylated the pro-apoptotic protein BAD at serine 112. Phosphorylation of BAD at serine 112 specifically suppressed BAD-mediated apoptosis. Further in-

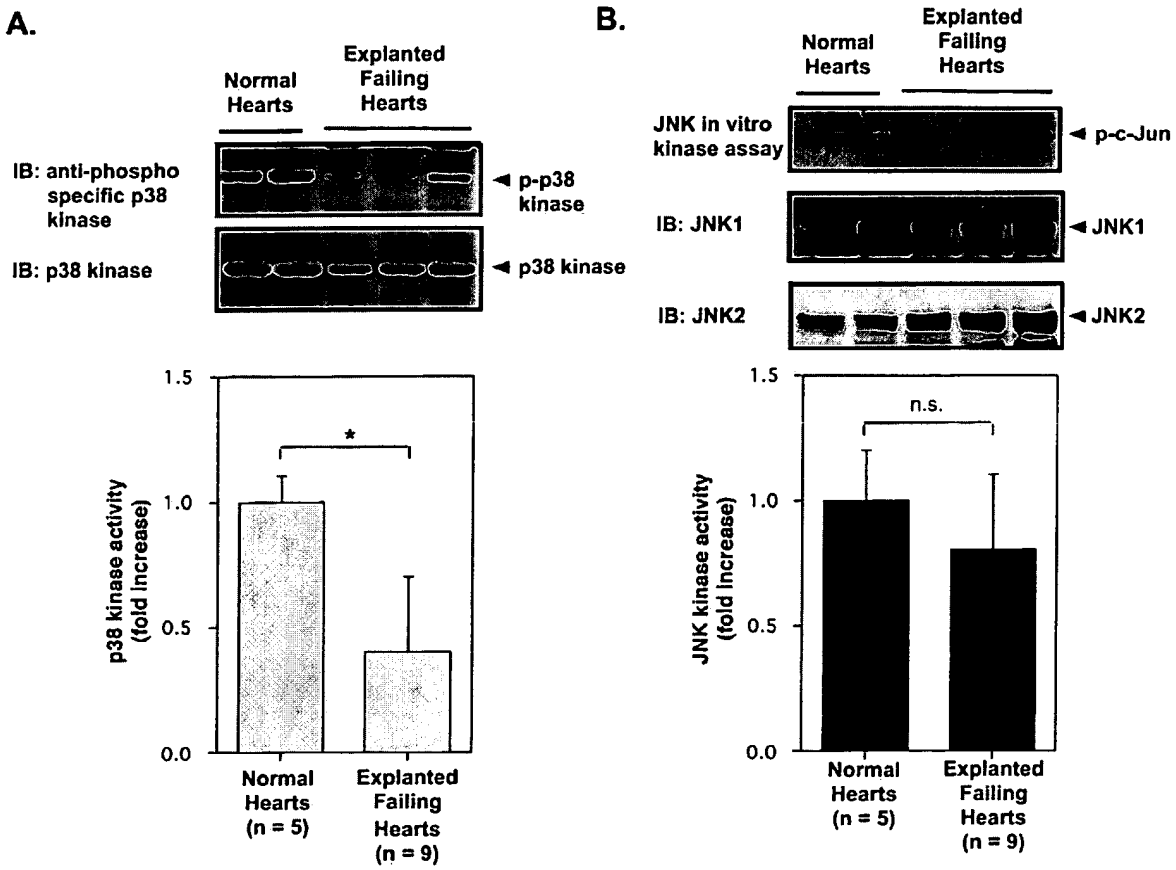

Fig. 2. p38 kinase and JNKs in failing and non-failing hearts. (A) p38 kinase activity in whole extracts was measured by Western blot analysis with a phospho-specific p38 antibody (upper). No difference in the amount of p38 kinase was observed in lysates from any of the heart samples by Western blot analysis with anti-p38 kinase antibody (lower). Densitometric analysis showed that p38 kinase activity was reduced in failing human hearts. Results were normalized for all experiments by arbitrarily setting the densitometry of control heart samples (non-failing hearts) to 1.0 (shown is mean±S.D.). (B) JNK activity was measured by in vitro kinase assay using c-Jun (1–89) fusion protein as a substrate. Western blots were performed with an anti phospho-specific c-Jun antibody for JNK activity assay (upper). No difference in the amount of JNK1/2 protein was observed in samples by Western blot analysis with anti-JNK (lower) and c-Jun substrate by Ponceau staining (data not shown).

vestigation is needed to define the precise role of ERK1/2 and p90RSK activation in failing human hearts.

Recently, Kato et al. [21] have reported that BMK1 activation is also protective against apoptotic cell death. BMK1 is highly expressed in cardiac myocytes and activated by reactive oxygen species in the adult guinea pig heart [8]. Recently, we have demonstrated that BMK1 is activated in hypertrophied myocardium induced by chronic pressure-overload [22]. MEK5-dependent BMK1 activation results in the phosphorylation of MEF2A and MEF2C, which are transcription factors belonging to the myocyte enhancer factor-2 (MEF2)-family [23]. Since BMK1 activation was significantly decreased in failing human hearts in the present study, it will be interesting to evaluate critically the role of this MAP kinase in diminished contractility of the failing heart.

In conclusion, multiple MAP kinases, p90RSK, and Src were differentially regulated in human failing myocardium of patients with idiopathic dilated cardiomyopathy and may be involved in the pathogenesis of this clinical syndrome.

Acknowledgements

The authors wish to thank Dr C. Yan for their invaluable assistance and critical reading of this manuscript. This study was supported by grants from National Institutes of Health (HL44721 and HL49192 to B.C. Berk, HL52318 to R.A. Walsh, and HL66919 to J. Abe), a grant-in-aid for Scientific Research (No. 12770337 to Y.T.) from the Ministry of Education, Science, Sports and Culture, Japan, and a grant from Kanae Foundation (to Y.T.).

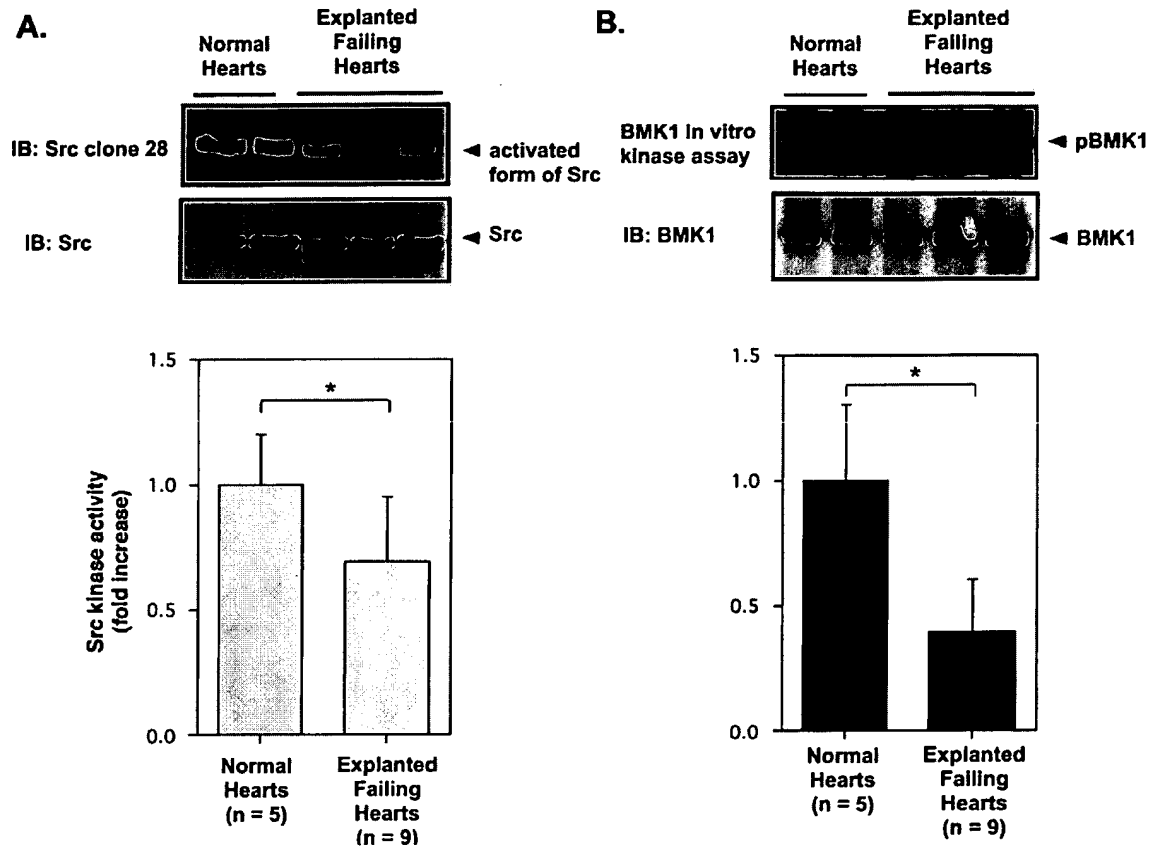

Fig. 3. Src and BMK1 in failing and non-failing hearts. (A) Src kinase activity in whole extracts was measured by Western blot analysis with a Src antibody clone 28 which recognizes the activated form of Src (upper). No difference in the amount of Src was observed in lysates from any of the heart samples by Western blot analysis with anti-Src antibody (lower). (B) BMK1 activity was analyzed by autophosphorylation in an immune complex kinase assay (upper). BMK1 protein level was assayed by Western blot analysis with anti-BMK1 antibody. No difference in the amount of BMK1 was observed in immunoprecipitates from any of the heart samples with anti-BMK1 antibody (lower). Densitometric analysis indicated that Src and BMK1 kinase activity was decreased in failing hearts compared with normal hearts (shown is mean±S.D.).

References

[1] Takeishi Y, Chu G, Kirkpatrick DM et al. In vivo phosphorylation of cardiac troponin I by protein kinase Cβ2 decreases cardiomyocyte calcium responsiveness and contractility in transgenic mouse hearts. J Clin Invest 1998;102:72–78.

[2] Takeishi Y, Bhagwat A, Ball NA et al. Effect of angiotensin-converting enzyme inhibition on protein kinase C and SR proteins in heart failure. Am J Physiol 1999;276:H53–62.

[3] Jalili T, Takeishi Y, Song G et al. PKC translocation without changes in Gαq and PLC-β protein abundance in cardiac hypertrophy and failure. Am J Physiol 1999;277:H2298–2304.

[4] Bowling N, Walsh RA, Song G et al. Increased protein kinase C activity and expression of Ca^{2+}-sensitive isoforms in the failing human heart. Circulation 1999;99:384–391.

[5] Sugden PH, Clerk A. 'Stress-responsive' mitogen-activated protein kinases (c-Jun N-terminal kinases and p38 mitogen-activated protein kinases) in the myocardium. Circ Res 1998;83:345–352.

[6] Lee JD, Ulevitch RJ, Han J. Primary structure of BMK1: a new mammalian map kinase. Biochem Biophys Res Commun 1995;213:715–746.

[7] Clerk A, Michael A, Sugden PH. Stimulation of multiple mitogen-activated protein kinase sub-families by oxidative stress and phosphorylation of the small heat shock protein, HSP25/27, in neonatal ventricular myocytes. Biochem J 1998;333:581–589.

[8] Clerk A, Fuller SJ, Michael A, Sugden PH. Stimulation of 'stress-regulated' mitogen-activated protein kinases (stress-activated protein kinases/c-Jun N-terminal kinases and p38-mitogen-activated protein kinases) in perfused rat hearts by oxidative and other stresses. J Biol Chem 1998;273:7228–7234.

[9] Takeishi Y, Abe J, Lee JD et al. Differential regulation of p90 ribosomal S6 kinase and big mitogen-activated protein kinase 1 by ischemia/reperfusion and oxidative stress in perfused guinea pig hearts. Circ Res 1999;85:1164–1172.

[10] Abe J, Berk BC. Reactive oxygen species as mediators of signal transduction in cardiovascular disease. Trends Cardiovasc Med 1998;8:59–64.

[11] Takahashi E, Abe J, Gallis B et al. p90RSK is a serum-stimulated NHE1 kinase: regulatory phosphorylation of serine 703 of Na^+/H^+ exchanger isoform-1. J Biol Chem 1999;274:20206–20214.

[12] Takeishi Y, Jalili T, Hoit BD et al. Alterations in Ca^{2+} cycling proteins and Gαq signaling after left ventricular assist device support in failing human hearts. Cardiovasc Res 2000;45:883–888.

[13] Abe J, Takahashi M, Ishida M, Lee JD, Berk BC. c-Src is required for oxidative stress-mediated activation of big mitogen-activated protein kinase 1 (BMK1). J Biol Chem 1997;272:20389–20394.

[14] Tseng H, Peterson TE, Berk BC. Fluid shear stress stimulates mitogen-activated protein kinase in endothelial cells. Circ Res 1995;77:869–878.

[15] Griffith CE, Zhang W, Wange RL. ZAP-70-dependent and -in-

dependent activation of Erk in Jurkat T cells. Differences in signaling induced by H_2O_2 and Cd3 cross-linking. J Biol Chem 1998;273:10771–10776.

[16] Cook SA, Sugden PH, Clerk A. Activation of c-Jun N-terminal kinases and p38-mitogen-activated protein kinases in human heart failure secondary to ischaemic heart disease. J Mol Cell Cardiol 1999;1:1429–1434.

[17] Takahashi E, Abe J, Berk BC. Angiotensin II stimulates $p90^{rsk}$ in vascular smooth muscle cells. A potential Na^+/H^+ exchanger kinase. Circ Res 1997;81:268–273.

[18] Abe J, Baines CP, Berk BC. Role of mitogen-activated protein kinases in ischemia and reperfusion injury: the good and the bad. Circ Res 2000;86:607–609.

[19] Bonni A, Brunet A, West AE et al. Cell survival promoted by the Ras-MAPK signaling pathway by transcription-dependent and -independent mechanisms. Science 1999;286:1358–1362.

[20] Tan Y, Ruan H, Demeter MR, Comb MJ. p90(RSK) blocks bad-mediated cell death via a protein kinase C-dependent pathway. J Biol Chem 1999;274:34859–34867.

[21] Kato Y, Tapping RI, Huang S et al. Bmk1/Erk5 is required for cell proliferation induced by epidermal growth factor. Nature 1998;395:713–716.

[22] Takeishi Y, Huang Q, Abe J, et al. Differential activation of mitogen-activated protein kinase family and p90 ribosomal S6 kinase in hypertrophied myocardium induced by pressure-overload. J Mol Cell Cardiol 2001 (in press)

[23] Kato Y, Kravchenko VV, Tapping RI et al. BMK1/ERK5 regulates serum-induced early gene expression through transcription factor MEF2C. EMBO J 1997;16:7054–7066.

Exhibit K

Oncogene (1999) 18, 813–822

http://www.stockton-press.co.uk/onc

Constitutive activation of the 41-/43-kDa mitogen-activated protein kinase signaling pathway in human tumors

Rika Hoshino[1], Yuji Chatani[2], Takao Yamori[3], Takashi Tsuruo[3,4], Hiroya Oka[5], Osamu Yoshida[5], Yutaka Shimada[6], Shigeki Ari-i[6], Hiromi Wada[7], Jiro Fujimoto[8] and Michiaki Kohno[1]

[1]Laboratory of Cell Regulation, School of Pharmaceutical Sciences, Nagasaki University, 1–14, Bunkyo-machi, Nagasaki 852–8131; [2]Gifu Pharmaceutical University, Gifu 502–8585; [3]Cancer Chemotherapy Center. Japanese Foundation for Cancer Research, Tokyo 170–8455; [4]Institute of Molecular and Cellular Biosciences, University of Tokyo, Tokyo 113–8657; [5]Department of Urology, and [6]Department of Surgery and Surgical Basic Science, Graduate School of Medicine, Kyoto University Faculty of Medicine, Kyoto 606-8507; [7]Department of Thoracic Surgery, Chest Disease Research Institute, Kyoto University, Kyoto 606-8507; [8]1st Department of Surgery, Hyogo College of Medicine, Hyogo 663-8501, Japan

The 41-kDa and 43-kDa mitogen-activated protein (MAP) kinases play a pivotal role in the mitogenic signal transduction pathway and are essential components of the MAP kinase cascade, which includes MAP kinase kinase (MEK) and Raf-1. As aberrant activation of signal transducing molecules such as Ras and Raf-1 has been linked with cancer, we examined whether constitutive activation of the 41-/43-kDa MAP kinases is associated with the neoplastic phenotype of 138 tumor cell lines and 102 primary tumors derived from various human organs. Constitutive activation of the MAP kinases was observed in 50 tumor cell lines (36.2%) in a rather tissue-specific manner: cell lines derived from pancreas, colon, lung, ovary and kidney showed especially high frequencies with a high degree of MAP kinase activation, while those derived from brain, esophagus, stomach, liver and of hematopoietic origin showed low frequencies with a limited degree of MAP kinase activation. We also detected constitutive activation of the 41-/43-kDa MAP kinases in a relatively large number of primary human tumors derived from kidney, colon and lung tissues but not from liver tissue. Many tumor cells, in which point mutations of *ras* genes were detected, showed constitutive activation of MAP kinases, however, there were also many exceptions to this observation. In contrast, the activation of the 41-/43-kDa MAP kinases was accompanied by the activation of Raf-1 in the majority of tumor cells and was completely associated with the activation of MEK and p90[rsk] in all the tumor cells examined. These results suggest that the constitutive activation of 41-/43-kDa MAP kinases in tumor cells is not due to the disorder of MAP kinases themselves, but is due to the disorder of Raf-1, Ras, or some other signaling molecules upstream of Ras.

Keywords: 41-/43-kDa MAP kinases (ERKs); MEK; aberrant activation; human tumor; carcinogenesis

Introduction

Posttranslational modification of proteins by phosphorylation plays a central role in the regulation of many cellular events which include cell proliferation and differentiation. This ubiquitous form of reversible covalent modification of proteins is mediated by protein kinases, which are key components in a network of integrated signaling pathways (Cohen, 1992; Hunter, 1995; Pawson, 1995).

The 41- and 43-kDa MAP kinases (ERK2 and ERK1, respectively) (Ray and Sturgill, 1987; Boulton *et al.*, 1991), which have originally been identified as molecules whose tyrosine phosphorylation is commonly induced in cells treated with a variety of mitogenic agents (Cooper *et al.*, 1984; Kohno, 1985), are ubiquitous components of signal transduction pathways (Nishida and Gotoh, 1993; Cobb and Goldsmith, 1995; Seger and Krebs, 1995). They are activated by phosphorylation on both threonine and tyrosine residues by dual specificity kinases, MAP kinase/ERK kinase (MEK) 1 and 2. MEK activity is in turn regulated by serine phosphorylation catalyzed by MEK activators. The major MEK activator is a serine/threonine kinase, Raf-1. It has also been reported that the activated Ras-mediated translocation of Raf-1 to the plasma membrane is one of the necessary events for Raf-1 to be activated following phosphorylation (Avruch *et al.*, 1994). The identity of the kinase(s) that phosphorylate Raf-1, however, is poorly understood at present.

The protein kinase cascade described above (the MAP kinase cascade) is activated in many cell types by diverse extracellular stimuli which elicit a wide array of physiological responses such as cell division, differentiation, and secretion (Nishida and Gotoh, 1993; Cobb and Goldsmith, 1995; Seger and Krebs, 1995). The 41- and 43-kDa MAP kinases are serine/threonine kinases that phosphorylate and modulate the function of many proteins with substantial regulatory functions. These include other protein kinases (such as p90[rsk]), cytoskeletal proteins (such as microtuble-associated proteins), other enzymes (such as cytoplasmic phospholipase A_2), and transcription factors (such as Elk-1) (Davis, 1993). Thus, the MAP kinases are thought to function as key intermediaries in intracellular signal transduction networks.

Aberrant expression and/or activation of signal transducing proteins have been linked with cancer. For example, overexpression of the epidermal growth factor receptor tyrosine kinase (c-*erb* B-1) gene (Yao *et al.*, 1988), loss of the amino-terminal regulatory domain to produce active c-Raf-1 kinase (Nakatsu *et al.*, 1985), and point mutations of the *ras* oncogenes to produce constitutively active Ras proteins (Shimizu *et al.*, 1983;

Correspondence: M Kohno
Received 29 May 1998; revised 17 August 1998; accepted 17 August 1998

Barbacid, 1987; Bos, 1988) have been observed in several human cancers. In this respect, active mutants of MEK-1, made constitutive by deleting N-terminal amino acids 32–52, as well as by changing regulatory phosphorylated serines (residues 218 and 222) to glutamic acid, have recently been shown to transform mammalian cells (Mansour *et al.*, 1994; Cowley *et al.*, 1994; Brunet *et al.*, 1994). However, few studies have examined disorders of the MAP kinase cascade in naturally occurring human tumors.

In this study, we have examined whether constitutive activation of the MAP kinase cascade is associated with the neoplastic phenotype of 138 cell lines derived from various human tumors. Constitutive activation of the 41-/43-kDa MAP kinases was observed in 50 tumor cell lines: cell lines derived from pancreas, colon, lung, ovary and kidney showed especially high frequencies of constitutive MAP kinase activation. We also detected constitutive activation of the MAP kinases in a large number of primary human tumors derived from colon, lung and kidney tissues but not from liver tissue.

Results

Constitutive activation of the 41-/43-kDa MAP kinases in human tumor cell lines

Activation of the 41-/43-kDa MAP kinases in tumor cells was examined by three different assay procedures: by measuring the appearance of their active forms which show reduced mobility in SDS–PAGE due to phosphorylation of specific tyrosine and threonine residues (Chatani *et al.*, 1992), by measuring their tyrosine phosphorylation, and by performing a direct *in vitro* kinase assay of the immunoprecipitates using myelin basic protein (MBP) as the substrate. These analyses consistently gave essentially identical results (Figure 1). As the basal level of MAP kinase activity varied significantly from cell line to cell line, we determined the kinase activity in each cell line under conditions of cell proliferation (exponentially growing phase), serum-starvation, and growth-stimulation (by the addition of 10% fetal bovine serum [FBS] to serum-starved cells for 10 min). In non-tumorous cells, significant activation of the MAP kinases was observed only under serum-stimulated conditions: the MAP kinase activities of five lines of human diploid fibroblasts (SF-TY, WI38, TIG-3. TIG-7 and skin fibroblasts) under proliferating conditions were between 8.8 ~ 19.1% (average = 13.5 ± 4.1%) of the levels observed under growth-stimulation conditions. Thus, tumor cells were considered to be positive (constitutive activation of the MAP kinases occurs) if, under proliferating conditions, their MAP kinase activity exceeded 20% of the level observed under growth-stimulation conditions.

We did not detect significant activation of the 41-/43-kDa MAP kinases in 26 out of the 138 cell lines analysed (18.8%), even when the cells were serum-starved for 48 h and then growth-stimulated for 10 min with 10% FBS or with a mixture of 20 ng/ml each of

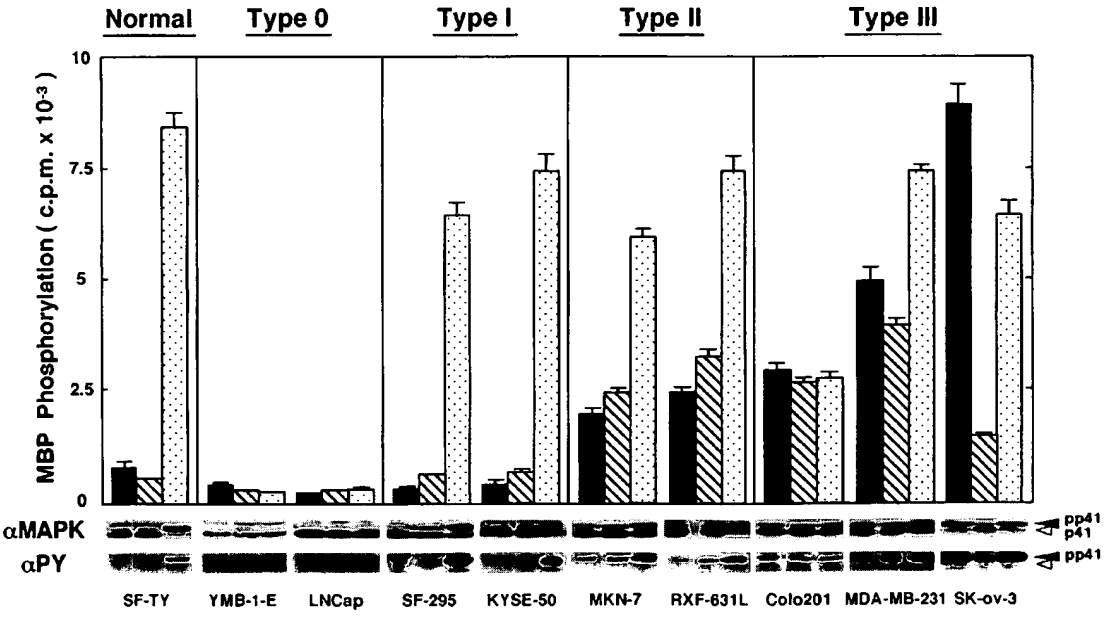

Figure 1 Activation of the 41-/43-kDa MAP kinases in human tumor cell lines derived from various organs. The 41-/43-kDa MAP kinase activity in each cell line was determined under conditions of cell proliferation (CP; ■), serum-starvation (SS; ▨), and growth-stimulation (GS; ■). The MAP kinase assay was performed by incubating cell lysates (10 μg of protein) with anti-MAP kinase antibody followed by the kinase reaction as described under Materials and methods; radioactivity incorporated into MBP was determined. Each value represents the mean ± S.D. of duplicate determinations of a representative experiment. Cell lysates (15 μg of protein) were resolved by SDS–PAGE, blotted, probed by anti-MAP kinase antibody (αMAPK) or anti-phosphotyrosine antibody (αPY), followed by ECL detection. Closed arrowheads indicate positions of the phosphorylated (activated) forms of 41-kDa MAP kinase (pp41), while open arrowheads indicate positions of its unphosphorylated forms (p41). Data shown are representative of two to three separate experiments that gave essentially the same results. Tumor cells were classified into four groups by comparing the level of MAP kinase activity under proliferating conditions with that under growth-stimulation conditions

PDGF and EGF (data not shown): all these tumor cells apparently required FBS or PDGF/EGF for their growth. The proliferation of these cells appears to depend on a signaling pathway(s) which does not involve these MAP kinases; these tumor cells were classified as 'type 0'. In 62 tumor cell lines (44.9%), activation of the MAP kinases was observed under growth-stimulation conditions but not significantly under proliferating conditions as in normal diploid fibroblasts; these tumor cells were classified as 'type I'. These two types of tumor cells (type 0 and type I) are those in which constitutive activation of the 41-/43-kDa MAP kinases was not detected. In contrast, constitutive activation of the MAP kinases was detected in 50 cell lines (36.2%). The degree of activation varied significantly among the different cell lines: tumor cells whose MAP kinase activity under proliferating conditions exceeded 50% of the level of that under growth-stimulation conditions were classified as 'type III' (strong positive), and the rest as 'type II'.

Representative results of such analyses on several tumor cell lines are shown in Figure 1, and data on the 138 cell lines are summarized in Table 1. Tumor cell lines derived from pancreas, colon, lung, ovary and kidney showed especially high frequencies of constitutive MAP kinase activation with a high degree of MAP kinase activation, while those derived from brain, esophagus, stomach, liver and of hematopoietic origin showed low frequencies of constitutive MAP kinase activation with only a limited degree of MAP kinase activation.

Constitutive activation of the 41-/43-kDa MAP kinases in human primary tumor tissues

We determined the activity of 41-/43-kDa MAP kinases in primary tumors of colon, lung, kidney and liver (adenocarcinomas of colon and lung, renal cell carcinomas, and hepatocellular carcinomas, respectively), which was compared with the activity in corresponding non-tumorous tissues derived from the same individual. It was rather difficult to categorize the constitutive activation of MAP kinases in some cases, because the activity appeared to be elevated not only in the tumor tissues but also in the non-tumorous tissues. This was particularly the case for tumors of the colon and lung (Figure 2). Many tumor cells have been reported to produce growth factors such as TGF-α and PDGF, which then stimulate the proliferation of tumor cells themselves (in an autocrine fashion) and also of the surrounding normal cells (in a paracrine fashion) (Sporn and Todaro, 1980). Thus, the elevated MAP kinase activity observed in some non-tumorous tissues could be the result of such a paracrine stimulation of normal cells by growth factors produced by tumor cells. Alternatively, reactive changes such as inflammation and the immunoresponse may be at the basis of the increased MAP kinase activity of the non-tumorous tissues that surround tumors. In this study, MAP kinase was tentatively considered to be constitutively active when the activity in the tumor tissue samples was greater than (i) the average of that of the 102 non-tumorous tissue samples (^{32}P-radioactivity incorporated into MBP was 4580 ± 1240 c.p.m. in the standard assay condition employed; that of tumor tissue samples was 8750 ± 2480 c.p.m.) and (ii) 1.5-fold of that in the matched non-tumorous tissue samples. Tumors in which MAP kinase activity exceeded the average of that of the non-tumorous tissue samples but was less than 1.5-fold of that in the matched non-tumorous tissue were considered to be false-positives of constitutive MAP kinase activation, and the others were classified as negative.

Representative results of such analyses in several cases of lung and liver tissues are shown in Figure 2, and data on 34 cases of colon tissues, 34 cases of lung tissues, 11 cases of kidney tissues, and 23 cases of liver tissues are summarized in Table 2. In this context, we have previously shown that constitutive activation of the MAP kinases occurs in 12 out of 25 cases of human renal cell carcinoma (Oka *et al.*, 1995). Thus, in support of the results in established tumor cell lines, primary tumors derived from colon, lung and kidney showed high frequencies of constitutive MAP kinase activation, while liver tumors did not show significant activation of the 41-/43-kDa MAP kinases.

Constitutive activation of the 41-/43-kDa MAP kinases is always associated with the constitutive activation of MEK

Constitutive activation of the 41-/43-kDa MAP kinases in tumor cells can be induced through several mechanisms, which include the activation of 41-/43-kDa MAP kinases themselves, the activation of upstream signaling molecules such as MEK, Raf-1 and Ras (Nishida and Gotoh, 1993; Cobb and Goldsmith, 1995; Seger and Krebs, 1995), and the inactivation of MAP kinase phosphatase (Sun *et al.*, 1993; Ward *et al.*, 1994). In order to gain insight into the molecular mechanisms of constitutive activation of 41-/43-kDa MAP kinases, we first examined the possible participation of a *ras* gene mutation. Many tumor cells, in which point mutations of *ras* genes were detected (Bos, 1988; Kawaguchi *et al.*, 1997), showed constitutive activation of MAP kinases. However, there were also many exceptions to this observation (Table 3). We then examined the possible association of the activation of Raf-1 kinase (an activator of MEK), MEK (the activator of MAP kinases) and p90^{rsk} (a substrate of MAP kinases) with the constitutive activation of 41-/43-kDa MAP kinases in tumor cells, by determining the activities of these kinases under conditions of cell proliferation, serum-starvation and growth-stimulation. To detect the activation of Raf-1 and p90^{rsk}, we examined their phosphorylation by monitoring the mobility sifts in SDS–PAGE (activation of these kinases is reportedly accompanied by increased serine/threonine phosphorylation, which results in the decrease in their mobilities in SDS–PAGE) (Daum *et al.*, 1994; Sturgill *et al.*, 1988); to detect the activation of MEK, we determined the GST-ERK2^{K52R} phosphorylation activity of anti-MEK1 antibody-immunoprecipitates in an *in vitro* kinase assay. The representative results of analyses of several tumor cells are shown in Figure 3, and the data on 38 tumor cell lines are summarized in Table 4 (21 cell lines were positive for the constitutive activation of MAP kinases and 17 cell lines were negative). The activation of 41-/43-kDa MAP kinases was accompanied by the activation of Raf-1 in the majority of

tumor cells and was completely associated with the activation of MEK and of $p90^{rsk}$ in all the tumor cell lines examined. We also determined the activities of Raf-1 and $p90^{rsk}$ by an *in vitro* kinase assay of the

Table 1 Activation of the 41-/43-kDa MAP kinases in 138 human tumor cell lines derived from various organs

	MAP kinase activation				
	Negative		*Positive*		
Derived organ	*Type O*	*Type I*	*Type II*	*Type III*	*Total*
Brain	0	6 KG-1-C SF-295* SNB-75* SNB-78* T98G U251*	3 A-172 SF-268* SF-539*	0	9
Esophagus	0	9 KYSE-30 KYSE-50 KYSE-70 KYSE-220 KYSE-270 KYSE-350 KYSE-450 KYSE-510 KYSE-520	2 KYSE-150 KYSE-410	0	11
Stomach	2 AZ-521 SCH	5 MKN1* MKN28* MKN74* St-4* TMK1	4 KATO III MKN7* MKN45* NUGC-3	0	11
Liver	0	6 Hep3B HepG2 HLF Huh-6 Huh-7 PLC	1 HLE	0	7
Pancreas	1 KMP-2	4 KMP-1 KMP-4 KP-1 NL KP-2	2 BxPC-3 SUIT-2	3 KMP-3 KMP-5 KP-3	10
Colon	3 Colo320 HCT-15* KM-12*	7 CoCM-1 CCK81 DLD-1 HCC-2998* Lovo RCM-1 SW837	2 BM314 HCT-116*	5 CaR-1 Colo201 HT-29* TCO WiDr*	17
Lung	5 DMS273* LK-2 SBC-1 SBC-2 VMRC-LCD	8 ABC-1 EBC-1 HCCY1 LU65A RERF-LC-MA RERF-LC-MS RERF-LC-OK SBC-5	4 A549* NCI-H226* NCI-H522* SBC-3	4 DMS114* LU99B NCI-H23* NCI-H460*	21
Kidney	1 VMRC-RCW	4 ACHN* CCF-RC2 NC65 VMRC-RCZ	2 CAKI-1 RXF-631L*	2 CAKI-2 RPMI-SE	9
Bladder	0	4 EJ-1 HBT5637 J82 KK47	1 HT1197	1 T24	6

continued

Table 1 *continued*

	MAP kinase activation				
	Negative		*Positive*		
Derived organ	*Type O*	*Type I*	*Type II*	*Type III*	*Total*
Breast	4 MCF-7* MRK-nu-1 YMB-1 YMB-1-E	2 BSY-1* HBC-5*	0	2 HBC-4* MDA-MB-231*	8
Ovary	1 OVCAR-5*	1 OVCAR-8*	1 OVCAR-4*	3 OVCAR-3* SK-OV-3* TYK-nu	6
Prostate	2 LNCaP PC3	1 PC93	2 DU145 TSU-PRL	0	5
Skin	0	1 B16	1 Mewo	1 LOX-IMVI*	3
Miscellaneous					
Hematopoietic cells	6 Jurkat K562 Molt-3 RAJI RPMI 1788 TALL-1	2 HL60 RPMI 8866	0	0	8
Neuroblastoma	1 GOTO	2 SKNMC TGW	0	1 NB-1	4
Sarcoma	0	0	1 KT006	2 HT1080 RD	3
Total	26	62	26	24	138

The 41-/43-kDa MAP kinase activity in each of 138 human tumor cell lines was determined under conditions of cell proliferation, serum-starvation, or growth-stimulation: representative results of such analyses on several cell lines are shown in Figure 1. Tumor cells were classified into four groups by comparing the level of MAP kinase activity under proliferating conditions with that under growth-stimulation conditions, as described in the text. Tumor cell lines with an asterisk are those in which the activation of Raf-1, MEK and $p90^{rsk}$ was also examined (see Figure 3 and Table 4)

respective immunoprecipitates using GST-$MEK1^{K97A}$ or S6 peptide as a substrate (Tanimura *et al.*, 1998), and obtained essentially the same results as those shown in Figure 3 (data not shown). Furthermore, the constitutive activation of MAP kinases was always associated with the constitutive activation of MEK in all the primary tumor samples analysed (Figure 2).

Discussion

In this study, we demonstrated that the constitutive activation of the 41-/43-kDa MAP kinases was observed in a relatively large number of human tumors. Analyses of established cell lines suggested that the constitutive activation of MAP kinases was induced in tumors in a rather tissue-specific manner; tumor cells derived from pancreas, colon, lung, ovary and kidney tissues showed especially high frequencies of MAP kinase activation, while those derived from brain, esophagus, stomach, liver tissues and hematopoietic cells showed low frequencies with only a limited degree of MAP kinase activation (Table 1). Analyses of primary tumors obtained from patients with respective tumors at the time of surgical resection also gave similar results; tumors derived from colon, lung and kidney tissues showed high frequencies of MAP kinase activation, while tumors derived from liver tissue did not show any significant activation of the 41-/43-kDa MAP kinases (Table 2). Thus, although the MAP kinase cascade is an essential mitogenic signaling pathway in many types of cells (Nishida and Gotoh, 1993; Seger and Krebs, 1995), inappropriate activation of the cascade may not be important for the carcinogenesis of several tissues such as liver, stomach and esophagus. Deregulation of other cytoplasmic signaling pathways (such as JAK/Stat pathway) and/or inactivation of tumor suppressor proteins (such as Rb, p53, APC and $p16^{INK4a}$) has also been linked with cancer. These abnormalities may contribute more to the carcinogenesis of tissues whose derived tumor cells show only a low incidence of MAP kinase activation. In accordance with this possibility, inactivation of $p16^{INK4a}$, for example, has been reported to occur with high frequency in various cancers including those of the esophagus and liver (Chaubert *et al.*, 1997; Serrano, 1997).

We have recently reported that constitutive activation of the 41-/43-kDa MAP kinases occurs in 12 out of 25 cases of human renal cell carcinomas, in which MAP kinase activation shows a significant correlation with their histological grade (Oka *et al.*, 1995). This was also the case for the 11 cases of renal cell carcinomas analysed in this study (data not shown).

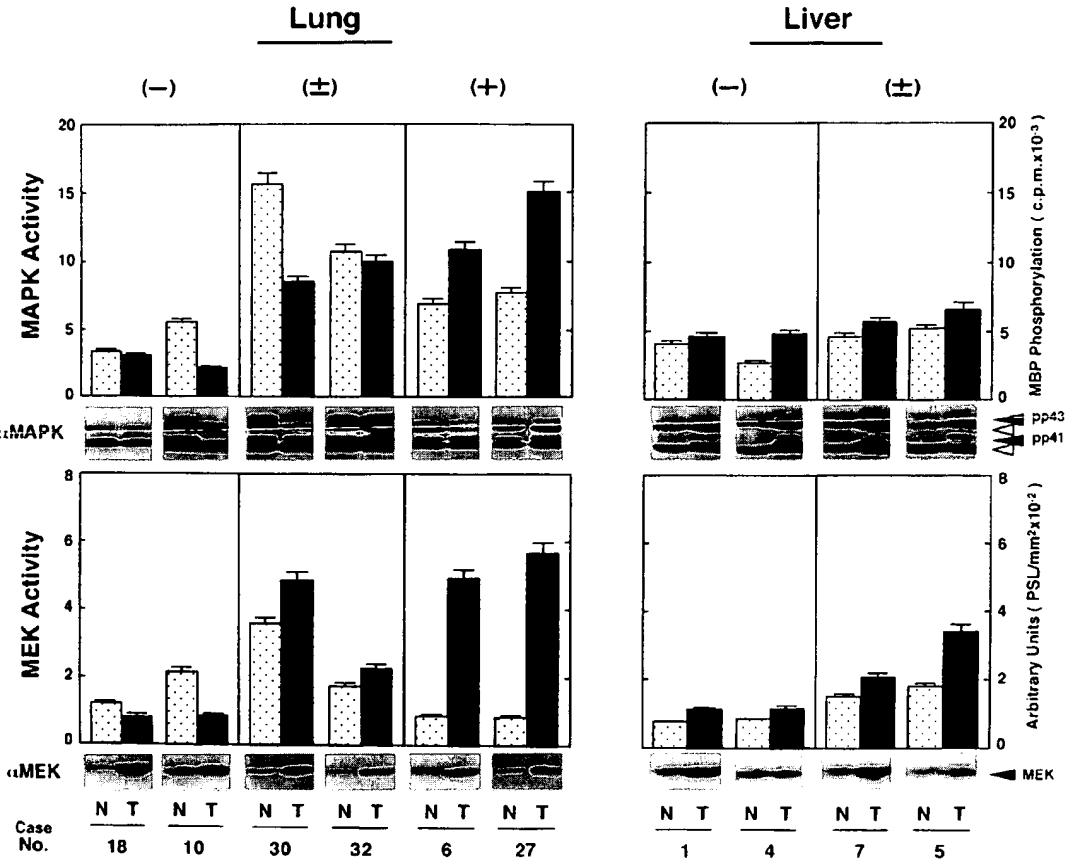

Figure 2 Activation of the 41-/43-kDa MAP kinases and MEK in human primary tumors derived from lung and liver tissues. Activities of the 41-/43-kDa MAP kinases and MEK in primary tumors of lung and liver (adenocarcinomas of the lung and hepatocellular carcinomas, respectively) (T) and in matched non-tumorous tissues (N) were determined. The MAP kinase assay (upper) and MEK assay (lower) was performed by incubating cell lysates (30 μg of protein for MAP kinase assay and 50 μg of protein for MEK assay) with respective antibodies followed by the kinase reaction. Radioactivity incorporated into MBP was determined by liquid scintillation spectrometer, and radioactivity incorporated into GST-ERK2^{K52R} was quantified with a Fujix Bioimaging analyzer BAS 1500. Each value represents the mean ± S.D. of duplicate determinations of a representative experiment. Cell lysates (30 μg of protein) were resolved by SDS–PAGE, blotted, and probed with anti-MAP kinase antibody or anti-MEK1 antibody, followed by ECL detection. Closed arrowheads indicate positions of the phosphorylated (activated) forms of 41- and 43-kDa MAP kinases (pp41, pp43) and of the MEK (MEK), while open arrowheads indicate positions of the unphosphorylated forms of the MAP kinases. Data shown are representative of two to three separate experiments that gave essentially the same results

In primary tumors derived from colon and lung tissues, such a positive correlation between MAP kinase activation and histological grade was not clearly observed. However, MAP kinase activation showed significant correlation with the differentiation grade of each of the tumor tissues from which the respective cell line was derived; five of 21 cell lines derived from well-differentiated tumor tissues (seven, esophagus; three, stomach; ten, colon; one, ovary) showed constitutive activation of the MAP kinases, while 14 of 20 cell lines derived from poorly-differentiated tumor tissues (four, esophagus; three, stomach; four, colon; five, lung; four, ovary) showed constitutive MAP kinase activation. Taken together, these results suggest that constitutive activation of the MAP kinase signaling pathway may play a role in the carcinogenesis of human tumors.

Activation of the 41-/43-kDa MAP kinases in tumor cells (established cell lines and primary tissues) was always associated with the activation of MEK, the activator of MAP kinases. Although constitutive activation of the MAP kinases can be induced through several mechanisms (Nishida and Gotoh, 1993; Cobb and Goldsmith, 1995; Seger and Krebs, 1995), our results showing the co-activation of MEK and MAP kinases is all the tumor cells analysed suggest that the constitutive activation of 41-/43-kDa MAP kinases in these tumor cells is not due to the disorder of MAP kinases themselves. These results also suggest that inactivation of the MAP kinase phosphatases, which lie downstream of the MAP kinases and inactivate them Sun *et al.*, 1993; Ward *et al.*, 1994), is not a cause of constitutive activation of 41-/43-kDa MAP kinases in tumor cells. These conclusions can be drawn from the fact that disorder of MAP kinases themselves or MAP kinase phosphatase induces the activation of 41-/43-kDa MAP kinases in the absence of the constitutive activation of MEK.

Rather, our results suggest that unregulated activation of some of the upstream signaling molecules such as MEK, Raf-1 or Ras play a causal role in the constitutive activation of 41-/43-kDa MAP kinases in tumor cells. With regard to this idea, it has recently

been reported that mutations in the MEK genes are very rare in human lung cancer (Bansal *et al.*, 1997). Our results, showing the co-activation of MEK and Raf-1 (an activator of MEK) in almost all the tumor cells analysed (Table 3), suggest that mutational activation of MEK as the primary cause of constitutive activation of MAP kinases in tumor cells is possible but unlikely; which is consistent with the previous observation described above (Bansal *et al.*, 1997). The SF-539 glioblastoma cell line, which displays constitutive activation of MEK and MAP kinases without Raf-1 activation, is the only exception in our analysis. In this case, MEK might be activated through a Raf-1-independent pathway. Alternatively, a mutational alteration which induces the activation of MEK itself might have occurred; this possibility remains to be examined in future study. Our results also indicate that, when compared with that in matched normal tissues, the expression level of MEK protein in tumor tissues has a tendency to be increased regardless of whether or not MEK/MAP kinase activation is induced. This is in strong contrast to the fact that the amount of 41-/43-kDa MAP kinases is not significantly different between tumor and normal tissues (Figure 2). Although overexpression of MEK itself has been reported not to induce the activation of MAP kinases and cell transformation (Mansour *et al.*, 1994; Cowley *et al.*, 1994; Brunet *et al.*, 1994), the significance and mechanistic basis of its overexpression require additional investigation.

Constitutive activation of the 41-/43-kDa MAP kinases in many tumor cells seems to be a consequence of the activation of Ras, because point mutations of *ras* genes have been observed in these cells. However, there are also many tumor cells which do not show abnormal activation of the MAP kinases, although point mutations of *ras* genes were detected (Table 2). Alternatively, activation of the MAP kinases can be induced through Ras-independent

Table 2 Activation of the 41-/43-kDa MAP kinases in human primary tumors

Derived organ	*MAP kinase activation* −	±	+	*Total*
Colon	17	10	7	34
Lung	10	13	11	34
Kidney	4	2	5	11
Liver	16	7	0	23

The 41-/43-kDa MAP kinase activity in primary tumors of colon, lung, kidney and liver (adenocarcinomas of colon and lung, renal cell carcinomas, and hepatocellular carcinomas, respectively) was determined, which was compared with the activity in corresponding non-tumorous tissues derived from the same individual: representative results of such analyses on several cases are shown in Figure 2. MAP kinase was considered to be constitutively active (+) when the activity in the tumor tissue was greater than the average of that of the 102 non-tumorous tissues and also greater than 1.5-fold of that in the matched non-tumorous tissue. Tumors, the MAP kinase activity of which exceeded the average of the non-tumorous tissue samples but was less than 1.5-fold of that in matched non-tumorous tissue samples, were classified as false-positives of constitutive MAP kinase activation (±), and the others were classified as negative (−)

Table 3 Correlation between the 41-/43-kDa MAP kinase activation and *ras* gene mutation

Cell line	*Derived organ*	ras *gene mutation*	*MAP kinase activation*
T24	Bladder	H-*ras* (12*)	+ (Type III)
HT1080	Connective tissue	N-*ras* (61*)	+ (Type III)
HT1197	Bladder	N-*ras* (61*)	+ (Type II)
A549	Lung	K-*ras* (12*)	+ (Type II)
LU65A	Lung	K-*ras* (12*)	− (Type I)
KMP1	Pancreas	K-*ras* (12*)	− (Type I)
KMP2	Pancreas	K-*ras* (12*)	− (Type 0)
KMP3	Pancreas	K-*ras* (12*)	+ (Type III)
KMP4	Pancreas	K-*ras* (12*)	− (Type I)
KMP5	Pancreas	K-*ras* (12*)	+ (Type III)

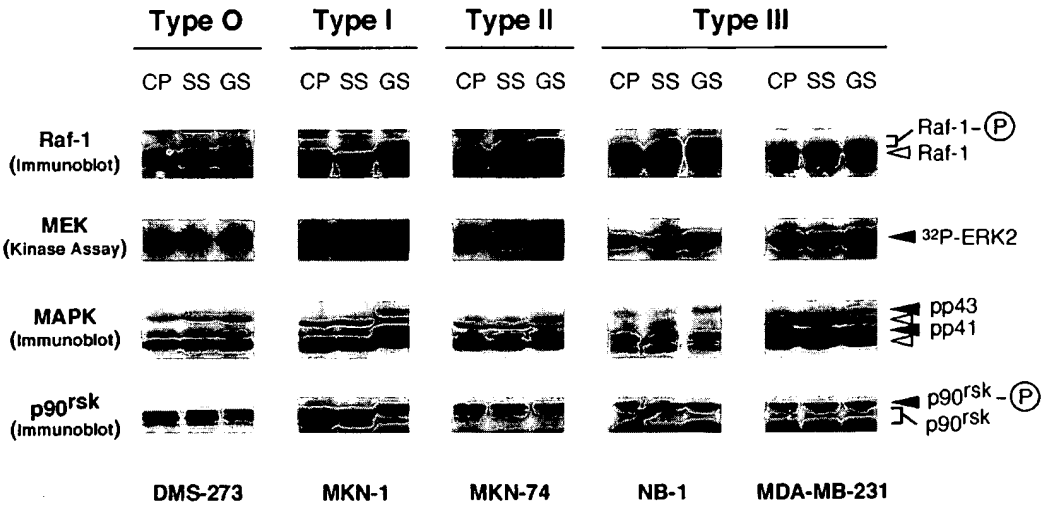

Figure 3 Activation of Raf-1, MEK, 41-/43-kDa MAP kinases and $p90^{rsk}$ in several human tumor cell lines. Activation of Raf-1, 41-/43-kDa MAP kinases and $p90^{rsk}$ was examined in each cell line under conditions of cell proliferation (CP), serum-starvation (SS) and growth-stimulation (GS) by monitoring the appearance of their more slowly migrating forms (phosphorylated forms; Raf-1-P, pp43/pp41 and $p90^{rsk}$-P). For the analyses, cell lysates (20 μg of protein) were resolved by SDS–PAGE, blotted and probed with anti-Raf-1 antibody, anti-MAP kinase antibody or anti-$p90^{rsk}$ antibody, followed by ECL detection. Activation of MEK was determined by incubating cell lysates (30 μg of protein) with anti-MEK1 antibody followed by the kinase reaction: ^{32}P incorporation into GST-$ERK2^{K52R}$ is shown by autoradiography (^{32}P-ERK2). Data shown are representative of two to four separate experiments that gave essentially the same results

Table 4 Correlation between activation of the 41-/43-kDa MAP kinases and those of $p90^{rsk}$, MEK and Raf-1 in several human tumor cell lines

	$p90^{rsk}$		MEK		Raf-1	
MAP kinase activation	n	*Activation* (%)	n	*Activation* (%)	n	*Activation* (%)
Positive	21	21 (100)	21	21 (100)	21	20[a] (95.2)
Negative	17	0 (0)	17	2[b] (11.8)	17	1[c] (5.9)
Total	38	21 (55.3)	38	23 (60.5)	38	21 (55.3)

Activation of 41-/43-kDa MAP kinases, $p90^{rsk}$, MEK and Raf-1 was determined in 38 tumor cell lines; these are those in Table 1 with asterisk. Representative results of such analyses on several tumor cells are shown in Figure 3. [a]Cell line which does not show the activation of Raf-1 is SF-539; [b]Cell lines which show the activation of MEK are HCC-2998 and KM-12; [c]Cell line which shows the activation of Raf-1 is KM-12

pathways: no mutations have been detected in H-, K-, or N-*ras* genes in 12 cases of renal cell carcinomas, although constitutive activation of the MAP kinases has been clearly observed in these tumor cells (Oka *et al.*, 1995). Thus, although the precise cause of the constitutive activation of the MAP kinase signaling pathway is unclear in many tumor cells, it may be the result of a disorder of Raf-1 or some other signaling molecule upstream of Ras (such as receptor tyrosine kinases, GRB2, SOS, Shc, etc.) (Hunter, 1997), which remains to be elucidated. In support of this idea, constitutive activation of the 41-/43-kDa MAP kinases is observed in A431 human vulval carcinoma cells which express a high level of EGF receptors; A431 cells are classified as type II tumor cells with regard to the activation of the MAP kinases (data not shown).

Many tumor cell lines (26 out of the 138 cell lines analysed in this study) were found to possess novel characteristics with regard to the activation of their 41-/43-kDa MAP kinase signaling pathway; these 'type 0' tumor cells did not show any significant activation of Raf-1, MEK and 41-/43-kDa MAP kinases, even when they were serum-starved for 48 h and then growth-stimulated for 10 min with 10% FBS or with a mixture of 20 ng/ml each of PDGF and EGF. Although all these tumor cells expressed Raf-1, MEK and 41-/43-kDa MAP kinases to similar degrees as those observed in other types of tumor cells (Figure 3), their proliferation appeared not to depend on the activation of the MAP kinase pathway. We did not observe a significant difference between several growth characteristics (growth rate in monolayer culture, growth efficiency in soft agar, etc.) of type 0, type I, type II or type III tumor cells (data not shown). The MAP kinase cascade is the major cytoplasmic kinase pathway activated by numerous mitogenic stimuli which interact with a diversity of structurally distinct receptors (Nishida and Gotoh, 1993; Cobb and Goldsmith, 1995; Seger and Krebs, 1995), and it has also been shown that the activation of the pathway is necessary for the proliferation of fibroblasts (Mansour *et al.*, 1994; Cowley *et al.*, 1994; Brunet *et al.*, 1994). However, our present findings suggest the existence of a novel mitogenic signaling pathway(s) which does not involve these well-characterized signaling molecules. The precise mechanism by which proliferation of the type 0 tumor cells is regulated remains to be determined.

In summary, we have demonstrated that constitutive activation of the MAP kinase signaling pathway is observed in a relatively large number of human tumors; tumor cells derived from pancreas, colon, lung, ovary and kidney tissues show especially high frequencies of MAP kinase activation. Our results also point to the possibility that specific inhibitors may be developed against signaling molecules such as MAP kinases and MEK for cancer therapy, and especially for the treatment of tumors in which constitutive activation of the 41-/43-kDa MAP kinases occurs.

Materials and methods

Materials

A polyclonal anti-MAP kinase antibody was raised against residues 299–321 (RIEVEQALAHPYLEQYYDPSDEP) of 41-kDa MAP kinase (ERK2) and was shown to recognize both the 41- and 43-kDa MAP kinases (Chatani *et al.*, 1992; Chatani *et al.*, 1995). The polyclonal anti-Raf-1 antibody (C-12) and polyclonal anti-$p90^{rsk}$ antibody (C-21) were obtained from Santa Cruz Biotechnology, Inc. The monoclonal anti-MEK1 antibody was from Transduction Laboratories, and the monoclonal anti-phosphotyrosine antibody (4G10) were from Upstate Biotechnology, Inc. The cDNA for $ERK2^{K52R}$(Rossomando *et al.*, 1992) was expressed in *Escherichia coli* as a GST-fusion protein, which was purified by affinity chromatography using GSH-Sepharose (Pharmacia Biotech Inc.) (Smith and Corcoran, 1990). Other chemicals and reagents were of the purest grade available.

Cell lines and tissues

The human tumor cell lines examined in this study were purchased from the American Type Tissue Culture Collection, obtained through the Japanese Cancer Research Resources Bank, or described elsewhere (Shimada *et al.*, 1992; Iwasaki *et al.*, 1995; Kawaguchi *et al.*, 1997; Kawada *et al.*, 1998). Each cell line was maintained under recommended and standard conditions; the majority of non-hematopoietic cells were cultured in Dulbecco's modified Eagle's medium supplemented with 10% FBS, while the cells of hematopoietic origin were grown in RPMI 1640 medium supplemented with 10% FBS. For experimental use, subconfluent cell cultures in the respective growing medium were rendered quiescent by incubation for 48 h in serum-free medium (Dulbecco's modified Eagle's medium or RPMI 1640 medium containing 2 mg/ml of bovine serum albumin [Boehringer Mannheim], 1 μg/ml of insulin [Sigma], 2 μg/ml of transferrin [Sigma], 30 Na_2SeO_3, and 10 mM HEPES, pH 7.4), and were then growth-stimulated with 10% FBS for 10 min. Samples of human primary tumors and normal tissues were obtained at the time of surgical resection under the permission of patients' Informed Consent; these samples were snap frozen in liquid nitrogen and stored at −80°C.

Cell lysis and immunoprecipitation

Cells were washed twice with ice-cold phosphate-buffered saline, scraped from plates into a hypotonic cell lysis buffer (25 mM Tris-HCl, pH 7.4, 25 mM NaCl, 1 mM sodium orthovanadate, 10 mM NaF, 10 mM sodium pyrophosphate, 25 mM β-glycerophosphate, 25 mM p-nitrophenylphosphate, 20 nM okadaic acid, 0.2 mM sodium molybdate, 0.5 mM EGTA, 1 mM phenylmethylsulfonyl fluoride, 10 μg/ml leupeptin, and 1% aprotinin), and then flash-frozen in liquid nitrogen. After three freeze-thaw cycles, cells were lysed by passing them through a 25-gauge needle followed by sonication for 60 s. Tissue samples were homogenized on ice in the hypotonic cell lysis buffer, followed by sonication for 60 s. Lysates were cleared by centrifugation at 12000 *g* for 30 min, and protein concentrations were determined using the BCA protein assay reagent (Pierce). Cell lysates (10~30 μg of protein) were then immunoprecipitated by incubating for 3 h at 4°C with each of the respective antibodies preabsorbed to protein-A Sepharose (Pharmacia Biotech Inc.) (Iwasaki *et al.*, 1996). For protein kinase assays, immunoprecipitates were then washed twice with a kinase buffer (50 mM Tris-HCl, pH 8.0, 25 mM $MgCl_2$, 0.5 mM EGTA, 1 mM dithiothreitol, and 10% glycerol).

Protein kinase assays

41-/43-kDa MAP kinases and MEK activities were measured in an immune complex kinase assay as described previously (Iwasaki *et al.*, 1996; Tanimura *et al.*, 1998). Briefly, each immunoprecipitate prepared as described above was incubated for 30~60 min at 30°C with 20 μM ATP and 1~2 μCi of [γ-^{32}P]ATP (Amersham) in 30 μl of the kinase buffer: 41-/43-kDa MAP kinase assays were performed with 7.5 μg of MBP (Sigma) as a substrate, and MEK assays were performed using 2 μg of GST-ERK2^{K52R}. Radioactivity incorporated into MBP was determined by liquid scintillation spectrometry (for assays of 41-/43-kDa MAP kinases), or the incorporation of ^{32}P into GST-ERK2^{K52R} was examined by SDS–PAGE followed by autoradiography using a Fujix Bioimaging analyzer BAS 1500 (Fujix Photo Film Co., Tokyo, Japan) (for assays of MEK). In each experiment we determined the activities of MAP kinases/MEK in the cell lysate (5 μg of protein) of Raf-1-transformed NIH3T3 cells (Li *et al.*, 1993); these were used as internal standards in each experiment to normalize the activities of MAP kinases/MEK.

Western blot analysis

Cell lysates prepared as described above were separated by SDS–PAGE, electrophoretically transferred onto an Immobilon-P membrane (Millipore), and probed with anti-Raf-1 antibody, anti-MEK1 antibody, anti-MAP kinase antibody, anti-p90^{rsk} antibody, or anti-phosphotyrosine antibody. Immunoreactive bands were then visualized by enhanced chemiluminescence (ECL) (Amersham) (Chatani *et al.*, 1995; Iwasaki *et al.*, 1996).

Acknowledgements
We thank Drs Ei-ichi Tahara, Hidetoshi Tahara, Sakuji Toyama and Mayumi Ono for various tumor cell lines, Dr Michael J Weber for the cDNA for ERK2^{K52R}, and Dr Patrick Hughes for critical reading of the manuscript. This work was supported in part by Grants-in-aid for Scientific Research from the Ministry of Education, Sciences, Sports and Culture of Japan.

References

Avruch J, Zhang XF and Kyriakis JM. (1994). *Trends Biochem. Sci.*, **19**, 273–283.
Bansal A, Ramirez RD and Minna, JD. (1997). *Oncogene*, **14**, 1231–1234.
Barbacid M. (1987). *Annu. Rev. Biochem.*, **56**, 779–827.
Bos JL. (1988). *Mutation Res.*, **195**, 255–271.
Boulton TG, Nye SH, Robbins DJ, Ip NY, Radziejewska E, Morgenbesser SD, DePinho RA, Panayotatos N, Cobb MH and Yancopoulos GD. (1991). *Cell*, **65**, 663–675.
Brunet A, Pages G and Pouyssegur J. (1994). *Oncogene*, **9**, 3379–3387.
Chatani Y, Tanaka E, Tobe K, Hattori A, Sato M, Tamemoto H, Nishizawa N, Nomoto H, Takeya T, Kadowaki T, Kasuga M and Kohno M. (1992). *J. Biol. Chem.*, **267**, 9911–9916.
Chatani Y, Tanimura S, Miyoshi N, Hattori A, Sato M and Kohno M. (1995). *J. Biol. Chem.*, **270**, 30686–30692.
Chaubert P, Gayer R, Zimmermann A, Fontolliet C, Stamm B, Bosman F and Shaw P. (1997). *Hepatology*, **25**, 1376–1381.
Cobb MH and Goldsmith EJ. (1995). *J. Biol. Chem.*, **270**, 14843–14846.
Cohen P. (1992). *Trends Biochem. Sci.*, **17**, 409–413.
Cooper JA, Sefton BM and Hunter T. (1984). *Mol. Cell. Biol.*, **4**, 30–37.
Cowley S, Paterson H, Kemp P and Marshall CJ. (1994). *Cell*, **77**, 841–852.
Daum G, Eisenmann-Tappe I, Fries HW, Troppmair J and Rapp UR. (1994). *Trends Biochem. Sci.*, **19**, 474–479.
Davis RJ. (1993). *J. Biol. Chem.*, **268**, 14553–14556.
Hunter T. (1995). *Cell*, **80**, 225–236.
Hunter T. (1997). *Cell*, **88**, 333–346.
Iwasaki S, Tsuruoka N, Hattori A, Sato M, Tsujimoto M and Kohno M. (1995). *J. Biol. Chem.*, **270**, 5476–5482.
Iwasaki S, Hattori A, Sato M, Tsujimoto M and Kohno M. (1996). *J. Biol. Chem.*, **271**, 17360–17365.
Kawada M, Uehara Y, Mizuno S, Yamori T and Tsuruo T. (1998). *Jpn. J. Cancer Res.*, **89**, 110–115.
Kawaguchi Y, Takebayashi H, Kakizuka A, Arii S, Kato M and Imamura M. (1997). *Cancer Lett.*, **116**, 53–59.
Kohno M. (1985). *J. Biol. Chem.*, **260**, 1771–1779.
Li PM, Fukazawa H, Yamamoto C, Mizuno S, Tanaka K, Hori M, Yaginuma S, Saito T and Uehara Y. (1993). *Oncogene*, **8**, 1731–1735.
Mansour SJ, Mattern WT, Hermann AS, Candia JM, Rong S, Fukasawa K, Vande Woude GF and Ahn NG. (1994). *Science*, **265**, 966–970.
Nakatsu Y, Nomoto S, Oh-uchida M, Shimizu K and Sekiguchi M. (1985). *Cold Spring Harbor Symp. Quant. Biol.*, **51**, 1001–1008.
Nishida E and Gotoh Y. (1993). *Trends Biochem. Sci.*, **18**, 128–131.
Oka H, Chatani Y, Hoshino R, Ogawa O, Kakehi Y, Terachi T, Okada Y, Kawaichi M, Kohno M and Yoshida, O. (1995). *Cancer Res.*, **55**, 4182–4187.
Pawson T. (1995). *Nature*, **373**, 573–580.
Ray LB and Sturgill TW. (1987). *Proc. Natl. Acad. Sci. USA*, **84**, 1902–1906.
Rossomando A, Wu J, Weber MJ and Sturgill TW. (1992). *Proc. Natl. Acad. Sci. USA*, **89**, 5221–5225.
Seger R and Krebs EG. (1995). *FASEB J.*, **9**, 726–735.
Serrano M. (1997). *Exp. Cell Res.*, **237**, 7–13.
Shimada Y, Imamura M, Wagata T, Yamaguchi N and Tobe T. (1992). *Cancer*, **69**, 277–284.

Shimizu K, Goldfarb M, Suard Y, Perucho M, Li Y, Kamata T, Feramisco J, Stavnezer E, Fogh J and Wigler MH. (1983). *Proc. Natl. Acad. Sci. USA*, **80**, 2112–2116.

Smith DB and Corcoran LM. (1990). *Current Protocols in Molecular Biology*, Vol.2. Ausubel FM, Brent R, Kingston RE, Moore DD, Seidman JG, Smith JA and Struhl K. (eds), Greene Publishing Associates and Wiley-Interscience, John Wiley & Sons: New York, pp. 16.7.1–16.7.6.

Sporn MB and Todaro GT. (1980). *N. Engl. J. Med.*, **303**, 878–880.

Sturgill TW, Ray LB, Erikson E and Maller JL. (1988). *Nature*, **334**, 715–718.

Sun H, Charies CH, Lau LF and Tonks NK. (1993). *Cell*, **75**, 487–493.

Tanimura S, Chatani Y, Hoshino R, Sato M, Watanabe S, Kataoka T, Nakamura T and Kohno M. (1998). *Oncogene*, **17**, 57–65.

Ward Y, Gupta S, Jensen P, Wartmann M, Davis RJ and Kelly K. (1994). *Nature*, **367**, 651–654.

Yao M, Shuin T, Misaki H and Kubota Y. (1988). *Cancer Res.*, **48**, 6753–6757.

Exhibit L

Biochem. J. (2001) 357, 297–303 (Printed in Great Britain)

Mitogen-activated protein kinases control p27/Kip1 expression and growth of human melanoma cells

Marcin KORTYLEWSKI*†, Peter C. HEINRICH*, Maria-Elisabeth KAUFFMANN*, Markus BÖHM‡, Andrzej MACKIEWICZ† and Iris BEHRMANN*[1]

*Department of Biochemistry, RWTH Aachen, Pauwelsstrasse 30, 52074 Aachen, Germany, †Department of Cancer Immunology, University School of Medical Sciences at Greatpoland Cancer Center, Garbary Street 15, 61866 Poznan, Poland, and ‡Department of Dermatology, University of Münster, Von Esmarch-Strasse 56, 48149 Münster, Germany

The mitogen-activated protein kinases (MAPKs) extracellular signal-regulated protein kinase (ERK)1 and ERK2, involved in regulating cell growth and differentiation, are constitutively active in A375 and WM239 human melanoma cells. Using PD098059, an inhibitor of MAPK kinase (MEK), we investigated the role of persistently activated ERK1/2 in cell growth. The inhibition of MAPK activity induced a dose-dependent growth arrest in G_0/G_1 phase. Correspondingly, we observed the up-regulation of the cyclin-dependent kinase (Cdk) inhibitor p27/Kip1 and hypophosphorylation of the retinoblastoma protein. Further studies showed that PD098059 treatment significantly decreased Cdk2 kinase activity, most probably owing to an augmented level of p27/Kip1 associated with cyclin E–Cdk2 complexes. The accumulation of p27/Kip1 protein in A375 cells was attributed to its increased stability. Our findings suggest that constitutively active ERK1/2 kinases contribute to the growth of melanoma cells by negative regulation of the p27/Kip1 inhibitor.

Key words: PD098059, proliferation, protein stability.

INTRODUCTION

The mitogen-activated protein kinases (MAPKs) comprise a family of protein serine/threonine kinases mediating signals from a variety of extracellular stimuli. The mitogenic activation of extracellular signal-regulated protein kinase (ERK)1 and ERK2 kinases involves their threonine phosphorylation as well as tyrosine phosphorylation by the dual-specificity MAPK kinases also called MAP kinase/ERK kinase (MEK)1/2. The MEKs in turn are phosphorylated and activated by Raf, which initiates the signalling after its binding to the activated GTP-bound Ras protein. On activation, MAPKs translocate to the nucleus, where they phosphorylate and activate various transcription factors controlling the expression of their respective target genes, and are most frequently involved in the regulation of cell growth and differentiation [1]. Constitutive activation of mitogenic pathways is generally thought to contribute to cell transformation. The expression of constitutively active forms of MEK1/2 kinases was reported to cause transformation of murine fibroblasts and induce tumour formation in nude mice [2]. So far no naturally occurring constitutively active mutated forms of MAPK and MEK have been found. However, several upstream components of the MAPK cascade (Ras, Raf) and its downstream targets (Jun, Fos) are products of proto-oncogenes, emphasizing the relevance of this signalling pathway for promoting cell growth [3].

Several studies have suggested the involvement of the constitutively active MAPK cascade in melanoma development. The overexpression of activated H-*ras* in cultured human melanocytes changed their phenotype into one resembling transformed melanoma cells [4]. Activating *ras* mutations were observed in approx. 20 % of primary melanomas and at even higher rates in metastatic and recurrent melanomas [5,6], suggesting a role of activated Ras in promoting progression of the disease. The importance of the Ras signalling cascade for melanoma growth was further underlined by a recent study in a transgenic mouse model: it was shown that oncogenesis and maintenance of melanoma required the continuous presence of activated Ras [7].

Here we investigate the relevance of constitutively active MAPKs in human melanoma cells and show that their inhibition leads to G_0/G_1 arrest and to up-regulation of the inhibitor of cyclin-dependent kinases (Cdks) p27/Kip1.

EXPERIMENTAL

Cells and reagents

A human A375 malignant melanoma cell line established from a solid tumour was purchased from A.T.C.C. (CRL-1619). Human primary WM902b and metastatic WM239, WM9 malignant melanoma cells were obtained from Dr R. S. Kerbel (Sunnybrook Health Science Center, Toronto, Canada). Human Mel Inv metastatic melanoma cells were kindly provided by Dr A. Bosserhoff (Department of Pathology, RWTH Aachen, Germany). Cells were grown in RPMI 1640 medium supplemented with 5 % (for general culture) or 1 % (for growth assays) (v/v) fetal calf serum, 50 μg/ml penicillin and 100 μg/ml streptomycin in a humidified air/CO_2 (19:1) atmosphere. PMA, puromycin, MG132, U0126 and PD098059 were purchased from Calbiochem (Bad Soden, Germany).

Growth inhibition assay

Viable cells (3×10^3) were seeded in triplicate into 96-microwell plates; PD098059 or vehicle only (DMSO) was added to the medium at various concentrations. After 4 days of culture, an

Abbreviations used: Cdk, cyclin-dependent kinase; ERK, extracellular signal-regulated protein kinase; GAPDH, glyceraldehyde-3-phosphate dehydrogenase; MAPK, mitogen-activated protein kinase; MEK, MAPK kinase (MAP kinase/ERK kinase); pRb, retinoblastoma protein.

[1] To whom correspondence should be addressed (e-mail behrmann@rwth-aachen.de).

XTT {sodium 3′-[1-(phenylaminocarbonyl)-3,4-tetrazolium]-bis-(4-methoxy-6-nitro)benzenesulphonic acid hydrate} colorimetric assay (Roche, Mannheim, Germany) was performed as described previously [8]. The percentage growth inhibition was calculated in relation to the growth of control cells.

DNA staining and flow cytometry

For the analysis of DNA content, 5×10^5 cells were stained with propidium iodide by using the CycleTEST Plus DNA Reagent Kit (Becton Dickinson, Heidelberg, Germany) in accordance with the manufacturer's protocol. Fluorescence data were collected with a FACScalibur (Becton Dickinson) and further analysed using the ModFit 2.0 software (Verity Software, Topsham, ME, U.S.A.).

Immunoblotting analysis

Cells were lysed on the dish in lysis buffer A containing 1% (v/v) Triton X-100, 1% (w/v) sodium deoxycholate, 0.1% SDS, 20 mM Tris/HCl, pH 7.2, 158 mM NaCl, 5 mM EDTA, 50 mM NaF, 1 mM Na_3VO_4, 1 mM PMSF, 5 μg/ml aprotinin and 5 μg/ml leupeptin. Lysates were further cleared by centrifugation at 12000 *g* and the protein concentration was determined with the Bio-Rad protein assay reagent (Munich, Germany). Equal amounts of protein were used for SDS/PAGE gels, transferred to PVDF membrane (GelmanSciences, Dreieich, Germany) and probed with the respective antibodies. The antibodies used were polyclonal phospho-specific anti-(p44/42 MAPK) antibodies (threonine-202/tyrosine-204; New England Biolabs, Schwalbach, Germany), monoclonal anti-p21 antibodies (SX118; PharMingen, Heidelberg, Germany), polyclonal anti-ERK1 (C-16), anti-ERK2 (C-14), anti-Cdk2 (M2), anti-Cdk4 (H-303), anti-(cyclin E) (C-19), anti-p18 (N-20), anti-p27 (C-19), anti-(retinoblastoma protein) (anti-pRb) (C-15) and monoclonal anti-(cyclin D1) (R-124) antibodies (Santa Cruz Biotechnology, Heidelberg, Germany). Detection and quantification of signals generated by the enhanced chemiluminescence method (Amersham, Braunschweig, Germany) was performed on the Lumi-Imager with LumiAnalyst Software (Roche).

Immunoprecipitation

Before immunoprecipitation, cells were extracted in lysis buffer B containing 0.5% Nonidet P40, 50 mM Hepes, pH 7.5, 150 mM NaCl, 25 mM β-glycerophosphate, 15 mM pyrophosphate, 25 mM NaF, 5 mM EGTA, 1 mM EDTA, 1 mM Na_3VO_4, 1 mM PMSF, 5 μg/ml aprotinin and 5 μg/ml leupeptin. After adjustment to equal protein concentrations, lysates were incubated overnight at 4 °C with 1 μg of polyclonal antibodies against human cyclin E (C-19) or against human Cdk4 (H-303) (Santa Cruz Biotechnology). The immunoprecipitates were later collected with Protein A–Sepharose, washed three times with lysis buffer and analysed further by SDS/PAGE. Western blot analysis was performed with polyclonal anti-p27 antibodies (C19); after stripping, the blot was redeveloped with polyclonal anti-Cdk2 antibodies (M2) or anti-Cdk4 antibodies (H-303) (Santa Cruz Biotechnology). The detection of cyclin E was not possible, probably owing to co-migration of cyclin E with the heavy chains of the anti-(cyclin E) antibodies.

Immunocytochemistry and confocal fluorescence microscopy

Cells grown to subconfluence on coverslips were fixed in 2% (w/v) paraformaldehyde at room temperature for 20 min. After being washed three times with PBS, the cells were permeabilized with 0.2% (v/v) Triton X-100 and incubated first with polyclonal anti-p27 antibodies (C19; Santa Cruz Biotechnology) and then with secondary FITC-conjugated antibodies. The fluorescence images were observed with a laser-scanning microscope LSM 510 (Zeiss, Halbergmoos, Germany), with an Apochromat 63× objective lens, 488 nm laser excitation and a 505 nm bandpass emission filter.

Histone H1 kinase assay

Histone H1 kinase assays were performed as described by Hermeking et al. [9]. In brief, the anti-Cdk2 (M2) immunoprecipitates prepared from 150 μg of lysate protein were incubated for 20 min at 30 °C in 20 μl of kinase buffer [20 mM $MgCl_2$/10 mM EGTA/40 mM Hepes (pH 7.0)] with 1 μg of histone H1 (Roche) and 1 μl of 300 mCi/mmol [γ-^{32}P]ATP (Amersham). After stopping the reaction with 2× SDS sample buffer, phosphorylated proteins were resolved by SDS/PAGE [12% (w/v) gel] and signals were analysed with a Storm 840 PhosphorImager with the ImageQuant software (Molecular Dynamics).

RNA isolation and Northern blot analysis

Total RNA was isolated with the RNeasy kit from Qiagen (Hilden, Germany). RNA (5 μg) was denatured, size-fractionated by electrophoresis in a 1% (w/v) agarose/formaldehyde gel and transferred to a GeneScreen Plus nylon membrane (DuPont NEN Research Products, Boston, MA, U.S.A.). Detections of p27 mRNA were performed with human p27 cDNA labelled with [α-^{32}P]dATP with the use of a random primer labelling kit (Roche). After stripping of the blot, hybridization with a glyceraldehyde-3-phosphate dehydrogenase (GAPDH) cDNA probe was used to control the loading and transfer of RNA. Signals were quantified with a Storm 840 PhosphorImager with the ImageQuant software (Molecular Dynamics) and normalized to the GAPDH values.

RESULTS

Constitutive activation of the MEK/MAPK pathway in A375 cells

We have shown previously that the specific activation of tyrosine phosphatase SHP-2, often acting as an adaptor to the Ras/MAPK pathway, did not affect the growth behaviour of transfected human A375 melanoma cells [8]. By testing the activity state of ERK1 and ERK2 MAPKs in Western blot analysis with antibodies recognizing specifically the tyrosine-phosphorylated forms of both proteins, we observed elevated levels of phosphorylation, predominantly of ERK2 and to a much smaller extent that of ERK1. The intensity of the phosphospecific bands did not decline on serum starvation of the cells for 24 h (Figure 1A). Treating the cells with serum or PMA did not significantly increase MAPK phosphorylation. Thus ERK1 and ERK2 MAPKs seem to be constitutively active in A375 melanoma cells.

To investigate the contribution of MEK to the pronounced ERK1/ERK2 phosphorylation, we used PD098059, a highly specific inhibitor of MEK activation [10]. Incubation of A375 cells with PD098059 dose-dependently decreased the MAPK activation. In concentrations exceeding 5 μM, ERK1/ERK2 phosphorylation was diminished to undetectable levels without any major effect on the total level of MAPK protein (Figure 1A). Similar to A375 cells, we found constitutively activated and not further PMA-inducible ERK1 and ERK2 also in another human metastatic melanoma cell line, WM239, but not in other primary

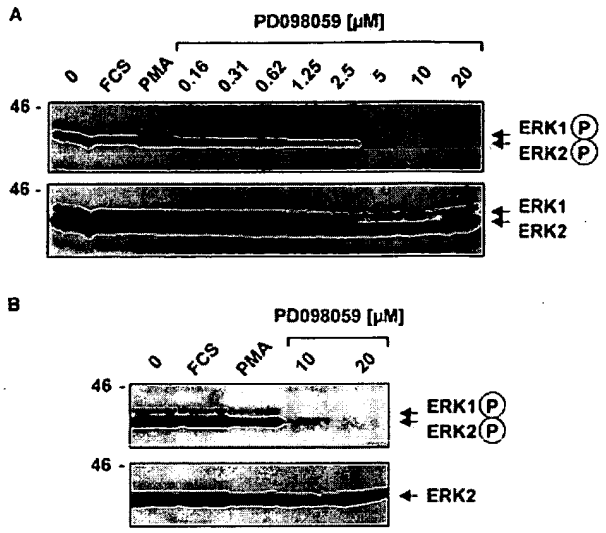

Figure 1 MAPKs are constitutively tyrosine-phosphorylated in human A375 and WM239 melanoma cells

A375 (**A**) and WM239 (**B**) cells starved for 24 h in medium without serum were treated thereafter for 30 min with fetal calf serum (10%, v/v), PMA (100 nM) or PD098059 at the indicated concentrations. Equal amounts of total cell lysates (50 μg of protein) were separated by SDS/PAGE [8.75% (w/v) gel] followed by a Western blot analysis with phospho-specific anti-p44/42 MAPK antibodies. After being stripped, the blot was redeveloped with anti-ERK1 and/or anti-ERK2 antibodies to demonstrate equal loading. The positions of a molecular mass marker (in kDa) and of ERK1 and ERK2 are indicated.

(WM902b) and metastatic (WM9 and Mel Inv) melanoma cell lines (Figure 1B, and results not shown). As expected, the activities of MAPKs in WM239 cells could be decreased by treatment with PD098059 at concentrations above 10 μM. These results indicate that constitutive activation of MAPK in human melanoma cells is the result of a constant positive regulation by members of Ras/MAPK pathway located further upstream.

PD098059 inhibits the growth of A375 cells

We analysed the effect of PD098059 on the proliferation of A375 and WM239 cells (Figure 2A). PD098059 at concentrations ranging from 5 μM to 20 μM exerted a dose-dependent growth inhibitory effect on the cells within 4 days of incubation. Unexpectedly, low inhibitor concentrations seemed to promote the proliferation of A375 slightly but not that of WM239 cells. Nevertheless, the extent of growth inhibition induced by higher concentrations of PD098059 correlated with the decrease in ERK1/ERK2 phosphorylation demonstrated in Figure 1.

To characterize this effect further, we performed a cell cycle analysis by measuring the DNA content of A375 cells incubated with 10 μM PD098059 for different periods (Figure 2B). A strong growth-inhibitory effect was visible after 24 h, with a significant decrease in the number of dividing cells. After 48 h almost 99% of the cells were arrested in the G_0/G_1 phase. A longer incubation with the inhibitor further increased the ratio of sub-G_1 events from less than 1% to over 7% of all counted events, indicative of apoptotic cells. WM239 cells reacted to the inhibition of MEK in a similar way (results not shown). PD098059 therefore induces a G_0/G_1 arrest in both tested human melanoma cell lines and, secondarily, with greatly prolonged incubation times might additionally decrease cell survival.

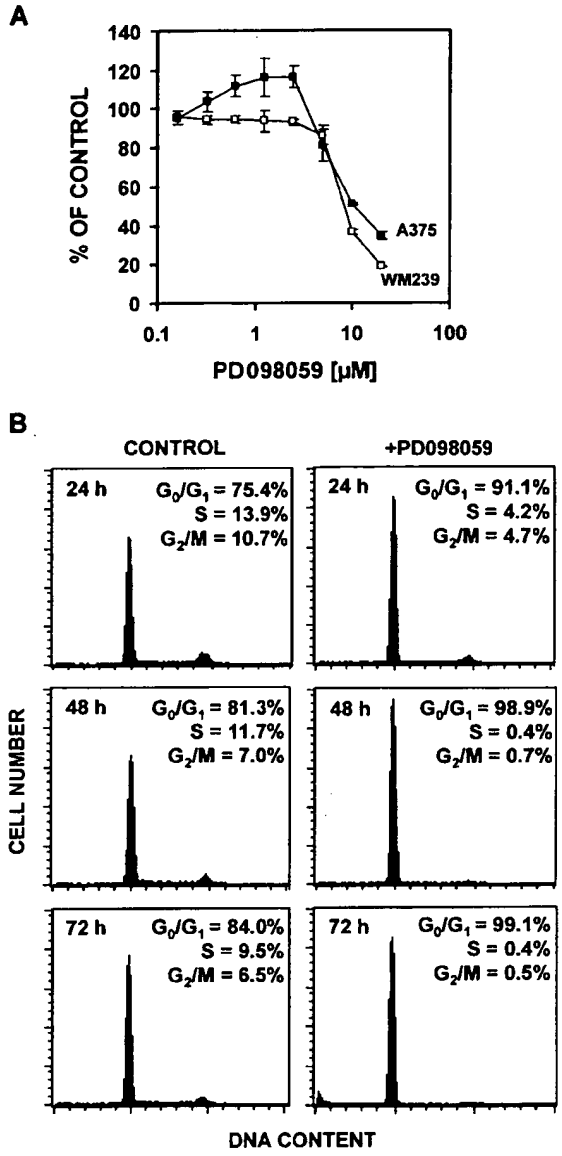

Figure 2 Effect of PD098059 on the growth of human melanoma cells

(**A**) A375 cells (■) or WM239 (□) (initial density 3000 cells per well) were cultured for 4 days in the presence of PD098059 at different concentrations. Growth was assessed by an XTT test; values were recalculated in relation to controls treated with vehicle only [0.05% (v/v) DMSO]. Error bars represent the S.D. for triplicate samples. (**B**) For cell cycle analysis, cells were incubated in medium with or without the addition of 10 μM PD098059 for the durations indicated. After staining of DNA with propidium iodide, fluorescence was measured with a FACScalibur (Becton Dickinson), and the data were quantified further with ModFit 2.0 software (Verity Software). Sub-G_1 values were excluded from the calculation.

Inhibition of MAPKs by PD098059 leads to the up-regulation of p27/Kip1 protein

To explain the effect of PD098059 on G_0/G_1 arrest we examined the protein levels of negative regulators of cell cycle progression, the Cdk inhibitors. Incubation of A375 and WM239 cells with PD098059 resulted in the accumulation of p27/Kip1 protein (Figures 3A and 3B). In A375 cells the effect became detectable after 24 h, when p27/Kip1 protein amounts were increased 2.5-fold above the respective control levels, reached a maximum

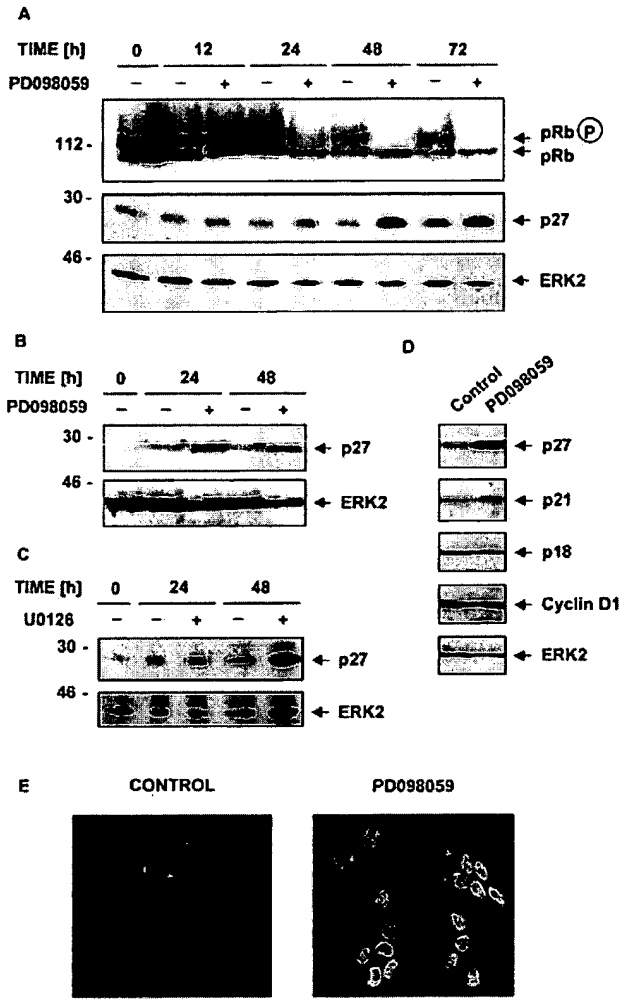

Figure 3 MEK inhibition results in up-regulation of p27/Kip1 expression in human melanoma cells

Stimulation-dependent accumulation of p27/Kip1 protein in A375 (**A**, **C–E**) and WM239 (**B**) cells. (**A–D**) Western blot analysis of cells treated with 10 μM PD098059 (**A**, **B**, **D**) or 1 μM U0126 (**C**) in comparison with controls incubated with vehicle only [0.05% (v/v) DMSO] for the durations indicated. Equal amounts of total cell lysates (50 μg of protein) were separated by SDS/PAGE on 6% (for Rb detection) or 12.5% (for p27 and ERK2 detection) gels. Blots were developed with anti-Rb, anti-p27, anti-p21, anti-p18 and anti-(cyclin D1) antibodies. After being stripped, blots were redeveloped with anti-ERK2 antibodies to demonstrate equal loading. The positions of molecular mass markers (in kDa) and of hyperphosphorylated and hypophosphorylated pRb (pRbP and pRb respectively), Cdk inhibitors, cyclin D1 and ERK2 are indicated. (**E**) Nuclear localization of p27/Kip1 in A375 cells. Indirect fluorescence of cells stained intracellularly with anti-p27 antibodies, revealed with FITC-conjugated secondary antibodies and observed with a laser-scanning microscope with a Zeiss Apochromat objective (63 ×) and identical measurement parameters in both control and PD098059-treated cells.

after 48 h (5-fold increase) and stayed elevated for up to 72 h of stimulation. The level of a control protein, ERK2, remained unchanged. Apparently the time course of p27/Kip1 protein accumulation correlates well with the abrogation of cell growth (Figure 2). A similar effect of the p27/Kip1 up-regulation coinciding with a strong G_0/G_1 growth arrest was efficiently induced also by U0126, another inhibitor of ERK activation structurally unrelated to PD098059 (Figure 3C, and results not shown).

The protein level of other Cdk inhibitors present in A375 cells, p18/INK4c and p21/Cip1, did not significantly change in the course of PD098059 treatment (Figure 3D). Because A375 cells lack the expression of both p15/INK4b and p16/INK4a genes [11] and the protein levels of two other inhibitors, p19/INK4d and p57/Kip2, were hardly detectable, p27/Kip1 might be a specific target of MAPK-dependent regulatory pathways. It is also worth noting that the expression of cyclin D1, which reportedly can be regulated by ERK kinases in a variety of cell types [3,12,13], remained unchanged on incubation with PD098059 (Figure 3D).

The function of p27/Kip1 as an inhibitor of cell cycle progression depends on its proper nuclear localization [14]. As determined by indirect immunofluorescence, p27/Kip1 resided almost exclusively in nuclei of untreated A375 cells and the inhibition of MAPK activity strongly enhanced the observed nuclear signals (Figure 3E). Thus it seems plausible that augmented amounts of nuclear p27/Kip1 could negatively influence the activity of Cdks, which are responsible for the inactivation of pRb. pRb, a key regulator of the cell cycle, is inactivated by its hyperphosphorylation, thereby allowing cell cycle progression. As expected, in PD098059-treated A375 cells, the accumulation of p27/Kip1 was paralleled by the disappearance of hyperphosphorylated pRb (Figure 3A). It decreased to the lowest level after only 24 h of incubation with PD098059 and remained low. Interestingly, after 72 h of treatment we also observed a decrease in the total level of Rb protein.

Decrease in Cdk2 kinase activity correlates with the association of p27/Kip1

To test whether the observed effect of the hypophosphorylation of Rb protein could result from the decreased activity of Cdk2 kinase, the major target of p27/Kip1 inhibition, we performed a histone H1 kinase assay. As shown in Figure 4(A), abrogation of MAPK signalling had a strong inhibitory effect on phosphorylation of the Cdk2-dependent histone H1. The Cdk2 activity dropped below 80% of the initial value after 6 h of incubation with PD098059 and decreased to approx. 30% of its normal level after 18 h. Therefore the maximal decrease in Cdk2 activity correlates with accumulation of p27/Kip1. In addition, we found increased amounts of p27/Kip1 at relatively stable levels of Cdk2 that could be co-precipitated with cyclin E after 18 h of PD098059 treatment (Figure 4B). However, we were unable to detect the presence of p27/Kip1 in anti-Cdk4 immunoprecipitates (Figure 4B).

PD098059 increases p27/Kip1 protein stability in A375 cells

The up-regulation of p27/Kip1 on inhibition of MEK/MAPK signalling seems to be controlled post-transcriptionally because no significant changes in the amount of p27/Kip1 mRNA were observed in A375 cells treated with PD098059 for up to 24 h (Figure 5A). We examined whether inhibition of proteasome function in A375 cells could counteract the negative influence of the MAPK pathway on p27/Kip1 expression and lead to its accumulation. As shown in Figure 5(B), the proteasome inhibitor MG132 was able to up-regulate the p27/Kip1 protein level even more efficiently than PD098059 during the same incubation period. These results suggest that the abundance of p27/Kip1 in A375 cells can be regulated post-translationally by the ubiquitin–proteasome system. Indeed, the stability of p27/Kip1 protein in A375 cells was significantly enhanced by addition of the MEK inhibitor (Figure 5C). After blocking of translation with puromycin for 3 h the level of p27/Kip1 remained almost unchanged

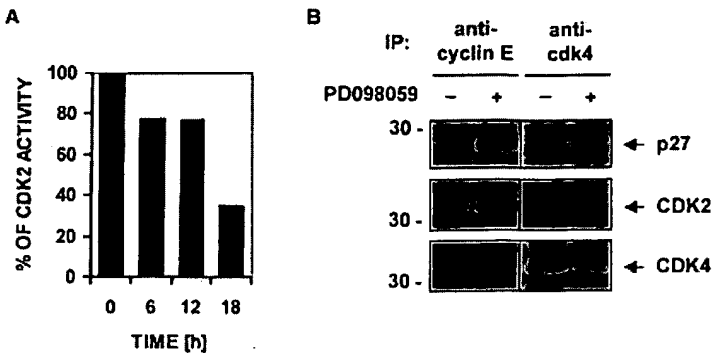

Figure 4 Inhibition of Cdk2 kinase activity correlates with the association of p27/Kip1 with cyclin E–Cdk2 complex

(**A**) Cdk2 immunoprecipitates prepared from lysates of A375 cells treated with 10 μM PD098059 or with vehicle only [0.05% (v/v) DMSO] for the indicated durations were used for a kinase assay with histone H1 as a substrate. After quantification of the signals with the Storm 840 PhosphorImager (Molecular Dynamics), values from different time points were recalculated in relation to respective controls. (**B**) Association of p27/Kip1 with complexes of Cdks immunoprecipitated (IP) with anti-(cyclin E) or with anti-Cdk4 antibodies from A375 cells treated for 18 h with 10 μM PD098059 or with vehicle only (0.05% DMSO). The immunoprecipitates from cell lysates containing equal concentrations of proteins were resolved by SDS/PAGE, blotted and developed with anti-p27, anti-Cdk2 and anti-Cdk4 antibodies. The position of a molecular mass marker is indicated (in kDa).

in PD098059-treated cells, whereas it decreased by approx. 70% in untreated controls. Similar results were obtained with cycloheximide, another inhibitor of translation (results not shown). We conclude that MAPKs regulate the level of p27/Kip1 in A375 melanoma cells by promoting protein degradation.

DISCUSSION

The results of our study provide evidence for a negative effect of constitutively active MAPKs on the expression of p27/Kip1 in human melanoma cells. Using the inhibitor PD098059 we have found that suppression of the permanent activity of ERK1/2 results in a strong nuclear accumulation of p27/Kip1 protein and correlates with a potent inhibition of cell growth. Additionally, the inhibition of MAPK signalling strongly decreased the kinase activity of Cdk2, which in complex with cyclin E or cyclin A constitutes the major target of inhibition by p27/Kip1 [15,16]. As expected, we also found increased amounts of p27/Kip1 associated with cyclin E–Cdk2 but not with cyclin D–Cdk4 complexes after treatment with PD098059.

The up-regulation of p27/Kip1 in A375 cells treated with PD098059 does not seem to occur at the level of its transcription, because we failed to detect any increase in the levels of p27/Kip1 mRNA. In contrast, we have observed an enhanced stability of p27/Kip1 protein. Thus the MAPK pathway seems to be involved in the negative control of this universal Cdk inhibitor by augmenting its degradation, thereby presumably supporting unrestricted cell growth. The negative regulation of p27/Kip1 levels by post-translational mechanisms, mainly by its increased proteolysis, seems to be a more general phenomenon, triggered for instance by growth factor stimulation [12,17]. A similar effect has been reported for murine NIH 3T3 fibroblasts stably transfected with an inducible c-Raf-1–oestrogen receptor cDNA [13]. Stimulation of the Raf/MAPK pathway abrogated p27/Kip1 protein expression. In contrast, the experiments with an analogous conditionally active c-Raf-1 protein in small-cell lung cancer cells yielded opposite results [18]. Raf activation in these cells was accompanied by a marked induction of p27/Kip1 and growth inhibitory effects. The specific cellular context might therefore critically influence the biological outcome of the MAPK signalling.

p27/Kip1 seems to be the only Cdk inhibitor that is down-regulated by mitogenic stimuli [17]. Accordingly, we were unable to detect any PD098059-dependent increase in protein expression of other cell-cycle inhibitors present in A375 and WM239 cells, such as p18/INK4c, p19/INK4d, p21/Cip1 or p57/Kip2. Although we cannot so far unequivocally determine whether the up-regulation of p27/Kip1 is a cause of the observed growth arrest, several reports suggest a role for p27/Kip1 in the control of proliferation of melanoma cells. Recently, the accumulation of p27/Kip1 has been demonstrated in melanoma cells during growth inhibition induced by interleukin 6 and oncostatin M or fibrillar collagen [8,19,20]. In contrast with the INK4 family of inhibitors (p15, p16, p18, p19), p27/Kip1 is rarely lost via genetic aberrations in tumours. Expression of p27/Kip1 was found to be high in normal melanocytes and in benign naevi, whereas in malignant melanomas the expression pattern was heterogeneous [21]. The level of p27/Kip1 significantly correlated with tumour thickness in the nodular subtype of primary melanoma but not in the superficially spreading subtype. Furthermore, the complete loss of p27/Kip1 expression had a potential prognostic value as an indicator of early relapse of the disease [21]. Interestingly, the nodular subtype of melanoma was previously shown to be associated with activating mutations in the *ras* gene [6,22]. The eventual inverse correlation between the expression of mutated Ras and the inhibitor p27/Kip1 could well be explained by the involvement of a constitutively active Ras–Raf–MAPK pathway in the negative regulation of p27/Kip1 expression. Further studies will be necessary to prove the prognostic potential of these two events, namely *ras* mutations and down-regulation of p27/Kip1 levels, as combined markers of melanoma aggressiveness.

Our results demonstrate a very potent growth-inhibitory action of PD098059 on human melanoma cells. So far, the effects of this specific inhibitor of MEK1 kinase have been studied in a murine B16 melanoma cell line. Englaro et al. [23] observed that blocking the mitogen-dependent activation of ERK1/2 kinases triggers the differentiation of murine B16 melanoma cells, promoting cell dendricity and melanogenesis. In our model cell lines the abrogation of constitutive activation of MAPKs arrested cell growth in the G_0/G_1 phase, which correlated in time with the accumulation of p27/Kip1 protein but did not lead to major

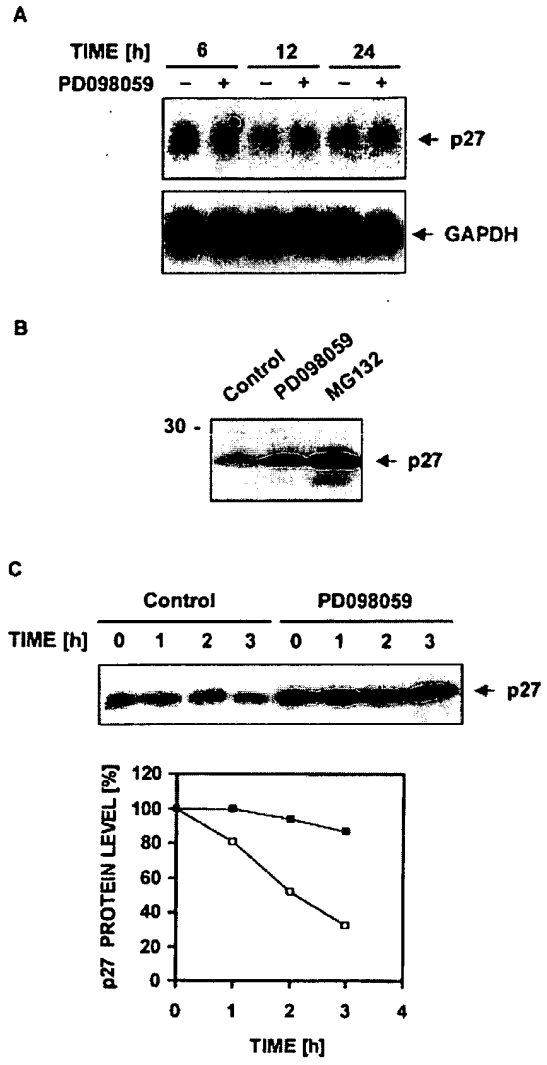

Figure 5 Abrogation of constitutive MEK/MAPK signalling does not up-regulate p27/Kip1 mRNA levels but increases its protein stability

(**A**) Northern blot analysis of p27/Kip1 and GAPDH (loading control) expression in A375 cells treated with 10 μM PD098059 or with vehicle only [0.05% (v/v) DMSO] for the durations indicated. (**B**) Immunoblot analysis of p27/Kip1 expression in A375 cells treated for 18 h with 10 μM PD098059, 5 μM MG132 or vehicle only. The position of a molecular mass marker is indicated (in kDa). (**C**) A representative Western blot analysis of p27/Kip1 protein levels in human A375 melanoma cells (upper panel) and its quantification (lower panel). Cells were treated for 24 h with 10 μM PD098059 (■) or with vehicle only (□); puromycin was then added and total cellular lysates were prepared at the indicated times. Western blot detection with anti-p27 was performed as described in the legend to Figure 3. The graph shows the quantification of p27/Kip1 signals with a Lumi-Imager (Roche), presented as percentages of the respective controls at the initial time points.

changes in cell dendricity or melanogenesis (results not shown). In addition, we have observed increased rates of cell death on long-term incubation with PD098059. A plausible explanation for this late effect could be provided by the postulated role of overexpressed p27/Kip1 as an apoptosis-promoting factor [17]. It could also result from partial degradation of Rb protein, which reportedly triggers the p53 apoptotic pathway [24], or from decreased expression of anti-apoptotic genes such as bcl-2, which was up-regulated in human melanoma cell lines transformed with the N-Ras oncogene [25].

Our finding that constitutive activation of MAPKs in melanoma cells is involved in the down-regulation of p27/Kip1 expression agrees well with the hypothesis that deregulation of p27/Kip1 might contribute to melanoma development [19,21]. The pharmacological approach targeting the Ras–Raf–MAPK pathway might represent a sensible way to inhibit melanoma growth. As reported recently, the chemical antagonist of Ras, farnesylthiosalicylic acid can efficiently restrain melanoma growth *in vitro* as well as in mice with severe combined immunodeficiency [26]. The efficient growth-inhibitory action of specific inhibitors of ERK1/2 activation underlines the potential of novel therapeutic approaches targeting members of the Ras–Raf–MAPK pathway in the treatment of human melanoma. Moreover, our study emphasizes the role of p27/Kip1 as a plausible key player in the control of melanoma cell proliferation.

We thank Professor Toshiyuki Sakai, Dr Anja Bosserhoff and Dr Fred Schaper for critical reading of the manuscript, and Bernd Giese for assistance in confocal microscopy. This work was supported by Volkswagen-Stiftung (Hannover), the START programme of RWTH Aachen, the State Committee for Scientific Research (Warsaw), Deutsche Forschungemeinschaft (Bonn), and Fonds der Chemischen Industrie (Frankfurt).

REFERENCES

1 Su, B. and Karin, M. (1996) Mitogen-activated protein kinase cascades and regulation of gene expression. Curr. Opin. Immunol. **8**, 402–411
2 Mansour, S. J., Matten, W. T., Hermann, A. S., Candia, J. M., Rong, S., Fukasawa, K., Vande Woude, G. F. and Ahn, N. G. (1994) Transformation of mammalian cells by constitutively active MAP kinase kinase. Science **265**, 966–970
3 Lloyd, A. C. (1998) Ras versus cyclin-dependent kinase inhibitors. Curr. Opin. Genet. Dev. **8**, 43–48
4 Albino, A. P., Sozzi, G., Nanus, D. M., Jhanwar, S. C. and Houghton, A. N. (1992) Malignant transformation of human melanocytes: induction of a complete melanoma phenotype and genotype. Oncogene **7**, 2315–2321
5 Ball, N. J., Yohn, J. J., Morelli, J. G., Norris, D. A., Golitz, L. E. and Hoeffler, J. P. (1994) Ras mutations in human melanoma: a marker of malignant progression. J. Invest. Dermatol. **102**, 285–290
6 Jafari, M., Papp, T., Kirchner, S., Diener, U., Henschler, D., Burg, G. and Schiffmann, D. (1995) Analysis of *ras* mutations in human melanocytic lesions: activation of the *ras* gene seems to be associated with the nodular type of human malignant melanoma. J. Cancer Res. Clin. Oncol. **121**, 23–30
7 Chin, L., Tam, A., Pomerantz, J., Wong, M., Holash, J., Bardeesy, N., Shen, Q., O'Hagan, R., Pantginis, J., Zhou, H. et al. (1999) Essential role for oncogenic Ras in tumour maintenance. Nature (London) **400**, 468–472
8 Kortylewski, M., Heinrich, P. C., Mackiewicz, A., Schniertshauer, U., Klingmüller, U., Nakajima, K., Hirano, T., Horn, F. and Behrmann, I. (1999) Interleukin-6 and oncostatin M-induced growth inhibition of human A375 melanoma cells is STAT-dependent and involves upregulation of the cyclin-dependent kinase inhibitor p27/Kip1. Oncogene **18**, 3742–3753
9 Hermeking, H., Funk, J. O., Reichert, M., Ellwart, J. W. and Eick, D. (1995) Abrogation of p53-induced cell cycle arrest by c-Myc: evidence for an inhibitor of p21WAF1/CIP1/SDI1. Oncogene **11**, 1409–1415
10 Davies, S. P., Reddy, H., Caivano, M. and Cohen, P. (2000) Specificity and mechanism of action of some commonly used protein kinase inhibitors. Biochem. J. **351**, 95–105
11 Gemma, A., Takenoshita, S., Hagiwara, K., Okamoto, A., Spillare, E. A., McMemamin, M. G., Hussain, S. P., Forrester, K., Zariwala, M., Xiong, Y. and Harris, C. C. (1996) Molecular analysis of the cyclin-dependent kinase inhibitor genes p15INK4b/MTS2, p16INK4/MTS1, p18 and p19 in human cancer cell lines. Int. J. Cancer **68**, 605–611
12 Takuwa, N. and Takuwa, Y. (1997) Ras activity late in G1 phase required for p27kip1 downregulation, passage through the restriction point, and entry into S phase in growth factor-stimulated NIH 3T3 fibroblasts. Mol. Cell. Biol. **17**, 5348–5358
13 Kerkhoff, E. and Rapp, U. R. (1997) Induction of cell proliferation in quiescent NIH 3T3 cells by oncogenic c-Raf-1. Mol. Cell. Biol. **17**, 2576–2586
14 Baldassarre, G., Belletti, B., Bruni, P., Boccia, A., Trapasso, F., Pentimalli, F., Barone, M. V., Chiappetta, G., Vento, M. T., Spiezia, S. et al. (1999) Overexpressed cyclin D3 contributes to retaining the growth inhibitor p27 in the cytoplasm of thyroid tumor cells. J. Clin. Invest. **104**, 865–874

15 Polyak, K., Lee, M. H., Erdjument-Bromage, H., Koff, A., Roberts, J. M., Tempst, P. and Massagué, J. (1994) Cloning of p27Kip1, a cyclin-dependent kinase inhibitor and a potential mediator of extracellular antimitogenic signals. Cell **78**, 59–66
16 Sherr, C. J. and Roberts, J. M. (1999) CDK inhibitors: positive and negative regulators of G1-phase progression. Genes Dev. **13**, 1501–1512
17 Lloyd, R. V., Erickson, L. A., Jin, L., Kulig, E., Qian, X., Cheville, J. C. and Scheithauer, B. W. (1999) p27kip1: a multifunctional cyclin-dependent kinase inhibitor with prognostic significance in human cancers. Am. J. Pathol. **154**, 313–323
18 Ravi, R. K., Weber, E., McMahon, M., Williams, J. R., Baylin, S., Mal, A., Harter, M. L., Dillehay, L. E., Claudio, P. P., Giordano, A. et al. (1998) Activated Raf-1 causes growth arrest in human small cell lung cancer cells. J. Clin. Invest. **101**, 153–159
19 Florenes, V. A., Lu, C., Bhattacharya, N., Rak, J., Sheehan, C., Slingerland, J. M. and Kerbel, R. S. (1999) Interleukin-6 dependent induction of the cyclin dependent kinase inhibitor p21WAF1/CIP1 is lost during progression of human malignant melanoma. Oncogene **18**, 1023–1032
20 Henriet, P., Zhong, Z. D., Brooks, P. C., Weinberg, K. I. and DeClerck, Y. A. (2000) Contact with fibrillar collagen inhibits melanoma cell proliferation by up-regulating p27KIP1. Proc. Natl. Acad. Sci. U.S.A. **97**, 10026–10031
21 Florenes, V. A., Maelandsmo, G. M., Kerbel, R. S., Slingerland, J. M., Nesland, J. M. and Holm, R. (1998) Protein expression of the cell-cycle inhibitor p27Kip1 in malignant melanoma: inverse correlation with disease-free survival. Am. J. Pathol. **153**, 305–312
22 Yasuda, H., Kobayashi, H., Ohkawara, A. and Kuzumaki, N. (1989) Differential expression of ras oncogene products among the types of human melanomas and melanocytic nevi. J. Invest. Dermatol. **93**, 54–59
23 Englaro, W., Bertolotto, C., Busca, R., Brunet, A., Pages, G., Ortonne, J. P. and Ballotti, R. (1998) Inhibition of the mitogen-activated protein kinase pathway triggers B16 melanoma cell differentiation. J. Biol. Chem. **273**, 9966–9970
24 Harbour, J. W. and Dean, D. C. (2000) Rb function in cell-cycle regulation and apoptosis. Nat. Cell Biol. **2**, E65–E67
25 Borner, C., Schlagbauer Wadl, H., Fellay, I., Selzer, E., Polterauer, P. and Jansen, B. (1999) Mutated N-ras upregulates Bcl-2 in human melanoma in vitro and in SCID mice. Melanoma Res. **9**, 347–350
26 Jansen, B., Schlagbauer-Wadl, H., Kahr, H., Heere-Ress, E., Mayer, B. X., Eichler, H.-G., Pehamberger, H., Gana-Weisz, M., Ben-David, E., Kloog, Y. and Wolff, K. (1999) Novel Ras antagonist blocks human melanoma growth. Proc. Natl. Acad. Sci. U.S.A. **96**, 14019–14024

Received 22 February 2001/26 March 2001; accepted 20 April 2001

Exhibit M

ELSEVIER

Cancer Letters 117 (1997) 41–50

CANCER LETTERS

TGFβ regulation of mitogen-activated protein kinases in human breast cancer cells

Randall S. Frey, Kathleen M. Mulder*

Department of Pharmacology, Pennsylvania State University College of Medicine, 500 University Drive, Hershey, PA 17033, USA

Received 21 February 1997; received in revised form 20 March 1997; accepted 20 March 1997

Abstract

We demonstrate herein the ability of transforming growth factor-beta-2 ($TGF\beta_2$) to potently activate extracellular signal-regulated kinase 2 (ERK2) in the highly TGFβ-sensitive breast cancer cell (BCC) line Hs578T. The ERK2 isoform was activated by 3-fold within 5 min of $TGF\beta_2$ addition to Hs578T cells. However, $TGF\beta_2$ only slightly activated ERK2 (1.5-fold) in the partially TGFβ-responsive BCC line MDA-MB-231. The magnitude of the difference in activation of ERK2 by $TGF\beta_2$ in the two cell lines paralleled the difference in the IC_{50} values for TGFβ inhibition of DNA synthesis; the IC_{50} value in the MDA-MB-231 cells was 32-fold greater than that in the Hs578T cells. Further, our data demonstrate that $TGF\beta_2$ activated the stress-activated protein kinase/Jun N-terminal kinase (SAPK/JNK) type of mitogen-activated protein kinases (MAPKs); maximal induction levels were 2.5-fold above basal values and were attained at 30 min after $TGF\beta_2$ treatment. Transient co-transfection of a luciferase reporter construct (3TP-Lux) containing three AP-1 sites and the plasminogen activator inhibitor-1 (PAI-1) promoter, in conjunction with a construct that directs expression of a dominant-negative mutant ERK2 (TAYF) protein, did not block the ability of TGFβ to induce AP-1 or PAI-1 activity. In contrast, TAYF ERK2 was able to block EGF and insulin-induced 3TP-Lux-reporter activity. These results indicate that in these BCCs, the activation of ERK2 by TGFβ is more tightly linked to the ability of TGFβ to inhibit DNA synthesis than to the ability to stimulate promoter regions important for TGFβ production and control of the extracellular matrix. In addition, this is the first demonstration that TGFβ can activate the SAPK/JNK type of MAPK in TGFβ-sensitive human BCCs. © 1997 Elsevier Science Ireland Ltd.

Keywords: TGFβ; Breast cancer cells; Signal transduction; ERK2; MAPK; SAPK/JNK

1. Introduction

The transforming growth factor beta (TGFβ) proteins are the major endogenous growth inhibitors secreted by breast cancer cells (BCCs). Unfortunately, many BCCs have lost responsiveness to the growth inhibitory effects of TGFβ [1–7]. Recent evidence indicates that restoration of the TGFβ receptor system to TGFβ-resistant BCCs can lead to reversion of malignancy in vivo [8]. These results indicate that an intact TGFβ response pathway is sufficient to reduce the malignancy of BCCs in vivo. However, some carcinoma cells remain resistant to the growth inhibitory effects of TGFβ, despite functional TGFβ receptors [9,10]. In these instances, defects in post-receptor signaling components are apparently involved. However, despite the well known nuclear

* Corresponding author. Tel.: +1 717 5316789; fax: +1 717 5315013; e-mail: kmm15@psu.edu.

0304-3835/97/$17.00
PII S0304-3835(97)00211-5

events modulated by TGFβ [11–13], the effects of TGFβ on cytoplasmic signaling components in BCCs have not been studied to date.

Mitogen-activated protein kinases (MAPKs) are key kinases in intracellular signal transduction pathways. This family of kinases are rapidly phosphorylated on threonine and tyrosine residues, thereby resulting in their activation. MAPKs are rapidly activated in response to many growth factors and hormones that influence cell proliferation and differentiation. To date, four subgroups of MAPKs have been identified [14]: the extracellular signal-regulated kinases (ERKs) [15,16], the Jun kinases (c-Jun amino-terminal kinases (JNK) or stress-activated protein kinases (SAPK)) [17,18], p38/MPK2 MAP kinase [19] and BMK1/ERK5 [20,21].

We have demonstrated previously that the sensitivity to the growth inhibitory effects of TGFβ in untransformed epithelial cells was associated with the ability of this cytokine to activate the Ras and ERK1 signaling components [22,23]. In contrast, TGFβ did not activate Ras or ERK1 in TGFβ-resistant cells [22,23]. Recently, we have demonstrated that TGFβ activation of ERK1 is blocked in epithelial cells expressing a dominant-negative mutant of Ras (RasN17), indicating that Ras is necessary for TGFβ activation of ERK1 [24]. Moreover, expression of RasN17 resulted in a blockade of the ability of TGFβ to regulate cell cycle events linked to the growth inhibitory effects of TGFβ, namely cyclin-dependent kinase-2 activity, cyclin A protein expression [24] and the cyclin-dependent kinase inhibitors $p27^{Kip1}$ and $p21^{Cip1}$ [25,26]. These studies suggest that the Ras/MAPK pathway may be one of the important signaling pathways that mediate the growth inhibitory response to TGFβ in untransformed epithelial cells.

In addition to ERK1, other cytoplasmic MAPKs have been shown to be activated by TGFβ. For example, a TGFβ-activated kinase (TAK1) has been identified and was shown to be a member of the MAPK kinase kinase (MAPKKK) family [27]. TAK1 activates a SAPK/ERK kinase (SEK), a kinase previously shown to activate the SAPK/JNKs [27]. However, no association between TAK1 activation by TGFβ and growth response was demonstrated [33,34]. More recently, TGFβ was shown to activate MAPKK6 in untransformed mink lung epithelial cells [28], but the functional significance of this event is not clear. In the current report, we demonstrate that $TGF\beta_2$ activates the ERK and SAPK/JNK families of MAPKs in BCCs in association with negative growth control by TGFβ. Moreover, our data suggest that the activation of MAPKs by TGFβ is more closely associated with the ability of TGFβ to inhibit DNA synthesis than with the ability of TGFβ to regulate AP-1-dependent gene expression important for both $TGF\beta_1$ production and control of the extracellular matrix.

2. Materials and methods

2.1. Materials

Polyclonal rabbit antibody directed against ERK2 (SC-154) was purchased from Santa Cruz Biotechnology (Santa Cruz, CA). Non-immune, whole molecule rabbit immunoglobulin (IgG) was obtained from Jackson ImmunoResearch Laboratories (West Grove, PA). Horseradish peroxidase-conjugated donkey anti-rabbit IgG was purchased from Amersham Corp. (Arlington Heights, IL). [γ-^{32}P]ATP (3000 Ci/mmol, BLU002H) and [^{3}H]thymidine (20 Ci/mmol, NET-027X) were purchased from Dupont NEN (Boston, MA). Myelin-basic protein (MBP) and insulin were obtained from Sigma (St. Louis, MO). Improved MEM (IMEM) was purchased from Irvine Scientific (Santa Ana, CA). $TGF\beta_2$ and $TGF\beta_3$ were generous gifts from P.R. Segarini (Celtrix Pharmaceuticals, Santa Clara, CA) and M. Morin (Pfizer Pharmaceuticals, Groton, CT), respectively.

2.2. Cell culture

Hs578T and MDA-MB-231 (American Type Culture Collection) were grown in IMEM–10% fetal bovine serum, with the addition of insulin (10 nM), as previously described [1]. The cells were all negative for the presence of mycoplasma as determined by staining with Hoechst dye.

2.3. Thymidine incorporation

BCC lines were plated at densities of 2×10^4 cells/cm^2 in 12-well plates. One day later, the medium was changed to serum-free IMEM for 13 h prior to TGFβ addition. BCC cultures were exponentially proliferat-

ing cultures approaching late log phase. [^{3}H]Thymidine incorporation was determined 24 h after the addition of TGFβ, as previously described [22].

2.4. In vitro ERK2 immunocomplex kinase assay and immunoblotting

BCCs were plated as for thymidine incorporation experiments except that 75 cm^2 flasks were used. Preparation of whole cell lysates, ERK2 immunoprecipitations, immunocomplex kinase assays and immunoblotting were performed as previously described [22].

2.5. In vitro SAPK/JNK immunocomplex kinase assay

BCCs were plated as for ERK2 assays. Cells were lysed and immunoprecipitated with rabbit SAPK/JNK antiserum [17] that recognizes all forms of SAPK/JNK as described previously [17]. SAPK/JNK activity was determined as described [17]. Briefly, immunocomplexed SAPK/JNK beads were added to GST-c-Jun (1–135) and incubated with [γ-^{32}P]ATP and $MgCl_2$ for 20 min at 30°C. The reaction was stopped with sample buffer and SDS-PAGE (10% acrylamide) was performed. Phosphorylation of GST-c-Jun was then quantitated by densitometric analysis of autoradiographs.

2.6. Transient transfections and reporter assays

Reporter assays were performed following transient co-transfection of expression plasmids for a dominant-negative mutant of ERK2 (TAYF) (obtained from M.J. Weber, University of VA) [46–48] and the 3TP-Lux reporter (obtained from J. Massagué) [49] in Hs578T cells. The 3TP-Lux reporter plasmid contains a luciferase expression unit under the control of three AP-1 sites and the plasminogen activator inhibitor-1 (PAI-1) promoter [49]. 3TP-Lux was used to monitor TGFβ induction of AP-1 and PAI-1 activities, as described previously [49–51]. Hs578T cells (6.66×10^3 cells/cm^2) were transfected by $CaPO_4$ co-precipitation using 1–20 μg of 3TP-Lux DNA, 100 ng renilla luciferase DNA (Promega, Madison, WI) and 3–12 μg of TAYF ERK2 DNA. One day after plating cells in IMEM–10% FBS, DNA was added for 18–21 h, followed by a treatment period of 8–48 h in serum-free IMEM in the presence or absence of TGFβ_3 (10 ng/ml) or EGF (20 ng/ml) and insulin (600 μg/ml). Cells were then harvested and lysed in reporter lysis buffer (Promega) and cell lysates were assayed for both firefly and renilla luciferase activities. The firefly luciferase activity, which reflects both AP-1 and PAI-1 activities in the 3TP-Lux reporter, was normalized to renilla luciferase to correct for transfection efficiency.

3. Results

3.1. TGFβ_2 activation of ERK2 is associated with sensitivity to the growth inhibitory effects of TGFβ in human breast cancer cells

TGFβ is a potent growth inhibitor of some epithelial-derived breast cancer cells (BCCs) [1]. Unfortunately, many BCCs have lost responsiveness to the growth inhibitory effects of TGFβ. Although defects in TGFβ receptors are clearly important in the development of resistance to TGFβ in BCCs, defects in post-TGFβ-receptor signaling components also appear to play a role in this resistance [40]. We have previously reported that mitogen-activated protein kinases (MAPKs) play an important role in TGFβ signal transduction pathways in untransformed epithelial cells. However, modulation of specific types of MAPKs have not been examined in BCCs. Moreover, although TGFβ isoform-specific differences in bind-

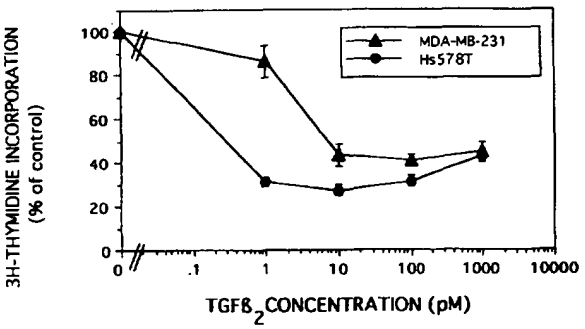

Fig. 1. Effect of TGFβ_2 on [^{3}H]thymidine incorporation in exponentially proliferating cultures of TGFβ-sensitive BCCs. Dose-dependent effects of TGFβ_2 on DNA synthesis in Hs578T and MDA-MB-231 BCCs. BCCs were incubated in serum-free IMEM prior to treatment with or without various concentrations of TGFβ_2 for 24 h. [^{3}H]Thymidine incorporation into DNA in TGFβ-treated cells was expressed as a percentage of levels in untreated cells. Points represent $\bar{x} \pm$ SD ($n = 3$).

Table 1

Growth parameters for TGFβ_2 inhibition of DNA synthesis of breast cancer cell lines

Cell line	IC_{50} (pM)	% Inhibition of DNA synthesis at 10 pM[a,b]
MDA-MB-231	8.0	57 ± 3
Hs578T[c]	0.25	73 ± 2

[a]10 pM = 0.25 ng/ml.
[b]Values represent $\bar{x}$ ± SD.
[c]IC_{50} values were approximated from the plot in Fig. 1.

ing to the TGFβ receptors R_I and R_{II} have been observed [41–43], TGFβ isoform-specific differences have not been examined with regard to MAPK activation. Since previous studies of TGFβ signaling components in untransformed cells have focused on the TGFβ_1 isoform [27,55–57], we investigated the effect of the TGFβ_2 isoform on DNA synthesis and ERK2 activation in BCCs. The two cell lines examined in this report both express functional TGFβ signaling receptors (R_I and R_{II}), with MDA-MB-231 cells expressing more TGFβ R_I and R_{II} than the Hs578T cell line [40].

Fig. 1 depicts the dose-dependent effects of TGFβ_2 on [^{3}H]thymidine incorporation into DNA in the BCC lines Hs578T and MDA-MB-231. Treatment of Hs578T and MDA-MB-231 cells, over a TGFβ_2 concentration range of 1–1000 pM for 24 h, resulted in a dose-dependent decrease in DNA synthesis, with IC_{50} values of 0.25 and 8 pM, respectively (Table 1). Maximal inhibition of DNA synthesis in the MDA-MB-231 and Hs578T cells was 57% and 73%, respectively, and occurred at a TGFβ_2 concentration of 10 pM (0.25 ng/ml). Thus, Hs578T cells were more sensitive to the growth inhibitory effects of TGFβ_2 than were MDA-MB-231 cells, with the IC_{50} value for DNA synthesis inhibition in the MDA-MB-231 cells being 32-fold higher than that of the Hs578T cells.

Fig. 2A depicts the phosphorylation of MBP by ERK2, as determined by an in vitro immunocomplex kinase assay after treatment of asynchronous, serum-free cultures of Hs578T and MDA-MB-231 cells with

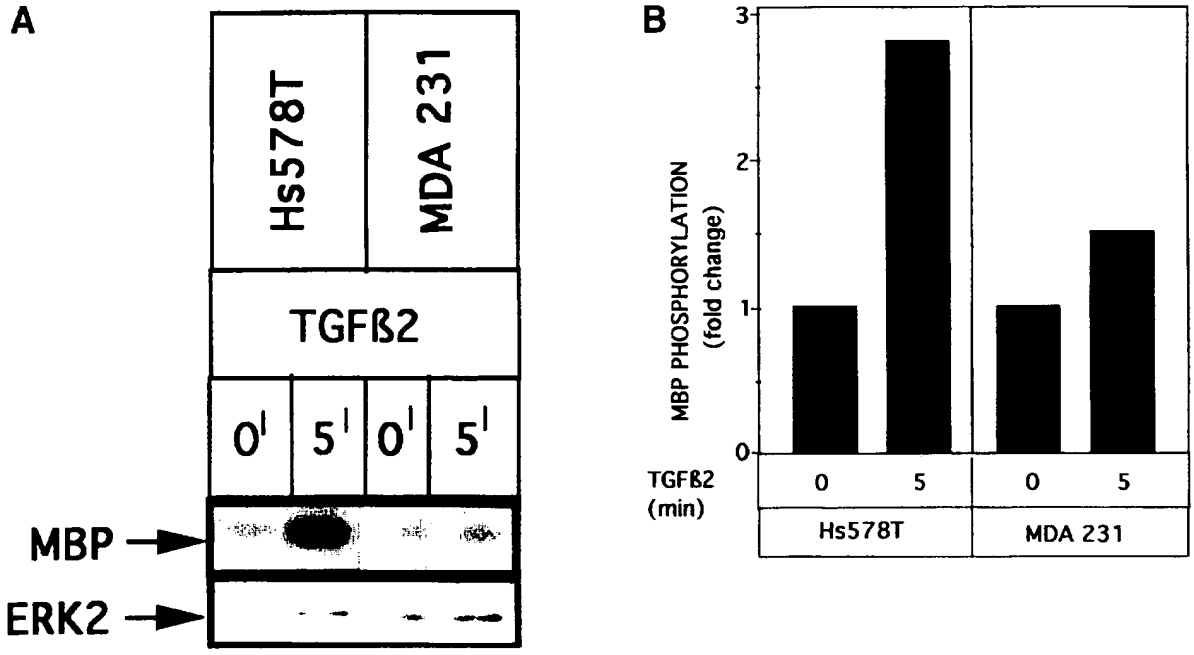

Fig. 2. Effect of TGFβ_2 on ERK2 activity in exponentially proliferating cultures of TGFβ-sensitive BCCs. (A) Top panel: in vitro phosphorylation of MBP by immunoprecipitated ERK2 from Hs578T and MDA-MB-231 cells treated with TGFβ_2 for the indicated times. Minimal phosphorylation of MBP was detected when cell lysates were incubated with non-immune rabbit IgG. Bottom panels: immunoblot analysis of ERK2 loading; no ERK2 was detectable when cell lysates were incubated with non-immune rabbit immunoglobulin. Results are representative of two similar experiments. (B) Plot of scan results from the autoradiograph shown in (A) after correction for ERK2 loading.

TGFβ_2 for 5 min. The lower panel of Fig. 2 depicts the gel loading of ERK2 as determined by immunoblotting of transferred proteins with an ERK2-specific antibody. The results of betagen scanning of the blot in Fig. 2A are shown in Fig. 2B, after correction for ERK2 loading. As indicated, ERK2 was activated by 3-fold within 5 min of TGFβ_2 treatment of Hs578T cells. Similar results were observed with the TGFβ_3 isoform. In contrast, ERK2 was only marginally activated in MDA-MB-231 cells. Thus, the level of activation of ERK2 by TGFβ_2 in these BCCs was associated with sensitivity to the growth inhibitory effects of TGFβ_2.

3.2. TGFβ_2 activation of SAPK/JNK

The stress-activated protein kinases (SAPKs) or Jun N-terminal kinases (JNKs) are activated by a number of factors including UV light and tumor necrosis factor-alpha (TNF-α). TNF-α is a potent growth inhibitor of BCCs that is distinct from TGFβ and binds to specific receptors that differ from TGFβ receptors [29]. We hypothesized that TGFβ, a potent growth inhibitor of BCCs, may also activate SAPK/JNK. Thus, we investigated the effect of TGFβ_2 on SAPK/JNK activity in TGFβ-sensitive BCCs. Fig. 3A depicts the phosphorylation of GST-c-Jun by SAPK/JNK, immunoprecipitated from asynchronous Hs578T cultures treated with TGFβ_2 for various periods of time. The results of densitometric scanning of GST-c-Jun phosphorylation by SAPK/JNK are shown in Fig. 3B. The results indicate that SAPK/JNK was activated by 2.5-fold within 30 min of TGFβ_2 addition to serum-free cultures of Hs578T cells. Similar results were seen with the TGFβ_3 isoform (data not shown). Thus, TGFβ can activate both the ERK2 and SAPK/JNK sub-families of MAPKs in TGFβ-responsive human BCCs. In contrast, BCCs that are resistant to the growth inhibitory effects of TGFβ do not display activation of MAPKs (data not shown).

3.3. TGFβ increases 3TP-Lux reporter activity through an ERK2-independent mechanism

We previously presented a model to explain the potential significance of the ability of TGFβ to activate ERK1 in association with an inhibition of cell growth [22]. This model was based upon previously published work regarding both TGFβ autoinduction and downstream effectors of ERK. That is, autoinduction of TGFβ_1 has been shown to be mediated by the AP-1 complex in the TGFβ_1 promoter and requires both c-Fos and c-Jun components [44]. In addition, ERK2 has been shown to efficiently activate transcription factors of the ternary complex factor (TCF) family, which permits ternary complex formation at the serum-response element of the c-fos promoter, resulting in an increase in both c-fos transcription and AP-1-dependent gene expression [52–54]. Accordingly, we hypothesized that the activation of ERK2 by TGFβ could lead to a growth inhibitory response, indirectly, by activating AP-1-dependent genes (i.e. TGFβ_1, PAI-1) thought to be important for the growth inhibitory response to TGFβ [22,44]. Here we have tested this model by determining whether ERK2 was required for the TGFβ-mediated increases in AP-1 and PAI-1 activities.

For these studies, we transiently co-transfected

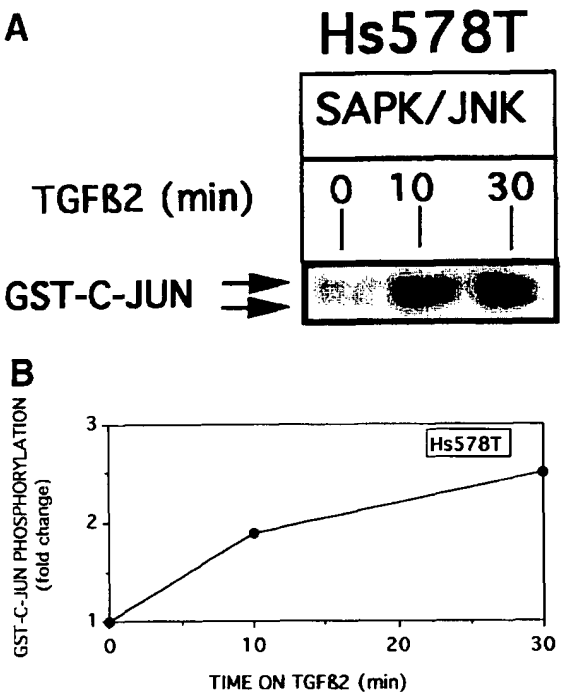

Fig. 3. TGFβ_2 activates SAPK/JNK in TGFβ-sensitive BCCs. (A) Kinetics for in vitro phosphorylation of GST-c-Jun by SAPK/JNK in TGFβ-sensitive Hs578T cells treated with TGFβ_2 for the indicated times. (B) Plot of densitometric scan results for GST-c-Jun autoradiograph in (A). Results are representative of two similar experiments.

Hs578T cells with a construct for expression of a dominant-negative mutant (TAYF) ERK2 protein, in conjunction with a luciferase reporter construct fused to three AP-1 sites and the PAI-1 promoter (3TP-Lux). As a positive control, we tested the effect of a combination of EGF and insulin on 3TP-Lux reporter activity. As indicated in Fig. 4A, treatment of transfected cells with EGF and insulin for 12 h led to an increase in 3TP-Lux reporter activity that was completely blocked when Hs578T BCCs were co-transfected with the TAYF ERK2 construct [46–48]. After a TGFβ treatment period of 8 or 48 h, in the absence of TAYF ERK2, a 4-fold increase in luciferase activity was observed, after correction for transfection efficiency with renilla luciferase (Fig. 4B,C, left side). Co-transfection of TAYF ERK2 (5 μg) with 3TP-Lux (1 μg) did not change 3TP-Lux activity in the absence of TGFβ. In addition, co-transfection of cells with 3TP-Lux and TAYF ERK2 in the presence of TGFβ, for time periods ranging from 8 to 48 h, also did not block TGFβ-induced 3TP-Lux activity (Fig. 4B,C, right side). In addition, co-transfection of TAYF ERK2 and 3TP-Lux at varying concentrations of TAYF ERK2 (0–12 μg) still resulted in no significant change in TGFβ-stimulated luciferase reporter activity (Table 2). Thus, it appears that TGFβ increases 3TP-Lux activity through an ERK2-independent pathway in TGFβ-sensitive BCCs.

4. Discussion

Extensive research efforts have focused on examining the mode of signal transduction by TGFβ through its receptors. TGFβ receptors lack intrinsic tyrosine kinase activity, but have serine-threonine kinase activity [30–32]. Several kinase cascades have been implicated in signal transduction for growth factors and cytokines. Many of these growth factors activate Ras, which in turn activates Raf and MEK. Activation of MEK often leads to the activation of MAPK, which can then enter the nucleus and acti-

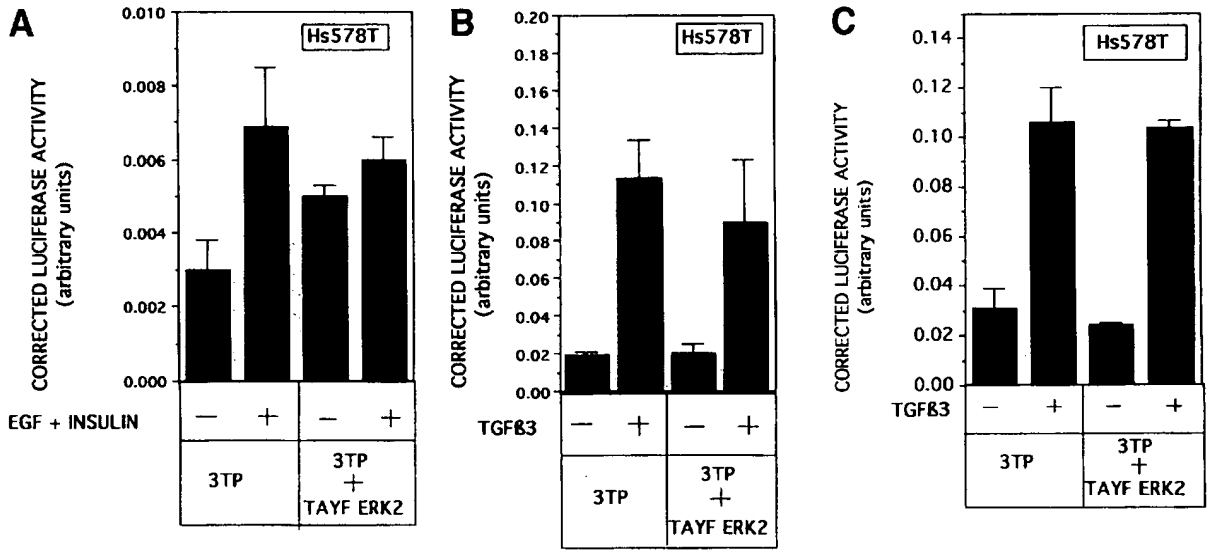

Fig. 4. 3TP-Lux activity in Hs578T BCCs transfected with TAYF ERK2. (A) Hs578T BCCs were co-transfected with 3TP-Lux (3TP) and dominant-negative mutant (TAYF) ERK2 expression plasmids. A renilla luciferase vector was co-transfected to correct for transfection efficiencies. The day after transfection, cells were incubated in serum-free IMEM in the presence or absence of EGF (20 ng/ml) and insulin (600 μg/ml) for 12 h, at which time cells were lysed and assayed for luciferase activity. Luciferase activity data are shown as arbitrary units which have been corrected for transfection efficiency using the dual luciferase assay system (Promega Corp., Madison, WI). (B) Hs578T BCCs were transfected as in (A). The day after transfection, cells were incubated in serum-free IMEM in the absence or presence of $TGF\beta_3$ for 8 h, at which time cells were lysed and assayed for luciferase activity. (C) Hs578T BCCs were transfected as in (A). The day after transfection, cells were incubated in serum-free IMEM in the absence or presence of $TGF\beta_3$ for 48 h, at which time cells were lysed and assayed for luciferase activity. Results are representative of four separate experiments and are expressed as the $\bar{x} \pm$ SD.

Table 2

Lack of effect of increasing concentrations of TAYF ERK2 on TGFβ-stimulated 3TP-Lux luciferase activity in Hs578T cells

μg TAYF ERK2 DNA	% Difference in luciferase activity[a]
0	0.95
3	0.86
6	1.18
12	1.17

[a]Percent difference in luciferase activity represents the fold change in luciferase activity after $TGF\beta_3$ treatment (10 ng/ml) for 48 h in TAYF ERK2-transfected cells relative to vector-transfected control cells. Experimental error was <15%.

vate a number of transcription factors. We now show that TGFβ activates the ERK and SAPK/JNK signaling components in human BCCs. The activation of ERK2 is greatest in BCCs that are the most responsive to the growth inhibitory effects of TGFβ. Moreover, the activation of ERK2 by TGFβ correlates with the IC_{50} for inhibition of DNA synthesis by TGFβ.

Although both ERK2 and SAPK/JNK were activated by $TGF\beta_2$ in the highly responsive BCC line Hs578T, the extent of activation was less than that observed for mitogenic factors and other cytokines [14]. This difference may be explained by the likelihood that ERK2 and SAPK/JNK activation by TGFβ is mediated by upstream components that differ from those utilized by other factors. Moreover, the level of activation of these MAPKs by TGFβ may be enhanced by the synergistic action of parallel pathways or by amplification downstream at the transcription factor level [35–37]. Thus, despite the difference in the magnitude of the activation observed, it is likely that the activation of ERK2 and SAPK/JNK by TGFβ reported herein represents a physiologically relevant signaling cascade leading to TGFβ responses.

Our data demonstrating a relationship between inhibition of DNA synthesis and MAPK activation by TGFβ in BCCs is similar to recent data obtained with the anticancer agent taxol [39]. Taxol causes cell cycle arrest and is an effective drug for the treatment of breast cancer [39]. Treatment of MCF-7 BCCs with this agent led to increased phosphorylation of raf-1 (and presumably increased activity) [39]. However, this effect was not observed until 24 h after treatment with taxol [39]. In contrast, here we show that TGFβ treatment of BCCs results in a much more rapid (5–30 min) activation of ERK2 and SAPK/JNK. Since the effect of taxol on raf-1 phosphorylation is delayed, the effect may be due to factors that are secreted in response to taxol [39]. In contrast, it is unlikely that other factors secreted in response to TGFβ explain the activation of MAPKs observed after a 5 min treatment with TGFβ. Accordingly, activation of MAPKs by TGFβ appears to be direct, indicating that the signaling pathways leading to the negative growth control by these two growth inhibitors in BCCs differ.

We have previously hypothesized that the association between the ability of TGFβ to activate ERK1 and to inhibit cell growth in untransformed epithelial cells might involve an activation of transcription factors involved in the induction of AP-1-dependent genes (i.e. $TGF\beta_1$ itself) [22,24], which can indirectly lead to growth inhibition. Along these lines, ERK2 and SAPK/JNK have been shown to efficiently activate transcription factors such as Elk-1/$p62^{TCF}$ and c-Jun. Activation of Elk-1/$p62^{TCF}$ results in ternary complex formation at the serum-response element of the c-fos promoter [52–54], with subsequent increases in c-fos transcription and AP-1-dependent gene expression. Activation of c-Jun by the SAPK/JNKs can also result in increased AP-1 activity. Both the $TGF\beta_1$ and PAI-1 promoters contain AP-1 sites that are activated by TGFβ and contribute to the TGFβ growth inhibitory response [44]. Thus, the findings reported herein, demonstrating the ability of TGFβ to activate ERK2 and the SAPK/JNKs [14,17], support and extend our original model.

Further, in the current report we have tested our model by asking whether expression of a dominant-negative mutant of ERK2 could block the TGFβ-mediated induction of AP-1 and PAI-1 activities. We have demonstrated that the ability of TGFβ to stimulate the activities of AP-1 and PAI-1, contained in the 3TP luciferase reporter utilized here, was not reduced by co-expression of a dominant-negative mutant of ERK2. In contrast, TAYF ERK2 was able to block EGF + insulin induced 3TP-Lux activity. Thus, it would appear that ERK2 is not required for the effects of TGFβ on AP-1 and PAI-1 activities in the Hs578T BCC line, although this may not be the case for untransformed epithelial cells [38]. In addition, the Hs578T and MDA-MB-231 cell lines used in this study appear to secrete similar amounts of TGFβ into their culture medium [45], despite the reduced

activation of ERK2 by TGFβ observed in the MDA-MB-231 cells (relative to the Hs578T cells). This finding would suggest that ERK2 activation by TGFβ is not directly associated with the AP-1-dependent production of TGFβ in these cell lines. In contrast, we observed a direct correlation between the IC_{50} values for inhibition of DNA synthesis by TGFβ and the level of MAPK activation by this polypeptide. Collectively, the data indicate that in these BCCs, the activation of ERK2 by TGFβ is more tightly linked to the growth inhibitory response of TGFβ than to the induction of AP-1-dependent gene expression by this polypeptide. It remains to be determined whether the SAPK/JNK type of MAPKs are required for control of AP-1-dependent gene expression in these cells.

Acknowledgements

This work was supported by N.I.H. grants CA51452, CA54816 and CA68444 to Kathleen M. Mulder. We thank P.R. Segarini (Celtrix Pharmaceuticals, Santa Clara, CA) and M. Morin (Pfizer Pharmaceuticals, Groton, CT) for the generous gifts of $TGF\beta_2$ and $TGF\beta_3$, respectively. We thank J.M. Kyriakis (Massachusetts General Hospital, Charlestown, MA) for SAPK antiserum and GST-c-Jun plasmid. We thank M.J. Weber (University of VA) for the TAYF ERK2 plasmid and J. Massagué (Sloan-Kettering, NY) for the 3TP-Lux plasmid.

References

[1] C.L. Arteaga, A.K. Tandon, D.D. VonHoff, C.K. Osborne, Transforming growth factor β: potential autocrine growth inhibitor of estrogen receptor-negative human breast cancer cells, Cancer Res. 48 (1988) 3898–3904.

[2] C. Knabbee, M.E. Lippman, L.M. Wakefield, K. Flanders, A. Kasid, R. Derynck, R.B. Dickson, Evidence that transforming growth factor-β is a hormonally regulated negative growth factor in human breast cancer cells, Cell 48 (1987) 417–428.

[3] M.H. Jeng, P.T. ten Dijke, K.K. Iwata, V.C. Jordan, Regulation of the levels of three transforming growth factor β mRNAs by estrogen and their effects on the proliferation of human breast cancer cells, Mol. Cell. Endocrinol. 97 (1993) 115–123.

[4] B.A. Arrick, M. Korc, R. Derynck, Differential regulation of expression of three transforming growth factor β species in human breast cancer cell lines by estradiol, Cancer Res. 50 (1990) 299–303.

[5] A. Butta, K. MacLennan, K.C. Flanders, N.P.M. Sacks, I. Smith, A. MacKinna, M. Dowsett, L.M. Wakefield, M.B. Sporn, M. Baum, A.A. Colletta, Induction of transforming growth factor beta1 in human breast cancer in vivo following tamoxifen treatment, Cancer Res. 52 (1992) 4261–4264.

[6] M.H. Jeng, V.C. Jordan, Growth stimulation and differential regulation of transforming growth factor-β1, TGFβ2, and TGFβ3 messenger RNA levels by norethindrone in MCF-7 human breast cancer cells, Mol. Endocrinol. 5 (1991) 1120–1128.

[7] M.E. Herman, B.S. Katzenellenbogen, Alterations in transforming growth factor-α and -β production and cell responsiveness during the progression of MCF-7 human breast cancer cells to estrogen-autonomous growth, Cancer Res. 54 (1994) 5867–5874.

[8] L. Sun, G. Wu, J.K.V. Willson, L. Zborowska, J. Yang, I. Rajkarunanayake, J. Wang, L.E. Gentry, X.F. Wang, M.G. Brattain, Expression of transforming growth factor β type II receptor leads to reduced malignancy in human breast cancer MCF-7 cells, J. Biol. Chem. 269 (1994) 26449–26455.

[9] T. Masui, L.M. Wakefield, J.F. Lechner, M.A. LaVeck, M.B. Sporn, C.C. Harris, Type beta transforming growth factor is the primary differentiation-inducing serum factor for normal human bronchial epithelial cells, Proc. Natl. Acad. Sci. USA 83 (1986) 2438–2442.

[10] C.S. Murphy, J.A. Pietenpol, K. Munger, P.M. Howley, H.L. Moses, c-myc and pRB: role in TGF-beta 1 inhibition of keratinocyte proliferation, Cold Spring Harbor Symp. Quant. Biol. 56 (1991) 129–135.

[11] I. Reynisdóttir, K. Polyak, A. Iavarone, J. Massagué, Kip/Cip and Ink4 inhibitors cooperate to induce cell cycle arrest in response to TGF-β, Genes Dev. 9 (1995) 1831–1845.

[12] C.J. Sherr, J.M. Roberts, Inhibitors of mammalian G_1 cyclin-dependent kinases, Genes Dev. 9 (1995) 1149–1163.

[13] M.G. Alexandrow, H.L. Moses, Transforming growth factor β and cell cycle regulation, Cancer Res. 55 (1995) 1452–1457.

[14] R.J. Davis, MAPKs: new JNK expands the group, Trends Biochem. Sci. 19 (1994) 470–473.

[15] T.G. Boulton, S.H. Nye, D.J. Robbins, N.Y. Ip, E. Radziejewska, S.D. Morgenbesser, R.A. DePinho, N. Panayotatos, M.H. Cobb, G.D. Yancopoulos, ERKs: a family of protein-serine/threonine kinases that are activated and tyrosine phosphorylated in response to insulin and NGF, Cell 65 (1991) 663–675.

[16] R. Seger, N.G. Ahn, T.G. Boulton, G. Yancopoulos, N. Panayotatos, E. Radziejewska, L. Ericsson, R.L. Bratlien, M.H. Cobb, E.G. Krebs, Microtubule-associated protein 2 kinases, ERK1 and ERK2, undergo autophosphorylation on both tyrosine and threonine residues: implications for their mechanism of action, Proc. Natl. Acad. Sci. USA 88 (1991) 6142–6146.

[17] J.M. Kyriakis, P. Banerjee, E. Nikolakaki, T. Dai, E.A. Rubie, M.F. Ahmad, J. Avruch, J.R. Woodgett, The stress-activated protein kinase subfamily of c-Jun kinases, Nature 369 (1994) 156–160.

[18] B. Derijard, M. Hibi, I.H. Wu, T. Barrett, B. Su, T. Deng, M.

Karin, R.J. Davis, JNK1: a protein kinase stimulated by UV light and Ha-Ras that binds and phosphorylates the c-Jun activation domain, Cell 76 (1993) 1025–1037.
[19] J. Han, J.D. Lee, L. Bibbs, R.J. Ulevitch, A MAP kinase targeted by endotoxin and hyperosmolarity in mammalian cells, Science 265 (1994) 808–811.
[20] J.D. Lee, R.J. Ulevitch, J. Han, Primary structure of BMK1: a new mammalian MAP kinase, Biochem. Biophys. Res. Commun. 213 (1995) 715–724.
[21] G. Zhou, Q. Bao, J.E. Dixon, Components of a new human protein kinase signal transduction pathway, J. Biol. Chem. 270 (1995) 12665–12669.
[22] M.T. Hartsough, K.M. Mulder, Transforming growth factor β activation of $p44^{mapk}$ in proliferating cultures of epithelial cells, J. Biol. Chem. 270 (1995) 7117–7124.
[23] K.M. Mulder, S.L. Morris, Activation of $p21^{ras}$ by transforming growth factor β in epithelial cells, J. Biol. Chem. 267 (1992) 5029–5031.
[24] M.T. Hartsough, R.S. Frey, P.A. Zipfel, A. Buard, S.J. Cook, F. McCormick, K.M. Mulder, Altered TGFβ signaling in epithelial cells when ras activation is blocked, J. Biol. Chem. 271 (1996) 22368–22375.
[25] J. Yue, A. Buard, K.M. Mulder, Blockade of TGFβ_3 up-regulation of $p27^{Kipl}$ and $p21^{Cipl}$ by expression of RasN17 in epithelial cells. Temporal and spatial determinants of specificity in signal transduction. Keystone Symp., 1997.
[26] K.M. Mulder, A. Buard, R.S. Frey, J. Yue, Ras requirement for the up-regulation of $p27^{Kipl}$ and $p21^{Cipl}$ expression by TGFβ in intestinal epithelial cells, 1997, submitted.
[27] K. Yamaguchi, K. Shirakabe, H. Shibuya, K. Irie, I. Oishi, N. Ueno, T. Taniguchi, E. Nishida, K. Matsumoto, Identification of a member of the MAPKKK family as a potential mediator of TGF-β signal transduction, Science 270 (1995) 2008–2011.
[28] T. Moriguchi, N. Kuroyanagi, K. Yamaguchi, Y. Gotoh, K. Irie, T. Kano, K. Shirakabe, Y. Muro, H. Shibuya, K. Matsumoto, E. Nishida, M. Hagiwara, A novel kinase cascade mediated by mitogen-activated protein kinase kinase 6 and MKK3, J. Biol. Chem. 271 (1996) 13675–13679.
[29] A.B. Roberts, M.B. Sporn, The transforming growth factor-betas. In: Peptides, Growth Factors and Their Receptors, Springer Verlag, Berlin, 1997, pp. 419–472.
[30] H.Y. Lin, X.F. Wang, E. Ng-Eaton, R.A. Weinberg, H.F. Lodish, Expression cloning of the TGF-β type-II receptor, a functional transmembrane serine/threonine kinase, Cell 68 (1992) 775–785.
[31] P. Franzen, P. ten Dijke, H. Ichijo, H. Yamashita, P. Schulz, C.H. Heldin, K. Myazono, Cloning of a TGFβ type I receptor that forms a heteromeric complex with the TGFβ type II receptor, Cell 75 (1993) 681–692.
[32] L. Attisano, J. Cárcamo, F. Ventura, F.M.B. Weis, J. Massagué, J.L. Wrana, Identification of human activin and TGFβ type I receptors that form heteromeric kinase complexes with type II receptors, Cell 75 (1993) 671–680.
[33] S. Ohta, Y. Hiraki, C. Shigeno, F. Suzuki, R. Kasai, T. Ikeda, H. Kohno, K. Lee, H. Kikuchi, J. Konishi, H. Bentz, D.M. Rosen, T. Yamamuro, Bone morphogenetic proteins (BMP-2 and BMP-3) induce the late phase expression of the proto-oncogene c-fos in murine osteoblastic MC3T3-E1 cells, FEBS Lett. 314 (1992) 356–360.
[34] M. Centrella, T.L. McCarthy, E. Canalis, Transforming growth factor β is a bifunctional regulator of replication and collagen synthesis in osteoblast-enriched cell cultures from fetal rat bone, J. Biol. Chem. 262 (1987) 2869–2874.
[35] M.V.V.S. Prasad Vara, J.M. Dermott, L.E. Heasley, G.L. Johnson, N. Dhanasekaran, Activation of Jun kinase/stress-activated protein kinase by GTPase-deficient mutants of $G\alpha_{12}$ and $G\alpha_{13}$, J. Biol. Chem. 270 (1995) 18655–18659.
[36] A.B. Vojtek, J.A. Cooper, Rho family members: activators of MAP kinase cascades, Cell 82 (1995) 527–529.
[37] A. Minden, A. Lin, T. Smeal, B. Dérijard, M. Cobb, R. Davis, M. Karin, c-Jun terminal phosphorylation correlates with activation of the JNK subgroup but not the ERK subgroup of mitogen-activated protein kinases, Mol. Cell. Biol. 14 (1994) 6683–6688.
[38] F. Basolo, L. Fiore, F. Ciardiello, S. Calvo, G. Fontanini, P.G. Conaldi, A. Toniolo, Response of normal and oncogene-transformed human mammary epithelial cells to transforming growth factor β1 (TGFβ1): lack of growth-inhibitory effect on cells expressing the simian virus 40 large-t antigen, Int. J. Cancer 56 (1994) 736–742.
[39] M.V. Blagosklonny, T.W. Schulte, P. Nguyen, E.G. Mimnaugh, J. Trepel, L. Neckers, Taxol induction of $p21^{WAF1}$ and p53 requires c-raf-1, Cancer Res. 55 (1995) 4623–4626.
[40] E. Kalkhoven, B.A.J. Roelen, J.P. de Winter, C.L. Mummery, A.J.M. van den Eijnden-van Raaij, P.T. van der Saag, B. van der Burg, Resistance to transforming growth factor β and activin due to reduced receptor expression in human breast tumor cell lines, Cell Growth Diff. 6 (1995) 1151–1161.
[41] G.-H.K. Zhou, G.L. Sechrist, S. Periyasamy, M.G. Brattain, K.M. Mulder, Transforming growth factor β isoform-specific differences in interactions with type I and II transforming growth factor β receptors, Cancer Res. 55 (1995) 2056–2062.
[42] G.H. Zhou, G.L. Sechrist, M.G. Brattain, K.M. Mulder, Clonal heterogeneity of the sensitivity of human colon carcinoma cell lines to TGFβ isoforms, J. Cell. Physiol. 165 (1995) 512–520.
[43] A. Moustakas, H.Y. Lin, Y.I. Henis, J. Plamondon, D. O'Connor-McCourt, H.F. Lodish, The transforming growth factor β receptors types I, II, and III form hetero-oligomeric complexes in the presence of ligand, J. Biol. Chem. 268 (1993) 22215–22218.
[44] S.J. Kim, P. Angel, R. Lafyatis, K. Hattori, K.Y. Kim, M.B. Sporn, M. Karin, A.B. Roberts, Autoinduction of transforming growth factor beta 1 is mediated by the AP-1 complex, Mol. Cell. Biol. 10 (1990) 1492–1497.
[45] C.L. Arteaga, T.C. Dugger, S.D. Hurd, The multifunctional role of transforming growth factor (TGF)-βs on mammary epithelial cell biology, Br. Cancer Res. Treat. 38 (1996) 49–56.
[46] M. David, E. Petricoin, C. Benjamin, R. Pine, M.J. Weber, A.C. Larner, Requirement for MAP kinase (ERK2) activity in interferon alpha- and interferon beta-stimulated gene expression through STAT proteins, Science 269 (1995) 1721–1723.

[47] J.H. Her, S. Lakhani, K. Zu, J. Vila, P. Dent, T.W. Sturgill, M.J. Weber, Dual phosphorylation and autophosphorylation in mitogen-activated protein (MAP) kinase activation, Biochem. J. 296 (1993) 25–31.

[48] J.H. Her, J. Wu, T.B. Rall, T.W. Sturgill, M.J. Weber, Sequence of pp42/MAP kinase, a serine/threonine kinase regulated by tyrosine phosphorylation, Nucleic Acids Res. 19 (1991) 13743.

[49] J.L. Wrana, L. Attisano, J. Carcamo, A. Zentella, J. Doody, M. Laiho, X.F. Wang, J. Massagué, TGF beta signals through a heteromeric protein kinase receptor complex, Cell 71 (1992) 1003–1014.

[50] L. Attisano, J.L. Wrana, E. Montalvo, J. Massagué, Activation of signaling by the activin receptor complex, Mol. Cell. Biol. 16 (1996) 1066–1073.

[51] R. Wieser, L. Attisano, J.L. Wrana, J. Massagué, Signaling activity of transforming growth factor beta type II receptors lacking specific domains in the cytoplasmic region, Mol. Cell. Biol. 13 (1993) 7239–7247.

[52] R. Marais, J. Wynne, R. Treisman, The SRF accessory protein Elk-1 contains a growth factor-regulated transcriptional activation domain, Cell 73 (1993) 381–393.

[53] H. Gille, A.D. Sharrocks, P.E. Shaw, Phosphorylation of transcription factor p62TCF by MAP kinase stimulates ternary complex formation at the c-fos promoter, Nature 358 (1992) 414–417.

[54] R. Zinck, M.A. Cahill, M. Kracht, C. Sachsenmaier, R.A. Hiskind, A. Nordheim, Protein synthesis inhibitors reveal differential regulation of mitogen-activated protein kinase and stress-activated protein kinase pathways that converge on Elk-1, Mol. Cell. Biol. 15 (1995) 4930–4938.

[55] M. Ohtsuki, J. Massagué, Evidence for the involvement of protein kinase activity in transforming growth factor-beta signal transduction, Mol. Cell. Biol. 12 (1992) 261–265.

[56] J. Halstead, K. Kemp, R.A. Ignotz, Evidence for involvement of phosphatidylcholine-phospholipase C and protein kinase C in transforming growth factor-beta signaling, J. Biol. Chem. 270 (1995) 13600–13603.

[57] P.A. Gruppuso, R. Mikumo, D.L. Brautigan, L. Braun, Growth arrest induced by transforming growth factor beta 1 is accompanied by protein phosphatase activation in human keratinocytes, J. Biol. Chem. 266 (1991) 3444–3448.

Exhibit N

[CANCER RESEARCH 59, 227–233, January 1, 1999]

Epidermal Growth Factor (EGF) Receptor Blockade Inhibits the Action of EGF, Insulin-like Growth Factor I, and a Protein Kinase A Activator on the Mitogen-activated Protein Kinase Pathway in Prostate Cancer Cell Lines[1]

Thomas Putz, Zoran Culig, Iris E. Eder, Claudia Nessler-Menardi, Georg Bartsch, Hans Grunicke, Florian Überall, and Helmut Klocker[2]

Departments of Urology [T. P., Z. C., I. E. E., C. N-M., G. B., H. K.] and Medical Chemistry and Biochemistry [T. P., H. G., F. Ü.], University of Innsbruck, A-6020 Innsbruck, Austria

ABSTRACT

Epidermal growth factor (EGF) and insulin-like growth factor I (IGF-I) are potent mitogens that regulate proliferation of prostate cancer cells via autocrine and paracrine loops and promote tumor metastasis. They exert their action through binding to the corresponding cell surface receptors that initiate an intracellular phosphorylation cascade, leading to the activation of mitogen-activated protein kinases (MAPKs), which recruit transcription factors. We have studied the effects of EGF, IGF-I, and the protein kinase A (PKA) activator forskolin on the activation of p42/extracellular signal-regulated kinase (ERK) 2, which is a key kinase in mediation of growth factor-induced mitogenesis in prostate cancer cells. The activity of p42/ERK2 was determined by immune complex kinase assays and by immunoblotting using a phospho p44/p42 MAPK-specific antibody. EGF, IGF-I, and forskolin-induced PKA activity stimulate intracellular signaling pathways converging at the level of p42/ERK2. In the androgen-insensitive DU145 cell line, there is a constitutive basal p42/ERK2 activity that is not present in androgen-sensitive LNCaP cells. Constitutive p42/ERK2 activity is abrogated by blockade of the EGF receptor. Hence, it is obviously caused by an autocrine loop involving this receptor. The effects of EGF on p42/ERK2 are potentiated by forskolin in both cell lines. The blockade of PKA by the specific inhibitor H89 attenuates this synergism. This finding is in contrast to those obtained in several other systems studied thus far, in which PKA activators inhibited MAPKs. p42/ERK2 in DU145 cells is highly responsive to IGF-I stimulation, whereas no effect of IGF-I on p42/ERK2 can be measured in LNCaP cells. Moreover, our results demonstrate that selective blockade of the EGF receptor in prostate cancer cells does not only inhibit the action of EGF, but also IGF-I-induced activation of the MAPK pathway and the interaction with the PKA pathway. In conclusion, these findings offer new possibilities for a therapeutical intervention in prostate cancer by targeting signaling pathways of growth factors and PKA.

INTRODUCTION

Androgen ablation, the standard treatment for nonorgan-confined prostate cancer, intends to block the hormonal signaling cascade leading to the activation of the androgen receptor. In the hormone-responsive stage of the tumor, this treatment causes down-regulation of androgen-responsive genes and leads to apoptosis. Although androgen ablation is initially successful, tumors overcome androgen blockade and develop a hormone-unresponsive phenotype with resistance to therapy. Progression to therapy-refractory prostate cancer can be, in part, explained by the concept of hypersensitive tumor cells (1). These cells are highly responsive to residual circulating androgens, growth factors, and other cellular regulators.

In this respect, the mitogenic effects of growth factors are of utmost significance (2, 3). EGF[3] (3) and IGF-I are potent mitogens that play a regulatory role in proliferation of prostate cancer cells. It has been demonstrated that stromal prostate tissue supports the growth of cancer cells predominantly by secreting growth factors. Moreover, various autocrine loops have been postulated in prostate cancer cells. Additionally, EGF and IGF-I activate the androgen receptor in prostate cancer cells in the absence of androgen (4), and IGF-I has been suggested to promote prostate cell metastasis (5). In concordance with that observation, high serum levels of IGF-I have recently been shown to be associated with an increased risk for prostate cancer (6).

The androgen-independent human prostate cancer cell line DU145 and the androgen-sensitive prostate cancer cell line LNCaP are responsive to stimulation with EGF and IGF-I (3). These growth factors exert their effects through the corresponding receptors expressed in both cell lines. Ligand binding to the cell surface receptor initiates an intracellular phosphorylation cascade resulting in the activation of MAPKs, which recruit transcription factors and, thus, control transcriptional activity.

Among the subgroups of MAPKs (7–9), the ERKs function as key mediators of the mitogenic potential of growth factors. In general, the Ras/Raf/ERK cascade is associated with proliferative effects. For LNCaP cells, it has been reported that overexpression of a mutated Ras results in increased growth. The chemotherapeutic agent phenylacetate has reduced the phosphorylated forms of p42/ERK2 via the Ras pathway and has inhibited cell proliferation (10). An antisense oligonucleotide directed against Raf-1 has also demonstrated inhibitory effects in LNCaP cells (11).

The cAMP-inducible PKA (12) interacts with growth factor signaling. Inhibitory links of cAMP and the PKA pathway to the ERK cascade have been described in many systems (13–17). However, cAMP does not always attenuate MAPK action (18–22). The implications of these second messenger pathways on the ERK cascade in prostate cancer cells are unclear. For LNCaP cells, it has been shown that second messengers including cAMP mediate proliferative effects of the neuropeptide calcitonin (23). In ALVA-41 prostate cancer cells, a cAMP analogue has increased growth rate (24), whereas high cAMP levels have retarded the prostate cancer cell line PC-3 (25).

These findings have focused our interest on the mitogenic potential of growth factors and the interaction with the cAMP-raising PKA activator forskolin. To establish new routes for therapeutical intervention in prostate cancer, we investigate the effects of growth factors and second messenger pathways on the ERK signal transduction pathway. The androgen-independent, fast-growing human prostate cancer cell line DU145, derived from a brain metastasis, serves as a model for advanced prostatic carcinoma (26, 27). The androgen-sensitive, slow-growing prostate cancer cell line LNCaP, derived from a lymph node

Received 7/9/98; accepted 10/28/98.

The costs of publication of this article were defrayed in part by the payment of page charges. This article must therefore be hereby marked *advertisement* in accordance with 18 U.S.C. Section 1734 solely to indicate this fact.

[1] Supported by Austrian Science Foundation (FWF SFB 002-F 201 and 203) and Österreichische Krebshilfe-Krebsgesellschaft/Tirol.

[2] To whom requests for reprints should be addressed, at Department of Urology, Anichstrasse 35, A-6020 Innsbruck, Austria. Fax: 43-512-504-4817 or 43-512-504-4873; E-mail: Helmut.Klocker@uibk.ac.at.

[3] The abbreviations used are: EGF, epidermal growth factor; IGF-I, insulin-like growth factor I; PKA, protein kinase A; MAPK, mitogen-activated protein kinase; ERK, extracellular signal-regulated kinase; cAMP, cyclic adenosine 3′,5′-monophosphate; GST, glutathione S-transferase; HRP, horseradish peroxidase; TBS, Tris-buffered saline; ECL, enhanced chemiluminescence; TBST, Tris-buffered saline Tween 20.

metastasis, displays properties of prostate cancer early in development (28, 29).

We show that forskolin-induced PKA activity and the putative mitogens EGF and IGF-I activate intracellular signaling pathways converging at the level of MAPK p42/ERK2. The basal activity of p42/ERK2 is constitutively elevated in the DU145 cell line. The effects of exogenously added EGF can be potentiated by forskolin in both cell lines. Moreover, our results demonstrate that blockade of the EGF receptor in prostate cancer cells attenuates not only the actions of EGF, but also IGF-I-induced activation of the MAPK pathway and the interaction with the PKA pathway.

MATERIALS AND METHODS

Cell Culture

LNCaP and DU145 cell lines were obtained from the American Type Culture Collection. Cells were maintained in RPMI 1640 (Hyclone, Logan, UT) with 10% FCS (Hyclone), 100 units/ml penicillin, and 0.1 mg/ml streptomycin (PAA Laboratories, Linz, Austria) at 37°C and 5% CO_2. Cells were routinely tested for mycoplasma by using a PCR ELISA kit (Boehringer Mannheim, Vienna, Austria). Before any experiment, cells were trypsinized and plated in 6-well plates (Falcon; Becton Dickinson, Lincoln Park, NJ; Costar, Cambridge, MA) in RPMI 1640 with 1% FCS and antibiotics. After serum starvation for 24 h, nearly confluent cells were incubated with growth factors, forskolin, and inhibitors. Treatment with EGF (Strathmann Biotech, Hannover, Germany), IGF-I (Biomol, Hamburg, Germany), forskolin (Sigma Chemical Co., St. Louis, MO), MAb-EGFR-528 (Santa Cruz Biotechnology, Santa Cruz, CA), Tyrphostin AG 1478 (Alexis, San Diego, CA), and H89 (Calbiochem, La Jolla, CA) was followed by subsequent MAPK assays.

MAPK Assays

Immune Complex Kinase Assays for p42/ERK2. After growth factor stimulation, cells were lysed in ice-cold buffer containing 50 mM Tris-HCl (pH 7.3), 5 mM EDTA, 50 mM NaCl, 5 mM $Na_4P_2O_7 \times 10\ H_2O$, 5 mM NaF, 5 mM Na_3VO_4, 2% Triton X-100, 6 μg/ml aprotinin, and 6 μg/ml leupeptin. Lysates were clarified by centrifugation at 13,000 *rpm* for 10 min at 4°C. The supernatant was precleared with 20 μl of Pansorbin-cells (Calbiochem) for 1 h on a shaker at 4°C. After removing Pansorbin-cells by centrifugation (3 min, 8000 *rpm*, 4°C), immune precipitation using an anti-p42/ERK2 rabbit polyclonal IgG (Santa Cruz Biotechnology) was performed overnight on a shaker at 4°C. Then, 20 μl of Pansorbin-cells were added and agitated for 1 h at 4°C. Immune complexes were collected by centrifugation (3 min, 8000 *rpm*, 4°C) and washed three times in lysis buffer and once in kinase buffer containing 25 mM Hepes (pH 7.5), 2 mM $MnCl_2$, and 20 mM $MgCl_2$.

The kinase reaction was performed by resuspending immune complexes in 20 μl of kinase buffer supplemented with 0.45 mg/ml GST-Elk1, 10 μM ATP, and 1 μCi/ml ATP^{32} (New England Nuclear, Dreieichenhain, Germany). After a 30-min incubation at 30°C, the reaction was stopped by adding electrophoresis sample buffer. Before electrophoresis, samples were boiled for 10 min and separated on a 14% SDS-polyacrylamide gel. Proteins were transferred to Immobilon-P membranes (Millipore, Bedford, MA) for 55 min at 300 mA in Towbin buffer containing 25 mM Tris, 192 mM Glycin, 20% methanol, and 3.5 mM SDS (pH 8.3). Then, membranes were exposed to autoradiography films (Amersham, Buckinghamshire, England) for 24 h.

After autoradiography, membranes were probed for detection of precipitated p42/ERK2 protein levels. Herefore, membranes were soaked in methanol and washed in TBS buffer containing 50 mM Tris-HCl (pH 7.5) and 150 mM NaCl for 5 min. After washing three times for 5 min in TBST containing 50 mM Tris-HCl (pH 7.5), 150 mM NaCl, and 0.05% Tween 20, membranes were blocked with TBST containing 1% nonfat dry milk for 1 h. Membranes were incubated for 2 h with anti-p42/ERK2 mouse monoclonal IgG (dilution, 1:666; Santa Cruz Biotechnology) in TBST containing 1% nonfat dry milk. After washing five times for 10 min in TBST, membranes were probed for 1 h with an HRP-conjugated antimouse antibody (dilution, 1:2000; Amersham) in TBST containing 1% nonfat dry milk. Proteins were visualized by the ECL detection reagents (Amersham) after washing five times in TBST and once in TBS.

Immunoblot of Phosphorylated p42/ERK2 and p44/ERK1. This assay uses a monoclonal antibody specific for activated p42/ERK2 and p44/ERK1. Cells were lysed in electrophoresis sample buffer and boiled for 5 min. After separation on 12% SDS-polyacrylamide gels, proteins were transferred to Immobilon-P membranes as described above. Membranes were washed in TBS buffer containing 50 mM Tris-HCl (pH 7.5) and 150 mM NaCl for 5 min. After washing three times for 5 min in TBST containing 50 mM Tris-HCl (pH 7.5), 150 mM NaCl, and 0.05% Tween 20, membranes were blocked with TBST containing 1% nonfat dry milk for 1 h. Membranes were incubated for 2 h with antibodies (Phospho-p44/p42 MAPK monoclonal antibody; dilution, 1:666; New England Biolabs, Beverly, MA) in TBST containing 1% nonfat dry milk. After washing five times for 10 min in TBST, membranes were probed for 1 h with an HRP-conjugated antimouse antibody (dilution 1:2000; Amersham) in TBST containing 1% nonfat dry milk. After washing five times in TBST and once in TBS, phosphorylated p42/ERK2 and p44/ERK1 proteins were visualized by the ECL detection reagents. In any experiment performed, there was no significant difference between the two assays (*i.e.*, autophosphorylation status of p42/ERK2 and the kinase activity toward GST-Elk1).

After immunoblotting with phospho-p44/p42 MAPK monoclonal antibodies, membranes were stripped to determine the corresponding protein levels. Herefore, membranes were soaked in methanol and washed in TBS buffer containing 50 mM Tris-HCl (pH 7.5) and 150 mM NaCl for 5 min. Then they were incubated with 62.5 mM Tris-HCl (pH 6.8), 100 mM mercaptoethanol, and 2% SDS for 30 min at 60°C. After washing five times for 5 min in TBST containing 50 mM Tris-HCl (pH 7.5), 150 mM NaCl, and 0.05% Tween 20, membranes were blocked with TBST containing 1% nonfat dry milk for 1 h and incubated for 2 h with anti-p42/ERK2 rabbit polyclonal IgG (dilution, 1:666; Santa Cruz Biotechnology) in TBST containing 1% nonfat dry milk. After washing five times for 10 min in TBST, membranes were probed for 1 h with an HRP-conjugated antirabbit antibody (dilution, 1:2000; Santa Cruz Biotechnology) in TBST containing 1% nonfat dry milk. Proteins were visualized by the ECL detection reagents after washing five times in TBST and once in TBS.

RESULTS

Basal Activity of p42/ERK2 Is Elevated in DU145 Cells. DU145 and LNCaP cells are model systems with different growth characteristics and phenotypes (26–29), reflecting the heterogeneity of human prostatic carcinomas. We addressed the question whether these distinct properties also are evident at the level of the mitotic ERK signaling pathway. Herefore, we investigated the activity of the MAPK p42/ERK2. The basal phosphorylation status of p42/ERK2 in human prostate cancer cell lines was determined after starvation for 24 h in RPMI containing 1% FCS. Activity of immunoprecipitated p42/ERK2 was then measured by phosphorylation of the transcription factor Elk1, which was expressed as a recombinant GST-fusion protein. Alternatively, the activation status of p42/ERK2 and p44/ERK1 was determined by Western blotting of the cell lysate with phosphospecific antibodies that detect p42/ERK2 and p44/ERK1 phosphorylated at threonine 202 and tyrosine 204. DU145 cells displayed elevated activity of p42/ERK2 when compared with LNCaP cells (Fig. 1). This finding clearly indicates a constitutively active MAPK in DU145 cells.

Inhibition of the EGF Receptor Blocks Constitutive Activation of p42/ERK2 in DU145 Cells. Exogenously added EGF enhanced activity of p42/ERK2 in LNCaP and DU145 cells (Fig. 2). We asked whether the constitutively active p42/ERK2 in DU145 cells could be associated with autocrine stimulation of the EGF pathway. For this purpose, we examined possibilities to down-regulate ERK activity by blocking the EGF receptor. Preincubation of DU145 cells with Tyrphostin AG 1478, a selective inhibitor of the tyrosine kinase of the EGF receptor, for 1 h resulted in decreased constitutive activity of p42/ERK2. This effect was concentration-dependent, showing a weak inhibition of p42/ERK2 phosphorylation with 3 nM Tyrphostin AG 1478 (data not shown). Treatment with 30 nM Tyrphostin AG 1478

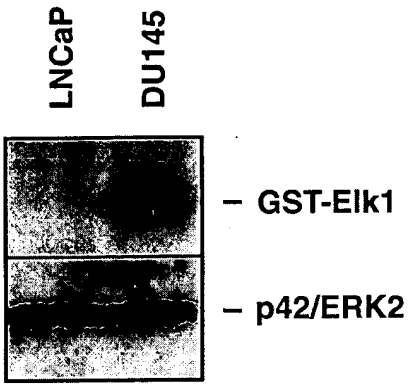

Fig. 1. Basal p42/ERK2 activity in DU145 prostate cancer cells is constitutively up-regulated. The activity of immunoprecipitated p42/ERK2 was determined by phosphorylation of GST-Elk1 after serum starvation for 24 h (*top*). Autoradiography was followed by Western blotting with an anti-p42/ERK2 monoclonal antibody, which represents the loading control for precipitated kinases (*bottom*).

resulted in a complete inhibition of constitutive p42/ERK2 activity (Fig. 3). Treatment of DU145 cells with 3 nM of the monoclonal antibody MAb-EGFR-528 for 1 h also abrogated constitutive p42/ERK2 activity. This antibody binds to a cell surface epitope of the EGF receptor and inhibits binding of EGF, thus, antagonizing EGF-stimulated tyrosine kinase activity. Taken together, these results provide evidence for an extracellular effector of the EGF receptor that stimulates the downstream kinase activity leading to a constitutive p42/ERK2 signal in DU145 cells, rather than a dominant positive signaling protein upstream of this MAPK.

The PKA Activator Forskolin and EGF Act Synergistically to Induce p42/ERK2 Activity in Prostate Cancer Cells. The intracellular signaling network of MAPKs is affected by various modulators. We focused on the regulatory links of the PKA activator forskolin to the ERK cascade. Fig. 4 shows a densitometric analysis of the time course of p42/ERK2 activity in response to EGF and forskolin. For these experiments, EGF concentrations that allowed the measurement of fine nuances in p42/ERK2 activities were determined. EGF doses were 2.5 ng/ml for DU145 and 10 ng/ml for LNCaP cells, respectively. Exogenously added EGF increased the phosphorylation of p42/ERK2 in both cell lines, whereas forskolin (20 μM), in the absence of any other supplement, displayed a weak stimulatory effect on p42/ERK2 activity in DU145 cells. No influence of forskolin on p42/ERK2 phosphorylation could be detected in LNCaP cells, even at higher concentrations (40 μM). However, incubation of cells with EGF and forskolin potentiated the effects of EGF on p42/ERK2 activity. The cooperative action of simultaneously added EGF and forskolin in DU145 cells was transient and less pronounced than in LNCaP cells and could be achieved predominantly in the early phase of p42/ERK2 induction. The low intensity of this p42/ERK2 costimulation and the failure to induce a costimulative activation of p42/ERK2 when DU145 cells were treated with forskolin before the EGF addition (data not shown) suggests a short-term additive effect, but not exclusively the involvement of PKA. The cooperative effect of EGF and forskolin was more evident in LNCaP cells. In this cell line, synergism also could be detected after 20 min of preincubation with forskolin (data not shown). Pretreatment for 30 min with H89 (10–25 μM), an inhibitor of PKA, abrogated the synergism of EGF and forskolin in LNCaP cells (Fig. 5), which indicates a PKA-dependent cooperative activation of p42/ERK2.

Different Effects of IGF-I on p42/ERK2 Activation in Androgen-insensitive and Androgen-sensitive cells. There is increasing evidence that IGF-I is an important growth factor in the pathogenesis of prostate cancer (30). IGF-I signaling shares both common and distinct pathways with EGF (31). Therefore, we were interested whether both growth factors activate p42/ERK2 in prostate cells in a similar manner. Fig. 6 demonstrates a response of p42/ERK2 in serum-starved DU145 cells after stimulation with 100 ng/ml IGF-I. We observed that IGF-I-induced p42/ERK2 kinetics was similar to that of EGF. In contrast to the findings in DU145 cells, no influence on p42/ERK2 activity could be measured in serum-starved LNCaP cells in a time range of 60 min with IGF-I concentrations from 50–200 ng/ml (data not shown). Fig. 6 shows a representative experiment in which LNCaP cells were treated with 100 ng/ml IGF-I. Our results with EGF in LNCaP cells demonstrated that, within 60 min,

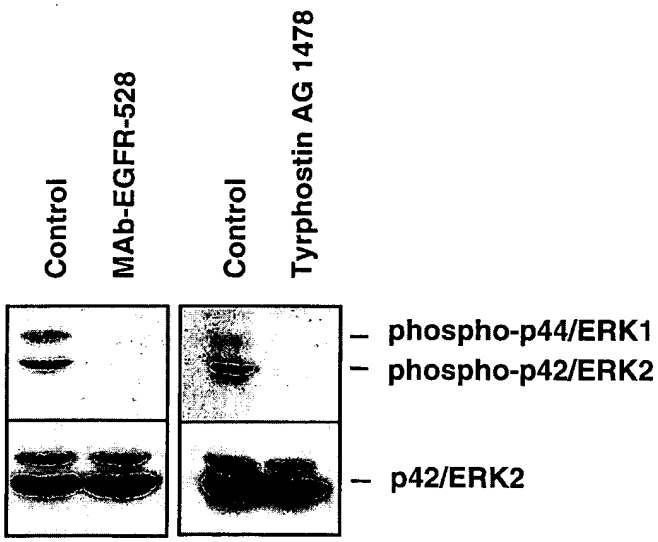

Fig. 3. Inhibition of the EGF receptor abrogates basal p42/ERK2 activity in DU145 cells. EGF receptor blockade for 1 h with 30 nM Tyrphostin AG 1478 and 3 nM MAb-EGFR-528 inhibits phosphorylation of p42/ERK2 in DU145 cells. The phosphorylation status of p42/ERK2 was determined by immunoblotting with a phospho-p44/p42 MAPK monoclonal antibody (*top*). The loading control was carried out with an anti-p42/ERK2 rabbit polyclonal antibody.

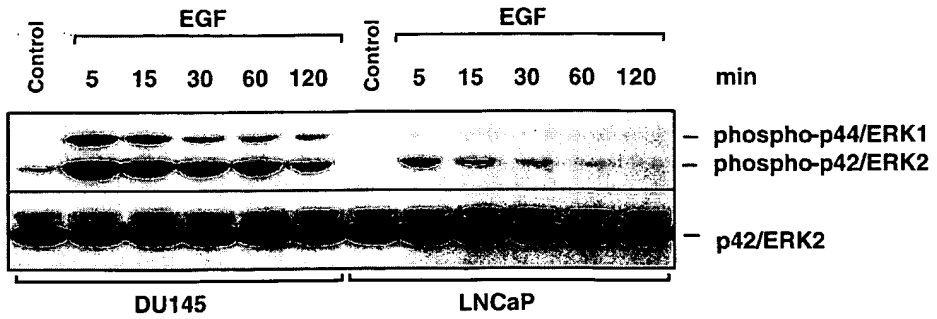

Fig. 2. EGF-induced activity of p42/ERK2 in DU145 and LNCaP cells. Cells were stimulated with 50 ng/ml EGF for the time indicated. The phosphorylation status of p42/ERK2 was determined by immunoblotting with a phospho-p44/p42 MAPK monoclonal antibody (*top*). The loading control was carried out with an anti-p42/ERK2 rabbit polyclonal antibody. Note that this antibody is cross-reactive with p44/ERK1 (*bottom*).

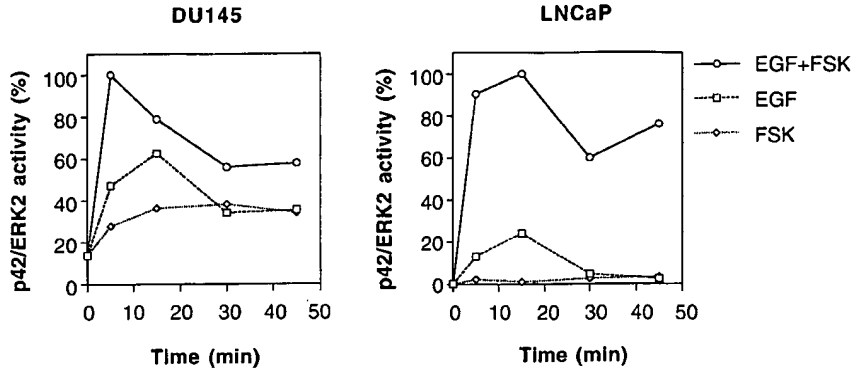

Fig. 4. Time course of p42/ERK2 activity in prostate cancer cells in response to EGF and forskolin treatment. Stimulation of p42/ERK2 was carried out with either EGF or forskolin and a simultaneously added combination of both. The phosphorylation status of p42/ERK2 was determined by immunoblotting with a phospho-p44/p42 MAPK monoclonal antibody, followed by densitometric analysis. A representative of three independent experiments is shown. *Left*, time course of p42/ERK2 activity of DU145 cells. Concentrations of the indicated kinase modulators were 2.5 ng/ml EGF and 20 μM forskolin (*FSK*). *Right*, time course of p42/ERK2 activity of LNCaP cells. Concentrations of the indicated kinase modulators were 10 ng/ml EGF and 40 μM forskolin (*FSK*).

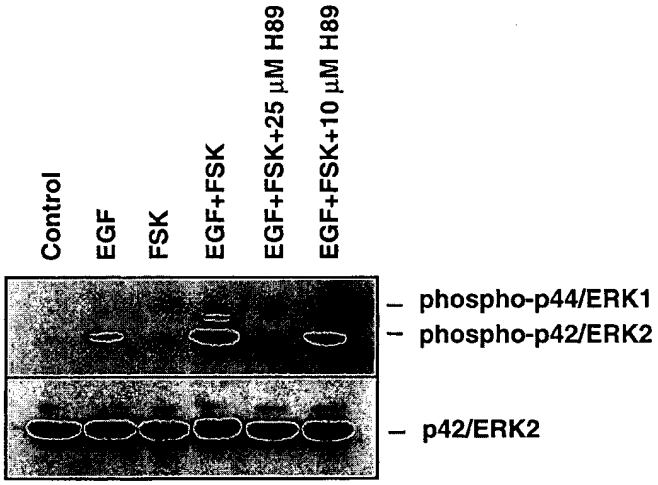

Fig. 5. Synergism of EGF and forskolin in LNCaP cells can be blocked by inhibition of PKA. LNCaP cells were stimulated for 15 min with 5 ng/ml EGF, 20 μM forskolin (*FSK*), or a combination of both. Costimulation was inhibited by preincubation with H89 for 30 min. The phosphorylation status of p42/ERK2 was determined by immunoblotting with a phospho-p44/p42 MAPK monoclonal antibody (*top*). The loading control was carried out with an anti-p42/ERK2 rabbit polyclonal antibody.

p42/ERK2 activation can be achieved. Consequently, IGF-I and EGF-activated pathways are either different or IGF-I receptor stimulation in LNCaP cells is insufficient for activating p42/ERK2.

The Blockade of the EGF Receptor in Prostate Cancer Cells Attenuates not only the Action of EGF, but also IGF-I-induced Activation of the ERK Pathway and Interaction with the PKA Pathway. The effective blockade of the constitutive activation of p42/ERK2 in DU145 cells (Fig. 3) supports the view of the EGFR as a central component in the activation of MAPKs. To address the question whether EGF and IGF-I pathways interact with each other, we investigated the effects of MAb-EGFR-528 on growth factor stimulation. As expected, preincubation of DU145 cells for 1 h with MAb-EGFR-528 (3–20 nM) abrogated the activity of p42/ERK2 induced by EGF (2.5 ng/ml; Fig. 7). Surprisingly, MAb-EGFR-528 also inhibited the IGF-I-induced (25 ng/ml) p42/ERK2 signal in DU145 cells (Fig. 7). Similar results were achieved when the selective inhibitor Tyrphostin AG 1478 (3–300 nM) was used to block the tyrosine kinase of the EGF receptor (data not shown). This result clearly indicates that EGF and IGF-I activate the ERK pathway via the involvement of the EGF receptor in DU145 cells.

Fig. 8 demonstrates that the EGF receptor blockade abrogates EGF-induced p42/ERK activation in LNCaP cells. This blockade also has implications on the actions of the PKA pathway on p42/ERK2 activity supported by the fact that forskolin activates this kinase only in combination with EGF in LNCaP cells. This is in line with the finding that the blockade of the EGF receptor in DU145 cells inhibited forskolin-mediated enhancement of basal p42/ERK2 activity (Fig. 8). Obviously, in this case, forskolin action on p42/ERK2 depends on autocrine growth factor loops.

In conclusion, EGF receptor blockade does not only inhibit EGF, but also IGF-I-induced mitogenic action and the synergistic effects of the PKA pathway on p42/ERK2. These findings offer new possibilities for therapeutical intervention in prostate cancer.

DISCUSSION

In the present study, we have investigated the activity of p42/ERK2 and its response to stimulation with growth factors and a PKA activator in prostate cancer cell lines. Previous studies have demonstrated the impact of growth factors on prostate cancer cell growth. For the androgen-independent prostate cancer cell line DU145, it has been shown that EGF stimulates thymidine incorporation and proliferation (32–34). High levels of EGF receptor expression (32, 35–39) and autocrine secretion of its ligands EGF and transforming growth factor α have been reported for this cell line (33, 34, 40, 41). Antibodies directed against the EGF receptor have been shown to decrease the growth rate of DU145 cells (38, 42) and to reduce autophosphorylation of the EGF receptor (38, 39, 43). Peng *et al.* (44) have induced G_1 cell cycle arrest of DU145 cells with EGF receptor blockade. Our finding that EGF receptor blockade inhibits constitutive p42/ERK2 activity is consistent with previous studies and suggests an up-regulated ERK activity due to autocrine growth factor loops in androgen-independent prostate cancer cells. It also supports the hypothesis that autocrine growth regulation via the EGF receptor offers

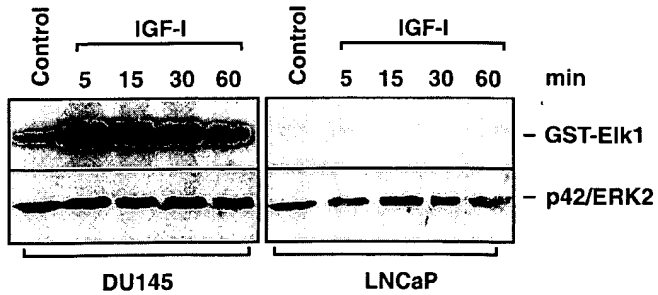

Fig. 6. Time course of p42/ERK2 activity in responses to IGF-I in DU145 and in LNCaP cells. Cells were stimulated with 100 ng/ml IGF-I for the time indicated. The activity of immunoprecipitated p42/ERK2 was determined by phosphorylation of GST-Elk1 (*top*). Autoradiography was followed by immunoblotting with an anti-p42/ERK2 monoclonal antibody, which represents the loading control for precipitated kinases (*bottom*).

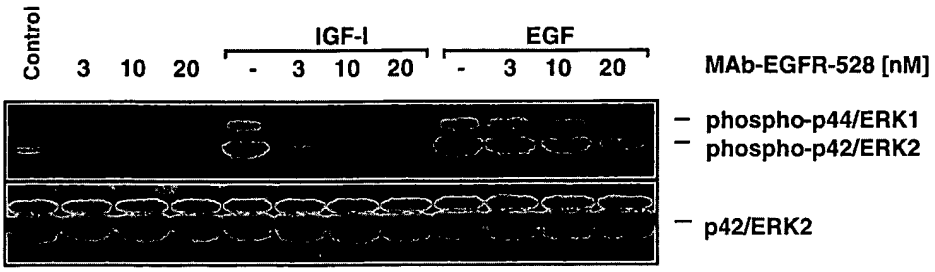

Fig. 7. EGF receptor blockade inhibits EGF and IGF-I-induced activation of p42/ERK2 in DU145 cells. Preincubation of DU145 cells for 1 h with the indicated concentrations of MAb-EGFR-528 was carried out before stimulation with IGF-I (25 ng/ml) or EGF (2.5 ng/ml) for 15 min. Phosphorylation of p42/ERK2 was determined by immunoblotting with a phospho-p44/p42 MAPK monoclonal antibody (*top*). The loading control was carried out with an anti-p42/ERK2 rabbit polyclonal antibody.

a possibility to bypass the need for normal levels of androgens in advanced tumors.

In androgen-sensitive LNCaP cells, p42/ERK2 is not constitutively activated, although autocrine phosphorylation of the EGF receptor has been reported for these cells (39, 45). This may be due to the expression of lower amounts of EGF and transforming growth factor α (40) and fewer EGF receptors (32, 35, 36, 39) than in DU145 cells. However, p42/ERK2 in LNCaP cells is activated by EGF. Therefore, our results support the concept that the reported growth-promoting effects of EGF in LNCaP cells (46, 47) are mediated, at least in part, by p42/ERK2.

The role of the PKA pathway in the regulation of p42/ERK2 has not been investigated in prostate cancer cells before our study. For various other cell lines, it has been demonstrated that second messenger pathways provide regulatory links to the Ras/Raf/ERK cascade, resulting in a subsequent reduction of MAPK activities (13–17). However, cAMP-raising substances do not always counteract ERK action. cAMP-mediated stimulation of ERK activities (18–22), as well as a lack of effects of forskolin on growth factor- or serum-induced MAPK activities (48, 49) has been reported. The influence of PKA on Ras/Raf interaction is regarded as a key regulatory step in integrating cAMP and growth factor signals into the ERK cascade. The underlying mechanism is cell type-specific and dependent on isotype expression of the signaling molecules involved. Differential regulation of Raf isotypes by cAMP (50, 51) has been reported. Additionally, phosphorylation of Raf-1 by PKA modulates its interaction with different members of the Ras family (52). Nevertheless, growth factor signaling via Ras/Raf-independent pathways should be taken into account (19, 53). PKA isotype expression also plays a role in the interaction with EGF receptor-mediated signal transduction pathways. In fact, a linkage of PKA-I to the adaptor protein Grb2 has been demonstrated (54) in mammary epithelial cells, which offers the possibility that PKA-I mediates mitogenic signaling of EGF and related growth factors.

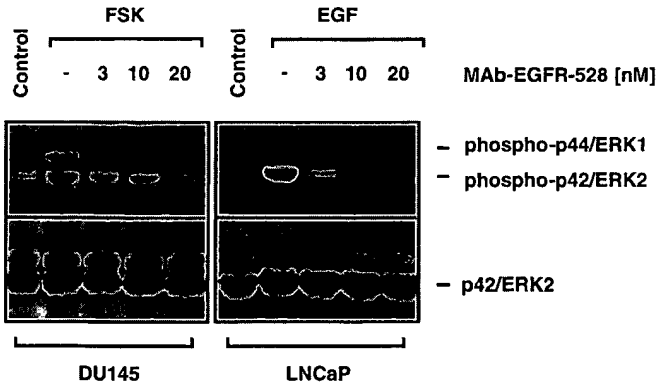

Fig. 8. EGF receptor blockade inhibits forskolin-induced activation of p42/ERK2 in DU145 cells and EGF-induced activation of p42/ERK2 in LNCaP cells. Preincubation of cells for 1 h with the indicated concentrations of MAb-EGFR-528 was carried out before stimulation with 10 ng/ml EGF or 40 μM forskolin for 15 min. Phosphorylation of p42/ERK2 was determined by immunoblotting with a phospho-p44/p42 MAPK monoclonal antibody (*top*). The loading control was carried out with an anti-p42/ERK2 rabbit polyclonal antibody (*bottom*).

Despite unresolved questions concerning the appropriate PKA and Ras/Raf/ERK interaction, we demonstrate that forskolin supports the EGF-induced p42/ERK2 activity in prostate cancer cell lines. This result provides evidence that cAMP-raising substances vigorously increase the mitogenicity of the ERK pathway at least in androgen-sensitive LNCaP cells.

Activation of p42/ERK2 in response to EGF stimulation is a common feature of the tested cell lines. In contrast, different effects of IGF-I can be detected in LNCaP and DU145 cells. Both cell lines have been shown to express the IGF-I receptor (55–59). mRNA levels for the IGF-I receptor have been reported to be higher in DU145 cells than in LNCaP cells (59), which is in line with higher IGF-I receptor concentrations in DU145 cells calculated in ligand binding studies (58). Previous studies concerning responses to IGF-I in prostate cells are, in part, contradictory. IGF-I has been demonstrated to stimulate thymidine uptake in DU145 (57, 58) but not in LNCaP cells (58), whereas IGF-I-induced growth stimulation in both DU145 (5, 56) and in LNCaP cells (5) has been reported. Peptide analogues of IGF-I that compete with IGF-I for binding and an antisense oligonucleotide to IGF-I receptor have inhibited the growth of DU145 and LNCaP cells in serum-free medium. Detection of autophosphorylated IGF-I receptors and IGF-I secretion has indicated the existence of an autocrine loop in these cells. In that study, no further increase in proliferation could have been measured in response to exogenously added IGF-I (59). Our results demonstrate that IGF-I is a potent activator of the ERK cascade in DU145 cells. Although the mitogenicity of IGF-I has been suggested, no corresponding p42/ERK2 activation can be measured in LNCaP cells as a consequence of IGF-I stimulation. The reasons for this unexpected result are unclear. A possible explanation for our finding is that IGF-I uses different mitogenic signaling pathways involving an ERK-independent mechanism in LNCaP cells. Moreover, it can be hypothesized that IGF-I receptor expression in LNCaP is not sufficient for inducing a measurable short-term downstream MAPK signal. In respect to the complexity of IGF-I and EGF actions, the interplay between the autocrine growth factor loops and receptor interactions could be of profound importance. This view is supported by our finding that blockade of the up-regulated ERK pathway evoked by MAb-EGFR-528 also abrogates IGF-I-induced p42/ERK2 activation in DU145 cells. Similar results have been reported by Connolly and Rose (57), who have demonstrated that the interruption of the EGF autocrine loop by an anti-EGF receptor antibody in DU145 cells results in a complete loss of IGF-I responsiveness.

Taken together, we demonstrate that the mitogenic effects of EGF, IGF-I, and forskolin-induced PKA in prostate cancer cells converge at the level of the MAPK p42/ERK2. Blockade of the EGF receptor was sufficient to abrogate autocrine effects, as well as the mitogenic action of exogenous growth factors. The fact that the inhibition of signal

transduction at the receptor level does not only abrogate EGF-induced p42/ERK2 activity but also IGF-I and forskolin-induced PKA action emphasizes the significance of the EGF receptor as a central component in MAPK signaling in prostate cancer cells and suggests possibilities for therapeutic intervention. EGF receptor-blocking antibodies, alone or in combination with PKA inhibitors, have been demonstrated to display antitumor activity in various human cancer cell lines *in vitro* and *in vivo*. Furthermore, EGF receptor-blocking antibodies and PKA inhibitors have already entered human clinical trials (60). In conclusion, the observations in our model system suggest that this therapeutical strategy should be further evaluated in prostate cancer treatment.

ACKNOWLEDGMENTS

We thank T. Sierek, E. Tafatsch, and M. Pöschl for technical assistance and K. Hellbert and F. Hochholdinger for helpful advice in performing MAPK assays.

REFERENCES

1. Culig, Z., Hobisch, A., Hittmair, A., Peterziel, H., Radmayr, C., Bartsch, G., Cato, A. C., and Klocker, H. Hyperactive androgen receptor in prostate cancer: what does it mean for new therapy concepts? Histol. Histopathol., *12:* 781–786, 1997.
2. Byrne, R. L., Leung, H., and Neal, D. E. Peptide growth factors in the prostate as mediators of stromal epithelial interaction. Br. J. Urol., *77:* 627–633, 1996.
3. Culig, Z., Hobisch, A., Cronauer, M. V., Radmayr, C., Hittmair, A., Zhang, J., Thurnher, M., Bartsch, G., and Klocker, H. Regulation of prostatic growth and function by peptide growth factors. Prostate, *28:* 392–405, 1996.
4. Culig, Z., Hobisch, A., Cronauer, M. V., Radmayr, C., Trapman, J., Hittmair, A., Bartsch, G., and Klocker, H. Androgen receptor activation in prostatic tumor cell lines by insulin-like growth factor-I, keratinocyte growth factor, and epidermal growth factor. Cancer Res., *54:* 5474–5478, 1994.
5. Ritchie, C. K., Andrews, L. R., Thomas, K. G., Tindall, D. J., and Fitzpatrick, L. A. The effects of growth factors associated with osteoblasts on prostate carcinoma proliferation and chemotaxis: implications for the development of metastatic disease. Endocrinology, *138:* 1145–1150, 1997.
6. Chan, J. M., Stampfer, M. J., Giovannucci, E., Gann, P. H., Ma, J., Wilkinson, P., Hennekens, C. H., and Pollak, M. Plasma insulin-like growth factor-I and prostate cancer risk: a prospective study. Science (Washington DC), *279:* 563–566, 1998.
7. Davis, R. J. MAPKs. new JNK expands the group. Trends Biochem. Sci., *19:* 470–473, 1994.
8. Denhardt, D. T. Signal-transducing protein phosphorylation cascades mediated by Ras/Rho proteins in the mammalian cell: the potential for multiplex signalling. Biochem. J., *318:* 729–747, 1996.
9. Zhu, X., and Liu, J. P. Steroid-independent activation of androgen receptor in androgen-independent prostate cancer: a possible role for the MAP kinase signal transduction pathway? Mol. Cell. Endocrinol., *134:* 9–14, 1997.
10. Danesi, R., Nardini, D., Basolo, F., Del Tacca, M., Samid, D., and Myers, C. E. Phenylacetate inhibits protein isoprenylation and growth of the androgen-independent LNCaP prostate cancer cells transfected with the T24 Ha-ras oncogene. Mol. Pharmacol., *49:* 972–979, 1996.
11. Lau, Q. C., Brüsselbach, S., and Müller, R. Abrogation of c-Raf expression induces apoptosis in tumor cells. Oncogene, *16:* 1899–1902, 1998.
12. Scott, J. D. Cyclic nucleotide-dependent protein kinases. Pharmacol. Ther., *50:* 123–145, 1991.
13. Wu, J., Dent, P., Jelinek, T., Wolfman, A., Weber, M. J., and Sturgill, T. W. Inhibition of the EGF-activated MAP kinase signaling pathway by adenosine 3′,5′-monophosphate. Science (Washington DC), *262:* 1065–1069, 1993.
14. Sevetson, B. R., Kong, X., and Lawrence, J. C., Jr. Increasing cAMP attenuates activation of mitogen-activated protein kinase. Proc. Natl. Acad. Sci. USA, *90:* 10305–10309, 1993.
15. Graves, L. M., Bornfeldt, K. E., Raines, E. W., Potts, B. C., Macdonald, S. G., Ross, R., and Krebs, E. G. Protein kinase A antagonizes platelet-derived growth factor-induced signaling by mitogen-activated protein kinase in human arterial smooth muscle cells. Proc. Natl. Acad. Sci. USA, *90:* 10300–10304, 1993.
16. Cook, S. J., and McCormick, F. Inhibition by cAMP of Ras-dependent activation of Raf. Science (Washington DC), *262:* 1069–1072, 1993.
17. Hordijk, P. L., Verlaan, I., Jalink, K., van Corven, E. J., and Moolenaar, W. H. cAMP abrogates the p21ras-mitogen-activated protein kinase pathway in fibroblasts. J. Biol. Chem., *269:* 3534–3538, 1994.
18. Englaro, W., Rezzonico, R., Durand-Clement, M., Lallemand, D., Ortonne, J. P., and Ballotti, R. Mitogen-activated protein kinase pathway and AP-1 are activated during cAMP-induced melanogenesis in B-16 melanoma cells. J. Biol. Chem., *270:* 24315–24320, 1995.
19. Faure, M., and Bourne, H. R. Differential effects on cAMP on the MAP kinase cascade: evidence for a cAMP-insensitive step that can bypass Raf-1. Mol. Biol. Cell., *6:* 1025–1035, 1995.
20. Frodin, M., Peraldi, P., and Van Obberghen, E. Cyclic AMP activates the mitogen-activated protein kinase cascade in PC12 cells. J. Biol. Chem., *269:* 6207–6214, 1994.
21. Calleja, R., Filloux, C., Peraldi, P., Baron, V., and Van Obberghen, E. The effect of cyclic adenosine monophosphate on the mitogen-activated proteinkinase pathway depends on both the cell type and the type of tyrosine kinase-receptor. Endocrinology, *138:* 1111–1120, 1997.
22. Sawada, T., Ohmichi, M., Koike, K., Kanda, Y., Kimura, A., Masuhara, K., Ikegami, H., Inoue, M., Miyake, A., and Murata, Y. Norepinephrine stimulates mitogen-activated protein kinase activity in GT1–1 gonadotropin-releasing hormone neuronal cell lines. Endocrinology, *138:* 5275–5281, 1997.
23. Shah, G. V., Rayford, W., Noble, M. J., Austenfeld, M., Weigel, J., Vamos, S., and Mebust, W. K. Calcitonin stimulates growth of human prostate cancer cells through receptor-mediated increase in cyclic adenosine 3′,5′-monophosphates and cytoplasmic Ca^{2+} transients. Endocrinology, *134:* 596–602, 1994.
24. Nakhla, A. M., and Rosner, W. Stimulation of prostate cancer growth by androgens and estrogens through the intermediacy of sex hormone-binding globulin. Endocrinology, *137:* 4126–4129, 1996.
25. Okutani, T., Nishi, N., Kagawa, Y., Takasuga, H., Takenaka, I., Usui, T., and Wada, F. Role of cyclic AMP and polypeptide growth regulators in growth inhibition by interferon in PC-3 cells. Prostate, *18:* 73–80, 1991.
26. Kozlowski, J. M., Fidler, I. J., Campbell, D., Xu, Z. L., Kaighn, M. E., and Hart, I. R. Metastatic behavior of human tumor cell lines grown in the nude mouse. Cancer Res., *44:* 3522–3529, 1984.
27. Stone, K. R., Mickey, D. D., Wunderli, H., Mickey, G. H., and Paulson, D. F. Isolation of a human prostate carcinoma cell line (DU 145). Int. J. Cancer, *21:* 274–281, 1978.
28. Gleave, M., Hsieh, J. T., Gao, C. A., von Eschenbach, A. C., and Chung, L. W. Acceleration of human prostate cancer growth *in vivo* by factors produced by prostate and bone fibroblasts. Cancer Res., *51:* 3753–3761, 1991.
29. Horoszewicz, J. S., Leong, S. S., Kawinski, E., Karr, J. P., Rosenthal, H., Chu, T. M., Mirand, E. A., and Murphy, G. P. LNCaP model of human prostatic carcinoma. Cancer Res., *43:* 1809–1818, 1983.
30. Cohen, P., Peehl, D. M., and Rosenfeld, R. G. The IGF axis in the prostate. Horm. Metab. Res., *26:* 81–84, 1994.
31. Rubin, R., and Baserga, R. Insulin-like growth factor-I receptor. Its role in cell proliferation, apoptosis, and tumorigenicity. Lab. Invest., *73:* 311–331, 1995.
32. MacDonald, A., and Habib, F. K. Divergent responses to epidermal growth factor in hormone sensitive and insensitive human prostate cancer cell lines. Br. J. Cancer, *65:* 177–182, 1992.
33. Connolly, J. M., and Rose, D. P. Secretion of epidermal growth factor and related polypeptides by the DU 145 human prostate cancer cell line. Prostate, *15:* 177–186, 1989.
34. MacDonald, A., Chisholm, G. D., and Habib, F. K. Production and response of a human prostatic cancer line to transforming growth factor-like molecules. Br. J. Cancer, *62:* 579–584, 1990.
35. Grasso, A. W., Wen, D., Miller, C. M., Rhim, J. S., Pretlow, T. G., and Kung, H. J. ErbB kinases and NDF signaling in human prostate cancer cells. Oncogene, *15:* 2705–2716, 1997.
36. Ching, K. Z., Ramsey, E., Pettigrew, N., D'Cunha, R., Jason, M., and Dodd, J. G. Expression of mRNA for epidermal growth factor, transforming growth factor-α and their receptor in human prostate tissue and cell lines. Mol. Cell. Biochem., *126:* 151–158, 1993.
37. Morris, G. L., and Dodd, J. G. Epidermal growth factor receptor mRNA levels in human prostatic tumors and cell lines. J. Urol., *143:* 1272–1274, 1990.
38. Fong, C. J., Sherwood, E. R., Mendelsohn, J., Lee, C., and Kozlowski, J. M. Epidermal growth factor receptor monoclonal antibody inhibits constitutive receptor phosphorylation, reduces autonomous growth, and sensitizes androgen-independent prostatic carcinoma cells to tumor necrosis factor α. Cancer Res., *52:* 5887–5892, 1992.
39. Sherwood, E. R., Van Dongen, J. L., Wood, C. G., Liao, S., Kozlowski, J. M., and Lee, C. Epidermal growth factor receptor activation in androgen-independent but not androgen-stimulated growth of human prostatic carcinoma cells. Br. J. Cancer, *77:* 855–861, 1998.
40. Connolly, J. M., and Rose, D. P. Production of epidermal growth factor and transforming growth factor-α by the androgen-responsive LNCaP human prostate cancer cell line. Prostate, *16:* 209–218, 1990.
41. Tillotson, J. K., and Rose, D. P. Endogenous secretion of epidermal growth factor peptides stimulates growth of DU145 prostate cancer cells. Cancer Lett., *60:* 109–112, 1991.
42. Connolly, J. M., and Rose, D. P. Autocrine regulation of DU145 human prostate cancer cell growth by epidermal growth factor-related polypeptides. Prostate, *19:* 173–180, 1991.
43. Zi, X., Grasso, A. W., Kung, H. J., and Agarwal, R. A flavonoid antioxidant, silymarin, inhibits activation of erbB1 signaling and induces cyclin-dependent kinase inhibitors, G1 arrest, and anticarcinogenic effects in human prostate carcinoma DU145 cells. Cancer Res., *58:* 1920–1929, 1998.
44. Peng, D., Fan, Z., Lu, Y., DeBlasio, T., Scher, H., and Mendelsohn, J. Anti-epidermal growth factor receptor monoclonal antibody 225 up-regulates p27KIP1 and induces G1 arrest in prostatic cancer cell line DU145. Cancer Res., *56:* 3666–3669, 1996.
45. Limonta, P., Dondi, D., Marelli, M. M., Moretti, R. M., Negri-Cesi, P., and Motta, M. Growth of the androgen-dependent tumor of the prostate: role of androgens and of locally expressed growth modulatory factors. J. Steroid. Biochem. Mol. Biol., *53:* 401–405, 1995.
46. Schuurmans, A. L., Bolt, J., Veldscholte, J., and Mulder, E. Regulation of growth of LNCaP human prostate tumor cells by growth factors and steroid hormones. J. Steroid. Biochem. Mol. Biol., *40:* 193–197, 1991.
47. Schuurmans, A. L., Bolt, J., and Mulder, E. Androgens stimulate both growth rate and epidermal growth factor receptor activity of the human prostate tumor cell LNCaP. Prostate, *12:* 55–63, 1988.

48. Seternes, O. M., Sorensen, R., Johansen, B., Loennechen, T., Aarbakke, J., and Moens, U. Synergistic increase in c-fos expression by simultaneous activation of the ras/raf/map kinase- and protein kinase A signaling pathways is mediated by the c-fos AP-1 and SRE sites. Biochim. Biophys. Acta, *1395:* 345–360, 1998.
49. Lowe, W. L., Jr., Fu, R., and Banko, M. Growth factor-induced transcription via the serum response element is inhibited by cyclic adenosine 3′,5′-monophosphate in MCF-7 breast cancer cells. Endocrinology, *138:* 2219–2226, 1997.
50. Hafner, S., Adler, H. S., Mischak, H., Janosch, P., Heidecker, G., Wolfman, A., Pippig, S., Lohse, M., Ueffing, M., and Kolch, W. Mechanism of inhibition of Raf-1 by protein kinase A. Mol. Cell. Biol., *14:* 6696–6703, 1994.
51. Erhardt, P., Troppmair, J., Rapp, U. R., and Cooper, G. M. Differential regulation of Raf-1 and B-Raf and Ras-dependent activation of mitogen-activated protein kinase by cyclic AMP in PC12 cells. Mol. Cell. Biol., *15:* 5524–5530, 1995.
52. Yee, W. M., and Worley, P. F. Rheb interacts with Raf-1 kinase and may function to integrate growth factor- and protein kinase A-dependent signals. Mol. Cell. Biol., *17:* 921–933, 1997.
53. Burgering, B. M., de Vries-Smits, A. M., Medema, R. H., van Weeren, P. C., Tertoolen, L. G., and Bos, J. L. Epidermal growth factor induces phosphorylation of extracellular signal-regulated kinase 2 via multiple pathways. Mol. Cell. Biol., *13:* 7248–7256, 1993.
54. Tortora, G., Damiano, V., Bianco, C., Baldassarre, G., Bianco, A. R., Lanfrancone, L., Pelicci, P. G., and Ciardiello, F. The RIα subunit of protein kinase A (PKA) binds to Grb2 and allows PKA interaction with the activated EGF-receptor. Oncogene, *14:* 923–928, 1997.
55. Kimura, G., Kasuya, J., Giannini, S., Honda, Y., Mohan, S., Kawachi, M., Akimoto, M., and Fujita Yamaguchi, Y. Insulin-like growth factor (IGF) system components in human prostatic cancer cell-lines: LNCaP, DU145, and PC-3 cells. Int. J. Urol., *3:* 39–46, 1996.
56. Figueroa, J. A., Lee, A. V., Jackson, J. G., and Yee, D. Proliferation of cultured human prostate cancer cells is inhibited by insulin-like growth factor (IGF) binding protein-1: evidence for an IGF-II autocrine growth loop. J. Clin. Endocrinol. Metab., *80:* 3476–3482, 1995.
57. Connolly, J. M., and Rose, D. P. Regulation of DU145 human prostate cancer cell proliferation by insulin-like growth factors and its interaction with the epidermal growth factor autocrine loop. Prostate, *24:* 167–175, 1994.
58. Iwamura, M., Sluss, P. M., Casamento, J. B., and Cockett, A. T. Insulin-like growth factor I: action and receptor characterization in human prostate cancer cell lines. Prostate, *22:* 243–252, 1993.
59. Pietrzkowski, Z., Mulholland, G., Gomella, L., Jameson, B. A., Wernicke, D., and Baserga, R. Inhibition of growth of prostatic cancer cell lines by peptide analogues of insulin-like growth factor 1. Cancer Res., *53:* 1102–1106, 1993.
60. Ciardiello, F., and Tortora, G. Interactions between the epidermal growth factor receptor and type I protein kinase A: biological significance and therapeutic implications. Clin. Cancer Res., *4:* 821–828, 1998.